High Temperature Processing of Kaolinitic Materials

by

Rachel Elizabeth Thomas

A thesis submitted to
The University of Birmingham
for the degree of
DOCTOR OF ENGINEERING

School of Chemical Engineering
College of Engineering and Physical Sciences
The University of Birmingham
February 2010

Abstract

Calcination, is the process of heating a substance, to a temperature below its fusing point, with a resultant loss of water. It is one of the most important techniques currently used to enhance the properties, and therefore value, of kaolin. The overall aim of this project was to provide a better understanding of the principles of the kaolin calcination reaction in order to enhance the efficiency, quality and sustainability of the Imerys calcining operations.

This research has shown a strong correlation between the chemistry of kaolin and the colour of the calcined product. This is due to the influence of contaminant materials on the colour of the hydrous kaolin, which in turn affects the calcined material. The strongest colour influencing factor is the presence of iron, particularly if it is present on the surface of the kaolin. Surface iron is currently reduced using a reductive bleaching process. This has an improving influence on even the most contaminated kaolins, however there can be quite a lot of interbatch variability.

Despite its effect on colour the chemistry of kaolin has little influence on post calcination reactivity. Reactivity is due to physical factors such as particle and agglomerate size and the penetration of heat into the material. Any kaolin will calcine to produce a low reactivity product; provided the heat is able to penetrate into the bed and that the material is able to remain at temperature for sufficient time for the calcination reaction to occur. Another outcome of the research was the discovery that a higher temperature and shorter time period has little on the end calcined product but has implications for lower energy usage.

For my Mum and Dad

One man’s magic is another man’s engineering

Robert Heinlein, Author (1907 – 1988)

Acknowledgements

I would like to thank my supervisors, Professor Stuart Blackburn, Dr Neil Rowson and Dr Richard Greenwood from Birmingham University and Richard Taylor from Imerys Minerals for their help and support throughout the project. I would like to extend special thanks to Dr Anabelle Legrix from Imerys who became involved late into the project, and without whom this thesis would not have happened.

I would also like to thank David Moseley, Darren Grose, Jon Morley, Mike Truscott, Martin Dunn, Allen Webb, Malcolm Soady, Becky Hamer, Jonathan Hearle, Jim Fooks and other members of the Performance and Filtration Minerals Europe Process Development Group for their assistance and patience with my many questions for the past four years. I am also very grateful for the help and guidance offered with sample testing by the Physical Testing and Analytical Chemistry groups at Par Moor Centre.

I would like to extend my thanks to my fellow EngD students at Imerys; Richard, Paul and Yao for their advice and support throughout the project and also to Harry and Sean for their help with experiments.

Finally, I owe a debt of gratitude to my Mum and Dad, my brother Edd and my friends, Melissa, Sarah, Katie, Mac, Angie and Grace for their understanding, endless patience, and encouragement when it was most required.

Contents

1 INTRODUCTION 1

1.1 The company 1

1.2 Product Description – Calcined Kaolins 3

1.2.1 Competitors 6

1.3 Statement of objectives 10

1.4 Thesis Layout 10

2 LITERATURE REVIEW 13

2.1 Formation of kaolin – Kaolinisation 13

2.1.1 Hydrothermal Theory 14

2.1.2 Weathering 16

2.1.3 Combination 17

2.1.4 Cornish clays 18

2.1.5 Sedimentary clay deposits 20

2.2 The structure and chemistry of kaolin 20

2.2.1 Kaolinite 23

2.2.2 Mica 28

2.2.3 Feldspar 30

2.2.4 Quartz 30

2.3 The calcination reaction 31

2.4 Time-Temperature-Transformation Diagram 40

2.5 The effect of impurities on colour after calcination 41

2.5.1 Iron 41

2.5.2 Organic materials 44

2.6 The effect of particle size on calcination 45

3 METHODS AND MATERIALS 48

3.1 Calcination 48
3.1.1 Tracer experiment 48
3.1.2 Laboratory calcinations to replicate multiple hearth kiln conditions 50
3.1.3 Thermocouple experiments 51

3.2 Sample Analysis 53
3.2.1 Colour 53
3.2.2 Soluble Aluminium 59
3.2.3 Nitrogen Determination 62
3.2.4 Carbon Determination 64
3.2.5 Particle size testing (Sedigraph) 65
3.2.6 Particle size testing (Sieve analysis) 68
3.2.7 X Ray Fluorescence 70
3.2.8 X Ray Diffraction 71
3.2.9 Thermal Analysis 73
3.2.10 Scanning Electron Microscopy 75
3.2.11 Surface Area Analysis 77
3.2.12 Freeman Rheometer 78
3.2.13 Oil Absorption 79

3.3 Production samples used 80
3.3.1 Source of samples 80
3.3.2 Beneficiation of samples in production 83

3.4 Laboratory Clay Treatments 89
3.4.1 Wet Blending 89
3.4.2 Dry Blending 90
3.4.3 Reductive Bleaching 90

3.5 Creating Various Feed Forms 91
3.5.1 Creating the different particle sizes 91
3.5.2 Milled Feed Preparation 93
3.5.3 Spray Dried Feed 93
3.5.4 Lump Feed 95
3.5.5 Prill Feed 95
3.5.6 Granulation 97

3.6 Regression Analysis methods 98

3.6.1 Single factor linear regression analysis 100
3.6.2 Multiple linear regression analysis 101

4 HERRESCHOFF KILN 103

4.1 Introduction 103

4.2 Industrial calciner configuration and operation 105

4.3 Investigating the residence time in a Herreschoff kiln 107
4.3.1 Titania tracer experiments 109
4.3.2 Talc tracer experiments 112

4.4 How to replicate a Herreschoff kiln under laboratory conditions 116
4.4.1 The use of reference samples 119

4.5 Conclusions 120

5 ARTIFICIAL CHEMISTRY 122

5.1 Introduction 122

5.2 The difference between Brazilian and Devon kaolin 123

5.3 Blending Ancillary Minerals with a Brazilian kaolin 132
5.3.1 Blending with Brazilian muscovite and Feldspar 132
5.3.2 Blending with Brazilian muscovite and Feldspar individually 135
5.3.3 Blending with different micas 141

5.4 Blending different kaolins 146

5.5 Western Area Herreschoff Feed with added fluxes 150

5.6 Conclusions 157

6 NATURAL CHEMISTRY 159

6.1 Introduction 159

6.2 The effect of beneficiation on the properties of hydrous kaolin 160

6.3 The effect of beneficiation on the properties of calcined kaolin 164

6.4 Expanding the data set to other production routes 169

6.5 Single Factor Trend Analysis 172
6.5.1 Brightness 172
6.5.2 Soluble Aluminium 173
6.5.3 Particle size 177
6.6 Multiple Linear Regression 180
6.6.1 Brightness 181
6.6.2 Soluble aluminium 187
6.6.3 Particle size 192
6.6.4 Testing the models 192
6.6.5 Difficulties with the models 194
6.7 The effect of bleaching on hydrous production samples 195
6.8 The effect of bleaching on calcined samples 198
6.9 Conclusions 201
7 THE EFFECT OF HEATING/COOLING RATE ON THE CALCINED PRODUCT 204
7.1 Introduction 204
7.2 Observed effects of different calcination methods 205
7.3 The use of thermocouples 210
7.4 Investigating the different methods of calcination using tall circular crucibles and thermocouples 213
7.4.1 Height in the kiln 221
7.4.2 Material of crucible construction 223
7.4.3 Heat gradient 224
7.4.4 The effect of conduction from the walls of the crucible 227
7.5 Investigating the method of calcination with tray crucibles and thermocouples 230
7.5.1 With support base in place 231
7.5.2 Without support base in place 235
7.6 Conclusions 241
8 PARTICLE SIZE AND MORPHOLOGY 242

8.1 Introduction 242

8.2 The effect of particle size on calcination 243

8.2.1 Particle size 245

8.2.2 Soluble Aluminium 250

8.2.3 Brightness 254

8.3 Heat transfer through different feed forms 258

8.4 The effect of particle morphology 266

8.5 Conclusions 278

9 CONCLUSIONS AND FURTHER WORK 280

9.1 Conclusions 280

9.2 Further Work 287

10 APPENDIX A 289

11 APPENDIX B 295

12 APPENDIX C 307

13 APPENDIX D 310

13.1 Determining the dominant mechanism of heat transfer in the kiln 310

13.1.1 An analytical model 311

13.1.2 Numerical model 313

14 REFERENCES 321

Table of Figures

Figure 1-1: A pie chart showing the distribution of sales by Supplier by volume in 2002. Suppliers described as 'Other' are domestic market suppliers, not selling into the worldwide market [10] 7
Figure 1-2: Distribution of identified Competitor Sales in 2002 by Country by volume [10] 8
Figure 1-3: Distribution of Imerys sales in 2002 by segment by volume [10] 9
Figure 1-4: Estimated distribution of competitor sales in 2002 by segment by volume [10] 9
Figure 2-1: Clay deposits in Cornwall and Devon [17] 19
Figure 2-2: Sheet structure of kaolinite 23
Figure 2-3: Silica Tetrahedra group 24
Figure 2-4: Octahedral alumina group 25
Figure 2-5: Structure of kaolinite 26
Figure 2-6: Schematic representation of the stacking arrangements for the octahedral sheets in kaolinite, dickite and nacrite [12] 27
Figure 2-7: Structure of muscovite [3] 29
Figure 2-8: Progression of the calcination physico-chemical reaction and transformations with temperature for kaolin and associated mineral species [3, 6, 8, 24-27] 32
Figure 2-9: Simultaneous Thermal Analysis of a Cornish kaolin. The two curves indicate the two thermal analyses: The black curve is a Differential Scanning Calorimetry curve, where an upwards peak indicates an endothermic reaction and a downwards peak shows an exothermic reaction. The grey line is a Thermogravimetric Analysis plot indicating the loss in weight as the reaction progresses 34
Figure 2-10: Graph showing transformations that occur, as kaolin is heated [24] 41
Figure 3-1: Arrangement of thermocouples in the crucible in order to investigate the rate of heat penetration into the crucible and its effect on the properties of the calcined product. 52
Figure 3-2: Thermocouple rig for fused silica tray crucibles 53
Figure 3-3: Yxy chromaticities in the CIE colour space [43] 55
Figure 3-4: L*a*b* colour space [43] 57
Figure 3-5: Schematic diagram of an inductively coupled plasma torch as used in a Thermo Electron Iris-AP Emission Spectrometer (TJA Solutions, Winsford, UK) 60
Figure 3-6: Particle size analysis using sedimentation [52] 66
Figure 3-7: Sieve Analysis 69

Figure 3-8: Location of Brazilian, French and Georgian deposits 81
Figure 3-9: Location of pits in Cornwall 82
Figure 3-10: Sectional view of a Centriquip 550C (Ashbrook Simon-Hartley, Clay Cross, UK) [66] 84
Figure 3-11: Carpco 5T/460 (Carpco SMS Ltd, Slough, UK) [66] 86
Figure 3-12: Stirred Media Mill Set Up 92
Figure 3-13: Mobile Minor spray drier with a rotary atomiser (GEA Process Engineering Inc, Maryland, US) 94
Figure 3-14: Laboratory-scale pug (Imerys Minerals Ltd, Par, UK) 96
Figure 3-15: Eirich mixer (Maschinenfabrik Gustav Eirich GmbH & Co. KG, Hardheim, Germany) with the mixing blades and bowl visible. 97
Figure 4-1: Diagrammatic representation of a multiple hearth calciner with eight hearths, showing an estimated temperature profile 106
Figure 4-2: Variation of the titania, TiO2, content of the calcined product sample during the period immediately following the titania tracer dosing addition 109
Figure 4-3: The change in talc content (inferred by MgO content) of the calcine product during the talc tracer dosing experiment 113
Figure 4-4: How the soluble aluminium content (which is linked to the reactivity) of the calcined kaolin is affected by exposure to a temperature of 1050 °C for varying duration 114
Figure 4-5: How the brightness of the calcined kaolin is affected by exposure to a temperature of 1050 °C for varying duration 115
Figure 4-6: The soluble aluminium content of Milled HF batch calcined at 1050 °C for varying durations 118
Figure 5-1: The relationship between temperature and brightness for Milled HF and Brazil 125
Figure 5-2: The effect of calcination temperature on the brightness of Brazil that has been soaked in Lee Moor process water 127
Figure 5-3: The relationship between temperature and percentage of soluble aluminium for Milled HF and Brazil 128
Figure 5-4: Simultaneous Thermal Analysis for Brazil kaolin where the blue line is a Differential Scanning Calorimetry plot (DSC) and the green line a Thermogravimetric Analysis 131
Figure 5-5: Simultaneous Thermal Analysis for Milled HF where the blue line is a Differential Scanning Calorimetry plot (DSC) and the green line a Thermogravimetric Analysis 131

Figure 5-6: The brightness of a Created Herreschoff Feed, Brazil and Milled HF when calcined at different temperatures. 134
Figure 5-7: The soluble aluminium level of a Created Herreschoff Feed, Brazil and Milled HF when calcined at different temperatures 134
Figure 5-8: The brightness of Brazil blended separately muscovite and feldspar when calcined at different temperatures compared with pure Brazil and Milled HF 137
Figure 5-9: The soluble aluminium levels of Brazil blended separately with Brazilian muscovite and feldspar when calcined at different temperatures compared with pure Brazil and Milled HF 138
Figure 5-10: The soluble aluminium levels of Brazilian muscovite and feldspar when calcined individually at different temperatures 139
Figure 5-11: The brightness of Brazil blended with different micas when calcined at different temperatures compared with pure Brazil and Milled HF 144
Figure 5-12: The soluble aluminium levels of Brazil blended with different micas when calcined at different temperatures compared with pure Brazil and Milled HF 144
Figure 5-13: The brightness of the Wheal Martyn Magnet Feed and Product (WM MGF and WM MGP)alongside the blend created from the mixing of magnet reject and magnet product samples (WM MGP and MGP), when calcined at different temperatures ... 148
Figure 5-14: The brightness of the calcined product with regards to temperature for all blends investigated 154
Figure 5-15: The effect of temperature on the brightness of WA HF and Milled HF 155
Figure 5-16: The soluble aluminium content of calcined product with regards to temperature 156
Figure 6-1: Brightness of Wheal Martyn Production Samples when calcined at 500, 700, 950 and 1050 °C compared with Milled HF when calcined at the same temperatures ... 165
Figure 6-2: The soluble aluminium content of Wheal Martyn Production Samples when calcined at 500, 700, 950 and 1050 °C 167
Figure 6-3: Brightness of the 1050 °C calcination for all four different production routes: Georgia, Lee Moor, Wheal Martyn and Blackpool 171
Figure 6-4: Soluble aluminium content of production samples when calcined at 950 °C and the weight of the hydrous sample used in the calcination 175
Figure 6-5: Soluble aluminium content of production samples when calcined at 1050 °C and the weight of the hydrous sample used in the calcination 176

Figure 6-6: Particle size of the production samples after being calcined at 1050 °C compared with the particle size of the hydrous feed the ringed samples are Lee Moor, second magnet run product and bleached product which skew the trend.....178
Figure 6-7: The particle size of the production samples after being calcined at 1050 °C compared with the kaolinite content of the hydrous feed.....179
Figure 6-8: Q-Q plot for the brightness of production samples after calcination at 500 °C related to the Aluminium, Kaolinite, Potassium, Feldspar and Iron content along with LOI and Hydrous Brightness as detailed in Equation 6-1.....182
Figure 6-9: Q-Q plot for the brightness of production samples after calcination at 500 °C related to the Aluminium, Kaolinite, Potassium, Feldspar and Iron content along with LOI and Hydrous Brightness as described in Equation 6-2.....183
Figure 6-10: Q-Q plot for the brightness of production samples after calcination at 950 °C, related to the aluminium, silica, iron and mica content as well as the hydrous yellowness, as detailed in Equation 6-3.....185
Figure 6-11: Q-Q plot for the brightness of production samples after calcination at 1050 °C, related to the aluminium, silica, kaolinite and mica content along with the hydrous brightness, as detailed in Equation 6-4.....186
Figure 6-12: Q-Q plot for the soluble aluminium content of the 950 °C calcination related to the Potassium and Mineraliser content, the hydrous brightness and the D30 and D50 values of the particle size distribution as detailed in Equation 6-5.....188
Figure 6-13: Q-Q plot for the soluble aluminium content of the 1050 °C calcination related to the hydrous brightness and the aluminium content as shown in Equation 6-7. 190
Figure 6-14: Q-Q plot for the soluble aluminium content of the 1050 °C calcination, with bleached Blackpool sample removed, related to the hydrous brightness and the aluminium content as shown in Equation 6-7.....191
Figure 6-15: The brightness of Wheal Martyn production samples when bleached at four different rates; 1.5, 3, 4.5 and 6 kg t^{-1} using sodium dithionite.....196
Figure 6-16: Effect of reductive bleaching with different quantities of sodium dithionite on the iron content of the kaolin.....197
Figure 6-17: Effect of iron content on the brightness of the hydrous kaolin.....198
Figure 6-18: The effect of bleaching on the brightness of the Wheal Martyn production samples after calcining at 1050 °C for 30 minutes. 199
Figure 7-1: Division of calcined kaolin for soluble aluminium testing.....205

Figure 7-2: The amount of soluble aluminium found in sections of kaolin calcined under different conditions. Dishes were segregated into six sections and then samples were taken from the top and bottom of each section and submitted for testing. 207
Figure 7-3: FC Feed calcined using the soak method at 1050 °C for 60, 30 and 15 minutes and at 1000 °C for 30, 20 and 15 minutes. Results shown are Brightness/soluble aluminium quantity (%/wt.%).....211
Figure 7-4: Milled Residue calcined at 1000 °C for 20 minutes using four different methods of calcination: soak, batch, soak/batch and batch/soak. Results are shown as Brightness / amount of soluble aluminium (% / wt.%) 213
Figure 7-5: Residue Milled soak calcined at 1000 °C for 20 minutes thermocouple data....214
Figure 7-6: Residue Milled batch calcined at 1000 °C for 20 minutes thermocouple data...216
Figure 7-7: Residue Milled soak/batch calcined at 1000 °C for 20 minutes thermocouple data 218
Figure 7-8: Residue Milled batch/soak calcined at 1000 °C for 20 minutes thermocouple data 219
Figure 7-9: Brightness and soluble aluminium data for FC Feed calcined using the soak method at 1000 °C for 30 and 15 minutes in circular crucibles, raised trays and standard level trays. Results are displayed as Brightness/amount of soluble aluminium (% / wt.%).....222
Figure 7-10: Brightness and soluble aluminium data for FC Feed calcined using the soak method at 1050 °C for 15 minutes in circular crucible, part-filled circular crucible and standard level tray. Results are displayed as Brightness/amount of soluble aluminium (% / wt.%).....223
Figure 7-11: Brightness and soluble aluminium data for FC Feed calcined using the soak and batch methods at 1050 °C for 15 minutes in a circular crucible. Results are displayed as brightness/amount of soluble aluminium (% / wt.%).....225
Figure 7-12: Photographs of sections through the crucible third layer (a), fourth layer (b) and the bottom layer (c). The ring of calcined kaolin around the outside of the crucible can be seen and is highlighted with a red dotted line in image (a). 226
Figure 7-13: The appearance of calcined and uncalcined kaolin in a circular crucible calcined at 1050 C for 15 minutes using the batch method.....226
Figure 7-14: FC Feed soak calcined at 1050 °C for 30 minutes with insulation in place thermocouple data.....227

Figure 7-15: Brightness and soluble aluminium data for FC Feed calcined using the soak and batch methods at 1050 °C for 15 minutes in a circular crucible. Results are displayed as brightness/amount of soluble aluminium (% / wt.%) 228
Figure 7-16: FC Feed batch calcined at 1050 °C for 30 minutes with insulation in place thermocouple data 229
Figure 7-17: Location of the two crucible based thermocouples along with sample division markings 230
Figure 7-18: Soluble aluminium results for FC Feed calcined at 1050 °C for 30 minutes in tray crucibles with full thermocouple rig, using the soak and batch calcination methods 232
Figure 7-19: FC Feed soak calcined at 1050 °C for 30 minutes thermocouple data, tray crucibles 233
Figure 7-20: FC Feed batch calcined at 1050 °C for 30 minutes thermocouple data, tray crucibles, thermocouple support base in place 234
Figure 7-21: Soluble aluminium results for Milled HF calcined at 1050 °C for 30 minutes in tray crucibles with only the thermocouple stand, resting on the fused silica base, using the soak and batch calcination methods. 235
Figure 7-22: Milled HF soak calcined at 1050 °C for 30 minutes thermocouple data, tray crucibles, no base to thermocouple support 237
Figure 7-23: Milled HF batch calcined at 1050 °C for 30 minutes thermocouple data, tray crucibles, no base to thermocouple support 238
Figure 7-24: Diagram to show the path of radiation inside the furnace without the thermocouple support base present 239
Figure 7-25: Diagram to show the path of radiation inside the furnace with the thermocouple support base present 240
Figure 8-1: The effect of temperature on the particle size of the calcined product of different feed forms with an intrinsic particle size of 40 wt.% less than 2 microns. 246
Figure 8-2: The effect of temperature on the particle size (wt.% less than 2 microns) of the calcined product of different feed forms created from the ultrafine material 247
Figure 8-3: The effect of temperature on the particle size (wt.% greater than 10 μm) of the calcined product of different feed forms created from the ultrafine material 248
Figure 8-4: The relationship between calcined particle size and hydrous bulk density for coarse and ultrafine Residue feed forms calcined at 500, 700, 950 and 1050 °C ... 249

Figure 8-5: The relationship between the temperature and the amount of soluble aluminium obtainable from the calcined product for Residue feed forms made from the coarse material 250
Figure 8-6: The relationship between the temperature and the amount of soluble aluminium obtainable from the calcined product for ultrafine Residue feed forms 252
Figure 8-7: The relationship between the soluble aluminium content of the calcined product and the hydrous brightness for four different calcination temperatures 253
Figure 8-8: The effect of temperature on the brightness of the calcined product of different feed forms created from coarse Residue 254
Figure 8-9: The effect of temperature on the brightness of the calcined product of different feed forms with an intrinsic particle size of 90 wt.% less than 2 micron..... 255
Figure 8-10: The effect of calcined particle size on the calcined brightness for coarse and ultrafine kaolins..... 256
Figure 8-11: The relationship between calcined brightness and hydrous bulk density for ultrafine and coarse feed forms 257
Figure 8-12: The relationship between hydrous brightness and calcined brightness size for all feed forms calcined at 500, 700, 950 and 1050 °C 258
Figure 8-13: Thermocouple data for Residue Milled Powder with an intrinsic particle size of 90 wt.% less than 2 µm when soak calcined at 1000 °C with 20 minutes at high temperature 259
Figure 8-14: Brightness and soluble aluminium data for three ultrafine Residue feed forms; Milled Powder,9 mm prills and Granules, calcined at 1000 °C for 20 minutes in circular crucibles, with thermocouple support in place 261
Figure 8-15: Thermocouple data for Residue 9 mm prills with a particle size of 90 wt.% less than 2 µm when soak calcined at 1000 °C with 20 minutes at high temperature..... 263
Figure 8-16: Thermocouple data for Residue granules with a particle size of 90 wt.% less than 2 µm when soak calcined at 1000 °C with 20 minutes at high temperature..... 264
Figure 8-17: SEM images at a magnification value of x20,000 showing hydrous kaolins A) Platy, B) Beauvoir, C) Blackpool LR, D) Blackpool FR and E) SC Residues..... 269
Figure 8-18: SEM images at a magnification value of x2000 showing kaolins calcined at 1050 °C for 30 minutes A) Platy, B) Beauvoir, C) Blackpool LR, D) Blackpool FR and E) SC Residues (shown at a magnification of x500)..... 271
Figure 8-19: The relationship between the quantity of fines in the hydrous feed (wt.% < 0.25 µm) and the change in particle size (wt.% less than 2 µm) as a the result of calcination at 1050 °C for 30 minutes, batch method 273

Figure 8-20: The relationship between the change in particle size (wt.% less than 2 microns) and the change in surface area as the result of calcination at 1050 °C for 30 minutes, batch method.....274
Figure 8-21: The oil absorption values for hydrous feeds and products after 1050 °C calcination for 30 minutes, batch method.....275
Figure 8-22: Theories of particle fusion, A) Face to face and B) House of cards 275
Figure 8-23: The oil absorption and surface area values for hydrous feeds and calcined products after 1050 °C calcination for 30 minutes, batch method 277
Figure 10-1: Front View of thermocouple support for use with tall circular crucible. Blue circles are 5 mm in diameter and are drilled completely through the support. 289
Figure 10-2: Side View of thermocouple support for use with tall circular crucible. Shaded areas should be cut to 2.5 cm deep. 290
Figure 10-3: Top View of thermocouple support for use with tall circular crucible. Shaded areas should be cut to 2.5 cm deep. 291
Figure 10-4: Front View of thermocouple support for use with flat rectangular crucibles. Blue circles are 5 mm in diameter and are drilled completely through the support. 292
Figure 10-5: Side View of thermocouple support for use with flat rectangular crucibles.....293
Figure 10-6: Top View of thermocouple support for use with flat rectangular crucibles. Shaded areas should be cut to 2.5 cm deep. 294
Figure 11-1: Dorr Oliver Operation in Production.....295
Figure 11-2: Bleaching Operation in Production 296
Figure 11-3: Milled HF Production Route 297
Figure 11-4: Brazil Production Route.....298
Figure 11-5: Wheal Martyn Production Route. Samples were taken at points marked with a blue star for Chapter 4: Artificial Chemistry and at points marked with a red star for Chapter 5: Natural Chemistry 299
Figure 11-6: Blackpool Production Route. Samples were taken at points marked with a red star for Chapter 5: Natural Chemistry 300
Figure 11-7: Lee Moor Production Route. Samples were taken at points marked with a red star for Chapter 5: Natural Chemistry 301
Figure 11-8: Georgia Production Route. Samples were taken at points marked with a red star for Chapter 5: Natural Chemistry 302
Figure 11-9: Beauvoir Production Route 303
Figure 11-10: Blackpool LR and Blackpool FR Production Routes.....304
Figure 11-11: Scalping Residues Production Route 305

Figure 11-12: Double Ground Clay Production Route 306
Figure 13-1: Illustration of the problem 310
Figure 13-2: Graph to show heat transfer into a fused silica dish 317
Figure 13-3: Graph to show the heat transfer into a fused silica dish when radiation is considered 319
Figure 13-4: The impact of radiation on the time taken for the fused silica dish to reach high temperature 320

Index of Tables

Table 1-1: List of Calcined kaolins produced by the Performance and Filtration minerals business group 5
Table 3-1: The percentage solids of the slurry for the three different kaolins used with the spray drier 93
Table 3-2: The amount of water added to the system for the three different kaolins when the Eirich mixer was in operation 98
Table 4-1: Showing the X-ray fluorescence results for calcined kaolin and talc (with results presented as percentage by weight of the elemental oxides) 108
Table 4-2: Showing MgO content of various calcined talc/kaolin blends determined by X-ray fluorescence 108
Table 4-3: Base Flow Energy, Stability Index and Flow Rate Index and Mass data for Talc, Calcined Kaolin and Titanium 111
Table 4-4: Colour, Particle Size and Soluble Aluminium values for Herreschoff Kiln Feed, Outlet and Milled Product 117
Table 4-5: Table showing the brightness and soluble aluminium content of Milled HF after calcining at 1050 °C for 30 minutes, using two different methods, batch and soak calcination. 117
Table 4-6: The range of values considered to constitute a normal reaction for Milled HF when calcined using the batch method of calcination at 1050 °C for 30 minutes 119
Table 4-7: The range of values considered to constitute a normal reaction for FC Feed when calcined using the batch method of calcination at 1050 °C for 30 minutes 120
Table 5-1: XRD results for Brazil and Milled HF 123
Table 5-2: XRF results and colour data for Brazil and Milled HF 124
Table 5-3: The nitrogen and carbon contamination of Brazil and Milled HF 126
Table 5-4: The amount of Brazil, feldspar and Brazilian muscovite required to make Created HF 132
Table 5-5: The XRF results and colour data for Brazilian muscovite, feldspar and the Created HF 133
Table 5-6: The ratio of mineral required to make both the Brazil/feldspar and Brazil/Brazilian muscovite blend 135
Table 5-7: The XRF results and colour data for Brazil blended with both muscovite and feldspar 136

Table 5-8: The maximum amount of aluminium obtainable from different minerals, calculated using the gravimetric factors calculated by Rudolf Loebel, the amount obtained as a result of a calcination at 950 °C for 30 minutes, batch method and the calculated values for the blends using experimental data 140
Table 5-9: XRF results for Chinese muscovite, phlogopite, Norwegian biotite and Lee Moor mica..... 141
Table 5-10: Ratio of minerals required to make each of the different Brazil/mica blends 142
Table 5-11: XRF results for Brazil blended with muscovite, phlogopite, biotite and mica found from the Lee Moor pit..... 143
Table 5-12: The XRD and XRF data and colour information for Wheal Martyn (WM) magnet samples, comprising Feed, Product and Rejects. 146
Table 5-13: The ratio of magnet reject and magnet product necessary to make the magnet blend 147
Table 5-14: The XRF data and colour information for the Wheal Martyn (WM) magnet blend 148
Table 5-15: XRD results for Milled HF and WA HF..... 151
Table 5-16: XRF Analysis of Western Area HF, standard HF and nepheline syenite..... 152
Table 5-17: The amount of nepheline syenite, sodium carbonate and Western Area (WA) HF needed to make the respective blends to raise the amount of fluxing agent content to 1.5, 2.0 and 2.4 wt.%..... 153
Table 6-1: XRD results for Milled HF Wheal Martyn (WM) Bleached sample..... 160
Table 6-2: XRD and XRF data for Wheal Martyn Production Samples 161
Table 6-3: The samples that were obtained from each of the Georgia, Lee Moor and Blackpool production route 169
Table 6-4: The R^2 value for six different factors and the brightness of the 1050 °C calcination product for all four production routes and the three production routes, omitting Georgia 170
Table 6-5: The R^2 value for a number of different factors in relation to the amount of soluble aluminium found in the product of Devon and Cornish kaolins being calcined at 950 and 1050 °C 174
Table 6-6: Colour, Particles size, XRD and XRF data for hydrous Littlejohns Magnet Samples, obtained from production and reductively bleached under laboratory conditions 193
Table 6-7: The predicted and laboratory product brightness and soluble aluminium content results for the batch calcination at 1050 °C for 30 minutes (Herreschoff replicating

conditions) of Littlejohns magnet feed, first magnet run product and second magnet run product the models used are shown in Equation 6-4 and Equation 6-6.....194
Table 7-1: The brightness and soluble aluminium content of Mulled HF after calcining at 1050 °C for 30 minutes, using two different methods, batch and soak calcination. .205
Table 7-2: Table showing XRD results for Milled HF calcined using the Batch/Soak method of calcination 209
Table 8-1: Particle size distributions for Milled Powder feed forms made from Residue obtained through sedigraph analysis 244
Table 8-2: Particle size distributions for Lump and Granular feed forms made from Residue 40, 73 and 90 wt.% less than 2 microns obtained through sieve analysis 245
Table 8-3: Summary of thermocouple data for ultrafine Residue milled powder when soak calcined at 1000 °C with 20 minutes at high temperature 260
Table 8-4: Summary of thermocouple data for ultrafine Residue 9 mm prills when soak calcined at 1000 °C with 20 minutes at high temperature 262
Table 8-5: Summary of thermocouple data for ultrafine Residue granules when soak calcined at 1000 °C with 20 minutes at high temperature 265
Table 8-6: XRD, Brightness and Particle size, Surface Area and Oil Absorption results for hydrous Platy, Beauvoir, Blackpool LR, Blackpool FR and SC Residues.....267
Table 8-7: Brightness and Particle size results for Double Ground, Beauvoir, Blackpool LR, Blackpool FR and SC Residues when calcined at 1050 °C for 30 minutes 270

Table of Equations

Equation 2-1: The kaolinisation of feldspar 13
Equation 2-2: Metakaolin reaction [6] 34
Equation 2-3: Spinel phase reaction 36
Equation 3-1: Determining XYZ colour values [43] 54
Equation 3-2: Determination of L*a*b* from X, Y and Z space [43]. 56
Equation 3-3: Determining the soluble aluminium content from the ICP reading of ppm 62
Equation 3-4:Determination of Nitrogen content in a sample using the Kjeldahl method of nitrogen testing 64
Equation 3-5: Stokes' law for a spherical particle, where D is the diameter of the spherical particle, v its equilibrium sedimentation velocity and K is calculated using Equation 3-6 65
Equation 3-6: Determination of K, for use in Equation 3-5, where ρ is the particle density, η the fluid viscosity, ρ_0 is the fluid density and g is the acceleration of gravity. 65
Equation 3-7: Determining the Coefficient of Determination (R^2) for a regression model where the sum of squared errors is also known as the residual sum of squares and the total sum of squares is proportional to the sample variance. 100
Equation 6-1: Determining the brightness of the product from the 500 °C calcination where Al = Aluminium content, Ka = Kaolinite content, K = Potassium content, F= Feldspar content, Fe = Iron content, LOI = Loss on Ignition and HB = Hydrous Brightness ... 181
Equation 6-2: Determining the brightness of the product of the 700 °C calcination, where K = Potassium content, F= Feldspar content, Fe = Iron content, LOI = Loss on Ignition and HY = Hydrous Yellowness 183
Equation 6-3: Determining the brightness of the product from the 950 °C calcination where Al = Aluminium content, Si = Silica content, Fe = Iron content, M = Mica content and HY = Hydrous Yellowness 184
Equation 6-4: Determining the brightness of the product from the 1050 °C calcination where Al = Aluminium content, Si = Silica content, Ka = kaolinite content, M = Mica content and HB = Hydrous Brightness 186
Equation 6-5: Determining the soluble aluminium content of the product from the 950 °C calcination where K = Potassium content, Min = Mineraliser content, D30 = d30 of particle size distribution of hydrous feed, D50 = d50 of particle size distribution of hydrous feed and HB = Hydrous Brightness 187

Equation 6-6: Determining the soluble aluminium content of the product from the 1050 °C calcination where Ka = Kaolinite content, Al = Aluminium content, Si = Silica content, F= Feldspar content, Fe = Iron content, M = Mica content, Min = Mineraliser content, se = wt.% of particles less than 2 µm in size and HB = Hydrous Brightness 189
Equation 6-7: Determining the soluble aluminium content of the product of the 1050 °C, where HB = Hydrous Brightness and Al = Aluminium content.....189
Equation 6-8: Determining the proportion of the hydrous sample less than 2 µm where L = LOI and Al = Aluminium content 194
Equation 6-9: Determining the hydrous brightness where Ka = Kaolinite content, Al = Aluminium content, Si = Silica content, K = Potassium content, Fe = Iron content, M = Mica content and Min = Mineraliser content.....195
Equation 13-1: Determining the heat transfer from air in the furnace to the crucible where m = mass in the dish (kg), Cp = specific heat capacity of the dish (kJ kg-1 K-1), T_d = temperature of the dish (K), h = heat transfer coefficient (W m-2 K-1), A = surface area of the dish (m2), T_f = temperature of the furnace (K), t = time (s) [92].....311
Equation 13-2: Rate of heating, rearranged from Equation 13-1, where m = mass in the dish (kg), Cp = specific heat capacity of the dish (kJ kg-1 K-1), T_d = temperature of the dish (K), h = heat transfer coefficient (W m^{-2} K-1), A = surface area of the dish (m^2), T_f = temperature of the furnace (K), t = time (s).....312
Equation 13-3: Integration of Equation 13-2, where m = mass in the dish (kg), Cp = specific heat capacity of the dish (kJ kg-1 K-1), T_d = temperature of the dish (K), h = heat transfer coefficient (W m-2 K-1), A = surface area of the dish (m^2), T_f = temperature of the furnace (K), t = time (s).....312
Equation 13-4: Correlation of Nusselt, Prandtl and Grashof numbers in a natural convection system. This correlation is valid for 10-4 ≤ Gr Pr ≥ 4x1014 and 0.0022 ≤ Pr ≥ 7640, where Nu = Nusselt number, Pr = Prandtl number and Gr = Grashof number [94]..314
Equation 13-5: Determining the density of air, where ρ = fluid density (kg m-3), P = standard air pressure, R = specific gas constant (kJ kmol-1 K-1), T = Temperature (K), RMM = Relative Molecular Mass [92].....315
Equation 13-6: Determining the viscosity of air, where µ0 = reference viscosity (cP), T = Temperature (K), S = Sutherland's constant = 120, T_{fs} = temperature of furnace (° R), T_{d0} = initial temperature of the dish (K) [92].....315
Equation 13-7: Determining the radiative heat transfer coefficient, where e = emissivity of grey body, σ = Stefan-Boltzman constant, T_d = temperature of the dish (K), T_f = temperature of the furnace (K) [89].....318

1 Introduction

1.1 The company

Established in 1880, Imerys Minerals Ltd has its origin in mining and metallurgy, with its core business in the extraction and processing of non-ferrous metals, it remained this way for almost a century. In the 1970s the company began to expand, entering the clay roof tile market, steel production and metal processing industry for the first time through the acquirement of other companies. After the takeover of Damrec (France), which specialised in refractories and ceramics in 1985, the company's business was structured around three sectors: Building Materials, Industrial Materials and Metals Processing [1].

From 1990 onwards, the company focused its development on Industrial Minerals and implemented an ambitious acquisitions policy. Ten different firms were bought, allowing Imerys to establish strong positions in various fields; kaolin, calcium carbonate, graphite, refractories, ball clays, ceramic bodies and technical ceramics. Between 1994 and 1998, Imerys doubled in size and by 1998 the business was structured around two sectors, Minerals Processing and Metals Processing [1].

In 1999, a milestone was reached with the acquisition of English China Clays (EEC). Founded in 1919, the UK based company and one of the world's foremost specialists in industrial minerals, specifically white pigments, and helped the Imerys group through acquisition to become a global leader in this sector. Following this takeover,

the Group focussed exclusively on Minerals Processing, withdrawing from activities that no longer corresponded to its core business, divesting its Metals Processing activity [1].

Since 2000, various other acquisitions have strengthened the group's position as experts at turning industrial minerals into speciality products, with high added value for customers. As of 16th November 2009, the group has more than 260 industrial sites in 47 countries on 5 different continents.

The company is split into four Business Units:

- Minerals for Ceramics, Refractories, Abrasives and Foundry
- Performance and Filtration Minerals
- Pigments for Paper
- Materials and Monoliths

The Performance and Filtration Minerals division is organised into two activities: Performance Minerals and Minerals for Filtration. In January 2009, the group employed 3,157 people at 60 industrial sites in 18 countries and during 2008 contributed 15% (€527 million) to the company's sales, 53% of which was from performance minerals [1].

Performance minerals are mineral additives based on kaolins, ground and precipitated calcium carbonate, perlite, diatomaceous earth, mica, feldspar, and fine ball clays added to finished or intermediary products for better functionality and

processability, lowering total raw material cost. The Performance Minerals division provides customers with tailor-made solutions in a highly technical field. This development of partnerships with customers is essential within the value-added markets of performance minerals. The main applications include [1]:

- Paints and coatings
- Plastics and films
- Rubber
- Sealants and adhesives
- Industrial and consumer products

1.2 Product Description – Calcined Kaolins

Calcination, the process of heating a substance to a point below its melting (or fusing) point, causing a loss of water, is one of the most important ways of enhancing the properties, and value of kaolin. Calcination decreases the discoloration of the clay, enhancing brightness and whiteness, but can also increase the abrasive nature of the particles, which can cause some processing difficulties due to a degree of aggregation of the particles. The extent of these changes is dependent on the temperature and duration of calcination and any impurities in the clay. Consequently, different kaolins will produce different qualities of calcined clay [2].

When kaolinite, the principal mineral in kaolin, is calcined, it undergoes a series of five reactions [3]. The initial reaction, which generally occurs around 100 – 150 °C, involves all absorbed moisture being driven off [4, 5]. Between 400 and 600 °C the

kaolinite undergoes a dehydroxylation reaction, the removal of chemically bonded water, to produce metakaolin, which also has a number of industrial applications, [6, 7].

The heating of kaolin above this temperature leads to the transformation of the metakaolin to the spinel phase by exothermic re-crystallisation. The exact reaction which takes place is subject to much debate and the only generally accepted theory is that a spinel-type phase forms along with some free silica although the type, its chemical formula and the mechanism of formation are all still under discussion. Above 1050 °C the defect-spinel begins to form hard crystals of mullite and at extremely high temperatures (above 1100 °C), cristobalite, a carcinogenic material which causes weaknesses in the refractory material, is formed [8].

There are three different methods of calcining kaolin: soak, soft and flash. Soak calcination involves exposing the kaolin, described as hydrous to high temperatures for a prolonged amount of time in order to guarantee the calcination is complete. The soft calcination method is similar, but it only exposes the clay to high temperatures for a limited amount of time in order to try and minimise the amount of abrasive particles formed. Flash calcination is different from the other two methods in that it involves a rapid temperature increase, usually to between 900 and 1000 °C within a fraction of a second, achieving a heating rate of 100,000 to 500,000 °C per second. The steam evolved from the kaolin cannot escape from the particles, causing the formation of sealed blisters, which are used to increase the opacity of paint thereby decreasing the amount needed in the formulation and costs for the manufacturer [9].

The calcination reaction may also be halted part way through, when temperatures of only 800 °C have been reached and the material is highly reactive. This material is termed metakaolin.

European Performance Minerals (EPM) produces a range of calcined kaolins; each geared for a different market segment. These are summarised in Table 1-1. EPM do not soak calcine any kaolins due to the markets they sell into, kaolins are soft, flash or part calcined.

Table 1-1: List of Calcined kaolins produced by the Performance and Filtration minerals business group

Name	Method of calcination	Use
Opacilite	Flash	Paint, Rubber and Films
Infilm	Soft with top cut adjustment	Antiblocking in films
Polarite	Soft and treated with silane	Insulation for wires and cables
Polestar 200P	Soft	Paint and Rubber
Polestar 200R	Soft	Insulation for Low to Medium voltage power cables
Polestar 501	Soft	Insulation for High voltage power cables
Metastar 501	Metakaolin	Cement and concrete
VLCC	Metakaolin	Ultramarine Blue pigments

Although Table 1-1 gives a general idea of the products Imerys sells, there are certain grades that are made to fulfil a customer's specific requirements. For example, there are up to 15 varieties of Polestar 200P that could be produced at any

one time. The products range in levels of reactivity (low to mid range soluble aluminium levels) and have different specifications for colour values, all to fit in with normal production. The general rule seems to be that if the value of the product is high enough then it will be produced.

1.2.1 Competitors

In 2002 the worldwide market for calcined kaolin was around 880 kT, of which Imerys had around a 27% share [10]. The market is divided fairly equally between Paper and Performance Minerals, but currently Imerys provide substantial material for the Paper market, which is currently under threat as calcined kaolins are being replaced by precipitated calcium carbonates (PCCs), also an Imerys product, as they are cheaper to produce.

Outside Europe, Imerys are relatively small players in regards to calcined kaolin for Performance Minerals; they have 25% of the world market, which decreases to 17.5% once European markets are accounted for. This difference arises because of the large amount of competitors based in North America compared to the rest of the world. The market there consumes more than twice the amount of calcined kaolin than the rest of the world put together and by citing production facilities near to customers, profit margins are maximised.

Figure 1-1 shows that Imerys have five main competitors in the world marketplace, Burgess, Engelhard, Huber, AGS/SOKA and Dorfner, of which the first three are based in America, AGS/SOKA and Dorfner are French and German respectively.

The strategy being implemented by American and European competitors are different. The high logistics costs of transporting calcined kaolin from America to Northern Europe and Asia mean that breaking into the European and Asian markets is difficult from purely US based facilities.

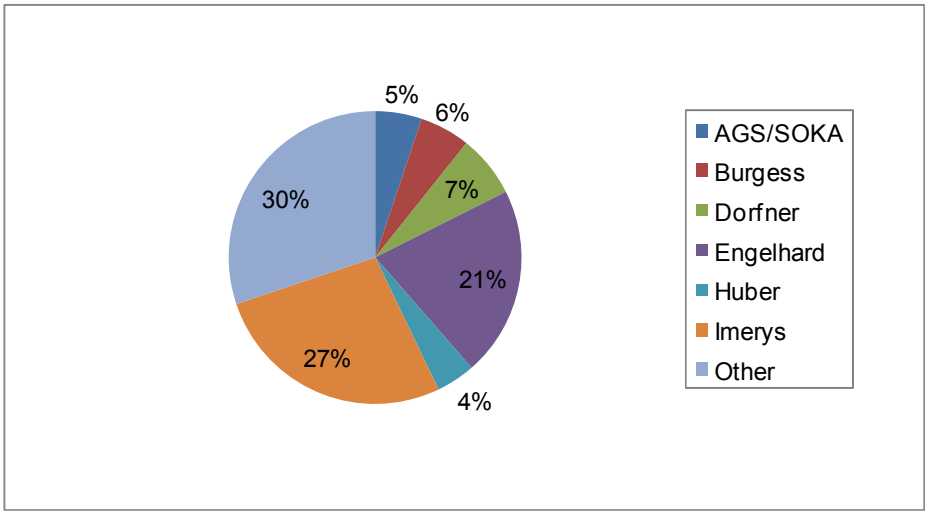

Figure 1-1: A pie chart showing the distribution of sales by Supplier by volume in 2002. Suppliers described as 'Other' are domestic market suppliers, not selling into the worldwide market [10]

Companies are instead likely to invest in local operations where they can expand production rather than export calcined kaolin or build new plants in a strategy termed glocalisation [11]. Imerys themselves are employing this tactic by buying calcining operations in Brazil, China and Hungary over the past couple of years. European companies, however, are seemingly concentrating on local accounts and markets, where they are already active and otherwise are only acting opportunistically.

From Figure 1-2 it can be seen that most of Imerys' competition is in Southern Europe. This is due to German-based Dorfner occupying most of the local market

and that the cost of transportation from the USA is much cheaper into Italy than anywhere else in Europe, allowing American firms to enter the marketplace.

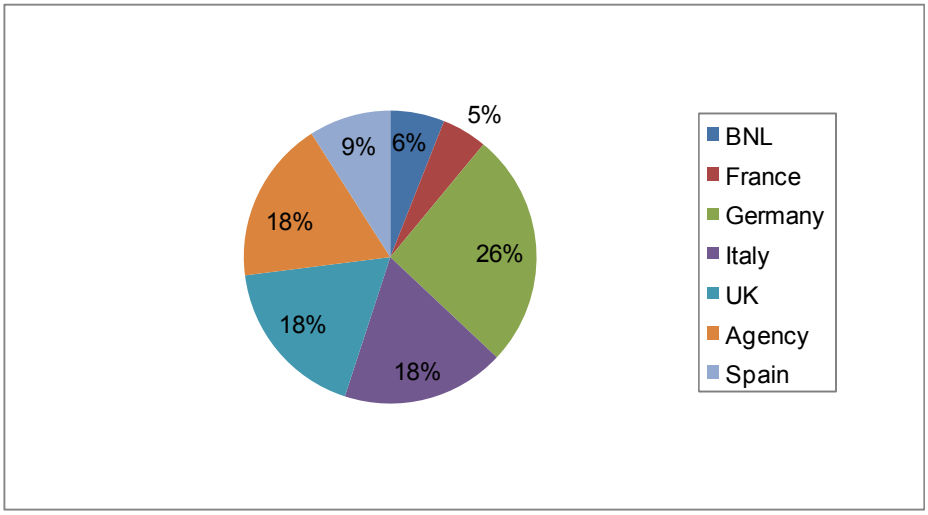

Figure 1-2: Distribution of identified Competitor Sales in 2002 by Country by volume [10]

Figures 1-3 and 1-4 show that the market areas for Imerys and their competitors are very similar. Paint and rubber sales, the traditional calcined kaolin markets, make up 87 % of Imerys' calcined kaolin sales and 78 % of their competitors, who have a higher percentage of sales into the sealants and adhesives market. Imerys only sell 3% by volume of their calcined kaolin into this sector, although it is an important area and very sensitive for many customers. Supply problems in the past have come close to shutting Coca-Cola production down worldwide.

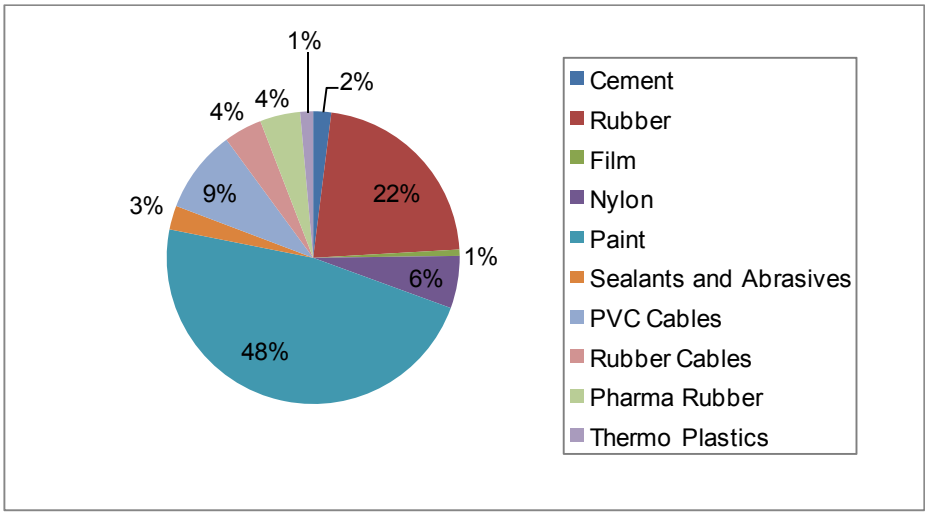

Figure 1-3: Distribution of Imerys sales in 2002 by segment by volume [10]

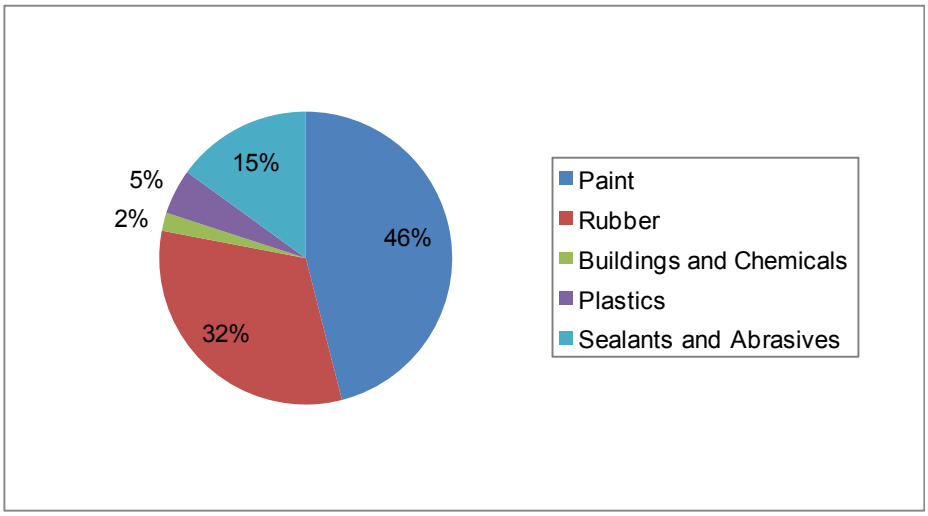

Figure 1-4: Estimated distribution of competitor sales in 2002 by segment by volume [10]

In recent years, Imerys have started to diversify into other areas of the market and currently obtain the greatest profit margin from the plastic film and nylon sectors, which competitors are currently not thought to be involved in. Pharmaceutical rubbers, such as those used to seal medicine bottles, which also have little

competitor involvement, have the smallest profit margin but provide a significant amount of local business for the calcining operations.

1.3 Statement of objectives

The overall aim of this thesis is to provide a better understanding of the principles of the kaolin calcination in order to enhance the efficiency, quality and sustainability of the Imerys calcining operations, and in particular, the soft calcination processes currently operated at the Lee Moor site in Devon.

This will be achieved through a series of laboratory scale experiments looking at the basic reaction conditions such as temperature and duration. The chemistry of kaolin will also be looked at, along with the feed form and the rate of heating of the clay. This work will help to develop an understanding of what is occurring when a kaolin is calcined.

1.4 Thesis Layout

Chapter 2 covers the possible theories of formation kaolin and how the different methods lead to variations in deposits. Also discussed is the structure of kaolinite and the other minerals that make up the kaolin matrix. This then leads to investigation of the calcination reaction and the effect of particle size and impurities such as iron and organic materials.

The different analytical methods to determine the chemical and physical properties of both the hydrous and calcined kaolins used throughout the project are detailed in Chapter 3. Also described are the methods used for the tracer experiments, laboratory clay treatments such as reductive bleaching and wet blending, and how to make various feed forms as well as the source of the different kaolins used throughout the investigations.

Chapter 4 concentrates on the industrial calciner configuration and operation and details the results from the residence time investigations carried out using titania and talc as tracer minerals. This information was then used as a basis in developing a method to replicate the kiln under laboratory conditions, which is also discussed.

In Chapter 5, a Brazilian (secondary deposit) and a Cornish (primary deposit) kaolin are investigated under different calcination conditions, varying temperature and duration. It is attempted to determine the cause for the differences in the product of the two kaolins by altering the chemistry of the Brazilian kaolin by blending it with different minerals including different micas and feldspar. This leads to an investigation with other kaolins including calcining blends of kaolin and fluxing agents and the investigation of blending samples from the magnet stage of operations and how the level of iron affects the calcined product.

Following on from Chapter 5, is Chapter 6 which more thoroughly investigates the natural variations in chemistry from different kaolin deposits and the changes that result in the calcined product. Samples were obtained from four different production

routes based in Cornwall, Devon and Georgia. The effect of beneficiation is determined on both the hydrous and calcined product. The product characteristics of the British kaolins will be analysed to determine the influencing factors on the brightness and reactivity of the product and to create predictive models. The effect of bleaching is then examined in more detail.

Chapter 7 investigates the effect of different calcination methods on the product using a series of thermocouples to examine the progression of heat through a tall, cylindrical crucible. The study will then expand to include the height of the sample in the kiln, the use of insulation around the crucible and the penetration of heat into the flat, rectangular crucibles that were used for all other experimentation as part of this project.

Chapter 8 examines the effect of particle size and morphology of the hydrous kaolin on the calcined product. A coarse kaolin is ground to produce a fine and an ultrafine feed. These three kaolins are then used to produce seven different feed forms: milled, spray dried, granules, 3 mm prills, 6 mm prills, 9 mm prills and lump. These are then calcined at different temperatures and using the rig developed for Chapter 7, the progression of heat throughout the crucible packed with different feeds is examined. In order to investigate the effect of the morphology of the particle, five very different kaolins will be chosen and calcined and the structure of the product and any differences examined.

Finally, in chapter 9 all the results are discussed and conclusions are presented.

2 Literature Review

2.1 Formation of kaolin – Kaolinisation

Kaolinite is the product of a chemical change, termed kaolinisation, which affects a precursor phase, commonly feldspar or muscovite. Some minerals present within the rock, such as quartz and tourmaline, may resist the kaolinisation process, whilst others, such as biotite, may decompose yielding contaminating products. In the case of the decomposition of biotite, or other unstable, iron-bearing silicates, the products include iron oxides and hydroxides, which discolour the, normally, white kaolin and so reduce its brightness value [12].

There are many different reactions that may have occurred as the rock was transformed into kaolin. In the basic reaction, sodium feldspar in the granite precursor is altered to kaolinite by the decomposition reaction shown in Equation 2-1.

$$2NaAlSi_3O_8 + H_2O + 2H^+ \rightarrow Al_2Si_2O_5(OH)_4 + 4SiO_2 + 2Na^+$$

Feldspar + Water → Kaolinite + Quartz

Equation 2-1: The kaolinisation of feldspar

The feldspar may also be converted into mica to a lesser or greater degree, depending on the environmental conditions and which reaction it favours, by a very similar pathway [13]. Under favourable conditions, mica and other materials in the granite are also sometimes converted to kaolinite.

The feldspar group consists of silicates of aluminium containing sodium, potassium, iron, calcium, or barium or combinations of these elements. The reaction shown above is that of sodium feldspar but the other types of feldspar are prone to transformation, most particularly potassium feldspar which has the same general formula and structure as sodium feldspar. When it is present, sodium feldspar is more readily kaolinised, but both are susceptible to the process [12].

The many different reactions that can occur mean that every deposit, given their unique geographic location, will have been exposed to a slightly different reaction scheme, resulting in noticeable variations in kaolinite quality around the world despite all the kaolinite deposits being created in similar ways. Determining the conditions under which the reactions take place represents a highly complex problem to geologists. There are two main methods of kaolinisation, hydrothermal and weathering alteration of the rock.

2.1.1 Hydrothermal Theory

The hydrothermal theory of formation is based on the idea that during the cooling of the granite, faults and fractures appeared which allowed solutions originating in the lower regions of the earth to permeate upwards and this started the kaolinisation process. In later periods, kaolinisation took place where these veins and faults allowed easier flow of conductive water, which was superheated by the heat produced from the radioactive decay of uranium into radon. The water was laden with chemicals and moved upwards from deep underground, continuing the alteration

of the feldspars in the granite, until it became trapped beneath a roof of impermeable rocks, at no great depth. This is known as the effect of the 'meteoric waters' [14].

The arguments in favour of the hydrothermal theory origin for china clay are listed below [14]:

- The great depth and form of the deposits, some are more than 200 m deep.
- The fact that unaltered rocks overlie kaolinised regions.
- The areas of most intense kaolinisation are around joints in the rock and veins of quartz.

In addition to the above points, extensive drilling by English China Clay Ltd (now Imerys) has shown that the typical kaolin body is funnel or trough-like in form, narrowing downwards. This feature, along with the fact that the granites in Cornwall are extensively mineralised with tin, copper and tungsten indicates hydrothermal activity was responsible for the formation of the deposits [15].

One style of kaolin occurrence, which is undoubtedly associated with hydrothermal activity, is solfatara, formed by the kaolinisation of acid volcanic rocks during the waning stages of volcanic activity. The original material may have been a volcanic glass and the kaolinised products include very fine grained silica minerals and alunite, ($KAl_3(SO_4)_2(OH)_6$) the formation of which reflects the presence of sulphur of volcanic origin [12]. Other deposits of china clay which are considered to have been formed via hydrothermal activity include those in China, Japan and Mexico [15].

2.1.2 Weathering

It has been known for a long time, that weathering of feldspathic rocks, especially in tropical climates, yields kaolin, releasing alkalis and silica. The weathering of granite rocks is thought to have happened during the Eocene period, approximately 50 million years ago. This period in time was characterised by a general increase in temperature on the Earth's surface to the point where most of the Earth was in tropical or sub-tropical conditions [16].

Because it is a chemical, rather than a physical weathering mechanism that is thought to occur to promote kaolinisation, one proposed mechanism is that of lateritic weathering, a form of weathering which only occurs in places where there is a definite division of the year into dry and wet seasons. During the wet season, the water soaks into the ground and changes some of the granite into kaolinite. When the dry season comes, the solution containing the by-products of the reaction will be drawn to the surface where it will evaporate, leaving some salts which would be washed away during the following wet season. This intensive extractive leaching removes most elements from the rock except aluminium and iron, which remain in the rock as hydrated oxides in the form of laterite and bauxite [16].

Weathering generally involves meteoric fluids at low temperatures (up to 40ºC) and generally occurs close to the surface. Weathering profiles depend on the topography, climatic factors and configuration of the unsaturated zone. Deep weathering may extend to depths in excess of 100 m [12].

The arguments in favour of weathering as a main method of china clay formation are as follows [14]:

- The low density and high porosity of the china clay matrix containing fragile, un-deformed kaolin stacks is incompatible with being formed under hydrothermal pressures as they would have been destroyed.
- The unlikelihood of kaolinite being stable under the conditions at which the hydrothermal action would take place. The upper temperature limit for the stability of kaolinite and its polymorphs is approximately 300ºC, though dickite, another kaolinite group mineral, replaces kaolin as the stable phase at temperatures of about 130ºC. Dickite is considered a good indicator of relatively high temperatures [12].

World-wide deposits which are considered to have been formed due to weathering include those in Australia, The Czech Republic, Germany, Indonesia and the Ukraine [14].

2.1.3 Combination

The deposits of china clay in the south-west of England and New Zealand do not exactly fit the ideal model for either hydrothermal or weathering formation. In these deposits, it is difficult to dissociate the effects of weathering from those of hydrothermal processes, because the product of high temperature hydrothermal processes are often affected subsequently by low temperature processes, including weathering [12].

In order to deal with the conflicting evidence, it has been theorised by several researchers that the best solution was to invoke a sequence of events, which involved both hydrothermal and weathering processes. This allows the hydrothermal phase to be seen as some form of 'softening up' process which renders the granite susceptible to a later phase of deep weathering, when the actual formation of the kaolinite took place [14].

2.1.4 Cornish clays

The geology of South-west England is dominated by the presence of a major composite Hercynian granite batholith, which extends throughout the counties of Devon and Cornwall as can be seen in Figure 2-1. China clay is produced from primary deposits within the granite, particularly from the St Austell pluton, which yields over 80% of kaolin production in the UK. Relatively minor amounts are produced from the Dartmoor granite, and other small deposits occur in the Land's End and Bodmin Moor granites [12]. The kaolinite content in the altered granite ranges between 10 and 20 percent in Cornwall [14].

These deposits are of international importance. With a potential annual production capacity in the UK for china clay of in excess of 3 million tonnes (80 – 90% of which is exported), this region was second only to the United States as a kaolin producer in the 1990s [14]. The importance of South-west England as a source of kaolinite in the form of china clay and ball clay arises as a consequence of special geological factors and by its proximity to the sea, which facilitates bulk export.

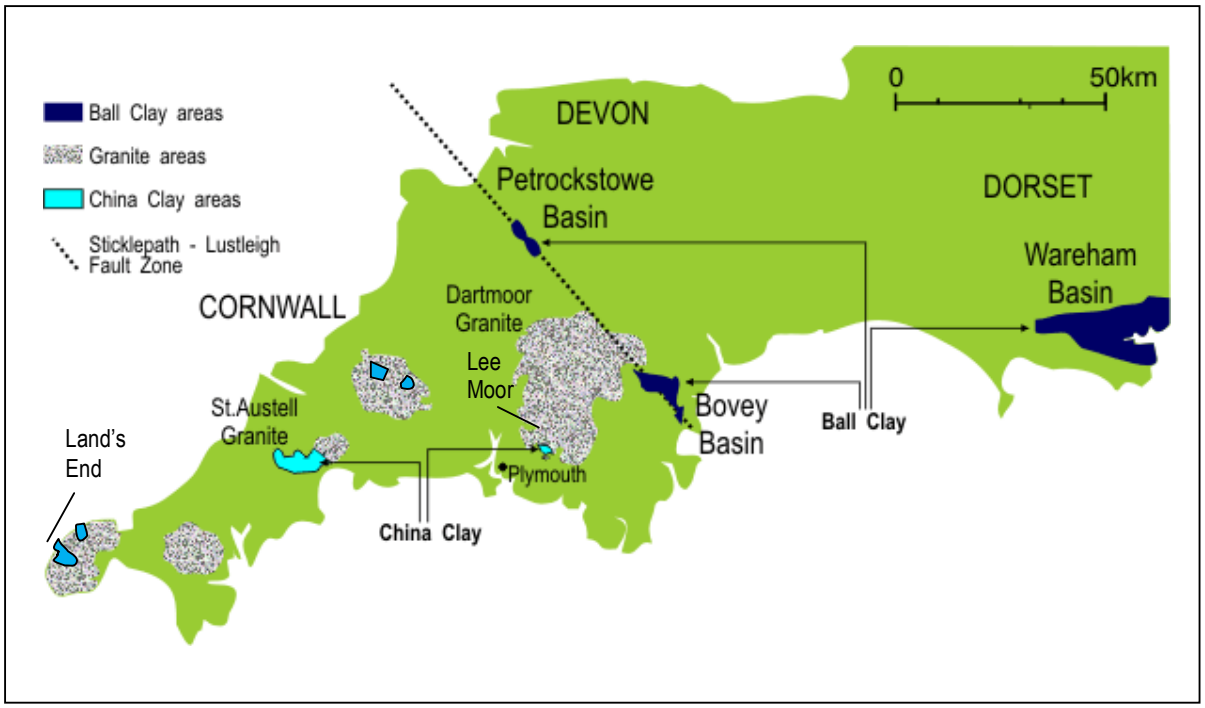

Figure 2-1: Clay deposits in Cornwall and Devon [17]

A very special combination of conditions were required to produce the high quality kaolin bodies in Devon and Cornwall, these are thought to be the following [15]:

- A relatively low iron content of the 'parent' granite
- A hydrothermal phase which destabilised the granite and formed a metastable matrix, making it susceptible to later kaolinisation
- A period of intense weathering that was sufficiently intense to alter completely the metastable granite matrix to form kaolin
- Mild conditions after kaolinisation occurred, lack of rapid erosion either by water or ice, allowing the kaolin matrix to be preserved in place.

2.1.5 Sedimentary clay deposits

Once kaolinisation had occurred, some deposits were subjected to further weathering and erosion. The deposits were transported to a different location from where they were formed, giving them the name secondary, or sedimentary, deposits. During transportation some of the heavier contaminants were deposited upstream and consequently, the main deposits are highly pure. Sedimentary clays are also finer than primary clays as a consequence of this transportation process.

Examples of such deposits are those in Georgia and South Carolina, USA which are the most extensive secondary kaolin deposits in the world. These kaolins were derived from deeply weathered crystalline rocks on the Piedmont plateau. At the beginning of the Cretaceous period (135 million years ago), the residual weathering products including kaolinite, quartz, partially altered feldspar, muscovite, smectite and minor amounts of magnetite and other heavy minerals, were stripped off and transported to the coastline by glaciers [15].

2.2 The structure and chemistry of kaolin

Kaolin is not usually pure kaolinite; instead it exists with a number of impurities. It is defined by the International Committee on Correlation of Age and Genesis of Kaolin as:

‘an earthy rock characterised by a significant content of kaolinite materials’ [18].

However, as this definition encompasses so many different materials, it is not very useful. A better definition is as follows:

'Kaolin is a clay consisting substantially of pure kaolinite, or related clay minerals, that is either naturally white; or can be beneficiated to white, or nearly white; will fire white, or nearly white. It is amenable to beneficiation to make it suitable for use in whiteware ceramics, paper, rubber, paint and similar uses [19].

The most valuable kaolins for commercial purposes tend to be purely white clays, which can be used as ceramic raw materials in the manufacture of china or whiteware, or as a filler or coating for paper. Examples of major impurities that greatly reduce the value of kaolin deposits include [12]:

- Iron oxides and hydroxides, which result in discoloured calcined products.
- Smectites (or other constituents), which adversely influence the behaviour of the kaolin slurries used in high speed paper coating due to their swelling behaviour in water.
- Contaminants such as silica and fine-grained feldspar, which produce an abrasive slurry, that causes undue wear to process machinery.

The amount and type of impurity that occur within the kaolin vary between, and even within, deposits. There are five main factors that have an impact on the impurities found in the kaolinite [12]:

- The method of formation – secondary deposits tend to be much purer than primary deposits.
- Conditions of formation – the conditions could be more/less favourable to different reactions, thus determining which reactions would occur, allowing different products to form in different areas. It is not just kaolinite that was formed due to hydrothermal activity and weathering, other clays could also be produced depending on the climate and rock conditions at the time of formation. For this reason, some kaolinite deposits are contaminated with other clays such as smectite and ball clays.
- Materials present in the parent rock – any impurities that occurred in the parent rock and were not kaolinised, or otherwise transformed, will be present in the kaolin when it is removed from the deposit.
- Place of formation – this links the conditions of formation and the materials present in the parent rock. Two separate locations may have originally contained the same materials in the parent rock, however, due to the different conditions kaolinisation took place under, they may not have reacted in the same way, producing kaolin deposits with different compositions.
- The particle size of both the kaolinite and the impurities is an important factor in determining how easily the kaolin can be purified. The majority of impurities exist in the coarsest particle fractions. A particle of around 10 cm in diameter

can be as little as 10% kaolinite and, for this reason, many beneficiation techniques can be involved in separating out the coarsest particles.

2.2.1 Kaolinite

Kaolinite, along with other clays, belongs to the phyllosilicate subclass of materials. In this subclass, rings of silica tetrahedrons are linked by shared oxygens to other rings in a two dimensional plane that produces a sheet-like structure, this sheet is then attached to another structure made from aluminium octahedral rings, as shown in Figure 2-2 [3].

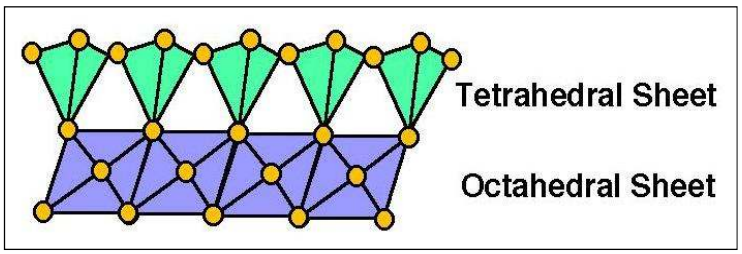

Figure 2-2: Sheet structure of kaolinite

Although hundreds of chemical analyses of kaolinite have been made, there is still little known for certain about the exact composition of most, if not all of the samples. The idealised composition by mass for a kaolinite ($Al_4(Si_4O_{10})(OH)_8$), is the following:

- SiO_2: 46.54 wt.%
- Al_2O_3: 39.5 wt.%
- H_2O: 13.96 wt.%

However this is seldom, if ever, found in nature [20].

A basic kaolinite particle is composed of a silica layer bonded to aluminium oxide/hydroxide layers. The silica layer consists of interconnected silicon atoms in tetrahedral co-ordination with oxygen atoms, as seen in Figure 2-3 [3].

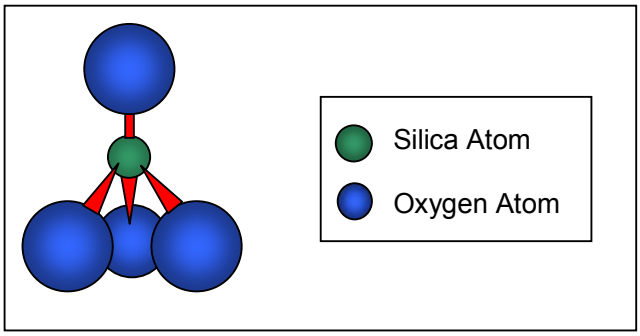

Figure 2-3: Silica Tetrahedra group

These tetrahedra form a hexagonally symmetric layer with one surface composed of three of the tetrahedral oxygens and the other surface made up of the single oxygen. The silicon atoms are located between the two. The surface containing single tetrahedral oxygen atoms is chemically connected to the alumina layer. The unbonded oxygens form a hexagonally open-packed layer [3].

The aluminium layer of kaolinite is often termed the gibbsite layer, as the layer has the same structure as gibbsite, an aluminium oxide mineral. Aluminium atoms are octahedrally co-ordinated with oxygen atoms and hydroxyl groups, as can be seen in Figure 2-4. The alumina molecules are then octahedrally interconnected to form a two-dimensional layer [3].

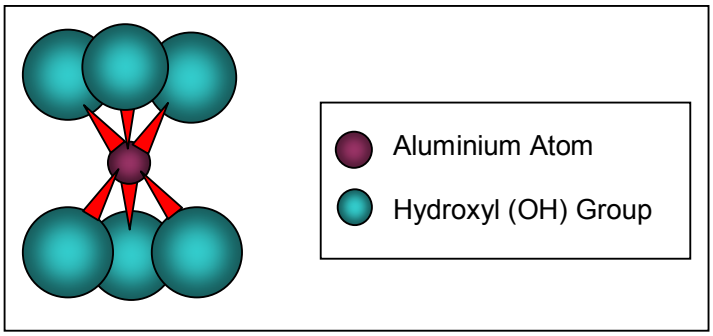

Figure 2-4: Octahedral alumina group

Only two-thirds of the octahedral positions in the gibbsite layer of kaolinite are filled by aluminium. The atoms are thought to be arranged so that two aluminiums are separated by a hydroxyl group above and below, thus making a hexagonal distribution in a single plane in the centre of the octahedral sheet. The reduction in the amount of aluminium present in the structure allows the electrical neutrality of the particle to be maintained [3].

The structure of kaolinite results from the combination of the silica and alumina layers into a hexagonal sheet. In the layer common to the octahedral and tetrahedral groups, the silicon and the aluminium share two-thirds of the atoms, and they become single oxygens instead of hydroxyl groups, the other third remaining as hydroxyl groups, as can be seen in Figure 2-5 [3].

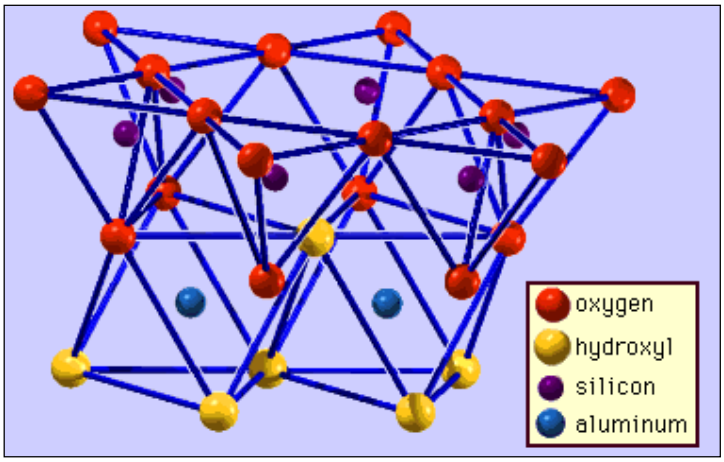

Figure 2-5: Structure of kaolinite

Hydrogen bonding between the alternating oxygen and hydroxyl surfaces causes these platelets to stack together. The resultant ideal kaolinite particle is then composed of three surfaces: the aluminium hydroxyl layer, the silicon oxygen layer, and an edge surface composed of aluminium, silicon, oxygen and hydroxyl groups [3]. This can be seen in Figure 2-5.

A naturally occurring sample of this mineral varies from the ideal particle only in its crystallinity, i.e. the regularity in its crystallographic directions, and the kind and number of cations adsorbed on the particle surface due to substitution of atoms of lower valence than aluminium in the lattice [3].

The kaolinite group of minerals includes dickite and nacrite, which rarely occur naturally, as well as kaolinite. The three minerals are polymorphs, i.e. they have the same chemical composition as each other but different structures [12].

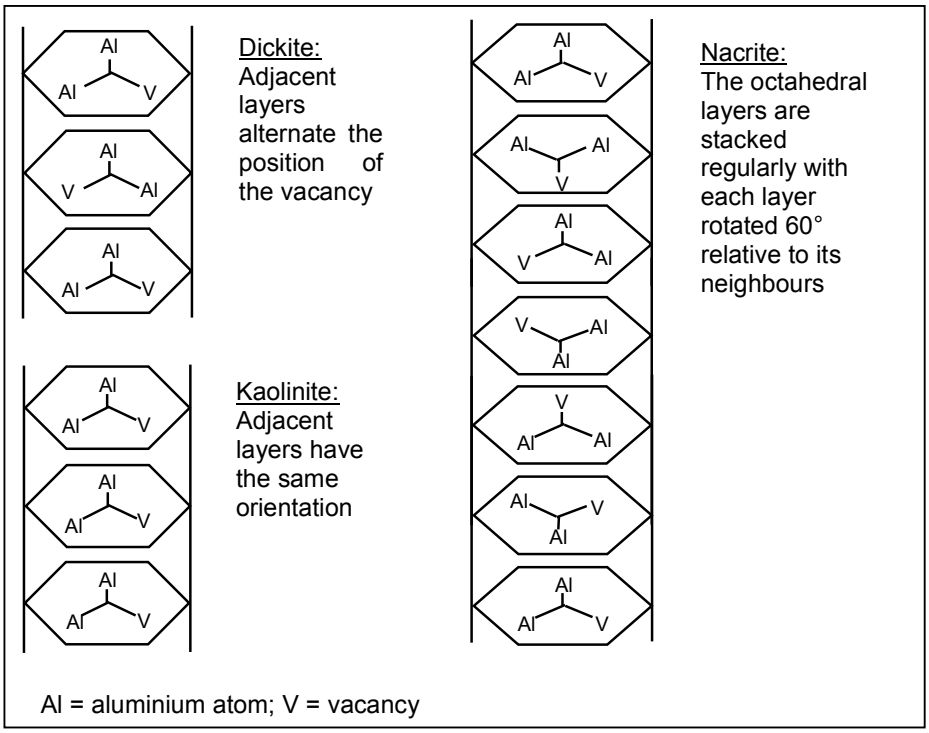

Figure 2-6: Schematic representation of the stacking arrangements for the octahedral sheets in kaolinite, dickite and nacrite [12]

As shown in Figure 2-6, dickite and kaolinite can be distinguished on the basis of the arrangement of the vacancy from sheet to sheet. In kaolinite, the vacancy is in the same position in each successive layer within a stack of sheets, whereas in dickite, it is in the same position in each alternate layer. This subtle distinction leads to kaolinite exhibiting triclinic symmetry and dickite monoclinic symmetry. The two minerals can be distinguished on the basis of careful X-ray diffraction analysis due to these differences [12].

Nacrite also differs in the way in which the fundamental layers are stacked, as shown in Figure 2-6. The position of the vacancy is repeated every 6th layer, causing nacrite

to demonstrate monoclinic symmetry. Kaolinite, dickite and nacrite all share a 7.1 Å basal spacing [12].

2.2.2 Mica

The mica group includes several closely related materials, which all have perfect basal cleavage which can be explained by the hexagonal sheet-like arrangement of its atoms. All minerals in the group are monoclinic and are similar in chemical composition.

Mica may occur as an impurity in kaolin, either as a constituent of the parent rock, which survived kaolinisation, or, in some deposits, as a product formed from feldspar in a similar method to the kaolinisation process. The layered structure of mica is similar to that of the clay minerals [21]. Generally speaking, they consist of an octahedral sheet bonded to two identical tetrahedral sheets, as can be seen in Figure 2-7 for muscovite. Muscovite is also known as potash mica due to the presence of potassium ions between the unit layers.

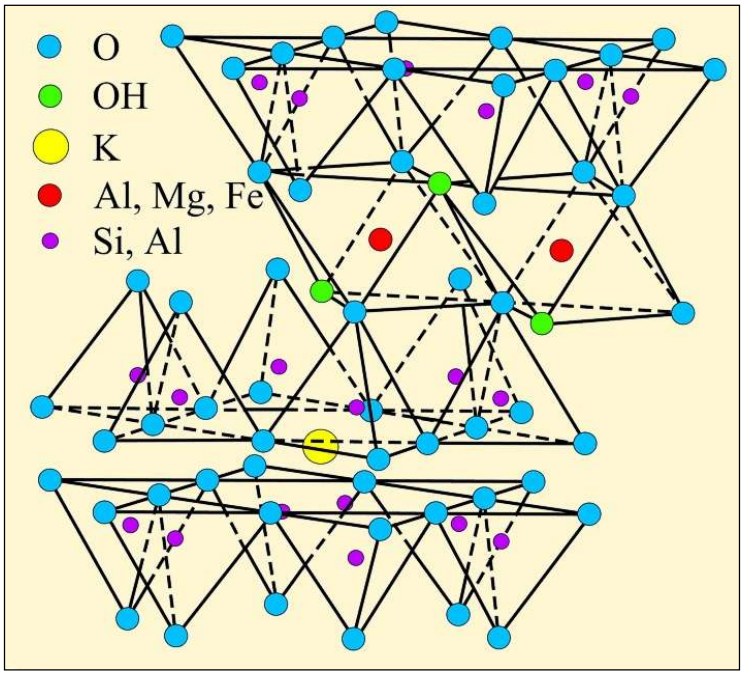

Figure 2-7: Structure of muscovite [3]

Different varieties of mica occur due to the presence of different cations at the centre of the structure. This gives them vastly different characteristics, not least the colour of the mica, which can vary widely from colourless to black. Coloured micas can have a detrimental effect on the clay product brightness, and all types of mica can have unfavourable effects on the rheology of clay-water suspensions [22].

Most micas are fairly coarse and can be removed with other coarse impurities during primary processing. It can however exist as fine grained material within the rock and tends to occur round the edges and in fractures and cleavages of the earlier minerals such as potassium feldspar and topaz [22].

This finer mica is more difficult to remove and can remain in the kaolin throughout the refining process, although micas, which have any magnetic cations, can be selectively removed using high intensity magnetic separation techniques.

2.2.3 Feldspar

The feldspar that most commonly occurs as a constituent in kaolin is potassium feldspar as it is less susceptible to the kaolinisation process than sodium feldspar. Feldspar generally exists around the edges of kaolin deposits, where the kaolinisation process was not sufficiently intense to change it into kaolinite, although in these regions it often transformed into mica [22].

Feldspar is a very hard material, it has a value of the 6 on Mohs hardness scale, compared to 2/2.5 for kaolinite and 10 for diamond [18]. It forms very angular fragments which may cause abrasion problems in some industrial applications. It is also a chemically reactive substance in some circumstances and can cause difficulties if present in a clay fraction that is to be chemically treated [22, 23].

2.2.4 Quartz

During the process of kaolinisation, silica is released from the rock, and although this is generally thought to move away from the kaolinised zone to form veins that exit the system, silica does occur in kaolin deposits in the form of quartz [22].

Quartz is made up entirely of silicon dioxide, SiO_2. Due to this chemical simplicity and general physical resistance, it is a very stable mineral and hardly breaks down during most hydrothermal and atmospheric weathering. For this reason, quartz is the most common mineral on the face of the Earth. It is found in nearly every geological environment and is at least a component of almost every rock type [22].

Uncontaminated varieties of quartz have a high brightness value and, when finely divided can enhance the brightness of kaolin. As it is chemically inert, it has no detrimental influence on the chemical properties of the clay. It is however a very hard mineral with a value of 7 on the Mohs hardness scale, hence harder than feldspar. The presence of quartz impurities can cause the kaolin to become more abrasive, potentially causing problems in certain applications [22].

If crystalline silica is of respirable size, it becomes a serious health risk as it can cause respiratory system diseases such as silicosis as well as aggravating existing respiratory system diseases and dysfunctions. The small particles also have an aggravating effect on both the skin and eyes.

2.3 The calcination reaction

Kaolin, also known as china clay, is principally made up of the mineral kaolinite, which has the idealised formula $Al_2Si_2O_5(OH)_4$. In many deposits, the kaolin also contains a variety of different impurities, such as mica, feldspar and quartz. The

quantity and quality of these contaminant minerals can have a profound effect on the kaolin once it is calcined.

Calcination, the process of heating a substance to a point below its melting or fusing point causing a loss of water from the structure, is one of the most important ways of enhancing the properties, and value, of kaolin. Once calcined, the kaolin becomes whiter and more chemically inert, enhancing its use in a wide range of products, such as paper, rubber, paint, plastic and refractory items.

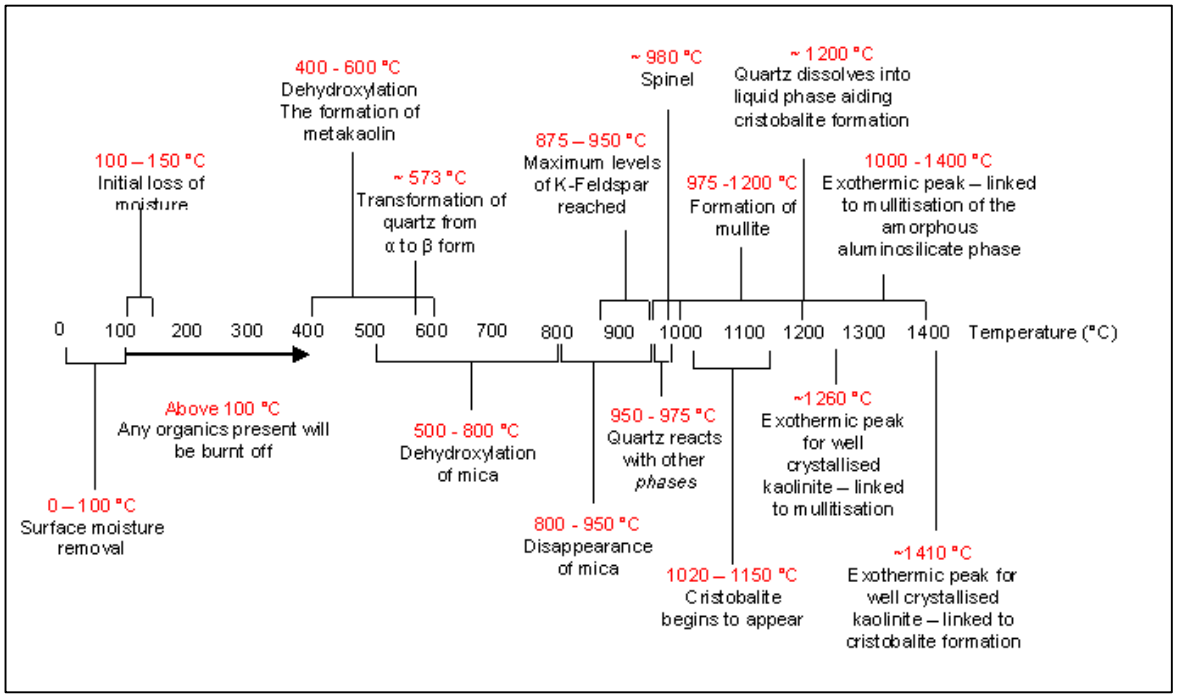

Figure 2-8: Progression of the calcination physico-chemical reaction and transformations with temperature for kaolin and associated mineral species [3, 6, 8, 24-27]

Most researchers will agree that when kaolinite is calcined, it undergoes a series of three principal reactions [3]. A series of different researchers have also identified,

alongside these reactions, a variety of complicated and critical reactions occurring between the other minerals present in the kaolin. The main distinguishable reactions, as summarised in the literature, are shown in Figure 2-8.

The Differential Scanning Calorimetry (DSC) plot in Figure 2-9 was generated for a typical Cornish kaolin. The method of analysis monitors the amount of heat necessary to establish nearly zero temperature difference between a substance and an inert reference material (usually an empty dish) as the two specimens are subjected to identical temperature regimes in an environment with a controlled heating rate [28]. The results are plotted as a graph of temperature against energy. This graph allows the identification of any endo/exothermic reactions that may take place and the temperature at which they occur.

The initial reaction, which generally occurs around 0 – 150 °C is characterised on the DSC plot in Figure 2-9 by an initial endothermic curve, where the temperature of the kaolin does not increase despite energy being applied to it [4, 5]. This reaction principally involves driving any physically bonded water from the kaolin. Typically, about 0.5 wt.% will be removed from a dry powder.

At temperatures above 100 °C, any organics present in the kaolin will be burnt off [5]. At low temperatures this may cause charring to the kaolin and some reduction in brightness of the product. Brightness is defined as the percentage of light reflected by a body compared to that reflected by a perfectly reflecting diffuser measured at a

nominal wavelength of 457 nm. It is an important characteristic, as bright, white calcined kaolin will generate a similarly bright, white artefact.

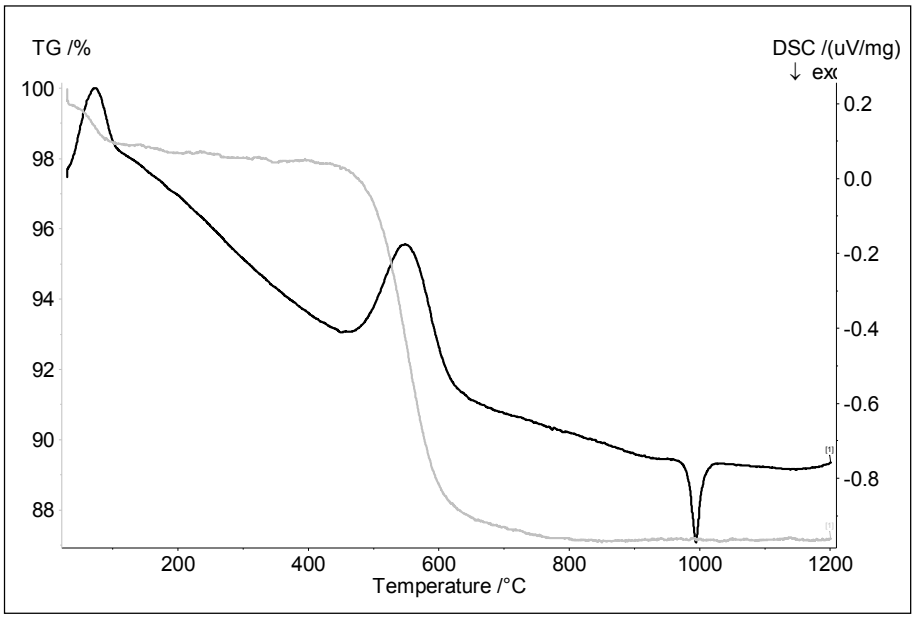

Figure 2-9: Simultaneous Thermal Analysis of a Cornish kaolin. The two curves indicate the two thermal analyses: The black curve is a Differential Scanning Calorimetry curve, where an upwards peak indicates an endothermic reaction and a downwards peak shows an exothermic reaction. The grey line is a Thermogravimetric Analysis plot indicating the loss in weight as the reaction progresses.

Between 400 and 600 °C, the kaolinite undergoes a dehydroxylation reaction, involving the removal of chemically bonded water, to produce metakaolin as shown in Equation 2-2 [6].

$Al_2Si_2O_5(OH)_4 \rightarrow Al_2Si_2O_7 + 2H_2O$

Kaolinite → Metakaolin + Water

Equation 2-2: Metakaolin reaction [6]

Heating to these high temperatures causes a change in the structure of the particle itself. Dehydroxylation causes an alteration in the co-ordination of the aluminium from six- to four-fold. The aluminium-oxygen tetrahedra then become 'stretched-out' over the unaltered silicon-oxygen network. This allows the particle to retain its basic hexagonal shape, with changes only occurring on one surface [6].

The point at which the dehydroxylation reaction starts to take place is indicative of the crystallinity of the structure, the impurities that are present within the kaolinite and the particle size. This part of the process requires a high energy input, and can be identified on the DSC curve in Figure 2-9 as a large endothermic curve between 450 and 700 °C.

This change of structure causes some complications to researchers. Powder X-Ray Diffraction (XRD) is commonly used to determine the crystallographic structure of powdered solid samples. It is commonly used to identify unknown substances, by comparing diffraction data against a database maintained by the International Centre for Diffraction Data. However, once the metakaolin region is reached, XRD becomes less helpful in determining compositional differences in the calcined product, as it often only registers an amorphous background phase. This is due to a loss of structure, which also causes the product to become optically duller and not as bright, which is detrimental to the value of the clay.

Whilst some researchers consider the dehydroxylation reaction to be irreversible others have shown that it is possible to re-hydrate metakaolin to some extent. The

resulting product has been found to be generally more disordered than the natural mineral, although it has been proposed that the amount of disorder in the product is dependent on the amount of crystallinity in the original sample, a theory which is yet to be disproved [3].

The third reaction, the transformation of the metakaolin to the spinel phase by exothermic recrystallisation, is shown in Figure 2-9 as the sharp exothermic peak at around 980 °C [8]. The exact reaction which takes place is subject to much debate, and the only generally accepted theory is that a spinel-type phase forms along with some free silica, although the type, its chemical formula as well as the mechanism of formation, are all the subject of debate [5]. One theory is that shown in Equation 2-3 [6].

$Si_4Al_4O_{14}$ → $Si_3Al_4O_{12}$ + SiO_2

Metakaolin → Spinel phase + Free silica

Equation 2-3: Spinel phase reaction

Spinel is a general term for a group of oxides which have the formula $X^{2+}Y_2^{3+}O_4$ (where X and Y are general chemical symbols). However, due to aluminium deficiencies in the metakaolin structure, vacancies will appear in the spinel which are integral to its structure and so the term defect-spinel is used [8]. Within the defect-spinel the aluminium has reverted back to its octahedral co-ordinated state [6].

The presence of the free amorphous silica, which is identified by some authors as part of the spinel phase, has been found to be absent in the presence of significant

alkali content. It has been determined that Mg^{2+}, Li^{+}, Cu^{2+} and Zn^{2+} promote the re-crystallisation of metakaolin, whilst Na^{+} and Ca^{2+} have little effect, and K^{+} and Ba^{2+} tend to slow the reaction down [4, 29].

In addition to the three main reactions, there are a number of others that are occurring at the same time and at higher temperatures. Between 500 and 800 °C, any mica which is present in the kaolin will be dehydroxylated. In a typical Cornish kaolin, the weight loss associated with this stage is approximately 0.5 wt.%; although, both the quantity and temperature will vary, depending on particle size and crystallinity.

Once temperatures of around 800 to 950 °C are reached, much of the mica present in kaolin had disappeared. The calcinations also showed that the amount of potassium feldspar increased to a maximum before declining or disappearing. The maximum potassium feldspar content generally occurs in the range from 875 to 950 °C, which is slightly above the temperature at which mica has disappeared. The breakdown of mica, therefore, appears to provide the raw materials for the new potassium feldspar formation [24].

A number of reactions involving quartz have also been identified. At around 573 °C, quartz undergoes a phase change, from the standard alpha form to the less dense and structurally less stable beta form. This temperature was identified through various Differential Scanning Calorimetry (DSC) traces. Consequently, between 950

and 975 °C this beta-quartz starts to react with the potassium-rich phases, causing them to melt [24].

At very high temperatures of around 1200 °C, any quartz present may dissolve in the liquid phase [24], and, this is considered to promote the formation of cristobalite. This is an undesirable reaction in any material that will be crushed and subsequently used in refractory applications, as it is classed as a Group 1 human carcinogen and can also cause lines of weakness to develop in refractory objects [25, 30].

A small exothermic peak present at approximately 1410 °C has been identified on DSC traces and is considered to be an indication of the formation of cristobalite in kaolin with a low quartz content [26]. Thereby, the presence of quartz reduces the temperature of cristobalite formation by just over 200 °C.

At temperatures above the spinel phase, the kaolinite continues to react. Between 975 and 1200 °C depending on the kaolin, mullite begins to form, expelling more silica from the structure [6, 8, 24]. An area of irregular exothermic activity, shown in a DSC trace in this temperature range indicates this reaction is taking place. The mullite, which forms from kaolin, has the formula $3Al_2O_3{\cdot}2SiO_2$ and is termed 3/2-mullite [8].

The formation of mullite is considered to be a two-stage process. When a well crystallised kaolinite was examined, two exothermic peaks occurred on a DSC trace. The first peak was broad and over the long temperature range of 1000 to 1400 °C is

due to mullite formation out of the amorphous aluminosilicate phase. The second peak, which is within the broad exotherm and occurs at around 1260 °C, is considered to be due to the conversion into mullite of the spinel phase [26, 27].

Some mullite begins forming at the same time as the spinel-phase, although this is small and poorly crystalline. Mullite initially has an elliptical shape with random orientation, but, as the temperature increases to around 1300°C, the crystallinity of the mullite increases and needle-like crystals begin to form, the orientation becomes more ordered and hexagonal-like. This arrangement is thought to stem from the original kaolinite sheets and the logical explanation is that the mullite needles are formed from the aluminium-oxygen octahedral chains of the spinel which are somehow preserved during mullite formation. This theory was supported by research that showed the growth of mullite proceeds at a lower temperature for a well-ordered kaolinite than a disordered kaolinite [8].

It has been determined that the rate of heating is important in the temperature of mullite formation. Mullite will form at a higher temperature when the heating is rapid [18]. With a Cornish kaolin, the amount of mullite reaches the theoretical value of about 55 wt% at about 1100°C in 25 hours, or at 1300°C in half an hour [4].

Mullite has a number of sought after properties: low thermal expansion, low thermal conductivity and excellent creep resistance. It is, however, very coarse and abrasive and can cause damage to machinery [8, 31]. In order for calcined kaolins to be suitable for application in the paint, polymer and paper industries, it is necessary to

prevent the formation of mullite. This is done by 'soft calcining' the kaolin for a short duration at temperatures below 1100 °C, creating a product which is white and with low reactivity, but without the abrasive nature.

2.4 Time-Temperature-Transformation Diagram

While the heating rate is an important factor in deciding the temperature at which transformations will occur at, generally speaking, the same transformations will occur irrespective of heating rate, and at lower rates of heating, the duration at temperature becomes important [32]. The effects are illustrated using the Time-Temperature-Transformation diagram (TTT-diagram) for a pure kaolinite; a unique diagram for kaolin and atmospheric pressure [24].

The most important feature of the TTT-diagram is that, at a given temperature, different mineral assemblages are possible, depending on the length of exposure time. As can be seen in Figure 2-10, many of the mineral assemblage fields are elongated so that they slope from higher temperatures to lower temperatures with increasing firing times.

This may be of great importance to commercial firing cycles because by firing at slightly higher temperatures the same product can be produced at a much reduced firing time. A significant reduction in firing costs may thus be achieved.

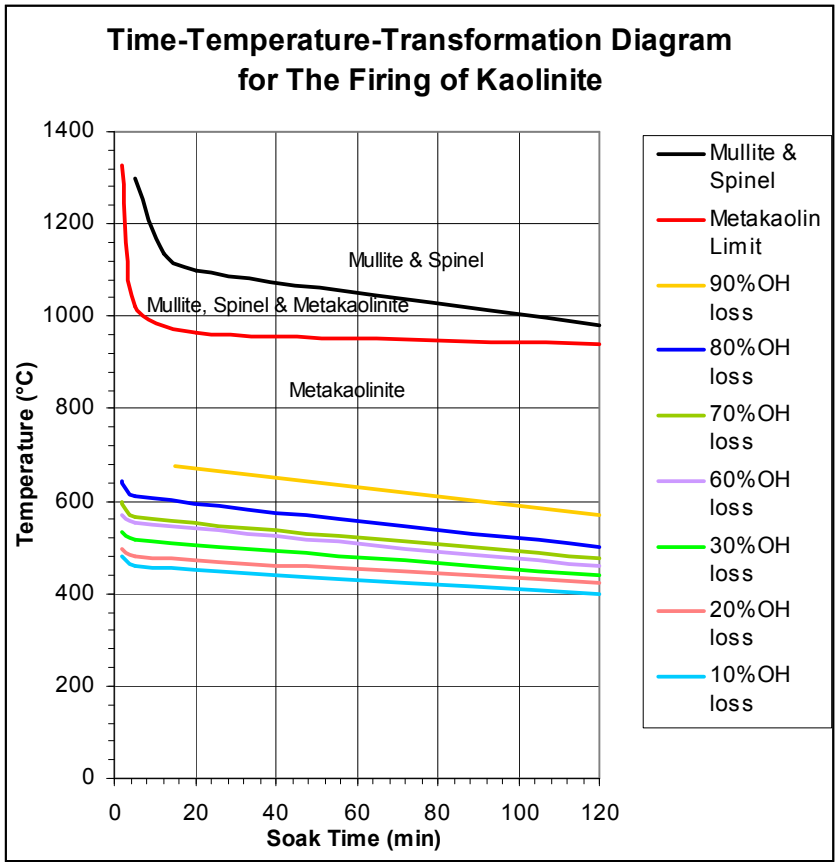

Figure 2-10: Graph showing transformations that occur, as kaolin is heated [24]

2.5 The effect of impurities on colour after calcination

2.5.1 Iron

The presence of iron in the clay becomes especially important if the clay is calcined. Heating the clay up to high temperatures causes the iron in the clay to be oxidised from the green/blue Fe^{2+} form, to the red Fe^{3+} form, which can turn the clay a shade of pink. With 'pure' kaolins, good correlations have been found between brightness, yellowness, light absorption coefficients and the analytical iron content at various

calcination temperatures from 700ºC upwards, allowing prediction of colour of the final product from the analytical iron content of the feed [33].

It has been shown that the brightness of samples varies with the calcination temperature, first decreasing and then improving again as the temperature is raised. The variation derives mainly from changes in light absorption rather than light scattering [34].

The increase in light absorption (reduction of the brightness) which occurs as the calcination temperature is raised towards 700°C is due mainly to the conversion of residual surface iron impurities to the intensely coloured red iron oxide, hematite. The decrease in light absorption, on heating above 700°C is due mainly to one or more solid state reactions involving ancillary materials [34].

Due to the complexity of these solid state reactions it is not possible to calculate light absorption or brightness figures for calcined mixtures from the properties of the individual components. Instead, prediction of colour occurs only after laboratory test firing of samples of each calciner feed [34].

It has been proven that a kaolin which has a high iron content before beneficiation, was favourably comparable, in terms of brightness, with kaolin that had naturally low iron content once both samples had been calcined. This is an important development for the china clay industry as high quality deposits are used up [2].

There are a number of different beneficiation methods, which can be used to remove iron (and other impurities) associated with kaolin. The common techniques include:

- Size classification for removing coarse minerals and for attaining the specific particle size distribution;
- Magnetic separation of the minerals containing iron;
- Reductive chemical bleaching to solubilise ferric species and reduce discoloration of remaining ferric sites;
- Froth flotation to separate micaceous, graphitic and titanoferrous minerals.

The beneficiation steps give a significant added value to a raw kaolin, although when the performance of the operation is compared with the overall cost, in most cases, it will not be cost effective [2].

The impact of iron in the kaolin can be reduced with the use of a reductive atmosphere during calcination and this area has been well-researched. This is due to transformations occurring to the iron species within the clay, with a preference for blue/green coloured Fe^{2+} species, rather than intensely red coloured Fe^{3+} species [35].

The use of reductive gases such as carbon monoxide can be replaced by the use of an additive which when burnt under conditions of low oxygen pressure produces the carbon monoxide, e.g. carbon black or ball clay. This gives a comparative colour improvement. Use of a reductive atmosphere, while improving whiteness at a lower calcination temperature, also reduces abrasiveness [36].

2.5.2 Organic materials

The effect of organic material on the kaolin depends on the kind and the amount contained within the kaolin material. In general, the organic material occurs in kaolin is several different ways: it may be present as discrete particles of wood, leaf matter, spores etc.; it may be present as organic molecules adsorbed on the surface of the kaolin particles; or it may be intercalated between the silicate layers. The discrete particles may be present in any size, from large chunks easily visible to the naked eye, which can be easily removed through screening in production, to particles of colloidal size, which are much more difficult to remove [3].

Kaolin can become contaminated with organic material through both natural and artificial means. During production, dispersants such as polyacrylate are routinely added to the suspension, preventing the kaolin from settling, therefore, making it easier to process through the system. The only chemical reaction undertaken for the hydrous kaolin is that of bleaching, which requires sodium dithionite and acidification, but it is assumed that the entire chemical added is used during the reaction.

Some kaolin production routes, depending on the water source, are affected by the presence of humic acid. This is a particular problem for operations in Devon, where the humic acid enters the water due to plant decay on the slopes surrounding the streams that feed the water circuit used in production. The concentration of the humic acid is highly variable, depending on the season and recent rainfall levels, with levels being particularly high after heavy rain in the winter, when organic matter has begun to decay in large amounts [37].

The effect of the humic acid content on the hydrous kaolin has been determined to be detrimental, with an accompanied increase in feldspar content in the pit wash, leading to an overall concurrent loss in product recovery [37]. Although the brightness of the hydrous kaolin has been determined to be unaffected, organic materials, which exist as surface contamination, have an effect on the clay colour once calcination has taken place.

Any organics that are present in low temperature calcination, have a charring effect, darkening the kaolin and turning it a grey colour. It has, however, been determined that organics are generally removed from the system and fully removed from the kaolin surface by around 800 °C, or possibly lower temperatures, provided that sufficient time is available for complete combustion to occur [5].

2.6 The effect of particle size on calcination

The particle size of hydrous kaolin is an important influencing factor on the characteristics of calcined kaolins. A kaolin with a fine particle size has a larger surface area, which means it will be more reactive than a coarse kaolin [3, 4, 38]. This increased reactivity leads to an increased rate of sintering and mullite formation as well as some initial shrinkage, which results in a decreased porosity [8, 39].

Thermal analysis of kaolins of different degrees of coarseness shows that, as the particle size decreases, the size of the exothermic reaction that is as a result of the spinel phase reaction, and intensity of the corresponding peak decreases. This is

considered to be due to the decrease in crystal phase formation due the fragmented state of the particles [40]. The decrease in crystallinity is also accompanied by a characteristic decrease in the onset of dehydroxylation temperature, and a prolonged period of dehydration [41].

There is also an additional effect when the particle size increases, whereupon the dehydroxylation and other reactions occur much slower. This phenomenon is found in particles larger than 20 μm and is thought to occur because the surface area is too small for the dehydroxylation reaction to happen as rapidly as in finer particles and the difference is identifiable using differential thermal analysis [40].

When two kaolins of different particle size, classified as medium and fine were soak calcined and the product examined using electron microscopy, the variations in the product were immediately noticeable. The fine hydrous particles produced a smaller aggregate, with an average size of around 0.7 μm compared to 1.2 to 2.2 μm for the medium sized particles. The fine particles, upon calcination, were discovered to have a higher void volume than the medium particles, which had a corresponding effect on the oil absorption of the product. This is due to the increase in porosity; the more pores that are present in the calcined structure, the more oil that can be absorbed [42].

It has been determined that opacity, the ability of a substance to block light, either through absorption or scattering is improved as particle size decreases. This is an important feature in calcined kaolin as it is primarily used in paint formulation, for

which opacity is highly important. This is accompanied by an increase in gloss, another desirable characteristic in the product [42].

3 Methods and Materials

3.1 Calcination

3.1.1 Tracer experiment

In order to determine the residence time of the multiple hearth kiln, located at the Lee Moor site in Devon, the feed kaolin was dosed first with titania, TiO_2 and secondly with talc, $Al_2Si_2O_5(OH)_2$. The concentration of these minerals was detected using X-ray fluorescence. Kaolin is added to the top of the multiple hearth kiln, in a semi-continuous matter using a loss-in weight feeder. Powdered kaolin feed is metered from the feed storage bin with the feeder into a discharge auger and through a rotary airlock valve, into the kiln. The feeder at the top of the calciner was adapted to incorporate a small hopper, which could be isolated by means of slide valve, situated directly over the discharge end of the screw. The hopper was loaded with 100 kg of tracer. The tracer powder was then discharged quickly into the auger and timing started. This configuration allowed the entirety of the mineral tracer to be dosed into the kiln in one go.

Calcined kaolin is discharged from the kiln through two drop holes, on either side of the kiln base, from which the calcined powder falls though to a discharge auger. This material is then moved and dropped into an air blast cooler, where the discharged calcined kaolin is both cooled and transported to a dust collector, from whence it is sent for milling to deagglomerate the particles.

Samples of the calcined material were taken from the exit of the kiln as it dropped from the kiln discharge point and before it passed into the air blast cooler. As the material being discharged is still at high temperature, samples were taken with an insulated steel long handled device, which was passed across the powder bed in a sweeping motion to obtain an even, characteristic sample of product. Approximately 0.1 kg of sample was taken each time.

In the initial titania experiment, both sides of the product stream were sampled, so as to determine whether there was any evidence of preferential flow through to one side of the kiln or the other. Samples were taken from side B every 5 minutes for the first 15 minutes, and then every minute thereafter until 60 minutes had elapsed. Further samples were then taken every 5 minutes until 75 minutes had passed. Side A was sampled every 5 minutes throughout the operation.

Once it had been determined that there was very little difference between the two sides as a result of the titania experiment, it was deemed not necessary to sample both sides for the talc trial. Samples were taken as the feed kaolin was dosed with talc, 5 minutes later and then every minute until 59 minutes had passed. Sampling then restarted at 80 minutes and samples were taken every five minutes until 170 minutes. One final sample was taken at 180 minutes after the original dosing took place.

3.1.2 Laboratory calcinations to replicate multiple hearth kiln conditions

All laboratory scale calcination experiments were carried out using a Carbolite GPC1300 Furnace (Carbolite Ltd., Hope, UK), controlled with a Eurotherm 2416 Controller (Eurotherm Ltd., Worthing, UK). The kiln has a heating area of 0.32 m by 0.43 m, a height of 0.25 m and is heated with APM (a nickel, chromium and aluminium alloy) wire heating elements which are located on the two sides of the kiln. At the base of the kiln, there is a refractory board (Saffil Ltd, Widnes, UK), which is 0.26 m by 0.33 m wide and 0.02 m thick. This is located in the centre of the kiln base and supports all samples during the heating/cooling cycle.

The crucibles used for the majority of the experimentation were fused silica (Scientific and Chemical, Bilston, UK) and were rectangular, 0.16 by 0.1 m, 0.025 m tall and with a wall thickness of 0.005 m. Prior to calcination, the empty crucible was weighed before the hydrous kaolin was carefully poured into the crucible, using a 50 ml plastic scoop, taking care to not compress the powder in doing so. The crucible was then weighed for a second time and the value recorded. This was done to ensure correct sample identification following the calcination and also to determine the loss on ignition, with the addition of fired weight data. This was a simple method of guaranteeing that a reaction had actually taken place, prior to the submission for other testing.

Four different methods of calcining were investigated as part of this work, the main two being batch and soak calcining. The other two methods investigated were batch/soak and soak/batch, a combination of the primary methods.

Soak calcining involves placing a powder filled crucible into a furnace when it is cold and leaving it inside until the temperature reaches the required level, allowing it to dwell at temperature for the required length of time, before letting it cool at a natural rate, before the sample is removed. Conversely, batch calcination, involves heating the furnace to the required temperature whilst it is empty and then placing the crucibles inside for the required length of time, before removing them and allowing them to cool naturally on a heat-proof surface.

A combination of the two methods was also investigated, where the kiln was heated up to the designated temperature with the sample inside, held at temperature for a specified amount of time and then the sample removed to cool outside of the kiln. This method was termed the Soak/Batch method.

The reverse method has also been examined, with the sample being put into the kiln when it was at the required temperature and was left to remain inside for the requisite time before the kiln was switched off and allowed to cool gradually. The sample was then removed when the kiln was returned to room temperature. This was described as the Batch/Soak method.

3.1.3 Thermocouple experiments

The rate of heating and its effect on the properties of the calcined product have been investigated using a rig of K-Type thermocouples with ceramic sheathing (TC Direct, Uxbridge, UK) and a six channel Ecograph T data recorder (Endress and Hauser Instruments International AG, Reinach, Switzerland).

Using a fibreboard (Unifrax Corporation, New York, USA) support, the level of penetration for the thermocouples has been staggered both across and downwards through the 0.11 m high 0.07 m diameter cylindrical crucible (Almath, Newmarket, UK). The arrangement can be seen in Figure 3-1, while the technical drawings can be seen in Appendix A.

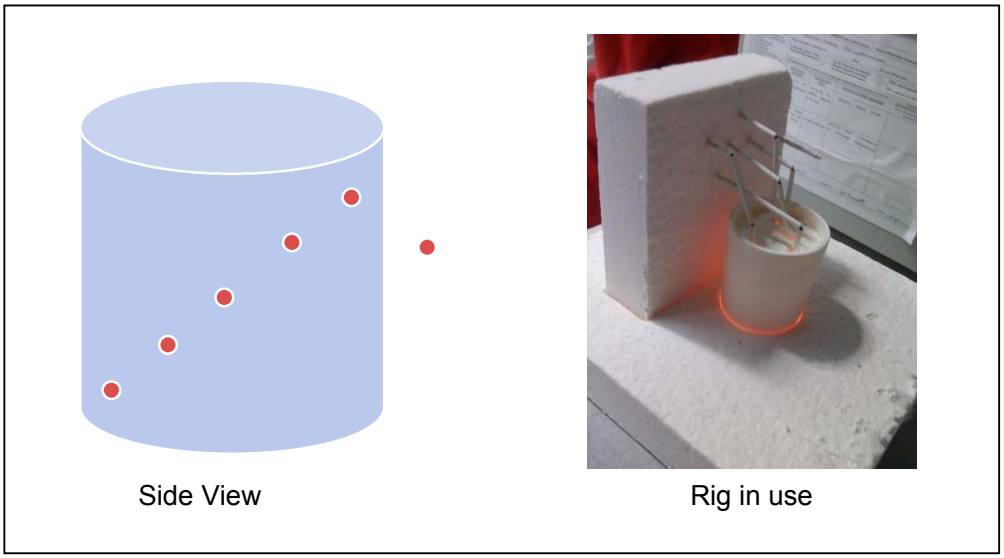

Figure 3-1: Arrangement of thermocouples in the crucible in order to investigate the rate of heat penetration into the crucible and its effect on the properties of the calcined product.

This rig has been used with all four different methods of calcination in order to better understand the relation between heating rate and product properties. An amended rig has also been used for the batch and soak calcination methods, with fused silica tray crucibles, this is shown in Figure 3-2, where the heat of the set-up when removed from the furnace can be seen in the glow around the crucibles. When used in experiments without the base, only the upright section was used. The technical drawings can be seen in Appendix A.

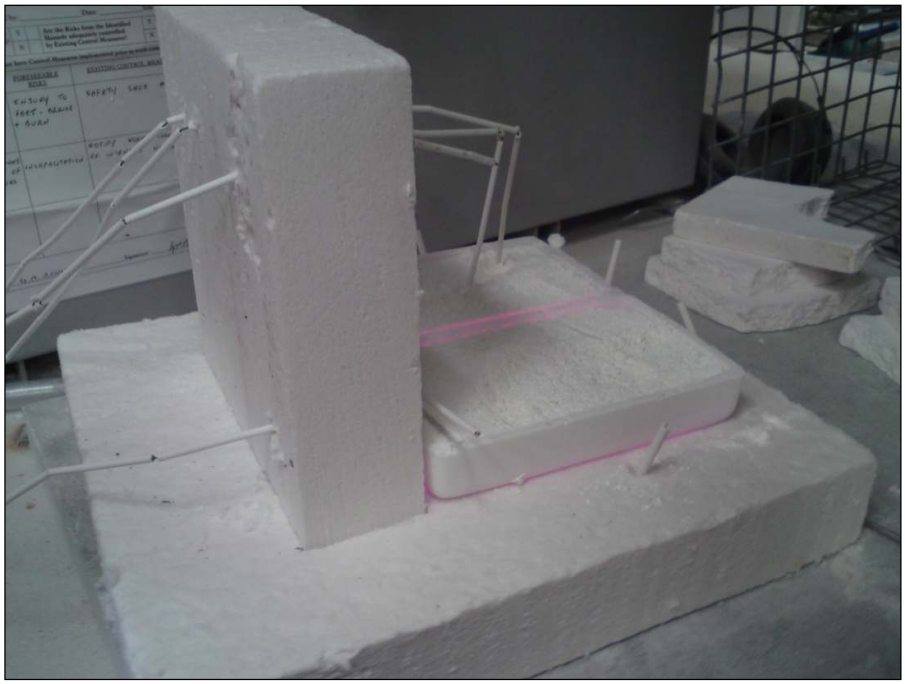

Figure 3-2: Thermocouple rig for fused silica tray crucibles

3.2 Sample Analysis

3.2.1 Colour

Whiteness/brightness values are very important for kaolin, as the possible uses are highly dependent on these values. There are a number of different techniques that are used world-wide to quantify colour.

The Commission Internationale d'Eclairage (CIE) (Vienna, Austria) created a set of colour spaces that specify colour in terms of human perception. It then developed algorithms to derive three imaginary primary constituents of colour - X, Y, and Z - that can be combined at different levels to produce the entire colour range that the human eye can perceive. The resulting colour model, CIEXYZ, as well as other CIE colour

models form the basis for all colour management systems. The goal of this standard is to produce consistent results, for a given CIE-based colour specification, on different devices, up to the limitations of each device [43].

There are several CIE-based colour spaces, but all are derived from the fundamental XYZ space. The XYZ space allows colours to be expressed as a mixture of the three tristimulus values X, Y, and Z. The term tristimulus is derived from the fact that colour perception results from a retinal response to three types of stimuli. After experimentation, the CIE set up a hypothetical set of primaries, XYZ, that correspond to the way the retina behaves [43].

The CIE defined these primaries so that all visible light maps into a positive mixture of X, Y, and Z, and so that Y correlates approximately to the apparent lightness of a colour. Generally, the mixtures of X, Y, and Z components used to describe a colour are expressed as percentages ranging from 0 percent up to, in some cases, just over 100 percent [43]. Yxy space expresses the XYZ values in terms of x and y chromaticity co-ordinates using the equations shown in Equation 3-1.

$$Y = Y$$

$$x = \frac{X}{(X + Y + Z)}$$

$$y = \frac{Y}{(X + Y + Z)}$$

Equation 3-1: Determining XYZ colour values [43]

The Z tristimulus value is incorporated into the new co-ordinates and does not appear by itself. This allows colour variation in Yxy space to be plotted on a two-dimensional diagram. Figure 3-3 shows the layout of colours in the x and y plane of Yxy space [43].

One problem with representing colours using the XYZ and Yxy colour spaces is that they are perceptually non-linear. It is not possible to accurately evaluate the perceptual closeness of colours based on their relative positions in XYZ or Yxy space. Colours that are close together in Yxy space may seem very different to observers, and colours that seem very similar to observers may be widely separated in Yxy space [43].

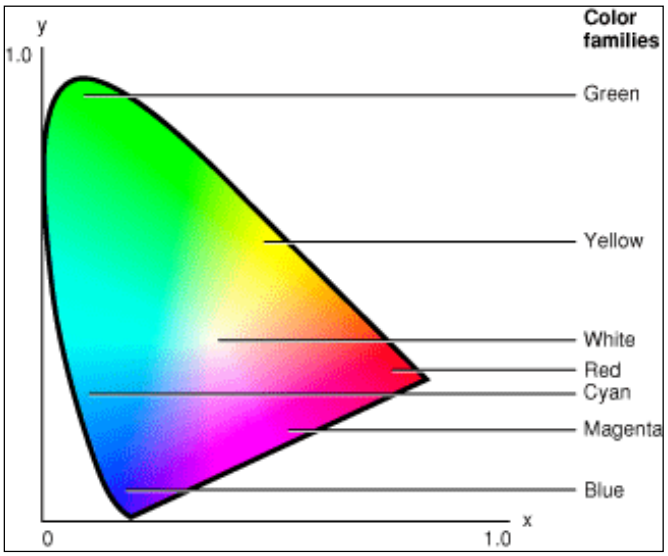

Figure 3-3: Yxy chromaticities in the CIE colour space [43]

L*a*b* space is a non-linear transformation of the XYZ tristimulus space. These spaces are designed to have a more uniform correspondence between geometric distances and perceptual distances between colours that are seen under the same

reference illuminant [43]. The values are worked out using the following calculations shown in Equation 3-2.

$$L^* = 116\left(\frac{Y}{Y_0}\right)\frac{1}{3} - 16$$

$$a^* = 500\left[\left(\frac{X}{X_0}\right)\frac{1}{3} - \left(\frac{Y}{Y_0}\right)\frac{1}{3}\right] L^*$$

$$b^* = 200\left[\left(\frac{Y}{Y_0}\right)\frac{1}{3} - \left(\frac{Z}{Z_0}\right)\frac{1}{3}\right]$$

Equation 3-2: Determination of L*a*b* from X, Y and Z space [43].

Where X, Y and Z are tristimulus values and X_0, Y_0 and Z_0 are tristimulus values for a perfect diffuser for the illuminant used [43]. L*a*b space is illustrated in Figure 3-4.

The a* value from the L*a*b* results show how red/green the sample is. A positive a* value means a red colouration of the sample (and probable iron contamination in kaolin samples), whilst a negative a* value indicates a green colouring of the sample. The L* value is the grey-scale. The closer the value for the sample is to 100, the whiter the substance will be. A positive b* value means the sample colour is yellow in colour, while a negative b* value indicates a blue colouring of the sample.

L*a*b* space represents colours relative to a reference white point, which is usually based on the whitest light that can be generated by a given device. Therefore, L*a*b* results are not completely device independent; as two numerically equal colours are truly identical only if they were measured relative to the same white point.

L*a*b* space is commonly used in applications where closeness of colour must be quantified [43].

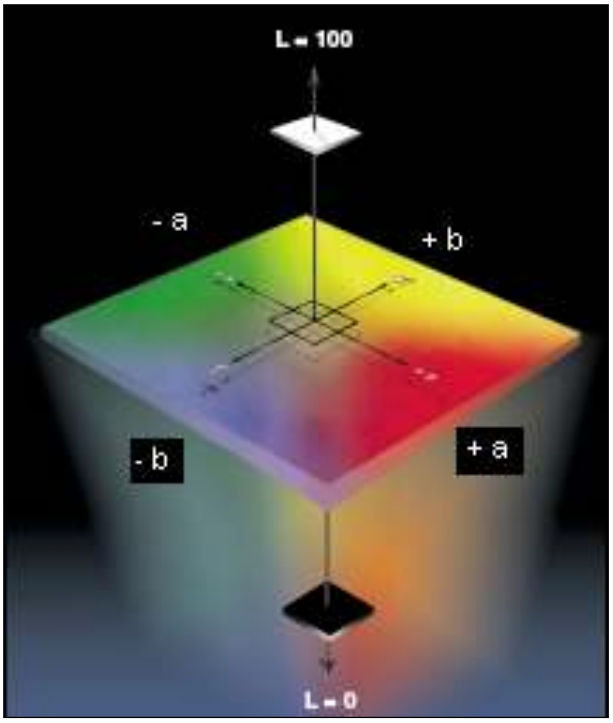

Figure 3-4: L*a*b* colour space [43]

The brightness and whiteness values quoted here, in this thesis, are based on ISO 2470:1999 - Measurement of diffuse blue reflectance factor (ISO Brightness) standard measurements [44]. They were developed by the paper industry as a standard method of measuring the brightness of pulp following bleaching.

Brightness in this instance is defined as the percentage of light at a nominal wavelength of 457 nm is reflected by a body compared to that reflected by a perfectly reflecting diffuser. Yellowness is the difference between the percentage of the light

reflected by a body compared to that reflected by a perfectly reflecting diffuser measured at a nominal wavelength of 571 nm and the brightness measurement [45].

Colour values were measured using a Datacolor Elrepho™ 450X (Datacolour Inc., New Jersey, USA), which is designed specifically for use by the paper industry [45]. The light source for Elrepho is a pulsed xenon flash lamp and the detector a SP2000 spectral analyser with a 256-photodiode array which enhances the precision of the measurement. A UV filter is in place for all measurements and only the visible light spectrum is analysed, the wavelength range for the instrument being between 360 and 700 nm [46].

A test surface is produced by milling 10 g of a 100% dry material to disperse it completely, then compressing it under fixed conditions to form a powder tablet. The tablet then placed on the Datacolor pedestal, which is moved into place below a 34 mm aperture. The reflectance values of this tablet are measured at various wavelengths in the visible spectrum, this is seen as a series of flashes by the operator, and the results recorded on the attached computer.

The primary standard employed by Imerys is an ISO Level 2 reflectance standard supplied and calibrated by Physikalisch-Technische Bundesanstalt (PTB, Germany) which is an ISO appointed primary calibration laboratory. A working standard is then used to calibrate the Datacolor, this is a ceramic tile, which has been previously calibrated against the primary standard and which is re-calibrated with a fresh standard every six months.

The machine is routinely calibrated with the working standard every six hours, along with a black trap which consists of an angled mirror which gives a reading of zero reflectance and a green tile, both of which are provided by Datacolour.

Repeat submission of a sample of Milled HF that had been batch calcined at 1050 °C for 30 minutes has shown the test to be extremely accurate with brightness values being ± 0.2 of the mean value, the quoted Imerys accuracy. The standard deviation on the data set is only 0.16, with an error of 0.12%. Other colour values show similarly accurate readings over the sample set.

3.2.2 Soluble Aluminium

In order to calculate the amount of soluble aluminium present in a calcined clay sample, approximately 0.1 g of sample was placed into a Pyrex™ test tube with a volume of approximately 24 cm^3, to which 10 ml of concentrated (16 M[47]) nitric acid, Analar grade, (Fisher Scientific, Loughborough, UK) was added before being capped with a glass stopper. Tubes were then placed in a rack and immersed in approximately 10 cm of boiling water in the boiling water bath, in a fume cupboard, for four hours before being allowed to cool.

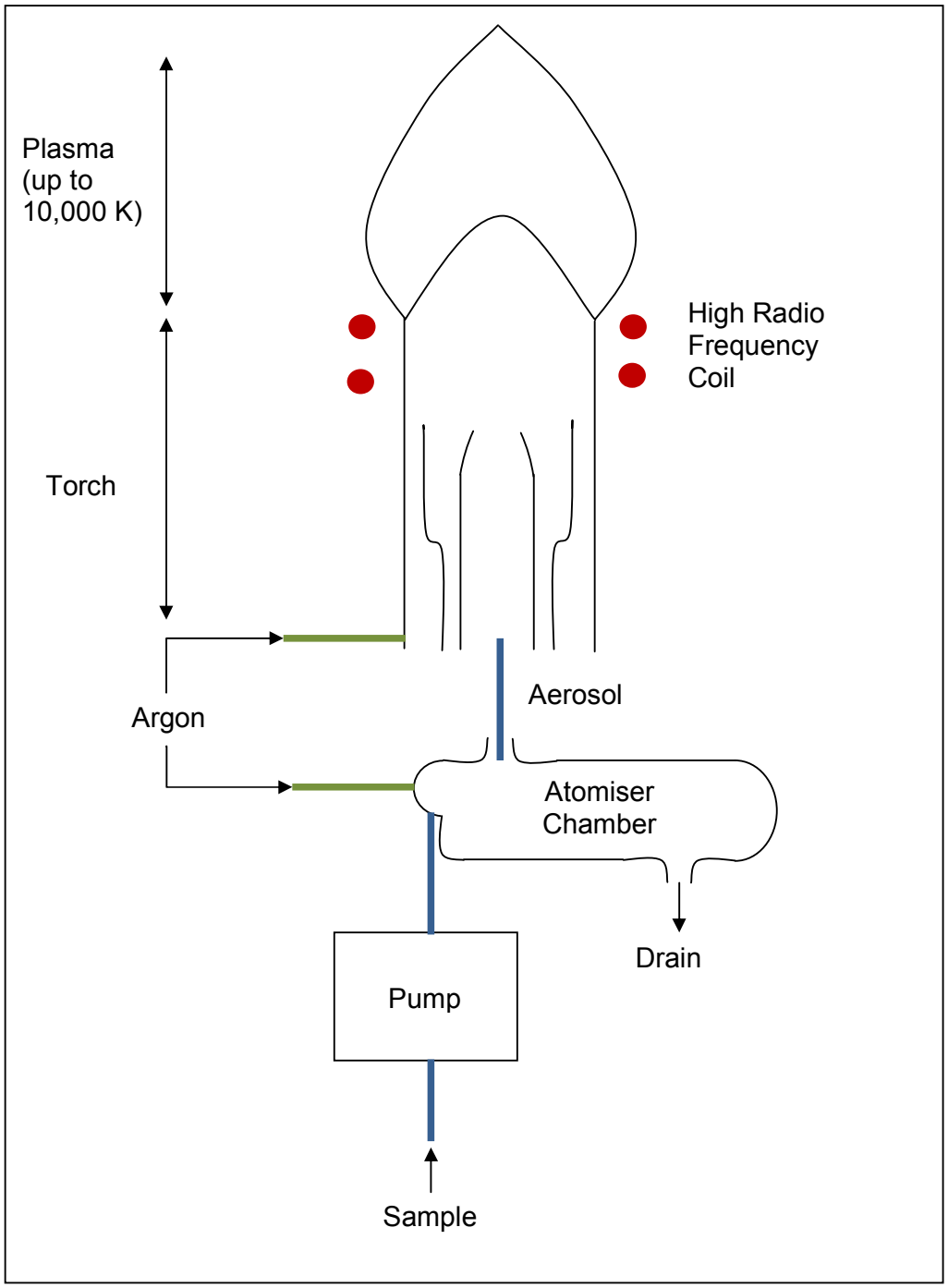

Figure 3-5: Schematic diagram of an inductively coupled plasma torch as used in a Thermo Electron Iris-AP Emission Spectrometer (TJA Solutions, Winsford, UK)

Once the samples were cooled to room temperature, the test tubes were filled to the top with approximately 13 cm^3 of distilled water and the solution was filtered through 12.5 cm No. 40/540 Whatman filter paper, into a 100 cm^3 glass volumetric flask. The filter was then washed with a small quantity of distilled water, into the 100 cm^3 flask and the filtered solute was then diluted to volume, again with distilled water. The solution was shaken thoroughly before being transferred into 6 cm^3 plastic test tubes and tested for aluminium content using a Thermo Electron Iris-AP Emission Spectrometer (TJA Solutions, Winsford, UK), which works using Inductively Coupled Plasma Atomic Emission Spectroscopy and is known as the ICP [48].

The ICP works by ionising argon gas, which is then turned into a plasma fireball using a spark from the high radio frequency coil. The plasma fireball is then maintained when the coil is transmitting a charge. When the solution that is to be analysed is atomised with argon and sprayed into the argon plasma fireball, as shown in Figure 3-5, it volatilises/vaporises on contact with the plasma, breaking it down into its ground state elements. These ground state elements absorb energy from the plasma fireball which causes them to become excited to higher energy levels, which is short lived before emitting light radiation, the wavelength of which is characteristic of the element present. It is operated entirely under vacuum. [49].

The light emitted is then passed over a series of gratings, and reflected in a succession of mirrors which cause the pin-point of light emitted from the plasma fireball to be spread into a spectrum. When this spectrum reaches the detector, it transforms the light into an electrical signal, which the attached computer can then

convert to parts per million. The amount of soluble aluminium, as a wt.% of the total sample, was then calculated using the formula shown in Equation 3-3 [48].

$$\%Al = \frac{(Aluminium\ content\ from\ ICP\ in\ ppm - blank\ ppm) x\ 100\ x\ dil.Factor\ x\ 100}{Sample\ weight\ in\ grams\ x\ 1{,}000{,}000}$$

Equation 3-3: Determining the soluble aluminium content from the ICP reading of ppm

In order to ensure the accuracy of the machine, which is quoted to be 0.1 ppm on pure solutions, a silicon standard solution, SpectrosoL (Fisher Chemicals, Loughborough, UK) is run before any analysis takes place and also as an unknown within the analysis batch. As it is a known quantity, the validity of the measurements for the other samples can be verified.

The error of the method has been tested by repeat submission of samples. The soluble aluminium content of a crucible of Milled HF batch calcined at 1050 °C for 30 minutes has been shown to have a standard deviation of 0.02 wt.% and an overall error of 0.015 %.

3.2.3 Nitrogen Determination

The Kjeldahl method of nitrogen testing, developed by Joseph Kjeldahl involves transforming all the nitrogen, in a weighed sample, into ammonium sulphate by digestion with sulphuric acid, alkalising the solution and distilling the residual ammonia into a boric acid receiver solution. The ammonia content is determined by direct titration of this receiver solution with hydrochloric acid [50].

In order to digest the sample ready for testing, 1 g of sample was added to a Buchi digesting unit (Buchi UK Ltd, Oldham, UK) along with 4 anti-bump balls (Fisher Chemicals, Loughborough, UK) and a single catalyst tablet (Buchi UK Ltd, Oldham, UK). Using a pipette, 10 ml of concentrated sulphuric acid, Analar grade (Fisher Chemicals, Loughborough, UK) was then added to the digestion unit which is then assembled with the scrubber and controller units (Buchi UK Ltd, Oldham, UK) and the digestion cycle started [50].

Once digestion is complete, the sample is transferred to the Buchi automatic distillation and titration unit (Buchi UK Ltd, Oldham, UK), which is filled with 40% Sodium Hydroxide solution (Fisher Chemicals, Loughborough, UK), 1% Boric acid (Fisher Chemicals, Loughborough, UK), distilled water and 0.01 M Hydrochloric Acid (Fisher Chemicals, Loughborough, UK). 5 ml of distilled water, 5 drops of indicator solution (Buchi UK Ltd, Oldham, UK) and a magnetic follower (Buchi UK Ltd, Oldham, UK) are added to a 250 ml conical flask (Fisher Chemicals, Loughborough, UK) is then placed in the receiver position. The unit will then carry out the distillation process automatically [50].

The distillate is then titrated with a 0.01 M hydrochloric acid solution using a burette (Buchi UK Ltd, Oldham, UK). The titration colour goes from green to blue to a gold/brown endpoint. A blank sample tube is then distilled using the Buchi apparatus at least three times or until a titration value is constant. Each 1 ml of 0.01 M hydrochloric acid used relates to 0.14006 mg of nitrogen being present in the sample.

Therefore, the amount of nitrogen present in parts per. million can be calculated using the formula in Equation 3-4.

$$ppm\ Nitrogen = \frac{(Titre - blank\ titre) \times 0.00014\ \times 100\ \times 10000}{Sample\ weight}$$

Equation 3-4:Determination of Nitrogen content in a sample using the Kjeldahl method of nitrogen testing

The method is verified using standard reference materials of known nitrogen content. A soil sample no.502-062 (Leco Corporation, Michigan, USA) containing 0.042% Nitrogen and Standard Reference Material 1551 Apple Leaves (Leco Corporation, Michigan, USA) containing 2.25% Nitrogen are used. These standards are analysed using 1 g and 0.25 g sample weights respectively. A bulk sample of silane treated china clay is analysed in triplicate alongside these standard materials. This bulk sample of silane treated kaolin is then used as a reference sample and run on a weekly basis [50].

3.2.4 Carbon Determination

The carbon content of the kaolin is measured directly by the Leco SC-444DR Analyser (Leco Corporation, Michigan, USA). Concentrations are determined by combusting a 1 g of kaolin sample at 1450 °C in a pure oxygen environment. This causes carbon-bearing compounds to break down and release the carbon, which oxidises to form CO_2. An Infrared cell reads the concentration of CO_2 gas present. This data can then be used to determine the carbon content of the sample [51].

A full range of standards containing 12, 6, 5, 3, 1 and 0.2 wt.% carbon (Leco Corporation, Michigan, USA) are analysed as unknowns before any unknown sample analysis is carried out. Four of these standards containing 0.2, 1, 3 and 6 wt.% carbon are positioned at regular intervals during bulk testing of samples to act as references [51].

3.2.5 Particle size testing (Sedigraph)

A particle falling due to gravity in a viscous liquid is acted upon by three forces: a gravitational force acting downward, a buoyant force acting upward, and a drag force acting upward. Sedimentation size analysis is based upon the fact that the measured equilibrium velocity of a particle through a viscous medium, resulting from the action of the gravitational force, can be related to the size of the particle by Stokes' law. Stokes' law for a sphere is shown in Equation 3-5 [52].

$$D = K\, v^{1/2}$$

Equation 3-5: Stokes' law for a spherical particle, where D is the diameter of the spherical particle, v its equilibrium sedimentation velocity and K is calculated using Equation 3-6

$$K = \left[18\, \frac{\eta}{(\rho - \rho_0)g}\right]$$

Equation 3-6: Determination of K, for use in Equation 3-5, where ρ is the particle density, η the fluid viscosity, ρ_0 is the fluid density and g is the acceleration of gravity.

This equation can be applied to a variety of suspensions, by assuming particles to be spherical. This reduces the accuracy of the method due to kaolin particles being not spherical, and instead the size of particles is given as an equivalent spherical diameter. However, when using sedimentation analysis, the falling rate of the particle is also taken into account as large particles fall at a faster rate than small particles, as shown in Figure 3-6, so aspect ratio issues are not as relevant [52].

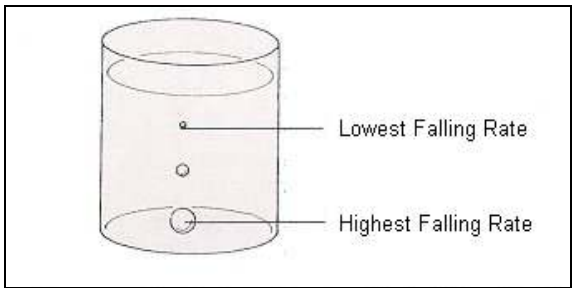

Figure 3-6: Particle size analysis using sedimentation [52].

Difficulties arise in determining the quantity of particles in each size class. This problem was solved by the use of soft X-rays to detect mass. The analysis cell is placed in the path of the X-ray beam, with a window on each side so that the X-rays can pass through the cell to the detector. Sedimenting particles inside the cell then cross the path of the X-ray beam, absorbing the X-rays. The amount of X-ray absorption directly indicates the mass concentration in the spatially separated collection of particles [52].

Measuring the rate at which particles of a certain density fall under the influence of gravity through a liquid of known density and viscosity provides all of the necessary

parameters to apply Stokes' law. The results are then presented as the size fraction below the equivalent sphere diameter.

Particle size was determined using a sedimentation technique, using a Mastertech Sedigraph 51 (Micrometrics Ltd., Dunstable, UK). A 5 g sample of material was mixed in a beaker with 5 ml of dispersant solution containing 1% w/v sodium carbonate and 0.5% w/v sodium hexametaphosphate along with 55ml of deionised water. The beaker was then subjected to ultra-sonic waves for approximately one minute in order to make sure the suspension was fully dispersed, before use with the Sedigraph.

Data is then logged into the computer and, when operating under normal mode the Sedigraph automatically prints a cumulative 'mass percent finer than' distribution, both as a curve and table. More comprehensive results, including a particle number distribution, can also be obtained [53].

This technique has an advantage over light-scattering based techniques as suspensions at high solid volume factions are too opaque for individual particles to be identified and measured. For a light-scattering based system to work, the suspension must either flow through a very narrow channel or undergo dilution in order for the scattered light to be able to pass through it. Studies have shown that a minimum of 5 to 10 % of the laser light needs to pass through the sample in order to perform reliable analysis. If 4 mm is selected as the minimum practical flow thickness, the solids content must be reduced to between 0.1 and 1 % by volume. At

this sample size, it is unlikely that a representative sample of the kaolin has been obtained and consequently results will not be accurate [54].

Repeat submission of a sample of Milled HF that had been calcined at 1050 °C for 30 minutes indicates that the test is reasonably accurate, with an error of only 1.25% for the percentage of the material less than 2 μm in size. The standard deviation on the 2 micron content for the set of samples is 1.7 wt.%.

3.2.6 Particle size testing (Sieve analysis)

There are a number of different techniques used to measure particle size. The most traditional method is a series of sieves with varying aperture size. Where a particle size distribution is required, a stack, or nest, of sieves may be used, progressing from the coarsest to the finest and with a tray at the base to collect fines. Such an arrangement is illustrated in Figure 3-7.

Figure 3-7: Sieve Analysis

The stack is placed on a sieve shaker and vibrated for 15 minutes, with a lid placed on top, after which the content of each sieve is brushed in order to aid the separation process. Once the material is satisfactorily separated, the contents of each sieve are weighed and a particle distribution created. The vibrations have a detrimental effect on any friable or cohesive particles and so affect the size distribution. This process is a very labour intensive and only suitable for particles in the size range 38 μm to 16 mm. There is also a high possibility for error as material will be lost in each sieve and during brushing [55].

3.2.7 X Ray Fluorescence

X-Ray Fluorescence is the spectroscopic analysis of secondary X-rays from the emission of materials excited by high energy X-rays [56]. This enables the elemental composition (based on oxides) of mineral powders to be determined. The program used by Imerys for kaolins, identifies the presence of silica, aluminium, iron, titania, calcium, magnesium, potassium and sodium. These elements were chosen due to the high occurrence in kaolin and for other minerals, other programs which record the presence of different elements can be used instead.

As part of this investigation, samples were examined for compositional variation using the XRF pressed powder technique. This gives a chemical analysis of various kaolins, giving results as percentages of the different oxides present. For each analysis, a mixture of 4 g of sample and 1 g of polyvinyl alcohol (PVA) powder (Fisher Chemicals, Loughborough, UK) was weighed into a container and shaken in a mixer mill for 5 minutes. The fully dispersed mixture was then placed in the well of a motorised laboratory pellet press and made into a pressed disc with a diameter of 32 mm.

These discs were then placed in aluminium dishes prior to analysis and were run on the PANalytical MagiX PRO Spectrometer (PANalytical, Almelo, The Netherlands) and the fluorescent intensities for each element recorded. The source of the excitation is a 4 kW rhodium tube and the detector is wavelength dispersive, allowing a large amount of flexibility in processing samples. Using the recorded intensities and

the known chemical composition of the standards, the calibration parameters for each element can be calculated by the operating software [57].

Before each operation, the XRF spectrometer was calibrated using a suite of standards of pressed powder. This consists of a series of check samples, such as ball clay, limestone, fire brick and soda feldspar, the compound content of which are certified by the Bureau of Analysed Samples, Middlesbrough, UK. In order to verify the results, a series of calibration standards are also used. These consist of Imerys kaolins, from a similar area of extraction as the sample to be analysed in order to try and reduce matrix interference and so increase the accuracy of the test. The chemical properties of the standards have already been determined through both wet chemistry analysis techniques and glass bead XRF, both of which are considerably more accurate but more expensive and time consuming to run.

3.2.8 X Ray Diffraction

The mineralogical compositions of different kaolins were calculated using the X-Ray diffraction (XRD) technique. The process uses Bragg's law of crystallinity as a basis, which relates the wavelength of an X-ray to the specific spacing of the atomic planes [58]. In order for the analysis to be accurate all particles must be less than 10 microns due to the occurrence of peak shift, peak broadening and a decrease in peak intensity for larger particles when they are analysed [59]. Therefore, prior to testing, each 5 g of sample was wet ground inside a McCrone micronising mill with agate elements with 10 cm^3 of water for 15 minutes.

The sample was then filtered using an 11 cm No. 40 Whatman ashless filter paper in a Büchner funnel by applying a vacuum to the filter flask. Once filtered, this sample was placed in the oven at 80 °C until dry. The sample, once dry, was ground in an agate pestle and mortar in order to produce a well mixed, fine powder.

This powder was then transferred into a standard Philips circular sample holder whereupon the edge of a palette knife is used to spread the powder evenly across the holder before it was levelled with the top of the holder. The sample was then gently pressed using the powder press block and any remaining powder from around the sample holder removed using a dusting brush. This sample was then presented for analysis.

The sample was analysed using a PANalytical X'Pert Pro (PANalytical, Almelo, The Netherlands) which is regularly calibrated using a piece of Arkansas Quartz, (Bureau of Analysed Samples, Middlesbrough, UK), pure crystalline silica that does not degrade over time. The X'Pert Pro has a Copper tube X-ray source (filtered to give off Cu K α radiation) mounted on a scanning goniometer, which operates over an angle range of 3 to 60 °. The intensity of the X-rays being diffracted by the sample are then recorded at the different angles. From this data, the composition of the material and the proportions of each mineral present can be ascertained. In order to eliminate orientation effects, the sample spins during analysis.

3.2.9 Thermal Analysis

Differential Scanning Calorimetry (DSC) works by measuring the amount of heat necessary to establish nearly zero temperature difference between a substance and an inert reference material (usually an empty dish) as the two specimens are subjected to identical temperature regimes in an environment with a controlled heating rate [28].

The results are plotted as a graph of temperature against energy in milliVolts per. milligram (mV/mg), as this is the information the thermocouples receive. Graphs of energy in the form of Joules against temperature can be plotted, if further investigation into a temperature region is required. In order to do this, a series of calibration experiments needs to be carried out using samples with known melting points. This is quite a laborious and complicated process and, therefore, only usually performed when detailed information is required, as information in mV/mg is still comparable, allowing the differences in samples to be analysed.

These graphs allow the identification of any exothermic (gives out heat) and endothermic (requires heat) reactions which may occur, and the determination of the temperature at which they are initiated. This allows ideal process conditions for the required product to be developed.

Thermogravimetric analysis (TGA) is a technique in which the mass of a substance (and/or its reaction product(s)) is measured as a function of temperature while the substance is subjected to a controlled temperature program. Such analysis relies on

upon a high degree of precision in three measurements: weight, temperature and temperature change [28].

It is a useful technique to determine characteristics of materials such as degradation temperatures, absorbed moisture content and the levels of inorganic and organic components in the material. The results are plotted as a graph of temperature/time against mass and can therefore be plotted on the same axis as the DSC results.

There are generally several small differences between the traces for the same clay; and these are thought to be due to:

- The instrument itself – it is unlikely to produce results, which are exactly the same as each other due to the instrument not being 100% accurate.
- The amount of material in the crucible – although every effort is made to compact material into the crucible in the same manner each time the amount actually compacted in will differ slightly each time. This links to:
    - The amount of compaction – less, and more, compacted clays will behave differently during calcination.
    - The content of the sample – although taken from the same batch, the exact composition will differ slightly for example, one may have contained more quartz or mica, than the other.

All of these points add up to small errors of around 5% which was considered to be acceptable.

Differential Scanning Calorimetry (DSC) and Thermogravimetric Analysis (TGA) characterisation were performed using the Netzsch 409 Simultaneous Thermal Analyser (Netzsch, Selb, Germany). A correction file was made to compensate for any buoyancy effects which may occur as a result of heating to such high temperatures. This correction file is unique for each heating regime and, therefore, a different correction file should be produced if conditions are changed.

For sample analysis, one pan was left empty as a reference pan, and the other packed with approximately 70 mg of sample in order to minimise air effects and maximise sample size. Both pans were weighed, along with the sample, and the values entered on the computer as part of the operation program. Once the balance has been tared and the furnace closed securely, the analysis was started and allowed to proceed with no further intervention. The temperature profile used for testing as part of this investigation was a heating rate of 10 °C min^{-1} until 1200 °C was reached. The system was then allowed to cool using an air flow.

3.2.10 Scanning Electron Microscopy

In Scanning Election Microscopy (SEM), the image is formed by scanning an electron beam and collecting the signal from beam-sample interaction point by point. The signal collected from each point is then used to construct an image on the display. An electron microscope can help the user determine the following information [60]:

- Topography - The surface features of an object or "how it looks", its texture; direct relation between these features and materials properties (hardness, reflectivity...etc.)

- Morphology - The shape and size of the particles making up the object; direct relation between these structures and materials properties (ductility, strength, reactivity...etc.)
- Composition - The elements and compounds that the object is composed of and the relative amounts of them; direct relationship between composition and materials properties (melting point, reactivity, hardness...etc.)
- Crystallographic Information - How the atoms are arranged in the object; direct relation between these arrangements and materials properties (conductivity, electrical properties, strength...etc.)

SEM analysis was undertaken using a Jeol 6700F Field Emission Scanning Electron Microscope (Joel USA Inc, Massachusetts, USA). Magnifications up to x 20,000 are possible using this equipment. For imaging work, the acceleration voltage used was between 5 and 10 kV while the imaging probe current was set to 6×10^{-11} Amps.

Samples were prepared as suspensions of 50/50 by volume methanol/water and sprayed onto freshly cleaved mica. This was mounted on an adhesive carbon tab on an aluminium stub, before being gold/palladium sputter coated. This coating was carried out in order to avoid charge build-up on the specimen, reduce thermal damage, enhance secondary electron emission and reduce the associated image distortion.

For very coarse samples, where the bulk of the sample is greater than 10 μm, spraying was not possible, samples were instead sprinkled directly onto adhesive

carbon tabs, mounted on aluminium stubs to enable examination to take place. Samples were then sputter coated using the gold/palladium mix.

3.2.11 Surface Area Analysis

The specific surface area of a substance is the area of the particles contained per. unit mass, determined under specified conditions. The Tristar 3000 (Micrometrics, Dunstable, UK) was used to determine the Specific Surface Area of a powder or granulated substance by the Brunauer Emmett and Teller (B.E.T. method). This involves the measurement of the quantity of nitrogen gas that is adsorbed as a mono-molecular layer on the test sample [61].

The adsorption is carried at temperature close to the boiling point of the adsorbate. This is achieved by immersing the test sample in a Dewar flask containing liquid nitrogen. Under these specific conditions, the area covered by a molecule of gas is accurately known. Thus, the area of the test material may be determined by measuring the number of molecules adsorbed. The volume of nitrogen adsorbed is measured using a sensitive pressure transducer that measures the change in pressure occurring in the sample chamber and thereby quantifies the volume adsorbed [62].

In order to prepare a sample for testing using the Tristar 3000, approximately 1.5 g of a dry powdered sample was weighed and transferred to a sample tube, of known weight. The filled sample tube was then re-weighed and the result recorded before the sample tube was placed into the heating elements of the FloPrep 060

(Micrometrics, Dunstable, UK) and heated to 180 °C and allowed to de-gas using nitrogen and hydrogen for 30 minutes. This is an important stage as it removes any material which has been adsorbed either in prior work or during storage [62].

Once cooled, a filler tube is gently fed into the sample tube, taking care not to disturb the sample. The Dewar flask is then filled with liquid nitrogen and sample analysis is started with results given in $m^2 g^{-1}$. The test precision is quoted by Micrometrics as ± 3% and the instrument is ISO 9001:2000 compliant [62].

3.2.12 Freeman Rheometer

The powder flow properties of each of the powders involved in this study were carried out using a Freeman FT3 Powder Rheometer (Freeman Technology, Malvern, UK). Samples were prepared by measuring 160 ml of powder into the sample vessel and the mass required was recorded. A conditioning cycle was then performed before any testing was started [63].

The Freeman FT3 Powder Rheometer measures, the Basic Flowability Energy (BFE), the Stability Index (SI) and Flowrate Index (FRI). The BFE test consists of a standard conditioning cycle followed by a test cycle with a downward transverse tip speed set at 100 mm and a 10° negative helix. This produces a compaction effect at a high flow rate. The SI is measured by repeating the BFE measurement seven times on the same sample, with a conditioning cycle between each test. The value for the 7th test is then divided by the first to give the SI. The FRI test consists of four testing cycles with a downward 10° negative helix at tip speeds of

100/70/40/10 mm s^{-1} with a conditioning cycle between each test. The BFE at 10 mm s^{-1} is then divided by the BFE at 100mms$_{-1}$ to give a ratio [63].

3.2.13 Oil Absorption

When a powder is mixed with oil, the minimum weight of oil required to give a homogeneous paste is an indication of the void volume. This test is applied to dry powders only. The end point of the test is reached when the test material just reaches saturation point. This is when the maximum amount of linseed oil has been absorbed by the test material but insufficient so that it runs over the surface of the paste. This test complies with ISO 787 Part 5: Determination of oil absorption value [64].

The oil absorption of a powder was determined using a 10 g sample. The powder was weighed out and transferred to a glass plate measuring 300 by 300 mm. A few drops of linseed oil were added to the test material using a 25 ml burette. This was then mixed into the powder with a steel bladed palette knife until the mixture was homogeneous. The linseed oil was continually added to the mixture at the rate of 'a few drops at a time', with thorough mixing between each addition until the end point approached [64].

As the testing progresses it is noticeable that with each addition, the linseed oil was progressively less readily absorbed into the mixture. As the maximum capacity of the kaolin was approached (this is known to be 50 to 80 g per 100 g for calcined kaolins

and 40 to 60 g per 100 g for hydrous kaolin) the amount of linseed oil added each time was reduced until the end point was reached. This condition is recognised as when the paste spreads without cracking or crumbling and just adheres to the plate. The amount of linseed oil was then recorded [64].

3.3 Production samples used

3.3.1 Source of samples

Over the course of this investigation, samples have been obtained from several different production routes. The majority of these originated from Cornwall, although samples have also been acquired from Brazil, France, Georgia and Devon. The location of the Brazil, Beauvoir and Georgia Feed deposits are shown in Figure 3-8, while the Lee Moor, Milled HF, deposit is indicated in Figure 2-1.

The locations of the pits of the Cornish samples are indicated on Figure 3-9. Wheal Martyn, Blackpool, Littlejohns and Melbur kaolins come from individual pits, while Double Ground, Residue and SC Residue kaolins are a blend of Wheal Martyn, Blackpool and Littlejohns. Production routes for all kaolins used are illustrated in Appendix B.

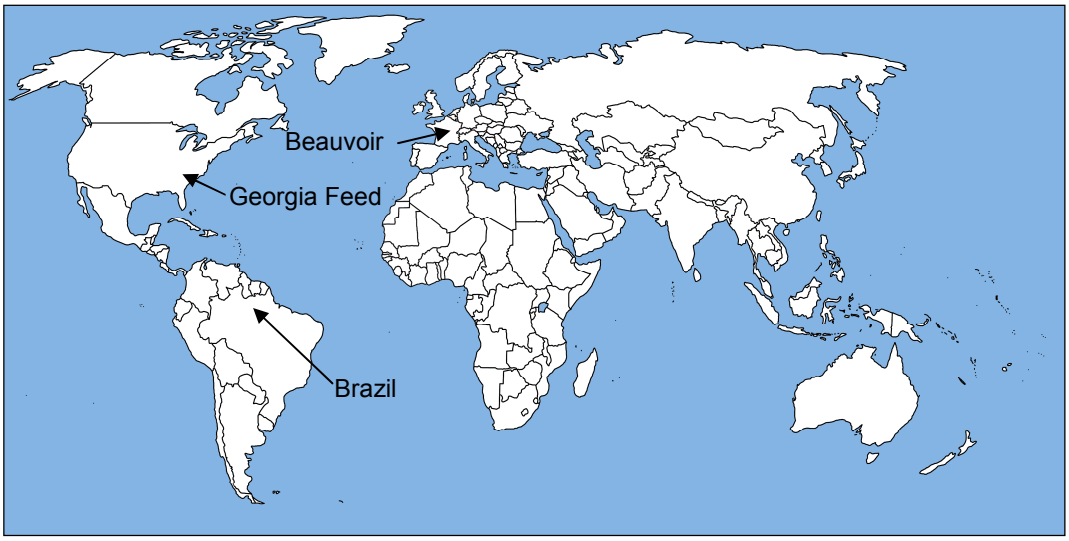

Figure 3-8: Location of Brazilian, French and Georgian deposits

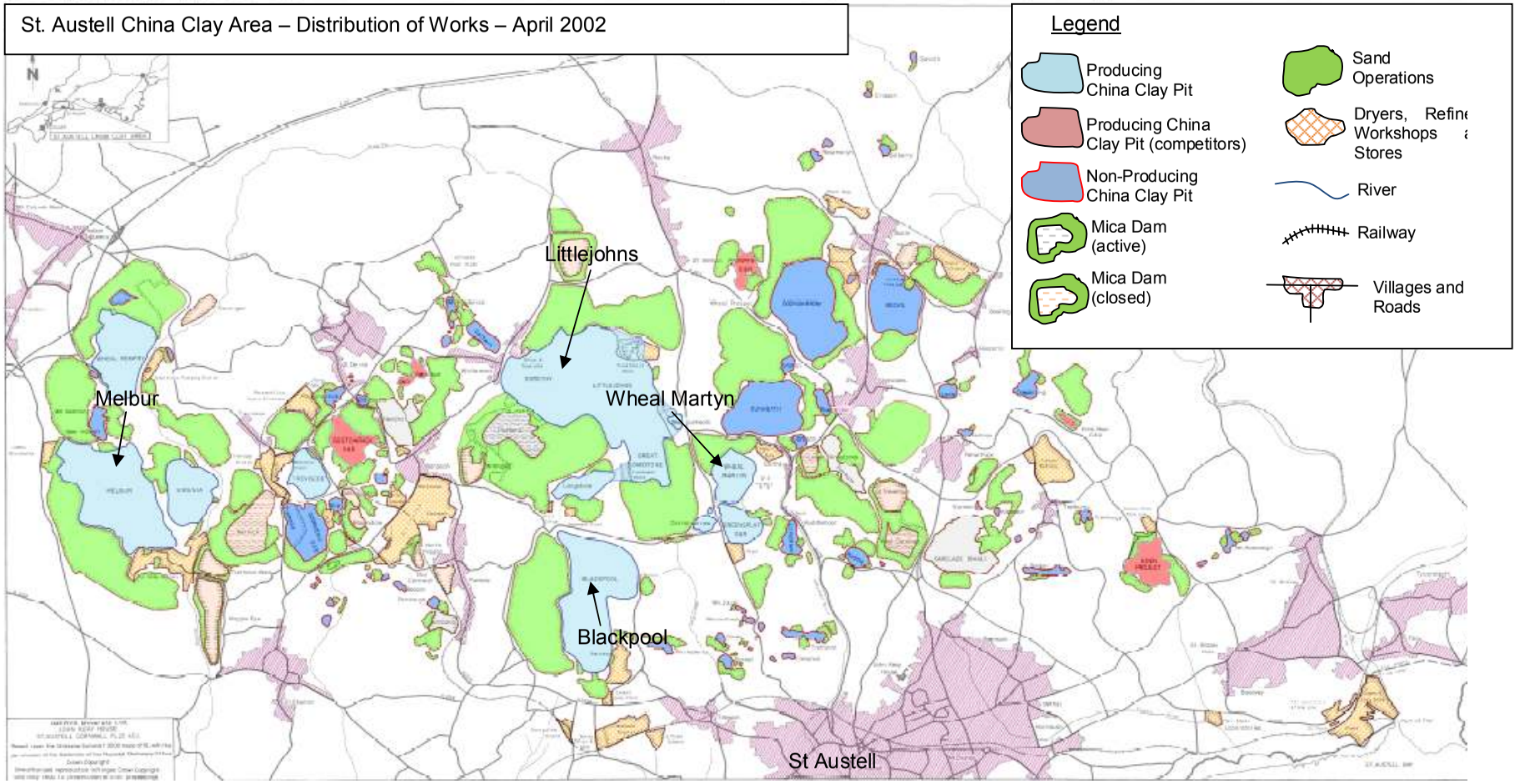

Figure 3-9: Location of pits in Cornwall

3.3.2 Beneficiation of samples in production

Due to the nature of the deposit and the varying purity, some kaolins require more beneficiation than others. The standard procedure for calcined feed is as follows:

- Dorr Oliver (Hydroseparators)
- Centrifuge
- Magnet Separation
- Bleaching
- Drying

The Dorr Oliver is a 15 m diameter, 350 m^3 settling tank, and slurry extracted from pits is fed into the centre of the tank. Three are used in series and employ the principles of gravity settling, allowing the larger particles, which contain most of the impurities to settle into a sludge at the bottom, with the finer particles allowed to overflow over the edge, ready to be collected for the next processing step. The residue from the first stage is diluted with water and then used as the feed for the second stage separator. The product from the second stage is combined with the first stage overflow. The second residue is diluted with water and fed into the third stage Dorr Oliver refiner. The product from the third stage is mixed in with the feed for the second stage of refining, with the third stage residue being sent to the mica dams. The product from the first and second stages becomes the feed for the centrifuge operations. The Dorr Oliver operation is illustrated as a flow sheet in Figure 11-1 from Appendix B.

The centrifuge used in operations by Imerys is a Centriquip 550C (Ashbrook Simon-Hartley, Clay Cross, UK), the cross-section view of which is shown in Figure 3-10. The centrifuge is used in operations to further refine the Dorr Oliver product, to decrease the particle size, ready for further processing e.g. bleaching, magnetic separation, etc. It operates continuously and works by spinning the suspended clay slurry at very high speeds, thereby increasing the gravitational factor by a factor of up to 3000 [65]. The settled solids accumulates at the bowl wall and are discharged by means of a helicoidally shaped screw known as a scroll, which pushes the solids from the cylindrical section of the bowl, up through the conical sections and towards the discharge ports. The liquid phase, known as the centrate, flows back down the centrifuge bowl, where if flows out over a weir plate and into a discharge pipe.

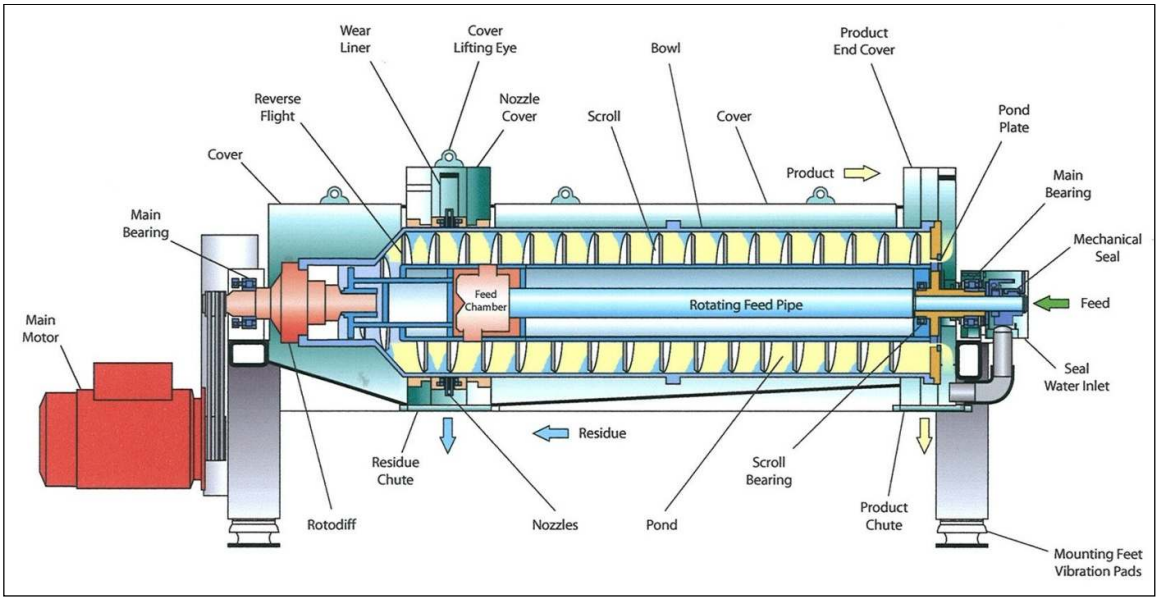

Figure 3-10: Sectional view of a Centriquip 550C (Ashbrook Simon-Hartley, Clay Cross, UK) [66]

Magnetic separation is used to reduce the iron content of the kaolin. All minerals, when subjected to a magnetic field, will respond in a particular manner and are classified into three groups; ferromagnetic, paramagnetic and diamagnetic. Ferromagnetic minerals are defined as strongly magnetised in a low magnetic field, while those that have a weak response are termed paramagnetic. Diamagnetic minerals are those that are essentially non-magnetic. Kaolin is termed paramagnetic and in order to generate the high field strengths required to achieve efficient separation in an economical way, superconducting magnets are used which require cryogens [67].

The Carpco 5T/460 (Carpco SMS Ltd, Slough, UK) used by Imerys as detailed in Figure 3-11 comprises a solenoidal coil sitting in a bath of liquid helium in a vacuum insulated vessel and is energised by introducing an electric current. In order to minimise helium losses, internal radiation shields within the cryostat are cooled using a mechanical cooler (cold head) to preferentially remove the heat. The cold head is supplied with very pure (99.9999%) helium gas from a compressor, which is cooled in turn by low temperature water from a chiller unit [67].

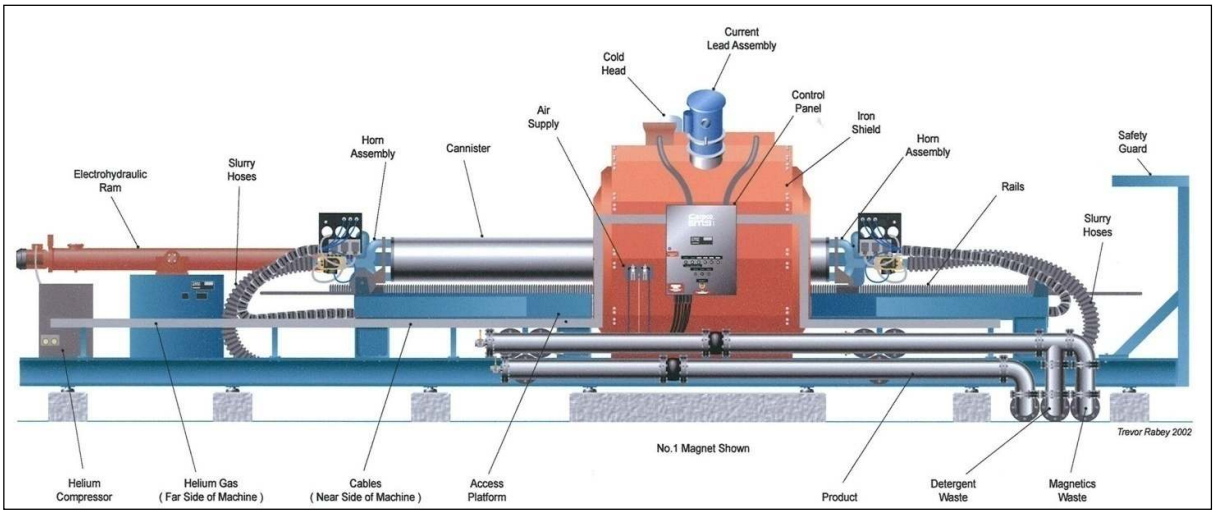

Figure 3-11: Carpco 5T/460 (Carpco SMS Ltd, Slough, UK) [66]

The magnetic separation process is performed within two active sections filled with a wire wool matrix, one at each end of a canister train positioned horizontally inside the magnet. During a cycle, one active canister is situated in the magnetic field and the matrix becomes magnetic. As kaolin slurry passes through the magnetised matrix, the iron based contaminants are attracted to the wire wool and become trapped, while the product is able to flow through the canister. At the end of the processing, the canister is removed from the magnetic field, and the magnetic material is removed from the matrix by flushing it with water, while the other canister is magnetised.

The colour of kaolin in its natural state varies depending on the type of staining on the surface of the kaolin particle. The most common surface contaminant is iron oxide. Sodium dithionite is a reducing agent in aqueous systems and is used to change the iron oxide from its insoluble highly coloured form to a less coloured and soluble iron sulphate. This method is known as reductive bleaching and reduces Iron

III (ferric) to Iron II (ferrous) [68]. The bleaching process used in production is illustrated as a flow sheet in Figure 11-2 in Appendix B.

Bleaching is carried out in a section of pipe termed the bleaching track. The sodium dithionite, a reducing agent (Fisher Scientific, Loughborough, UK) is made up with water in a mixing chamber, ready to dose to the kaolin stream as necessary. The amount of bleaching necessary is determined by an on-line brightness measurement system, Croma (Imerys Minerals Ltd, Par, UK) which automatically determines the dose of sodium dithionite needed for the kaolin being processed.

During the bleaching process, phosphoric acid is used as a source of phosphates which stop the iron reverting to the coloured Fe^{3+} form, while sulphuric acid is used to drop the pH down to 2.8, the optimum for the reaction to take place. Both are added directly to the kaolin stream prior to the sodium dithionite addition and all three chemicals are dispersed into the kaolin stream by an in-line mixer. The residence time within the bleaching track is around 10 to 15 minutes, before the addition of caustic, which is added in order to raise the pH to around 4, ready for landing to the dryer.

There are several technologies used for drying, but all are based on combinations of mechanical dewatering and thermal evaporation. For kaolin systems, mechanical dewatering is effected through use of either high-speed disk stack centrifuges or some form of pressure filter. In these systems, low density kaolin slurries (typically less than 20% solids content) are dewatered to the point where either viscous force

significantly affects fluid flow properties (centrifuges) or where cake permeability affects the rate of water removal (filtration), beyond these points it becomes impractical and uneconomic to dewater further.

At this point, thermal drying is then used to remove further water. Usually, thermal drying is used only to the point at which the constant drying rate occurs, once the loosely bound water is evaporated and the system enters the falling rate zone it is usually uneconomic to dry further. For most kaolin this equates to around 10-14% residual moisture. Thermal drying is usually achieved by combusting fuel to create and air stream of around 500 to 600 °C, this is then diluted with additional air to a temperature of 60 to 80 °C. The volume of air is set by the moisture carrying capacity of the air and hence it's drying potential. The aim is to use the minimum amount of fuel to achieve the drying requirement, so the exhaust air of the thermal dryer is always close to the dew point of the air at the exhaust temperature.

In order for the kaolin to be suitable for use in the Herreschoff kiln, it must be in milled form. The 10-14 wt.% moisture content material is put through an Altenburger swept air mill (Altenburger Maschinen Jäckering, GmbH, Hamm, Germany) which dries it to a moisture content of 0 wt.% ready to be calcined.

3.4 Laboratory Clay Treatments

3.4.1 Wet Blending

Brazil kaolin was blended with several different minerals in order to investigate the effect of mineral chemistry on the properties of the calcined product. The minerals/contaminants included three different pure micas, muscovite, biotite and phlogopite, which are rich in potassium, iron and magnesium respectively. Feldspar and mica obtained from a Devon operations site have also been included in this study. Blends were all made in order to increase the amount of contaminants in the kaolin to 11 wt.%, as this is the level of contamination typically found in the kaolin feed currently used as the feed for the Herreschoff kiln. The results were checked using XRF Analysis, where proportions are given in terms of wt.% for each elemental oxide.

In order to create the blend, 0.89 kg of kaolin was made into a slurry using 2.5 kg of water and 0.11 kg of contaminant mineral was added. The mixture was stirred using a Heidolph RK-6 mixer (Heidolph Instruments GmbH & Co.KG, Schwabach, Germany) for 30 minutes. The pH was adjusted to 4.0 using 5 wt.% sulphuric acid and the suspension was placed on a Buchner Filter before transferring to a piece of oven paper and drying in the oven at 80 °C overnight.

The sample was then milled using a Fritsch P14 mill (Fritsch GmBH, Idar-Oberstein, Germany) before calcination.

3.4.2 Dry Blending

As with the wet blending method, the amount of total contaminants in the Brazil was again increased to 11 wt.%. 0.89 kg of milled kaolin and 0.11 kg of milled contaminant mineral were added to a large plastic bag. The bag was then shaken thoroughly in order to integrate the kaolin and the contaminant. The contents of the bag were then ready for calcination.

3.4.3 Reductive Bleaching

This reductive bleaching method is the same as the one carried out in plant operations, as detailed in 3.3.2 Beneficiation of samples but on a much smaller scale. Dry, milled kaolin was mixed in a beaker with enough distilled water in order to make a fully suspended slurry, where the density is around 1.15 kg m^{-3}, with a solids concentration of around 15 wt.%. The pH of the slurry was then measured using a buffered pH meter and the pH adjusted to 2.8, the optimum pH for the reaction, with the use of 5% sulphuric acid [69].

An appropriate amount of sodium dithionite was weighed out; the quantity depending on the dosage (kg t^{-1}) required, and was gently stirred into the slurry in order to avoid the introduction of air. The slurry was then left to stand for 30 minutes, stirred occasionally and readjusted to pH 2.8 using 5% sulphuric acid as necessary.

After 30 minutes, if the pH is no longer rising and instead remains constant at 2.8, the reaction was deemed to be complete [68, 69]. The pH was then adjusted to 4.0 with 5 % sodium hydroxide and the sample placed on a Buchner Filter for filtering before

drying in the oven at 80 °C overnight. Once dried, a small sample was submitted for brightness testing, see Section 3.2.1 Colour, in order to determine how effective the bleaching process had been.

3.5 Creating Various Feed Forms

3.5.1 Creating the different particle sizes

Calcining trials required two ultra-fine kaolin products, of particle size 70 wt.% < 2 micron and 90 wt.% < 2 micron, respectively. 20 kg of each product were prepared from the same feed, Residue. Residue is a coarse, milled powder kaolin product of approximately 40 wt.% < 2 micron. To produce the finer products, a stirred media mill (Imerys Minerals Ltd, Par, UK) was used under wet conditions and operated as a close-circuit system so as to ensure maximum recovery and to speed up the process.

The kaolin was made into slurry with a density of 1180 kg m^{-3} using water. The pH was then corrected to pH 9.0 using sodium hydroxide and a sodium polyacrylate dispersant, was added at a dose of 1 kg t^{-1} in order to prevent the slurry from thickening [70].

A close-circuit continuous loop was created to pass 87.5 litres of slurry through a stirred media mill, containing 11 kg of 20/40 carbolite media (Carbo Ceramics, Houston, USA) until the desired particle size distribution was achieved. The slurry was pumped into the stirred media mill at a rate of 0.053 m^3 h^{-1} using a Watson Marlow peristaltic pump (Watson Marlow Bredel Ltd., Falmouth, UK).

The product from the stirred media mill was collected in a bucket and poured back into the feed bin at intervals of approximately 10 minutes. The set up is shown in Figure 3-12. The particle size distribution was measured at regular intervals using a Mastertech Sedigraph 51 (Micrometrics Ltd., Dunstable, UK), see section 3.2.5 Particle size testing (Sedigraph).

Figure 3-12: Stirred Media Mill Set Up

When the desired particle size distribution was reached, the slurry was screened using a 53 µm screen. The pH of the slurry was then reduced to pH 4.0 using sulphuric acid before being filtered on a Buchner vacuum filter and dried to 0 wt.% moisture in an oven set at 80 °C.

3.5.2 Milled Feed Preparation

Prior to milling, lump samples were pestle and mortared in order to be the correct feed size to be fed into the mill. Samples were milled using a laboratory scale Screened Hammer Mill (Machine Number 1526, International Combustion Ltd, London, UK) with a screen size of 350 μm.

3.5.3 Spray Dried Feed

Spray drying was carried out on a laboratory scale using a Mobile Minor spray drier with a rotary atomiser (GEA Process Engineering Inc, Maryland, US) as shown in Figure 3-13. During operation, the inlet temperature of the spray drier was set at 330 °C and the outlet cut-off temperature at 130 °C.

Slurry of each of the three different feeds of suitable viscosity to be fed into the atomiser, was made up in a 5 litre plastic beaker. The percentage of solids for each of the three kaolins was different, as shown in Table 3-1. The differences arose due to viscosity differences between the kaolin in suspension, a greater amount of water was needed to fluidise the fine particle kaolins efficiently.

Table 3-1: The percentage solids of the slurry for the three different kaolins used with the spray drier

Kaolin	Percentage solids (wt.%)
40 wt.% < 2 microns	41
73 wt.% < 2 microns	32
90 wt.% < 2 microns	25

Figure 3-13: Mobile Minor spray drier with a rotary atomiser (GEA Process Engineering Inc, Maryland, US)

During the spray drier operation, the slurry was continuously stirred in order to keep the slurry suspended. This was done using a Heidolph RK-6 mixer (Heidolph Instruments GmbH & Co.KG, Schwabach, Germany), set-up at a low speed so as not to introduce air into the system.

The slurry was pumped into the rotary atomiser using a Watson Marlow 505S Peristaltic Pump (Watson Marlow Bredel Ltd., Falmouth, UK) initially at a low speed of 8 rpm, increasing slowly until the system was stable at 24 rpm. The spray dried product was collected at the front of the equipment in 1 litre glass jars which were exchanged at regular intervals.

For each of the spray dried kaolins, the collection of dried product was around 90 wt.% of the feed entering the system, although this was slightly lower for the finer kaolins, where more kaolin particles were entrained in the air stream that is filtered using a bag filter before being expelled to air. Other losses are thought to occur as a result of the kaolin sticking to the inside of the spray drier, to internal pipes, and inside the pump tubing, as well as remaining inside the beaker and not entering the system at all.

3.5.4 Lump Feed

1.5 kg of kaolin was mixed with 0.15 kg of water for 10 minutes in a Kenwood mixer (Kenwood Electronics Europe BV, The Netherlands) in order to form a 10 wt.% moisture product, which is similar in characteristics to a production dried product. This 10 wt.% material was then dried in the oven at 80 °C.

3.5.5 Prill Feed

1.5 kg of kaolin was mixed with 0.5 kg of water for 10 minutes in a Kenwood mixer (Kenwood Electronics Europe BV, The Netherlands) in order to form a 25 wt.% moisture product.

The wetted product (25 wt.%) was then used as a feed for the laboratory-scale pug (Imerys Minerals Ltd, Par, UK), which consists of a Heligear HDMO motor (Opperman Gears Ltd., Newbury, UK) that turns a 29 cm long screw at a rate of 126 rpm. The screw is enclosed by a metal casing, and when the kaolin is fed into the

system, the rotating screw forces the material through an opening of variable size, allowing different sized products to be produced. The pug is shown in Figure 3-14.

The laboratory-scale pug was developed by Imerys in order to be able to replicate the pugging process carried out in production which is used to change the ceramic properties of the kaolin by introducing shear, making the product stronger and finer, both highly desirable properties.

Each kaolin was forced through the pug with exit diameters in place of 3 mm, 6 mm and 9 mm. When it exited the pug, the kaolin was in long spaghetti-like strands, which were dried in the oven at 80 °C before being broken into individual prills with length equal that of the diameter.

Figure 3-14: Laboratory-scale pug (Imerys Minerals Ltd, Par, UK)

3.5.6 Granulation

A blend of 2.7 kg of milled kaolin and 0.2 kg of water were mixed at a motor speed of 0.8 kW, using an Eirich mixer (Maschinenfabrik Gustav Eirich GmbH & Co. KG, Hardheim, Germany) as shown in Figure 3-15. Whilst in operation, a differing amount of water was added gradually to the powder, depending on the particle size of the feed. The amount of water added is shown in Table 3-2. As with the other techniques, more water was necessary for the finer kaolin.

Figure 3-15: Eirich mixer (Maschinenfabrik Gustav Eirich GmbH & Co. KG, Hardheim, Germany) with the mixing blades and bowl visible.

Table 3-2: The amount of water added to the system for the three different kaolins when the Eirich mixer was in operation

Kaolin	Amount of water (kg)
40 wt.% < 2 microns	0.5
73 wt.% < 2 microns	0.6
90 wt.% < 2 microns	0.7

Once the granules had begun to grow and were flowing freely in the mixer, a further 0.3 kg of dry kaolin was added, the mixer power was increased up to 1.8 kW for ten seconds before turning down to low power and allowing the material to tumble at the standard power of 0.9 kW for ten minutes. The contents of the mixer were then transferred to a lined oven tray and the sample was placed in the oven at 80 °C to be dried overnight.

Once dry, the material was dry-screened so that it was within the size range 1.4 mm to 0.5 mm. The 73 wt.% < 2 μm gave the highest yield of 39.9 wt.%. The other yields were 33.9 wt.% and 31.7 wt.% for the 40 wt.% < 2 μm and the 90 wt.% < 2 μm, respectively. The yield was not thought to be specific to particle size, but more related to the operation of the machine and rate of water addition.

3.6 Regression Analysis methods

Given a set of data, a linear regression model assumes that the relationship between the dependent variable, y and the independent variables, x is approximately linear. More specifically, regression analysis allows it to be determined how the dependent variable changes when any one of the independent variables is changed, while the others are held fixed [71].

Fitting a regression model requires several assumptions:

- Errors are uncorrelated random variables with a mean of zero
- Errors have constant variance
- Errors are normally distributed

Analysts should, however, always consider the validity of these assumptions and conduct analyses to examine the adequacy of the model [72].

Both the single factor and multiple factor regression analysis models used as part of this work used the method of least squares to determine a straight line through the data. The least squares technique is a mathematical method for finding the best-fitting curve to a given set of points by minimizing the sum of the squares of the offsets ("the residuals") of the points from the curve. The sum of the squares of the offsets is used instead of the offset absolute values because this allows the residuals to be treated as a continuous differentiable quantity. However, because squares of the offsets are used, outlying points can have a disproportionate effect on the fit [73].

The Coefficient of Determination (R^2) is often used to judge the adequacy of a regression model. It is often referred to as the amount of variability in the data explained or accounted for by the regression model. It is calculated using the formula shown in Equation 3-7 and varies between 1 and 0, where 1 indicates a perfect-fit. In is generally accepted in the scientific community that an R^2 value of 0.95 indicates a good-fit model [72].

$$R^2 = 1 - \frac{sum\ of\ squared\ errors}{total\ sum\ of\ squares}$$

Equation 3-7: Determining the Coefficient of Determination (R^2) for a regression model where the sum of squared errors is also known as the residual sum of squares and the total sum of squares is proportional to the sample variance.

For this work, the dependent variables were the brightness, soluble aluminium content and particle size of the product of calcination at 4 different temperatures, 500, 700, 950 and 1050 °C. There were fifteen independent variables considered: the aluminium, silica, potassium, iron, kaolinite, mica and feldspar and the loss on ignition (LOI) determined from XRF, the hydrous brightness and yellowness, along with the less than 2 μm content, the d30, d50 and d70 of the hydrous particle size distribution and the mineraliser content, the amount of potassium, sodium, calcium and magnesium present in the kaolin.

3.6.1 Single factor linear regression analysis

The single factor linear regression analysis for this project was carried out using Microsoft Excel 2007 (Microsoft Corporation). After enabling the Analysis ToolPak add-in program, the Regression analysis tool, was employed. As well as giving details of the R^2 value of the data, analysis tool also gives other information, such as how significant a factor is on the dependent variable and the standard error involved in the model.

3.6.2 Multiple linear regression analysis

Many applications of regression analysis involve situations in which there are more than one regressor variable. A regression model that contains more than one regressor variable is a called a multiple regression model. The multiple linear regression analysis carried our as part of this work was carried out using R Statistical Software version 2.8.1 (The R Foundation for Statistical Computing).

Data is collected in an Excel spreadsheet and saved as a csv type file. This removes the data from the spreadsheet format and separates it only by commas, allowing it to be read by the R Software. Initially, the software uses all fifteen independent variables in generating a model that is of best fit to the data. Alongside the formula for the model, the software, as in Microsoft Excel provides details on the error involved in the model and the significance of each factor to the model.

The least significant variable is then removed from the data set and the analysis run again until either the accuracy of the model, determined by the R^2 value decreases so that it is apparent that model is not sufficient to predict the dependent variable or each of the factors is of equal significance in creating the model. A factor is said to be significant to a model if the p-value, which is generated automatically by both Microsoft Excel and R, is smaller than 1×10^{-5} [74].

Quantile-quantile (Q-Q) plots can be generated using the R software in order to further analyse the accuracy of the generated model. As the R^2 is calculated using the sum of squared errors, as shown in Equation 3-7, this can sometimes be

misleading as two errors equidistant from the line of best fit can cancel each other out, causing a increase in R^2 which is not reflected in the ability of the model to predict the dependent variable [74].

4 Herreschoff kiln

4.1 Introduction

The multiple hearth (Herreschoff) calciner, based in Devon, is used to produce the majority of Imerys' UK-based soft calcined kaolin. It consists of eight hearths and operates continuously, capable of dealing with over 100 tonnes a day of 0 wt.% moisture, hydrous kaolin. The kiln is heated on hearths 4 and 6, where the gas temperature is around 1100 °C, although the burners can be manipulated depending on the product specifications.

The exact temperature profile of the kaolin as it moves through the kiln is not known, the extremely high temperatures it operates at, and the presence of moving parts makes sampling impossible. As such, detail on the residence time of individual particles is not known and this can have a significant impact on the product as the presence of either under and over calcined kaolin is detrimental.

With a view to improving product consistency, trials were performed to measure the residence time distribution of the kiln. First titania, TiO_2 and secondly talc, $Mg_3Si_4O_{10}(OH)_2$ were used to individually dope the kaolin and the concentrations of these mineral tracers were detected using X-ray fluorescence.

Calcination is carried out in a laboratory, due to the limited amount of material often available, which after the other necessary tests have been carried out can be as little as 100 g. The laboratory method was developed using samples of kiln feed, outlet

and milled product, which were obtained from production and submitted for XRD, XRF, brightness and particle size analysis. The kiln feed was then calcined under various different conditions, varying the duration and temperature of the calcination, until a suitable production replicating method was found.

During this work it was noted that the response to temperature was often variable, and as a result, it was determined necessary to include a reference sample in all experiments in order to verify that the calcination reaction had progressed in a typical fashion. In order to achieve this, Milled HF was calcined numerous times and the mean result of each of brightness, soluble aluminium and percentage of the particle size less than 2 μm determined. The error value for each property was calculated and by adding and subtracting this from the mean, a range of typical values for the calcination of Milled HF was determined.

4.2 Industrial calciner configuration and operation

The majority of soft calcined kaolin is produced using continuous multiple hearth calciner technology. The multiple hearth calciner equipment examined in this research consisted of eight hearths. The kiln is circular; 6.8 m in diameter; each hearth is 1.1 m high and has a diameter of 6.1 m. The distance between hearths is 0.93 m and the central column diameter is 0.87 m.

The multiple hearth kilns are configured so that the kaolin is fed into the top of the kiln and is then pushed towards a central drop hole by rabble arms, which are essentially a series of motorised rakes. On the second hearth, the kaolin moves from the inside of the kiln to the outside and falls through drop holes in the outside of the hearth as shown in Figure 4-1 [35]. The kaolin continues to fall alternately on the inside and the outside of the hearth as it progresses through the kiln.

Under standard operating conditions, air flow to the kiln is 8000 m^{-3} h^{-1}, whilst the feed rate to the kiln is approximately 5.3 tonnes h^{-1} of 0 wt.% moisture feed, although the rate may differ, depending on feed quality. The rotational speed and orientation of the blades on the rabble arms can be varied in order to change the residence time within the kiln. Burner settings can also be adjusted in order to give a specific temperature profile over the kiln. In this particular kiln, heating, to specific pre-set conditions, is provided with natural gas burners on the 4th and 6th hearths; these are controlled to meet product specifications.

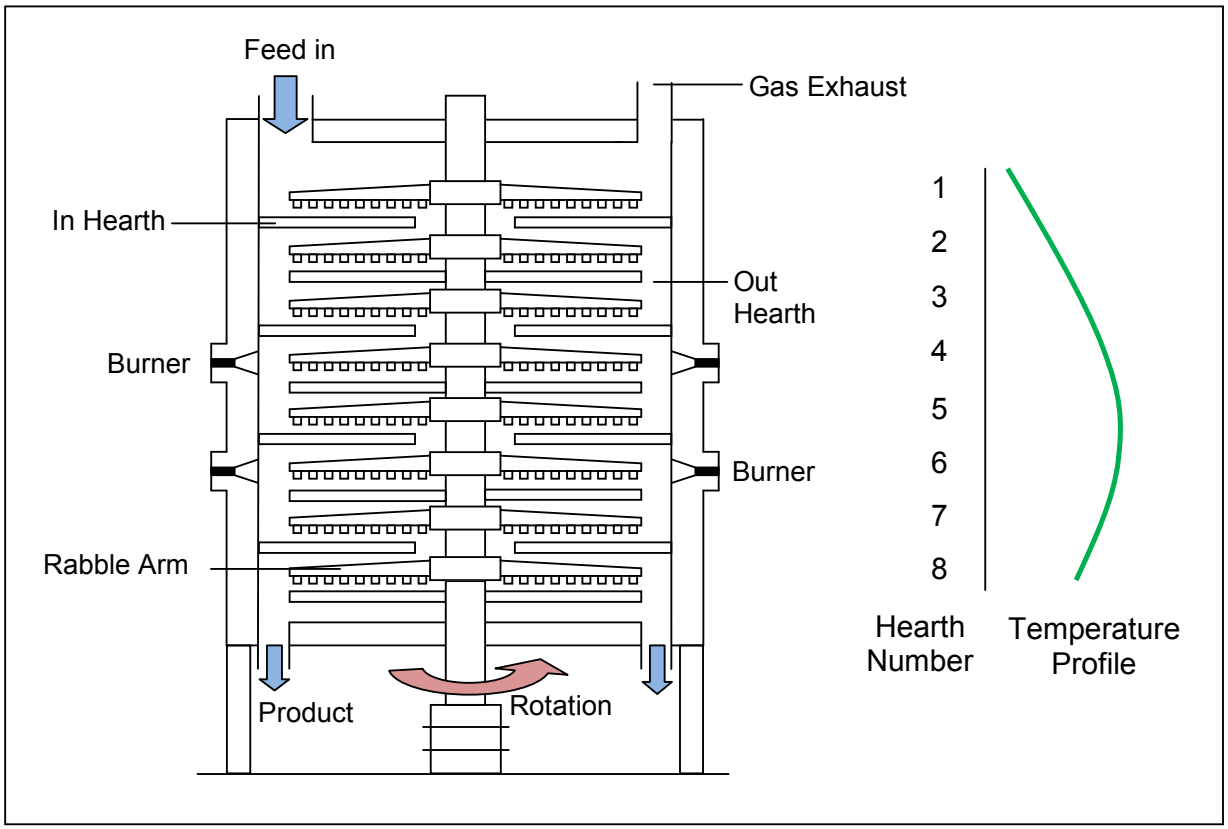

Figure 4-1: Diagrammatic representation of a multiple hearth calciner with eight hearths, showing an estimated temperature profile

The exact temperature profile of the kaolin as it moves through the kiln is not known, although it can be estimated as shown in Figure 4-1. This is due to a number of factors that makes sampling impossible: the kiln is in continuous operation; it is operating at extremely high temperatures and the presence of moving internal parts. As such, detail on the residence time distribution of individual particles is not known and this can have significant impact on the performance of the product.

From experiments carried out with a Herreschoff test rig, where the blade angles were set at 30°, it was determined that the path length for kaolin on the hearth was 7.2 m. The circumference of the kiln is 19.16 m and it can therefore be assumed that

the kaolin only covers 37% of each hearth. By using the flow rate of the feed, and the volume of material accumulated on the hearth, with the assumption that each of the eight hearths are the same, the residence time within the kiln is just less than 40 minutes. This model also assumes that plug flow behaviour is occurring in the kiln. In order to determine the accuracy of this timing, and with the hope of improving product consistency, trials were performed with tracer mineral, to determine the residence time distribution of the kiln.

4.3 Investigating the residence time in a Herreschoff kiln

In order to improve product consistency, trials using a tracer mineral were performed to measure the residence time distribution of the Herreschoff kiln. When choosing a mineral to use as a tracer, it was necessary to use a substance that would not react with the kaolin at temperature and that was easily identifiable even at low intensities. Titania, TiO_2 and talc, $Mg_3Si_4O_{10}(OH)_2$, were used to dope the kaolin individually as the titania and magnesium quantities could be easily distinguishable from the kaolin as neither is normally found in abundance in South West UK kaolins, using X-ray fluorescence. The XRF composition data of the talc, the titania and the kaolin grades used in this study are shown in Table 4-1.

Table 4-1: Showing the X-ray fluorescence results for calcined kaolin and talc (with results presented as percentage by weight of the elemental oxides)

	Al_2O_3	SiO_2	K_2O	Fe_2O_3	TiO_2	CaO	MgO	Na_2O	LOI
Kaolin (wt.%)	38.6	56.9	2.77	0.73	0.02	0.07	0.27	0.13	0.5
Talc (wt.%)	4.7	65.9	<0.01	0.09	0.01	0.29	28.66	<0.11	0.5
Titania (wt.%)	3	5	0	0	92	0	0	0	0

Table 4-1 shows that there is some MgO present in the kaolin used for the trials. It was, therefore, necessary to perform some calibration experiments so that the amount of talc present in the product could be determined. Samples with different talc/kaolin ratios were calcined, under controlled laboratory conditions, and the product examined using XRF, in order to ensure that the mineral tracer did not have a detrimental effect, such as particle aggregation, on the calcined kaolin product, and that it could still be detected after heating. The results are shown in Table 4-2. The particle size of the two tracer minerals used for the investigation is of similar distribution to that of the feed to the calcined with a 300 mesh (53 μm) size of less than 0.02 wt.% and with a 2 μm particle content of 83 wt.%.

Table 4-2: Showing MgO content of various calcined talc/kaolin blends determined by X-ray fluorescence

Talc/Kaolin ratio	0/100	1/99	3/97	5/95	10/90	20/80	50/50	100/0
MgO content (wt.%)	0.27	0.41	0.74	2.13	3.77	8.09	16.01	28.66

Samples of the calcined material were obtained from the exit of the kiln, as it dropped from the kiln discharge point and before it passed into the air blast cooler. These were then submitted for analysis.

4.3.1 Titania tracer experiments

As shown in Figure 4-2, Titania, TiO_2, begins to appear in the product at around 18 to 20 minutes. The level of TiO_2 then rises to a plateau, with a couple of recorded exceptions at 34 and 51 minutes where the TiO_2 levels reach 4.6 and 7.5 wt.% respectively. Once the plateau of around 0.4 wt.% TiO_2 is reached it does not descend during the period of the trial, it is presumed the remaining material is still entrained in the kiln else it has exited the kiln between sampling points.

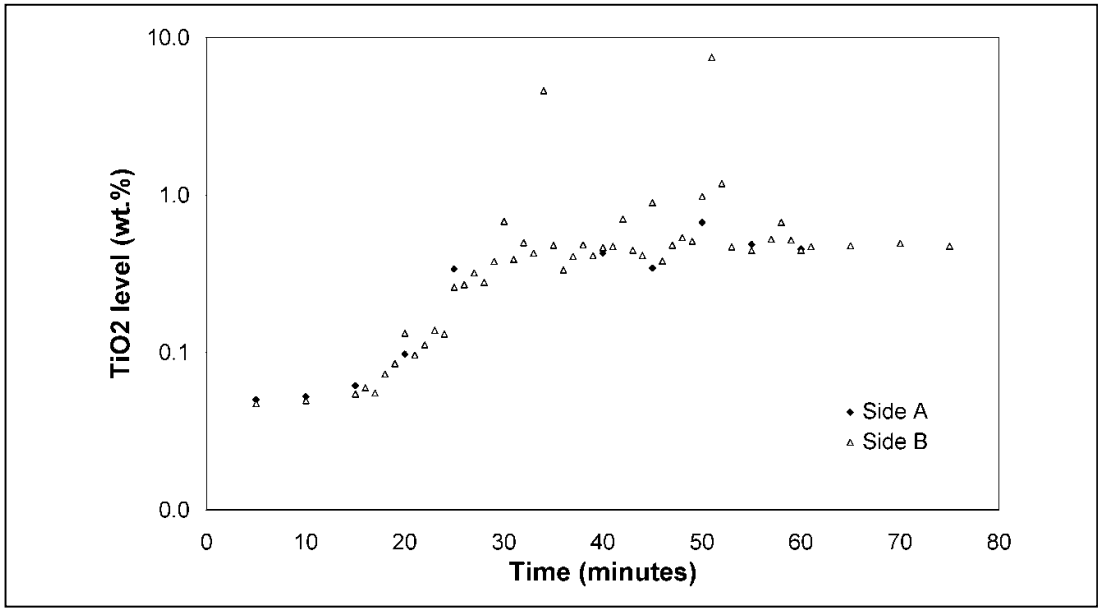

Figure 4-2: Variation of the titania, TiO2, content of the calcined product sample during the period immediately following the titania tracer dosing addition

The data shown in Figure 4-2, indicates that plug flow does not occur and that there is a great deal of short circuiting and recirculation, meaning that the simple geometric model that determined the residence time to be less than 40 minutes, is likely to be inaccurate. However, there is a high level of internal mixing occurring within the kiln, as both sides of the kiln show similar results, which suggests that only one side need be sampled for further tests.

The lack of TiO_2 in the first 20 minutes of sampling indicates that the titanium dioxide did not flow straight through the kiln, and was mixed in with the kaolin. The two large spikes that occur at 34 and 51 minutes giving values of 4.6 and 7.4 wt.% respectively, however, seem to show that some of the TiO_2 may have travelled down the kiln in fairly condensed clumps of material. If this is the case, it means that any mass balance results would be very unreliable because of the method of sampling. It could be possible for large portions of titania rich material to pass through into the product without being sampled. The total quantity of TiO_2 detected in samples from the kiln is around 33.6% of the total added to the kiln. It is unknown how long the remainder took to exit the kiln, as it was not identified by the sampling protocol used, which continued for only 75 minutes after the titania addition, based on the plug flow model calculation.

The difference in specific gravity for the two materials is thought to be the cause for some of the inaccuracies. Kaolin and calcined kaolin have a specific gravity values (relative to water) of 2.6 and 2.65 respectively, whilst TiO_2 has a much higher value of 4.2. It is, therefore, believed that the titania was not carried along with the bulk of

the kaolin inside the kiln, and instead travelled differently through the kiln; possibly, with some segregation from the kaolin or agglomeration. This difference in flow properties is reinforced by the Freeman Rheometer data for the materials, shown in Table 4-3.

Table 4-3: Base Flow Energy, Stability Index and Flow Rate Index and Mass data for Talc, Calcined Kaolin and Titanium

Mineral	Base Flow Energy (mJ)	Stability Index	Flow Rate Index
Talc	1019	0.952	2.29
Calcined Kaolin	799	1.02	1.76
Kaolin	296	1.18	2.27
Titania	3274	1.07	1.33

A perfect flowing powder would have a flow rate index of 1, as all four powders have a flow rate index of higher than one, this shows that all of them are sensitive to a change in flow rate, with talc and hydrous kaolin being slightly more responsive than the other two minerals investigated. The stability index seems to show all four powders are reasonably stable, as all four minerals have a value that is very close to 1, which identifies a completely stable powder.

However, the titania has a Base Flow Energy (BFE) of more than four times that of calcined kaolin, three times that of talc and eleven times greater than hydrous kaolin. This indicates that a greater amount of energy is required to move the titania than the standard kiln product or feed, and as this is the most important value for determining how the powder will react in an industrial situation. It can be seen that TiO_2 flows in a different manner to kaolin and is therefore not suitable to be used as a tracer for this

operation and the results shown in Figure 4-2 are believed to be a poor representation of the residence time for kaolin in the kiln.

The tracer used was therefore changed to talc. This was due to the more comparable flow properties of kaolin and talc, shown by the almost identical Flow Rate Index values and similar specific gravity values exhibited by the two minerals. The difference in Stability Index is considered minimal and although the Base Flow Energy for the three minerals differs it was hoped that this would not cause problems in the kiln.

4.3.2 Talc tracer experiments

The results for the talc experiment are shown in Figure 4-3. The talc begins to arrive at the outlet after about 20 minutes, which is the same as for the titania, shown in Figure 4-2. Some talc, however, remains in the kiln for up to 80 minutes. By the time 90 minutes have passed all of the dosed feed has passed through the kiln and the talc recovery is total. The peak amount of talc in the feed is at 43 minutes, when it is calculated that 4.2 wt.% of the product is talc. The mean time for a particle to spend in the kiln is determined to be 42 minutes, which equates to around 5.25 minutes per hearth.

The initial prediction, based on feed rates and known kiln geometry, was that the residence time would be just below 40 minutes. The difference between the measured value and the theoretical model value may be due to the way the feed moves through the kiln and subtle changes in kiln geometry due to thermal

expansion. The steady peak shown in Figure 4-3 indicates that the flow through the kiln is dominated by a plug flow regime, as expected. However, the large variation in residence time indicates that the flow of powder is not entirely uniform and that the feed follows a more complex, random route through the kiln.

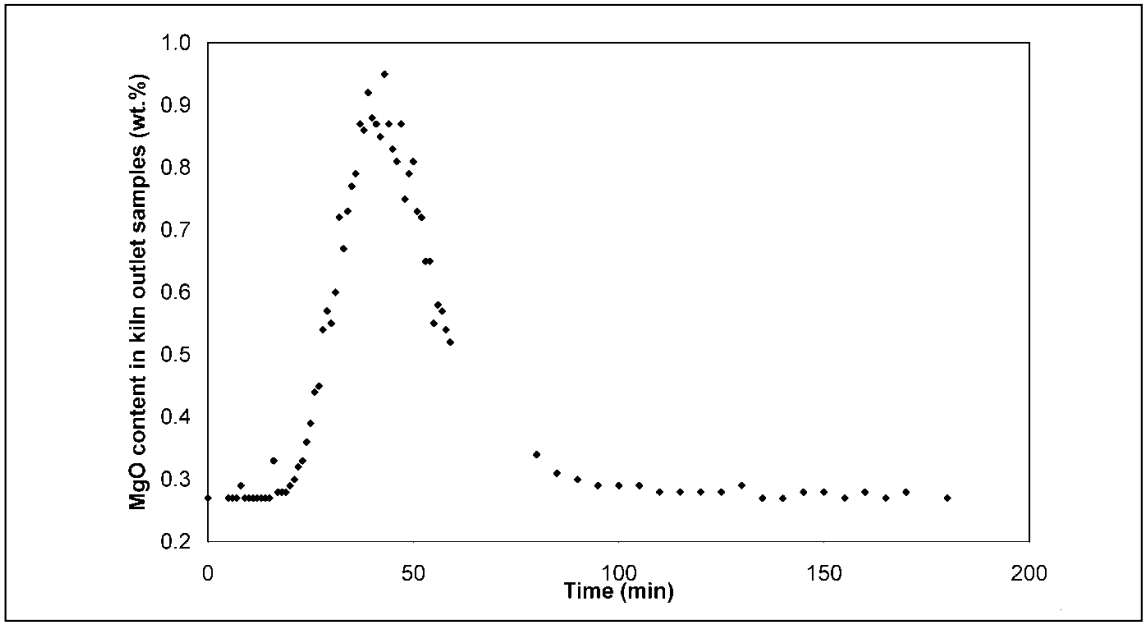

Figure 4-3: The change in talc content (inferred by MgO content) of the calcine product during the talc tracer dosing experiment

This does have some serious implication for the product and its consistency. If kaolin passes through the kiln in twenty minutes, it is highly unlikely that it has been properly calcined. As shown in Figure 4-4, a kaolin sample which has only been exposed to temperature for twenty minutes, under laboratory conditions, has a high level of soluble aluminium present; indicating that the calcined product has some reactivity associated with it. This is due to the calcination reaction not being completed, and the sample being made up of metakaolin. Once the spinel phase is reached, the amount of soluble aluminium present in the product decreases

dramatically. This can be seen in Figure 4-4 to be occurring at around 30 minutes. At the same time, the brightness level (as measured by light reflectance at a wavelength of 471 nm) is increased, as shown in Figure 4-5.

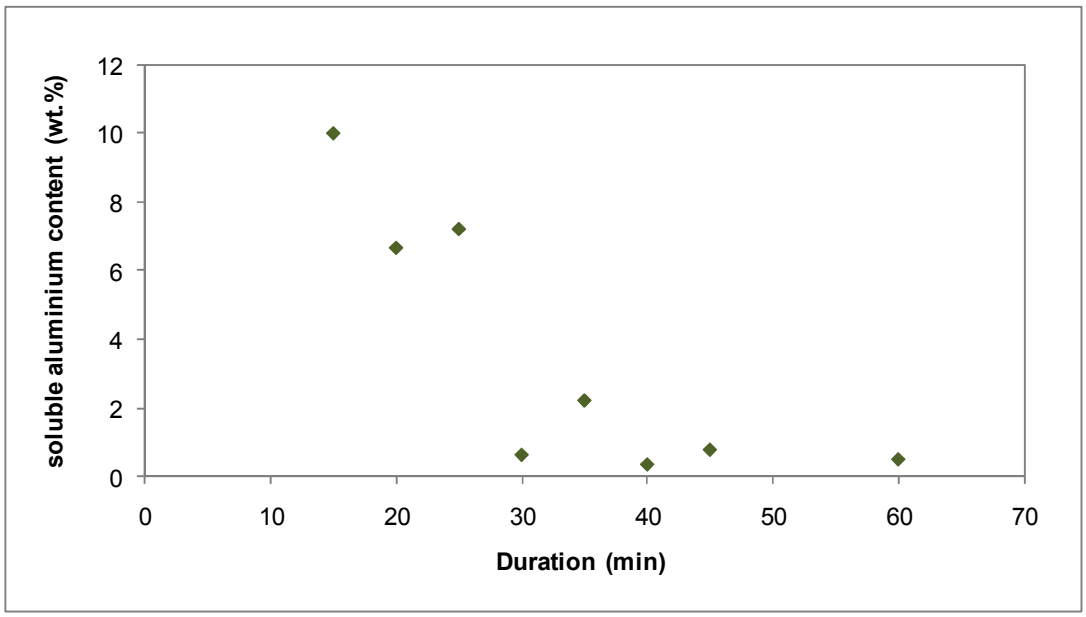

Figure 4-4: How the soluble aluminium content (which is linked to the reactivity) of the calcined kaolin is affected by exposure to a temperature of 1050 °C for varying duration

The data collected here suggests that there is around 15 wt.% of under-calcined product (calcined for less than 30 minutes) which, despite being low, is still high enough to have a detrimental effect for pharmaceutical applications, necessitating the dumping of material. There is also around 5 wt.% of material that is over-calcined (calcined for more than 1 hour) which will not significantly affect the easily identifiable characteristics of calcined kaolin: Figure 4-5 shows only a slight increase in brightness and Figure 4-4 a stable and low level of soluble aluminium.

However, kaolin calcined for more than 1 hour will contain mullite and be more abrasive, causing potential damage to process machinery for both Imerys and the customer. In order to reduce the amount of short-circuiting occurring within the system, the configuration of the rabble arms on hearth 1 was altered, introducing a degree of backward mixing before the kaolin moves through the kiln. This was found to reduce the problem of low soluble aluminium values in the product. If further long-term changes were to be made to the kiln, such as a different product were to be made, if further adjustments were to be made to the kiln, or if the feed material were to change, it is recommended that further tracer experiments should be carried out.

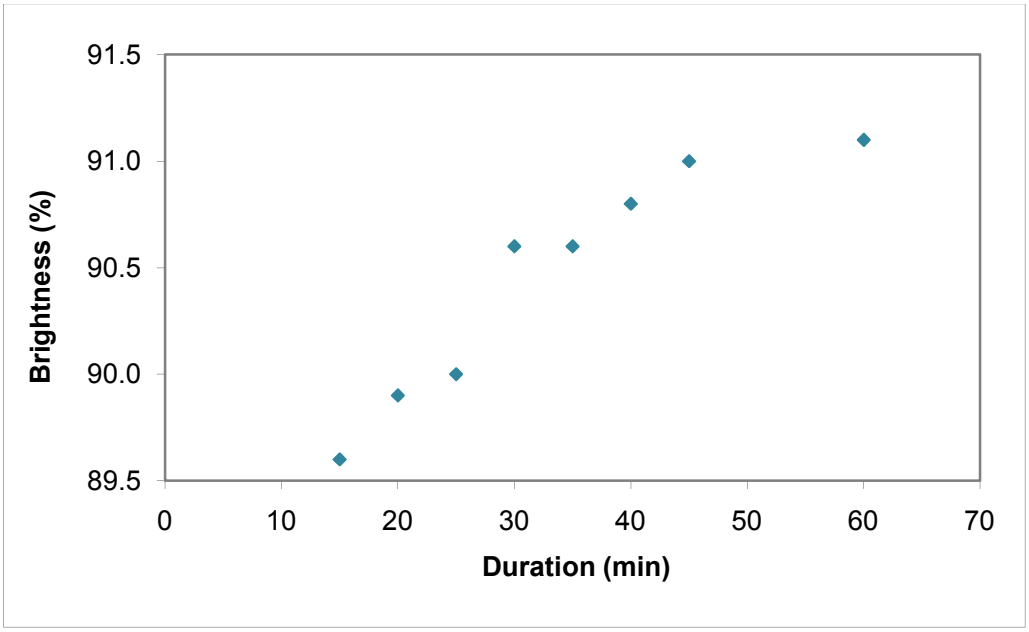

Figure 4-5: How the brightness of the calcined kaolin is affected by exposure to a temperature of 1050 °C for varying duration

4.4 How to replicate a Herreschoff kiln under laboratory conditions

The residence time within the Herreschoff kiln has a mean of 42 minutes. The exposure to temperature is very intense and the constant movement of the kaolin ensures that it is all evenly calcined. This is a difficult task to accomplish on a laboratory scale. However, it was necessary in order to be able to calcine a large variety of samples, of which there were occasionally only small amounts available. A calcined product from the Herreschoff kiln should have a brightness of 90 % ± 1.5 so that it can be used in paint applications and a soluble aluminium content, which indicates the reactivity, of below 5 wt.% [75, 76].

In order to develop a suitable method of replicating the conditions seen at the Herreschoff, samples were obtained from production and consisted of Kiln Feed, Kiln Outlet and Milled Kiln Product and submitted for brightness, particle size and soluble aluminium analysis. The results are shown in Table 4-4 and it can be clearly seen how the kaolin responds to calcination, becoming brighter and coarser. The difference in soluble aluminium content between the Kiln Outlet and Milled Kiln Product, is considered minimal.

Two methods of calcining were used to develop a method, soak and batch calcination. Soak calcining involves placing a crucible into a furnace when it is cold and leaving it inside until the temperature reaches the required level, allowing it to dwell at temperature for the required length of time, before letting it cool at a natural rate. This method is historically the method of calcining used when investigations are undertaken at a laboratory scale.

Table 4-4: Colour, Particle Size and Soluble Aluminium values for Herreschoff Kiln Feed, Outlet and Milled Product

	Kiln Feed	Kiln Outlet	Milled Kiln Product
Colour (%)			
Brightness	85.5	90.2	90.6
Yellowness	5.1	4.3	3.9
Particle Size (wt.%)			
< 2 µm	79.8	38.4	49.8
> 10 µm	1.2	9.7	4.2
Soluble Aluminium (wt.%)	N/A	1.23	2.42

Conversely, batch calcination, involves heating the furnace to the required temperature whilst it is empty and then placing the crucibles inside for the required length of time, before removing them and allowing them to cool naturally on a heat-proof surface.

After experiments, where the duration and temperature of calcination were varied for both methods, it was found that the most successful method of replicating conditions at the Herreschoff was that of batch calcining. The results of the testing can be seen in Table 4-5. Although the required brightness levels were close to being obtained using soak calcination, the soluble aluminium levels, which indicate the reactivity of the material, were far higher than expected. This indicated that the calcination reaction had not progressed to completion.

Table 4-5: Table showing the brightness and soluble aluminium content of Milled HF after calcining at 1050 °C for 30 minutes, using two different methods, batch and soak calcination.

	Soak calcination	Batch calcination
Brightness (%)	89.0	90.3
Soluble Aluminium (wt.%)	10.75	0.44

Although the soluble aluminium result for the batch calcined sample, shown in Table 4-5, is lower than that obtained from the production samples, shown in Table 4-4, it was determined that this was the most suitable duration as when the material was calcined for 25 minutes, the soluble aluminium level was considerably higher, as shown in Figure 4-6. The higher value of soluble aluminium obtained for the 35 minute calcination suggests that the reaction is not entirely predictable. Therefore, in order to not perform an experiment multiple times in order to obtain an average result, which is expensive and time consuming, it was decided to include a reference sample, of which the response to temperature was known, in order to confirm the validity of the result.

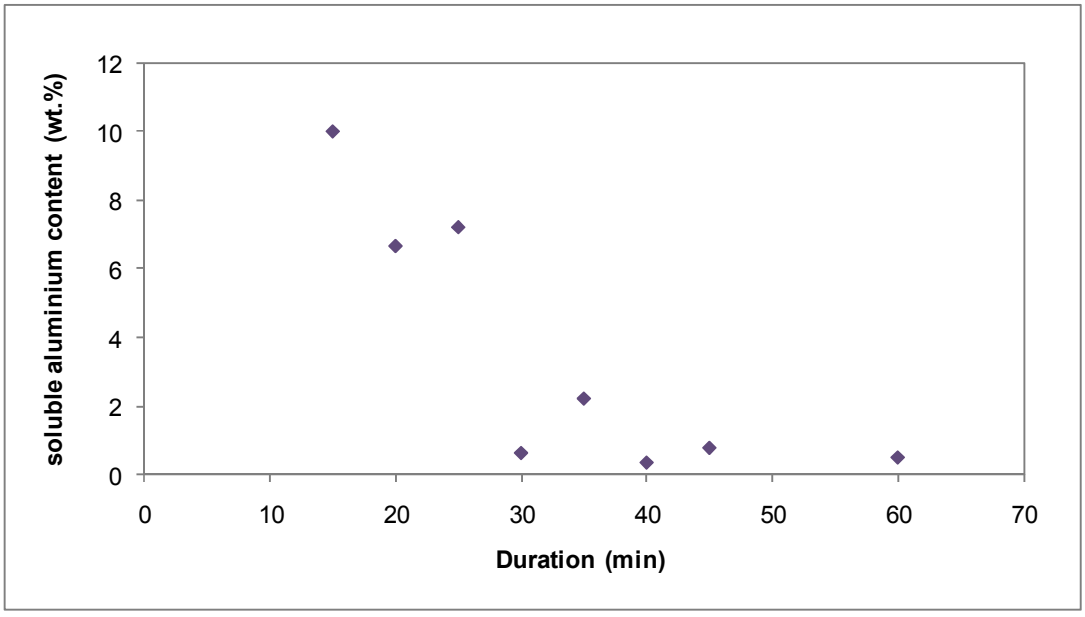

Figure 4-6: The soluble aluminium content of Milled HF batch calcined at 1050 °C for varying durations

4.4.1 The use of reference samples

Due to the unpredictability of the calcination reaction it was considered appropriate to use a reference sample in each experiment. The sample chosen to use as the reference material was Milled HF as it was known how that feed responded to the Herreschoff conditions.

A series of thirty Milled HF samples were batch calcined at 1050 °C for 30 minutes. The calcined material was then tested for brightness, soluble aluminium content and particle size. The results were analysed in terms of average (mean) and error ($4\sigma\ n^{-1/2}$) values for each property, and establishing the maximum and minimum values as the average plus/minus the error respectively. The standard calcination results for Milled HF are shown in Table 4-6.

Table 4-6: The range of values considered to constitute a normal reaction for Milled HF when calcined using the batch method of calcination at 1050 °C for 30 minutes

	Minimum	Maximum	Average
Brightness (%)	90.03	91.06	90.54
Particle size (wt.% less than 2 µm)	38.23	40.71	39.47
Soluble aluminium (wt.%)	0.18	1.34	0.76

Due to the volume of samples calcined as part of the project, it was necessary to obtain further reference material sample. As the Lee Moor deposit, from where the Milled HF was obtained, was no longer being operated, an alternative was sought. FC Feed originates from Lee Moor and despite undergoing further beneficiation compared to Milled HF, is of similar chemistry. Nevertheless, the new reference

sample was again calcined thirty times in order to develop a range of acceptable values which are shown in Table 4-7.

Table 4-7: The range of values considered to constitute a normal reaction for FC Feed when calcined using the batch method of calcination at 1050 °C for 30 minutes

	Minimum	Maximum	Average
Brightness (%)	90.69	91.11	90.90
Particle size (wt.% less than 2 µm)	38.66	41.34	40.0
Soluble aluminium (wt.%)	0	0.96	0.36

4.5 Conclusions

Under standard operating conditions, with a throughput of 5.3 tonnes h^{-1} of 0 wt.% moisture feed, the mean residence time inside the Herreschoff has been determined to be a mean of 42 minutes with the use of talc as a tracer. Talc was discovered to represent the flow properties of kaolin more accurately than titiania, which is understood to move at a different rate and by a different mechanism through the kiln to kaolin. This is probably due to discrepancies in the powder flow behaviour, as reflected in the properties determined with the Powder Flow Rheometer, and also the significant difference in specific gravity between the hydrous/calcined kaolin and the titania. However, if significant changes were to be made to the kiln, such as feed material or operating conditions, which encompasses the flow rate, rabble arm configuration and the number of feed entry points, it is recommended that further trials to determine residence time are undertaken.

In order to develop a suitable method of replicating Herreschoff conditions on a laboratory scale, samples were obtained from production of Kiln Feed, Kiln Outlet and Milled Kiln Product. By calcining the Kiln Feed under different conditions, varying the temperature, duration and method of calcination, it was determined that the most representative method was to calcine samples for 30 minutes at 1050 °C in silica trays using the batch method of calcination.

Due to the unpredictable nature of the calcination reaction, it was considered appropriate to use a reference sample in each experiment. The Kiln Feed, obtained from production was used and was calcined numerous times, before submitting samples for brightness, particle size and soluble aluminium content analysis. The results were then analysed in order to determine an acceptable range for the reference sample values to fall into. When the store of Milled HF was used up, the same testing procedure was performed with FC Feed, also originating from Devon, to provide a new reference material.

5 Artificial Chemistry

5.1 Introduction

Kaolinite is the primary mineral that makes up kaolin. Depending on the geographic location of the deposit, there are a number of contaminating minerals which may occur within the kaolin matrix, including mica, feldspar and quartz. It is known that kaolins with very different mineralogies react differently when calcined [34]. The Herreschoff kiln at Lee Moor is currently run with kaolin that has several ancillary minerals such as mica, feldspar and quartz. The failure of a very pure, Brazilian kaolin to match the product qualities of this feed led to an investigation into whether the overall mineralogy and any accompanying reactions were the cause of the differences.

Several different micas originating from China, Norway, Northern Europe, France and Cornwall were blended with the kaolin as well as with feldspar from Germany in order to artificially change the proportion of kaolinite in the kaolin.

In order to compare artificially blended minerals and the intrinsic chemistry of the kaolin, production samples were obtained from the magnet beneficiation stage of the Wheal Martyn production stream. The magnet product and reject streams were then 'back-blended' in an attempt to form a product with similar chemistry to the magnet feed.

Within other production areas of Imerys, fluxing agents are routinely blended with minerals in order to whiten the product. This was attempted with Western Area kaolin, using nepheline syenite and sodium carbonate. The results for this work are discussed in the following sections.

5.2 The difference between Brazilian and Devon kaolin

When Brazil, a Brazilian kaolin, and Milled HF, a Devon kaolin, were calcined at a series of different temperatures ranging from 300 to 1170 °C, there were distinct differences between the two kaolins in terms of the brightness and soluble aluminium results. The Brazilian kaolin is a newly mined secondary deposit and is, therefore, almost entirely contaminant free. The Milled HF however, is from the edges of a primary deposit, and, therefore, contains considerably more impurities. This can be seen from the XRD results, shown in Table 5-1. The production routes for the two kaolins are detailed in Figures 11-3 and 11-4 in Appendix B.

Table 5-1: XRD results for Brazil and Milled HF

Mineral (wt. %)	Brazil	Milled HF
Kaolinite	99.5	89
Mica	0	3
Quartz	0.5	1
Feldspar	0	7
Tourmaline	0	0
Albite	0	0

Some elemental contaminants, which are present only within the non-kaolinitic minerals, and some, such as iron which are also present within the kaolinite lattice have an effect on the calcined product [33]. Such impurities are identifiable using XRF analysis, the results of which are shown in Table 5-2. They indicate that the Milled HF contains a much larger percentage of potassium than the Brazil. This is most likely due to the presence of potassium feldspar and mica in the Devon deposit.

The amount of iron within the two kaolins is similar, which is probably due to the greater amount of beneficiation the Milled HF receives before it is suitable for use in the Herreschoff kiln, reducing the amount of iron present in the kaolin to an acceptable level.

Table 5-2: XRF results and colour data for Brazil and Milled HF

	Brazil	**Milled HF**
Oxide (wt.%)		
SiO_2	44.7	50.2
Al_2O_3	40.0	34.8
Fe_2O_3	0.51	0.48
TiO_2	0.43	0.0
CaO	0.02	0.03
MgO	0.01	0.18
K_2O	0.01	2.08
Na_2O	0.20	0.09
LOI	14.23	12.18
Colour (%)		
Brightness	88.3	85.5
Yellowness	4.3	5.1
Particle size (wt.%)		
< 2 µm	79.2	79.8

As shown in Figure 5-1, the brightness of the Devon clay decreases dramatically from the hydrous value when calcined at low temperatures. After around 500 °C, the

brightness of the Milled HF increases and once a temperature of 700 °C is reached, the brightness values are similar to those for Brazil.

The decrease in colour at 700 °C has been documented in previous research and it was concluded that the cause was due to the conversion of residual surface iron impurities (oxyhydroxide and gel coatings which were not removed during bleaching) to the intensely coloured red iron oxide, hematite [34]. The decrease in light absorption and increase in brightness on heating above 700 °C is probably due to one or more solid state reactions involving ancillary minerals [33].

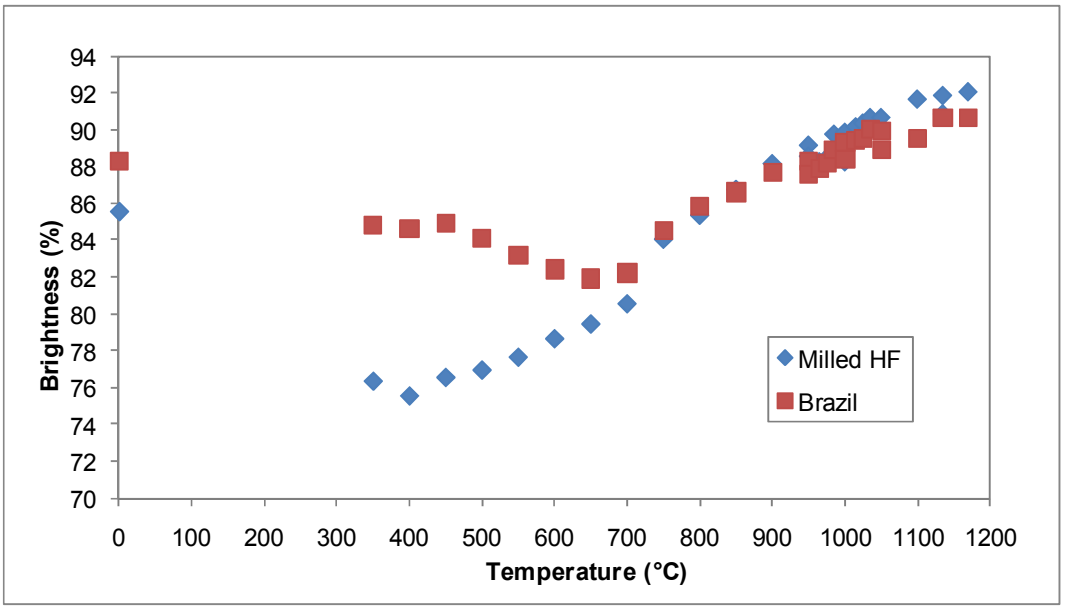

Figure 5-1: The relationship between temperature and brightness for Milled HF and Brazil

The increase in iron content, of 0.03 wt.% between the two kaolins may explain the decrease in brightness of the Brazil when compared to Milled HF at high temperatures, as illustrated in Figure 5-1. However, due to the small quantity of iron

and the distinct gap of 1 to 1.5 brightness points, it is likely there is an additional cause. This may be the presence of TiO_2 within the kaolin lattice. The occurrence of titanium dioxide is known to increase the amount of absorption in a particulate suspension and it is highly probable that it is having a similar effect here [77].

The reason for the initial dramatic decrease in brightness of Milled HF is debatable; the contamination of the deposit with mica and other impurities has been suggested along with the presence of organic contamination on the Milled HF, residual from the beneficiation process [37]. Yet, when the levels of organic contamination; the nitrogen and carbon levels, were examined, the Brazil was found to have significantly higher traces, see in Table 5-3.

Table 5-3: The nitrogen and carbon contamination of Brazil and Milled HF

	Carbon Content (wt.%)	Nitrogen Content (wt.%)
Devon	0.05	0.001
Brazilian	0.10	0.005

There are significant differences in the origin of these contaminants, however. During production, Brazil has around 3 kg t^{-1} of dispersant, polyacrylate added to it, along with around 1.6 kg t^{-1} of sodium carbonate. The only organic deliberately added to Milled HF during production is the dispersant, again polyacrylate, which amounts to around 0.45 kg t^{-1}.

The quantities between the two production routes, detailed above, are far lower than the organic contamination, shown in Table 5-3 suggests. This is because there are other organics, naturally present in the moorland water used in Milled HF production,

such as humic acid. This enters the water due to plant decay on the slopes surrounding the stream that feeds the Lee Moor water circuit. The concentration of this is highly variable, depending on season and recent rainfall; levels are particularly high after heavy rain in the winter when organic matter has begun to decay in large amounts [37].

In order to investigate whether the nature of the organics were causing the colour degradation at low calcination temperatures, a sample of the water was obtained from the Milled HF production site. A 600 g sample of Brazil was mixed with 2.5 litres of that water for several days in order that any organic contamination in the water had the greatest practical opportunity to interact with the kaolin. Once dried and milled, the kaolin was calcined at 300, 500, 700, 950 and 1050 °C in order to determine the colour response to temperature.

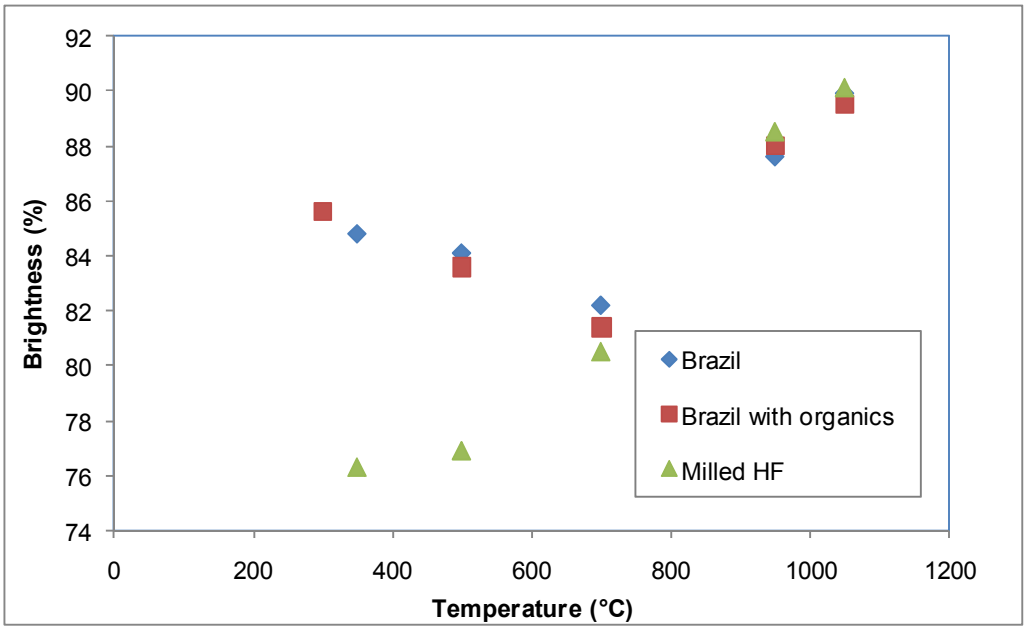

Figure 5-2: The effect of calcination temperature on the brightness of Brazil that has been soaked in Lee Moor process water

The brightness results for the Brazil soaked in Lee Moor water can be seen in Figure 5-2. Although there is some discolouration compared with the pure Brazil, any difference is only slight when compared to that between Milled HF and Brazil shown in Figure 5-2. This suggests that either the differences are not down to organic contamination, or that there was not sufficient organics within the water sample to cause a difference to the Brazil calcination process.

The experiment could be repeated with different concentrations of organics present in the water, as conducted by previous Imerys researchers [37]. This experiment would only be successful or meaningful if there are no synergetic reactions between the organic material and the other impurities of either kaolin or it may be that the organics are having a synergetic reaction with other elements in the Milled HF, such as the mica or the feldspar and hence a deterioration will not be seen with the Brazil.

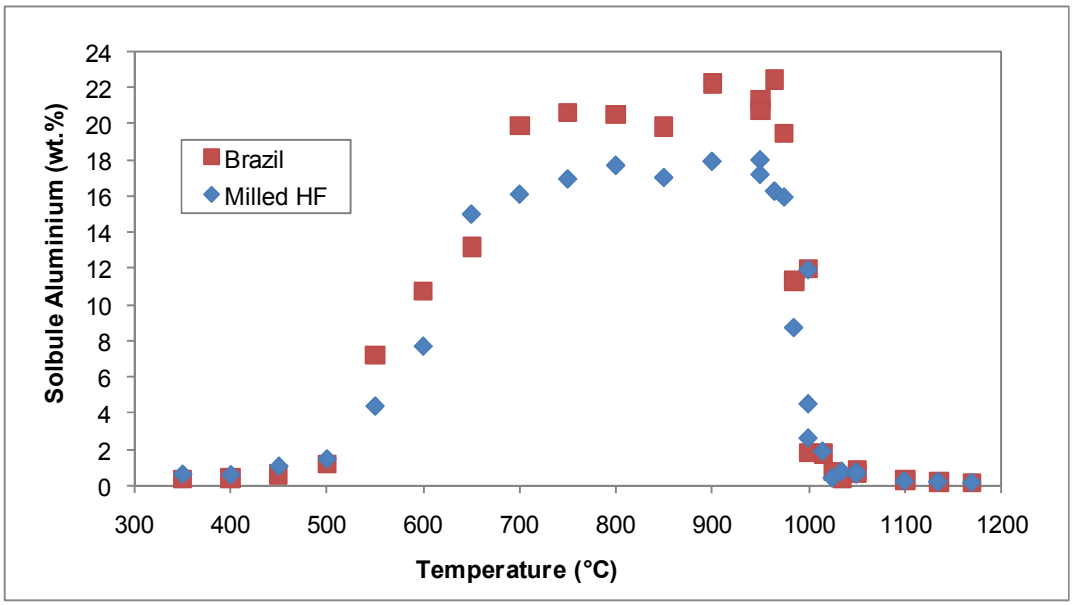

Figure 5-3: The relationship between temperature and percentage of soluble aluminium for Milled HF and Brazil

As can be seen in Figure 5-3, the trend for soluble aluminium levels in the calcined material are very similar in both clays investigated. Soluble aluminium is an indication of the reactivity of the product and is seen to initially increase with calcination temperatures above 500 °C. This is an indication of the start of the metakaolinite reaction, where the kaolinite is dehydroxylated to form metakaolin, an amorphous structure where the aluminium is easily leached out from the mineral lattice.

As the temperature increases further, to around 975 °C, the level of reactivity drops rapidly. This is around the temperature the spinel reaction is expected to start where-upon a crystalline structure is regained, albeit a different one to the hydrous kaolin, and the advantageous non-reactive properties of calcined kaolin are obtained.

The soluble aluminium results for the two kaolins are very similar, with a slightly lower maximum value for the Devon kaolin. This is due to different proportions of aluminium in the kaolins, as shown in Table 5-2. Using the information on gravimetric factors, calculated by Rudolf Loebel which states that the conversion factor for aluminium content from the Al_2O_3 obtained by XRF analysis is 0.52925, the XRF values for Brazil and Milled HF, shown in Table 5-2, indicate that the kaolins have the potential to release 23.29 and 18.41 wt.% aluminium during soluble aluminium testing [47]. A gravimetric factor is a number used to convert, by multiplication, the weight of one chemical into another. In general, gravimetric factors are calculated by dividing the atomic weight of the substance whose weight is sought by the atomic weight of the substance whose weight is known. However, the

calculation can become complicated when the number of atoms of the particular element in the numerator does not match the number of atoms present in the denominator. When this arises, coefficients are used to balance the calculation [78].

The maximum amount of soluble aluminium emitted by Brazil during testing was 22.42 wt.%, at 965 °C. The maximum soluble aluminium value for Milled HF was 17.94 wt.% as a result of the 950 °C calcination. This equates to 96 and 97 % of the theoretical maximum aluminium for Brazil and Milled HF respectively. The remaining aluminium may be trapped within particles and, therefore, not soluble by the nitric acid or it may be released at a temperature not investigated here. The amount of aluminium present within the kaolin can be related to the amount of kaolinite present, due to the contaminant minerals, mica, feldspar and quartz containing a lesser proportion of aluminium within their structure.

The differences between the two kaolins can be seen in the Differential Scanning Calorimetry (DSC) and Thermogravimetric Analysis curves shown in Figures 5-4 and 5-5. The dehydroxylation of kaolinite to produce metakaolin occurs between 450 and 600°C . There is a 14 wt.% loss in content from the Brazil kaolin and a 11.3 wt.% loss from the Milled HF. As a pure kaolinite is expected to lose around 13.9 wt.% of water, this shows that the Brazil sample is much purer than the Milled HF sample. The purity of the Brazil sample is also reflected in the narrow, extended peak for the exothermic spinel reaction, compared with the slightly wider and shorter peak for the Milled HF, indicating the presence of contaminants in the Devon kaolin [28].

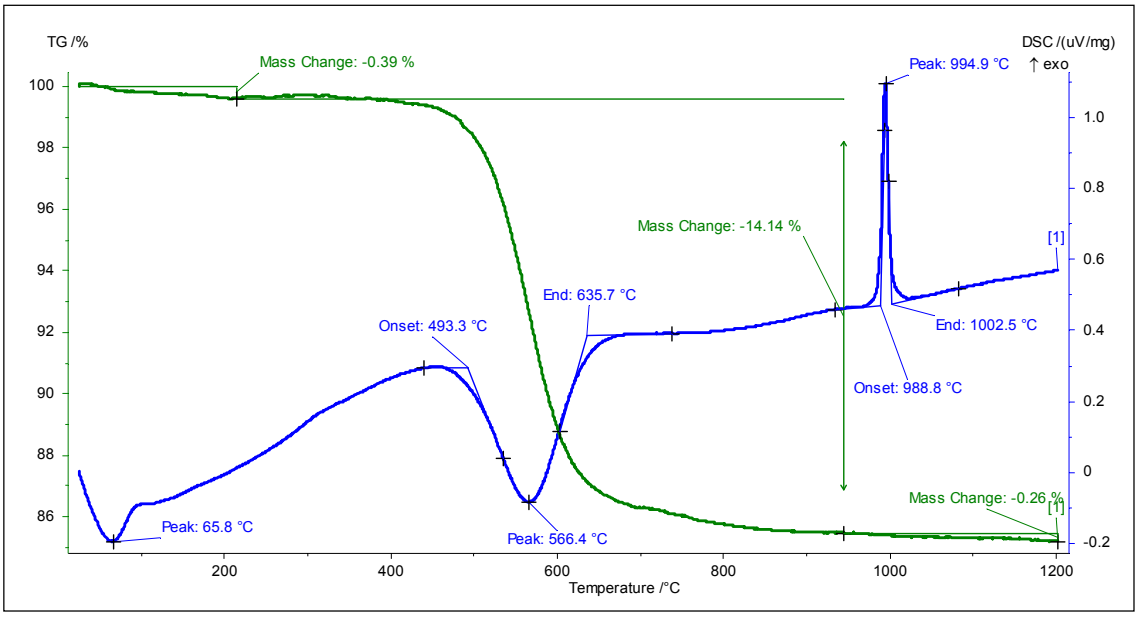

Figure 5-4: Simultaneous Thermal Analysis for Brazil kaolin where the blue line is a Differential Scanning Calorimetry plot (DSC) and the green line a Thermogravimetric Analysis

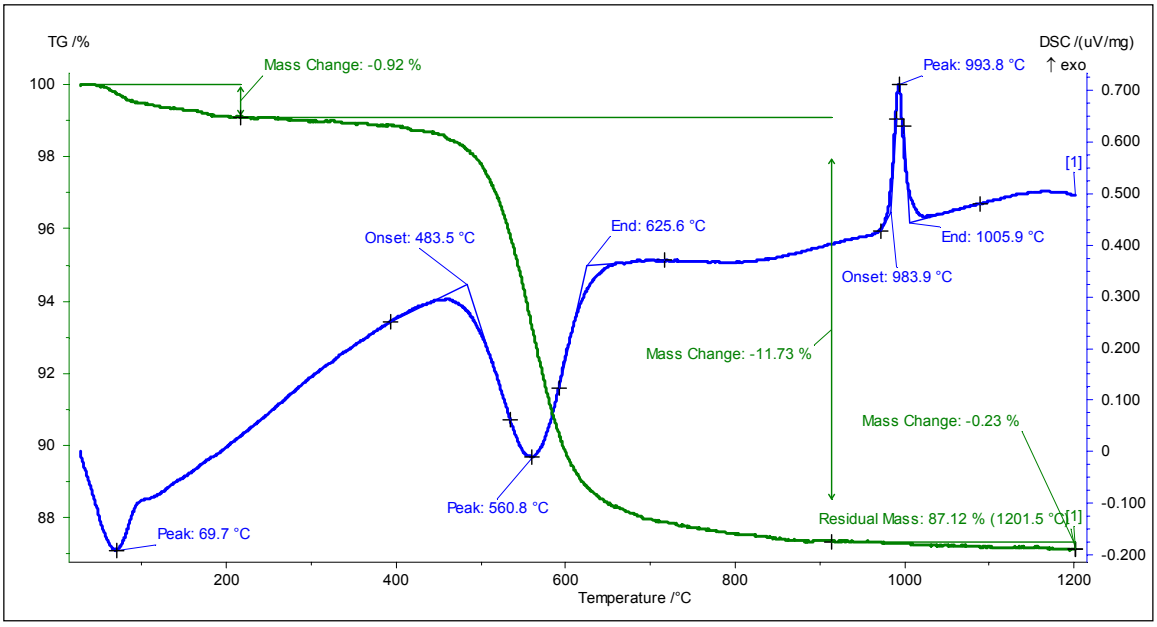

Figure 5-5: Simultaneous Thermal Analysis for Milled HF where the blue line is a Differential Scanning Calorimetry plot (DSC) and the green line a Thermogravimetric Analysis

To study the influence of mineral contaminants more fully, Brazil was blended with a series of minerals.

5.3 Blending Ancillary Minerals with a Brazilian kaolin

5.3.1 Blending with Brazilian muscovite and Feldspar

Brazil was wet blended with muscovite originating from Brazil, and orthoclase feldspar, mined in Germany, to match as closely as possible, the mineralogy of Milled HF obtained by XRF. The elemental composition is shown in Table 5-5, and should be compared with those for Brazil and Milled HF, shown in Table 5-2. The amount of mineral needed to generate a Created HF is detailed in Table 5-4.

Table 5-4: The amount of Brazil, feldspar and Brazilian muscovite required to make Created HF

Mineral	Brazil	Feldspar	Brazilian Muscovite
Amount (wt.%)	89.3	7.7	3.0

The blending process was reasonably successful as the XRF results, displayed in Table 5-5, were similar to that of the Milled HF, shown in Table 5-2. However, exact values were not possible due to chemical composition being a very complex relationship. In the hydrous state, the resultant blend was also brighter than Milled HF, 87.1 % compared to 85.5 %. The particle size of the Created HF was increased due to the presence of the impurities, which were coarser than Milled HF, a change from 79.8 to 67.8 wt.% less than 2 microns.

Table 5-5: The XRF results and colour data for Brazilian muscovite, feldspar and the Created HF

	Brazilian muscovite	Feldspar	Created HF
Oxide (wt.%)			
SiO_2	46.10	66.20	47.0
Al_2O_3	33.40	16.70	37.30
Fe_2O_3	3.59	0.03	0.59
TiO_2	0.26	0.01	0.41
CaO	0.10	0.13	0.05
MgO	1.00	0.18	0.03
K_2O	10.60	15.70	1.43
Na_2O	0.66	0.78	0.23
LOI	4.32	0.21	12.90
Colour (%)			
Brightness	76.9	74.1	87.1
Yellowness	2.0	5.1	4.5
Particle size (wt.%)			
< 2 µm	19.4	15.6	67.6

The blend was calcined at 500, 700, 950 and 1050 °C, as these temperatures were considered to be the most characteristic for the calcination reaction in both brightness and soluble aluminium values, see Figure 5-1.

The brightness results, shown in Figure 5-6 indicate that the Created HF does not replicate the Milled HF response to temperature with respect to brightness. Instead, it follows the Brazil curve very closely, with a constant value of comparatively reduced brightness and out of the three kaolins calcined, has the poorest colour value under standard soft calcination conditions.

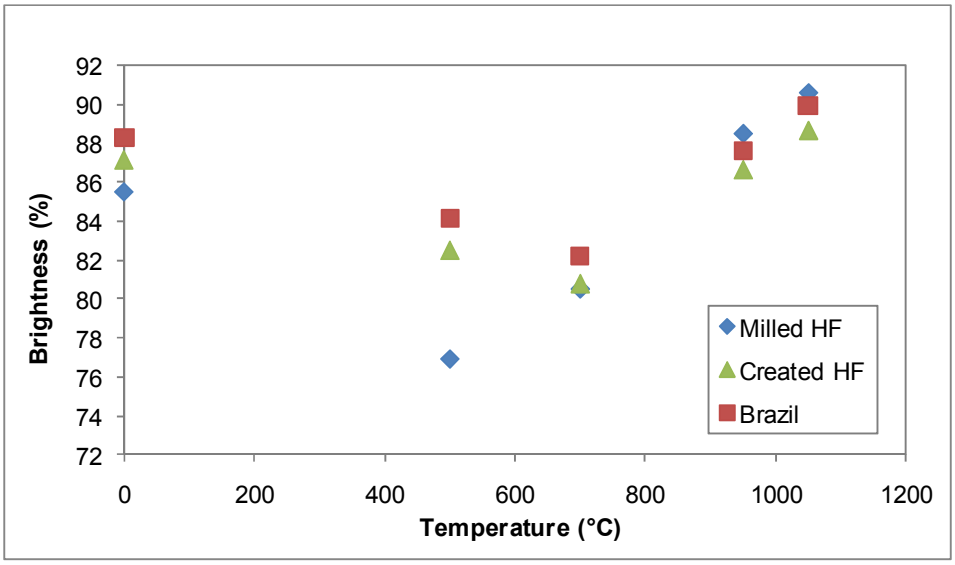

Figure 5-6: The brightness of a Created Herreschoff Feed, Brazil and Milled HF when calcined at different temperatures.

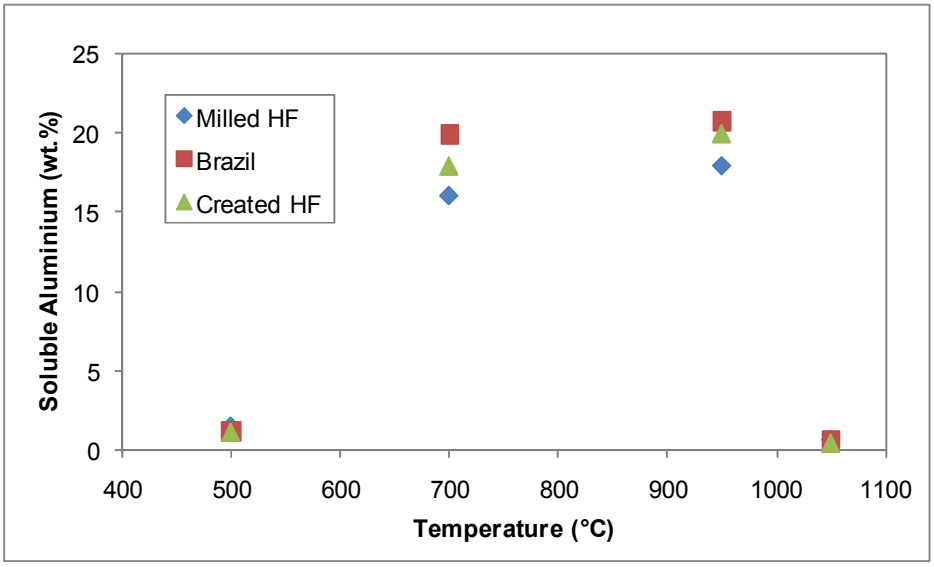

Figure 5-7: The soluble aluminium level of a Created Herreschoff Feed, Brazil and Milled HF when calcined at different temperatures

All three kaolins show a similar trend in their soluble aluminium results, as can be seen in Figure 5-7, with the maximum amount being extractable after fusing at 950 °C, the end of the metakaolin region and start of the spinel reaction. The amount

of aluminium extracted from each of the kaolins is closely related to the amount of aluminium found in the hydrous feed.

There is little change to the calcined product by adding micro-particles, it was therefore decided to blend Brazil with the Brazilian muscovite and feldspar separately, in order to investigate whether the two minerals had an individual impact on the calcination reaction.

5.3.2 Blending with Brazilian muscovite and Feldspar individually

The blends were made up of 89 wt.% Brazilian kaolinite and 11 wt.% contaminants so that they were comparable with Milled HF, the ratio of mineral needed to produce each blend is detailed in Table 5-6.

Table 5-6: The ratio of mineral required to make both the Brazil/feldspar and Brazil/Brazilian muscovite blend

	Brazil/feldspar blend	Brazil/Brazilian muscovite blend
Brazil	89.3 wt.%	89.3 wt.%
Feldspar	10.7 wt.%	0 wt.%
Brazilian muscovite	0 wt.%	10.7 wt.%

The two blends were calcined at 500, 700, 950 and 1050 °C to determine the influence of the minerals on the brightness and soluble aluminium content of the product. The XRF, colour and brightness results for the two blends are shown in Table 5-7 and indicate that both the Brazilian muscovite and feldspar have a detrimental effect on the colour of the hydrous Brazil, more noticeable with the blend containing the Brazilian muscovite than the feldspar blend. However the colours of

the two blends are still slightly higher than the values returned for Milled HF, detailed in Table 5-6.

Table 5-7: The XRF results and colour data for Brazil blended with both muscovite and feldspar

	Brazil and feldspar	Brazil and muscovite
Oxide (Wt.%)		
SiO_2	47.80	45.60
Al_2O_3	36.70	38.40
Fe_2O_3	0.47	0.85
TiO_2	0.39	0.44
CaO	0.04	0.03
MgO	0.00	0.10
K_2O	1.63	1.12
Na_2O	0.24	0.23
LOI	12.70	13.14
Colour (%)		
Brightness	87.6	86.3
Yellowness	4	5
Particle size (wt.%)		
< 2 µm	69.3	68.9

As shown in Figure 5-8, this detrimental effect continues throughout the calcination, with the largest difference being for the product of the 1050 °C calcination. As with the Created HF, a feldspar and Brazilian muscovite blend, the two individually blended minerals exhibit similar brightness curves to the starting kaolin, Brazil, with the significant feature of the lowest colour value being obtained at 700 °C. The muscovite blend exhibits the lowest brightness for all calcination temperatures, with the greatest difference being at 1050 °C where the calcined blend has a lower brightness than the hydrous blend. After 950 °C, Milled HF is the brightest calcined product.

The response to temperature may be due to the nature of minerals present in the kaolin. The form of mica used here, although essentially the same type of mica, muscovite, which occurs in the Devon region, was obtained from Brazil. As with kaolin deposits, different mica sources have distinct characteristics. This is due to different rates of formation and diverse contaminant elements being present, which lead to distinct chemical differences. The purity of the Brazilian muscovite is extremely high and it may, therefore, be having a slightly different effect to the impure Devon muscovite in the Milled HF.

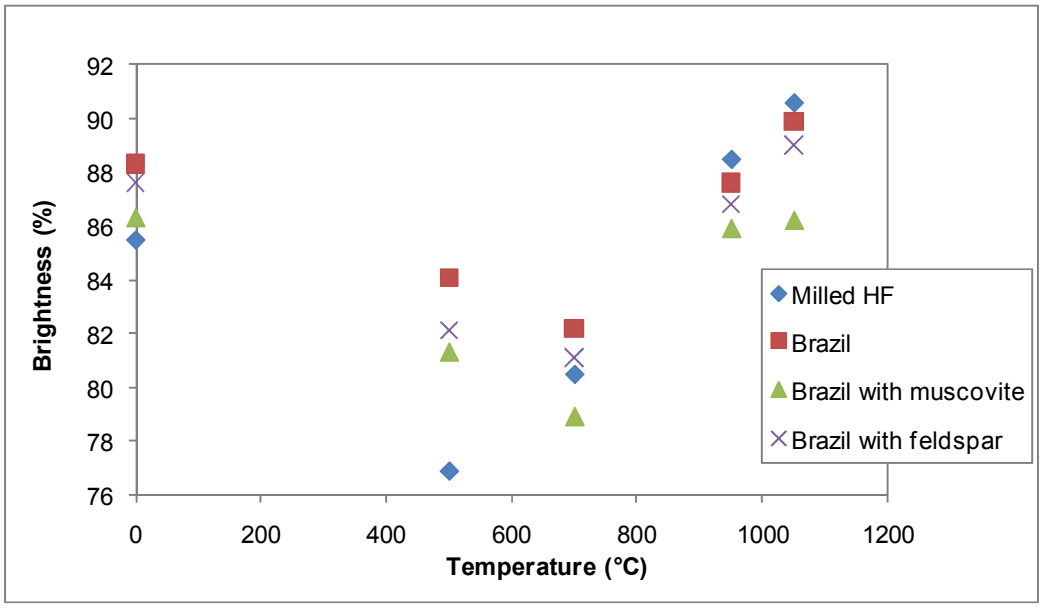

Figure 5-8: The brightness of Brazil blended separately muscovite and feldspar when calcined at different temperatures compared with pure Brazil and Milled HF

The soluble aluminium values for the 1050 °C calcination, shown in Figure 5-9, are all similar for the Milled HF, Brazil and muscovite calcinations, indicating that the same degree of calcination is occurring in the different experiments. However, for the feldspar blend, the value is higher, which indicates that the calcination reaction

has not progressed as far. The value is just less than 5 wt.%, and the sample can therefore still be considered soft calcined.

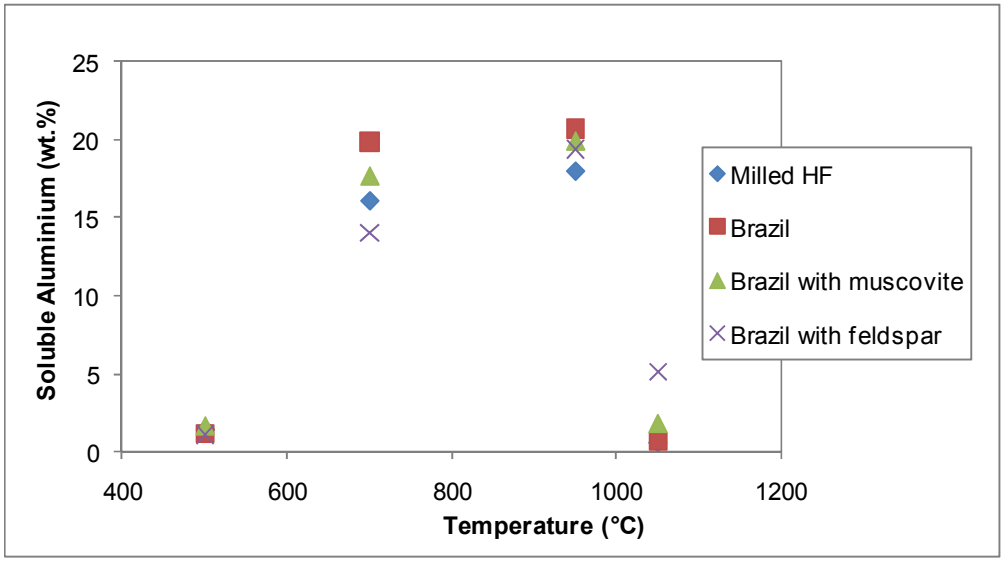

Figure 5-9: The soluble aluminium levels of Brazil blended separately with Brazilian muscovite and feldspar when calcined at different temperatures compared with pure Brazil and Milled HF

Due to the range of soluble aluminium results for the 700 °C it was decided to calcine both the Brazilian muscovite and feldspar individually to investigate whether they had any influence on the soluble aluminium level. As shown in Table 5-5, both muscovite and feldspar contain aluminium within the structure, but it is unknown whether this is released upon calcination. Samples were, therefore, calcined at 500, 700, 950 and 1050 °C and the results are shown in Figure 5-10.

As shown in Figure 5-10, the maximum amount of soluble aluminium retrieved from feldspar was 0.26 wt.% at 700 °C, with slightly more obtainable from the Brazilian muscovite, 1.45 wt.% was extracted from the 1050 °C calcination product. Using the

conversion factor determined by Rudolf Loebel, the amount of aluminium present in the Brazilian muscovite and feldspar, as detailed in Table 5-5, implies a maximum aluminium level of 8.84 and 17.68 wt.% for the Brazilian muscovite and feldspar respectively would be available to the solution [47]. It is clear that far less is released to solution in practice when the minerals are calcined individually.

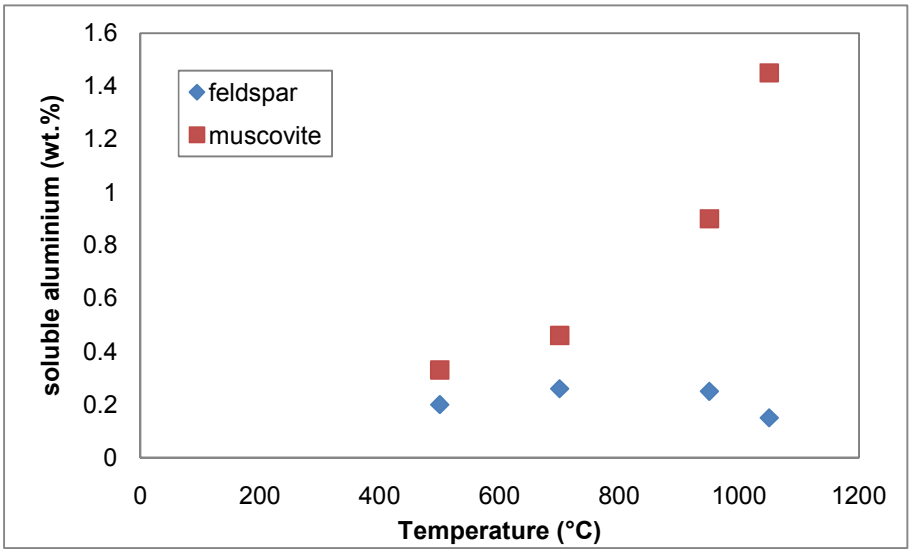

Figure 5-10: The soluble aluminium levels of Brazilian muscovite and feldspar when calcined individually at different temperatures

The theoretical amount of aluminium obtainable from each substance, along with the experimentally obtained values from the calcination of each mineral and mineral blend after calcining at 950 °C are shown in Table 5-8. Also displayed is the maximum amount of soluble aluminium obtainable where individual calcination results are used as a calculation basis. The calculated amounts of soluble aluminium obtainable from the blends using experimental values as a calculation basis are lower than the actual values obtained for the blends. These values are also, in turn

slightly lower than the theoretical amount available according to the gravimetric factors calculated by Rudolf Loebel.

Table 5-8: The maximum amount of aluminium obtainable from different minerals, calculated using the gravimetric factors calculated by Rudolf Loebel, the amount obtained as a result of a calcination at 950 °C for 30 minutes, batch method and the calculated values for the blends using experimental data

	Measured value after 950 °C calcination (wt.%)	Theoretical value (wt.%)	Value calculated from experimental (wt.%)
Brazil	20.71	23.29	-
Milled HF	17.94	18.41	-
Brazilian muscovite	0.90	17.68	-
Feldspar	0.25	8.84	-
Brazil and Brazilian muscovite blend	19.90	20.32	18.59
Brazil and Feldspar	19.38	19.42	18.52

For Brazil and Brazilian muscovite, 98% of the theoretical maximum level is obtained. While for the Brazil and feldspar blend, almost 100% of the maximum level of aluminium is obtained. Therefore, within the blend there must be some aluminium coming out of the feldspar and muscovite. It is not known whether this is due to locality of the kaolinite to the feldspar and muscovite and any accompanying reactions that may arise.

These results are still not comparable with Milled HF. Therefore, the study was expanded to include a variety of different micas, including one found in Devon, in order to investigate the influence of mica and attempt to replicate the deterioration in colour of the hydrous kaolin and the initial deterioration associated with calcining Milled HF at low temperatures.

5.3.3 Blending with different micas

Three different pure micas were blended with Brazil. These were muscovite, originating from China; biotite mined from a deposit in Norway and phlogopite, obtained from a supplier, (Minelco Ltd., Flixborough, England) which is thought to come from Northern Europe. These micas are rich in potassium, iron and magnesium respectively.

Table 5-9: XRF results for Chinese muscovite, phlogopite, Norwegian biotite and Lee Moor mica

	Lee Moor mica	Norwegian biotite	Phlogopite	Chinese muscovite
Oxide (wt.%)				
SiO_2	59.40	37.00	40.50	45.10
Al_2O_3	24.10	13.30	9.70	32.40
Fe_2O_3	1.83	22.31	9.23	5.15
TiO_2	0.40	3.45	0.17	0.75
CaO	0.60	0.21	1.09	0.04
MgO	0.43	13.22	27.46	0.66
K_2O	7.77	22.31	10.40	10.83
Na_2O	0.94	0.07	0.03	0.62
LOI	4.57	1.10	1.50	4.41
Colour (%)				
Brightness	74.9	15.2	35.7	72.8
Yellowness	3.6	5.6	10.1	5.1
Particle size (wt.%)				
< 2 µm	78.7	10.6	13.3	12.8

Mica was also obtained from the Devon area in order to try and compare the same mica chemistry as in Milled HF. The sample was obtained from a mica rich stream in the Milled HF production route, the underflow of the primary hydrocyclone within the pit. This meant that the Lee Moor mica sample was only 34 wt.% mica, it was otherwise comprised of 28 wt.% feldspar and 24 wt.% of kaolin, as well as 9 wt.%

quartz and 5 wt.% of albite. The XRF, colour and particle size data for the different micas used are shown in Table 5-9.

All blends were made up to 89 % kaolinite and 11 % contaminants. The amount of respective mica and Brazil needed for each of these blends is detailed in Table 5-10. These blends were then calcined at 500, 700, 950 and 1050 °C.

Table 5-10: Ratio of minerals required to make each of the different Brazil/mica blends

	Brazil and Lee Moor mica	Brazil and biotite	Brazil and phlogopite	Brazil and Chinese muscovite
Brazil	85.9 wt.%	89.3 wt.%	89.3 wt.%	89.3 wt.%
Respective mica	14.1 wt.%	10.7 wt.%	10.7 wt.%	10.7 wt.%

Table 5-11 shows that there are notable differences in the chemistry of the four blends and the chemistry of both Milled HF and Brazil. The blends made up from the different micas and Brazil all have slightly higher aluminium levels. There is also much more iron present in the four different blends than in either the Milled HF or Brazil. Significantly the amount of potassium does not increase with the presence of the different micas, as most K_2O is found in feldspar.

Table 5-11: XRF results for Brazil blended with muscovite, phlogopite, biotite and mica found from the Lee Moor pit

	Brazil and Lee Moor mica	Brazil and biotite	Brazil and phlogopite	Brazil and muscovite
Oxide (wt.%)				
SiO_2	47.65	45.18	45.51	45.40
Al_2O_3	37.10	35.63	36.45	38.67
Fe_2O_3	0.78	3.13	1.54	1.09
TiO_2	0.46	0.81	0.44	0.48
CaO	0.06	0.07	0.10	0.04
MgO	0.07	1.26	1.93	0.04
K_2O	1.07	1.04	0.94	1.05
Na_2O	0.16	0.10	0.11	0.13
LOI	12.65	12.77	12.99	13.09
Colour (%)				
Brightness	85.3	66.1	79.4	87.6
Yellowness	4.1	4.3	5.6	4.7

The results for the brightness of the different kaolin blends, when calcined at different temperatures, are shown in Figure 5-11. Each of the mica/Brazil blends follow the same trend as Brazil with regards to brightness and temperature. The Lee Moor mica blend and the Chinese muscovite blend, are much closer in value to the Brazil curve, than the biotite and phlogopite blends, for which the deterioration in brightness is more exaggerated, particularly at 700 °C.

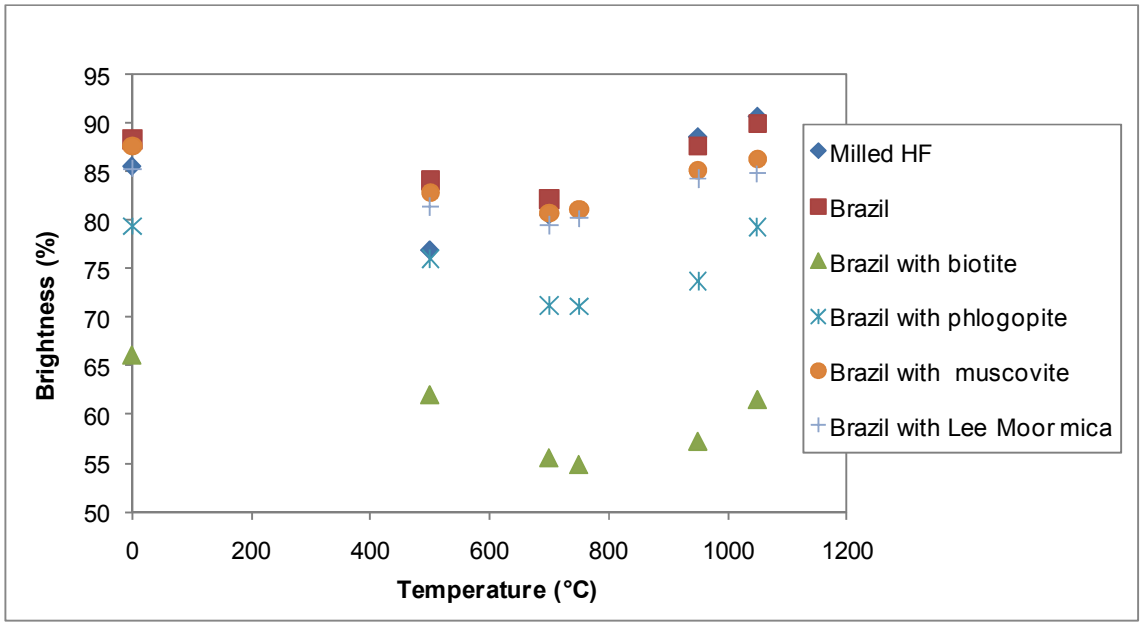

Figure 5-11: The brightness of Brazil blended with different micas when calcined at different temperatures compared with pure Brazil and Milled HF

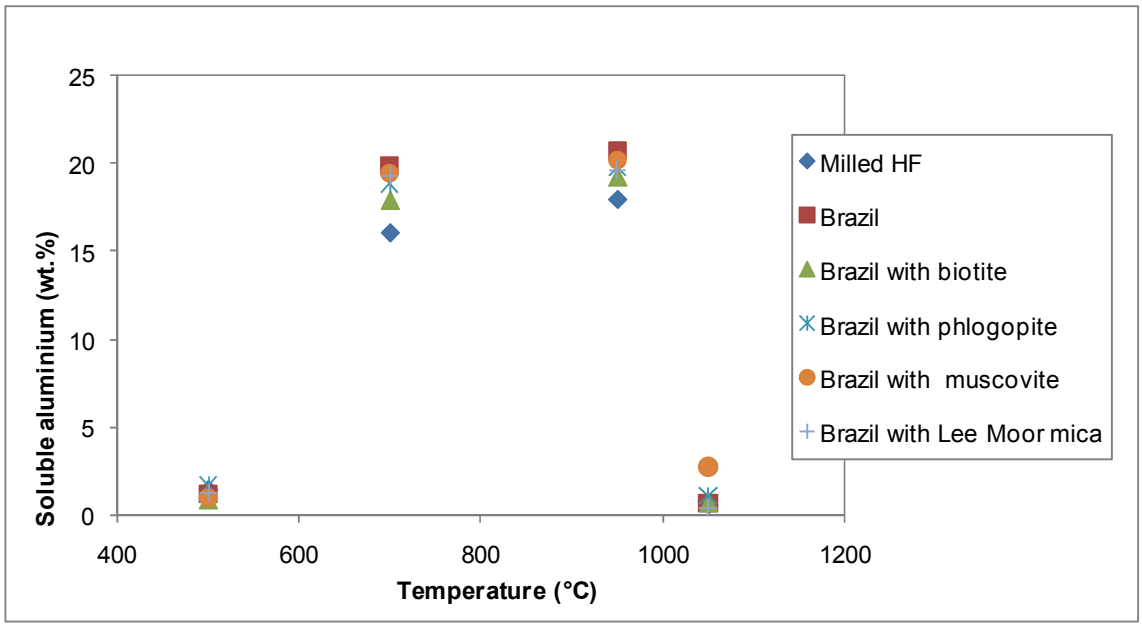

Figure 5-12: The soluble aluminium levels of Brazil blended with different micas when calcined at different temperatures compared with pure Brazil and Milled HF

Figure 5-12 shows that all four of the Brazil/mica blends follow the same pattern for soluble aluminium content as the temperature of calcination changes, with almost the same amount of aluminium released from the powder at 700 °C as at 950 °C. The amount of soluble aluminium in the calcined product does not seem to be comparable with the amount of aluminium in the structure as determined by XRF, although all four Brazil/mica blends do contain more aluminium than Milled HF.

The similarities shown by all five different Brazil/mica blends to the 'parent kaolin' seems to indicate that the wet blending method is not affecting the intrinsic chemistry of the kaolin. Instead, if a particle of a particular mineral impurity is next to a kaolin particle during the calcination reaction, and it is not able to react in immediate locality, there appears to be no reaction at all and instead, the effect on the kaolin is just one of dilution.

Kaolins which naturally contain different amounts of impurities may show a different response to temperature to both Milled HF and Brazil, it was therefore decided to look at blending different kaolins together.

5.4 Blending different kaolins

In order to investigate whether two kaolins blend more successfully than individual minerals with a kaolin, it was decided to examine production samples from the magnet stage of beneficiation, comprising the magnet feed, rejects and product. This stage was chosen due to the batch nature of the operation, making it easy to identify related samples, something which is difficult with continuous processes.

Table 5-12: The XRD and XRF data and colour information for Wheal Martyn (WM) magnet samples, comprising Feed, Product and Rejects.

Mineral (wt. %)	**WM Magnet Feed**	**WM Magnet Product**	**WM Magnet Rejects**
Kaolinite	93	95	78
Mica	6	4	19
Quartz	1	1	2
Feldspar	0	0	0
Tourmaline	0	0	1
Albite	0	0	0
Oxide (wt.%)			
SiO_2	48.00	48.00	48.10
Al_2O_3	37.00	37.00	35.60
Fe_2O_3	0.72	0.60	1.74
TiO_2	0.04	0.03	0.10
CaO	0.05	0.05	0.07
MgO	0.21	0.19	0.34
K_2O	1.66	1.49	3.25
Na_2O	0.02	0.03	0.07
LOI	12.33	12.54	10.77
Colour (%)			
Brightness	85.1	86.4	76.0
Yellowness	5.9	6.1	6.8

Samples were obtained from the Wheal Martyn production route. Wheal Martyn kaolin is from Cornwall and like the standard Herreschoff feed, Milled HF, it contains mica, feldspar and quartz but contains more kaolinite than Milled HF. The XRD and

XRF data, along with the colour data for the three magnet samples are shown in Table 5-12.

Using the amount of kaolinite and non-kaolinite material in the kaolin as a calculation basis, the magnet product was mixed with the magnet rejects in order to replicate as closely as possible, the magnet feed chemistry. The amount of kaolin needed to make the blend is shown in Table 5-13.

Table 5-13: The ratio of magnet reject and magnet product necessary to make the magnet blend

Magnet Sample	Rejects	Product
Amount (wt.%)	11.5	88.5

The XRF and colour data for the blend is displayed in Table 5-14, and shows that the blending has been successful when compared with the data from Table 5-12. The XRF data of the magnet feed closely matches that for the blend for all the oxides. This is in contrast to the individual mineral blending previously carried out.

The Magnet Feed and Magnet Product samples were calcined alongside the created blend at 500, 700, 950 and 1050 °C. The results for the brightness of the different kaolins when calcined are shown in Figure 5-13.

Table 5-14: The XRF data and colour information for the Wheal Martyn (WM) magnet blend

	WM Magnet Product and Rejects
Oxide (wt. %)	
SiO_2	47.51
Al_2O_3	37.18
Fe_2O_3	0.71
TiO_2	0.04
CaO	0.05
MgO	0.25
K_2O	1.64
Na_2O	0.06
LOI	12.57
Colour (%)	
Brightness	84.8
Yellowness	6

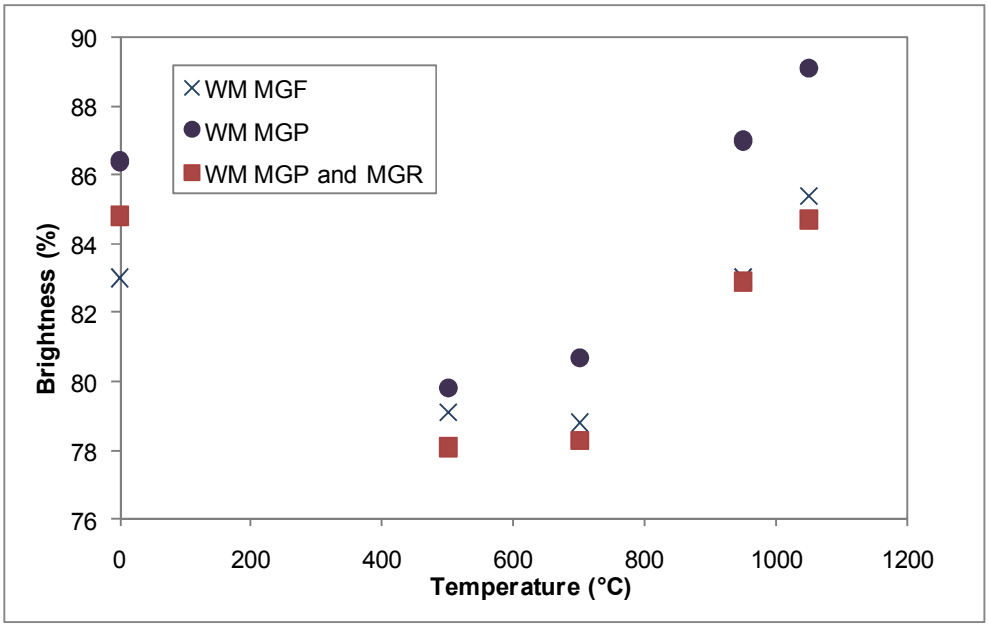

Figure 5-13: The brightness of the Wheal Martyn Magnet Feed and Product (WM MGF and WM MGP)alongside the blend created from the mixing of magnet reject and magnet product samples (WM MGP and MGP), when calcined at different temperatures

The presence of the different impurities is apparent in the difference in calcined brightness for the magnet feed and magnet product, most noticeable in the 950 °C

calcination with a difference of 4 brightness points. The differences also exist for the 700 and 1050 °C calcinations, with differences of 1.9 and 3.7 respectively, however, as a result of the 500 °C calcination the difference in brightness is much smaller, only 0.7.

Overall, the blending for the Wheal Martyn kaolins appears to have been successful, with the WM magnet product/magnet reject blend having a very similar reaction to temperature as the magnet feed. There is a slight decrease in colour for the blend sample at 500 and 1050 °C calcination temperatures, despite the hydrous blend being brighter. Overall, however, allowing for the error in brightness measurement technique, the values show no significant difference.

Whether the blend follows similar brightness trends to the magnet product, as with the Brazil blending work, because it is the main constituent, is difficult to determine without looking at how the magnet reject samples calcine separately in order to compare the effect of the contaminant kaolin and the main kaolin. However, due to the nature of the production sample, magnet reject samples are very dilute, only 450 g of the Wheal Martyn rejects was obtained from a 20 litre sample, this means that there was insufficient sample to calcine at the four required temperatures after the creation of the blend.

This work proves that where the minerals are intrinsic and of a similar natural chemistry, the blending process is much more successful than where the minerals are artificially blended into the matrix. This is reinforced by the similarity of the XRF

results for the hydrous kaolins, see Table 5-12 and Table 5-14 along with the calcination results.

5.5 Western Area Herreschoff Feed with added fluxes

Kaolin mined from the western area of Cornwall, a combination of Melbur and Virginia pits, has been used in a production scale trial at the multiple hearth Herreschoff kiln in Devon. Although promising, the results were not as good as those predicted by lab results or expectations based on feed clay properties. The final product brightness was found to be 87.5, with a yellowness value of 5.8, whereas the standard calciner product has a brightness of 90.5 ± 1.5 and a yellowness value of 4.0 ± 1.5 [75].

As can be seen from the XRD results in Table 5-15, there is a marked decrease in the amount of mica and feldspar present in the WA HF, compared to standard Herreschoff Feed, Milled HF. Both minerals are fluxing agents, which promote fusion during the calcination reaction, and it was thought that this absence may be affecting the reaction.

It was, therefore, decided to investigate increasing the content of potassium and other flux agents through chemical addition using two different minerals; sodium carbonate and nepheline syenite.

Table 5-15: XRD results for Milled HF and WA HF

Mineral	Milled HF (wt.%)	WA HF (wt.%)
Kaolinite	89	95
Mica	3	4
Quartz	1	1
Feldspar	7	0
Tourmaline	0	0
Albite	0	0

These two minerals were chosen because they are already used as fluxing agents by Imerys, albeit in the production of different industrial minerals. During the calcination of diatomaceous earth, (a product of World Minerals, a subdivision of Imerys' Performance Minerals and Filtration Europe (PFME) division), it is standard practice to add extra fluxing agent, sodium carbonate, in order to whiten the final product [79]. Nepheline syenite; meanwhile, is a standard flux supplement in ceramics applications, as it mimics natural feldspars found in kaolin and it has been found to promote fusion. It has an advantage over the use of feldspar found in Imerys production, because it is purer, making interpretation of results simpler as other compounds are not introduced into the blend.

From XRF analysis, detailed in Table 5-16, it has been determined that Western Area HF has a typical potassium content of 1.07 wt.% whilst standard Herreschoff feed has a standard potassium content of 2.08 wt.%.

Table 5-16: XRF Analysis of Western Area HF, standard HF and nepheline syenite

Oxide (wt.%)	WA HF	Milled HF	Nepheline syenite
SiO_2	46.72	50.2	58.0
Al_2O_3	38.40	34.8	23.0
Fe_2O_3	0.68	0.48	0.11
TiO_2	0.01	0.0	0.03
CaO	0.05	0.03	1.00
MgO	0.16	0.18	0.16
K_2O	1.07	2.08	9.13
Na_2O	0.11	0.09	7.84
LOI	12.8	12.18	0.95

The main compounds known to have a fluxing effect on the kaolin during calcination are those containing potassium, sodium and magnesium, as the melting points are within the temperature range of standard operations. The amount of such compounds in nepheline syenite is shown in Table 5-16. It is known that sodium carbonate (Na_2CO_3) has a flux content of 58.5 wt.%.

Determination of the amount of fluxing agent present in the minerals allowed appropriate quantities to be wet blended with the WA HF in order to raise the flux content to match that of the standard Herreschoff feed, Milled HF. A series of three blends were produced with either nepheline syenite or sodium carbonate to have fluxing agent contents of 1.5, 2.0 and 2.4 wt.%.

The quantities needed to make these blends are detailed in Table 5-17. These blends were then calcined along with a sample of the natural state WA HF which has a flux content of 1.0 wt.% at three different temperatures, 950°C, 1000°C and 1050°C

to determine partial brightness, yellowness and soluble aluminium curves for each of the blends.

Table 5-17: The amount of nepheline syenite, sodium carbonate and Western Area (WA) HF needed to make the respective blends to raise the amount of fluxing agent content to 1.5, 2.0 and 2.4 wt.%

Flux content (wt.%)	Nepheline syenite blends		Sodium Carbonate blends	
	Amount of nepheline syenite (wt.%)	Amount of WA HF (wt.%)	Amount of sodium carbonate (wt.%)	Amount of WA HF (wt.%)
1.0	0.0	100	0.0	100
1.5	2.9	97.1	0.80	99.2
2.0	6.0	94.0	1.6	98.4
2.4	8.5	91.5	2.4	97.6

The results shown in Figure 5-14 indicate a significant increase in brightness with temperature for all seven blends. However, there is no distinct link evident between the amount, or type, of flux and the brightness of the product. Any gains that were achieved are insignificant, in that they are only fractions of a point. A standard spread of brightness values would be ±0.25 brightness points and most values are within this range.

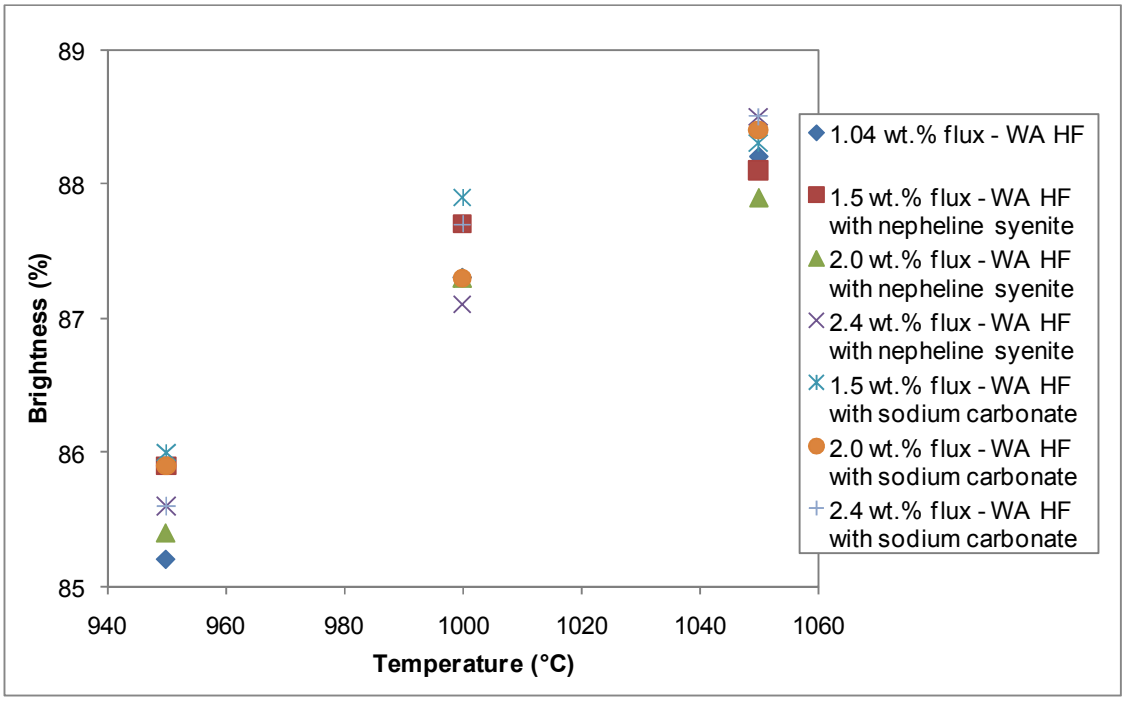

Figure 5-14: The brightness of the calcined product with regards to temperature for all blends investigated

The brightness value of the products from the 1050 °C calcinations were also considerably lower than that of the standard Herreschoff feed, Milled HF, which reaches a brightness value of between 90.5 and 91 when calcined under the same conditions. It is also interesting to note that the WA HF does not seem to have reached a plateau in brightness values, while the other kaolins investigated have by 1050 °C, including Milled HF, see Figure 5-1.

Whether WA HF would reach a plateau was investigated further by increasing the calcination temperature to 1150 °C and, as shown in Figure 5-15, the brightness of unblended WA HF continues to increase steadily with temperature, with no sign of plateauing. Ideally, the kaolin would be tested further at increasing temperature, but the method of calcination, opening the door and plunging the sample into the furnace

means that this is not feasible as it starts to involve dangerous temperatures for both the operator and the equipment.

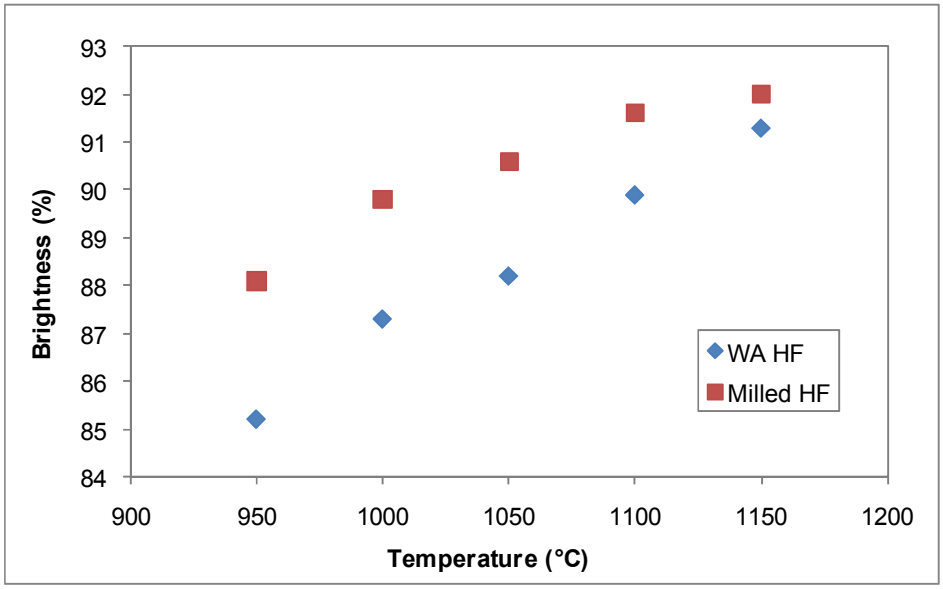

Figure 5-15: The effect of temperature on the brightness of WA HF and Milled HF

Whilst the nepheline syenite used in this investigation is a greyish colour, which lightens slightly upon calcination, any unfavourable effect on the total blend is considered unlikely due to the small quantity involved. Also, there is no significant difference between using the nepheline syenite and the very white sodium carbonate in the blends.

The results in Figure 5-16 show that, as expected the amount of soluble aluminium present in the calcined clay decreases with temperature. The standard Herreschoff feed has a soluble aluminium level of between 0.18 and 1.34 mass% when calcined under these Herreschoff replicating conditions, and most of the blends have values

which are considerably higher than this, particularly those blends composed of nepheline syenite.

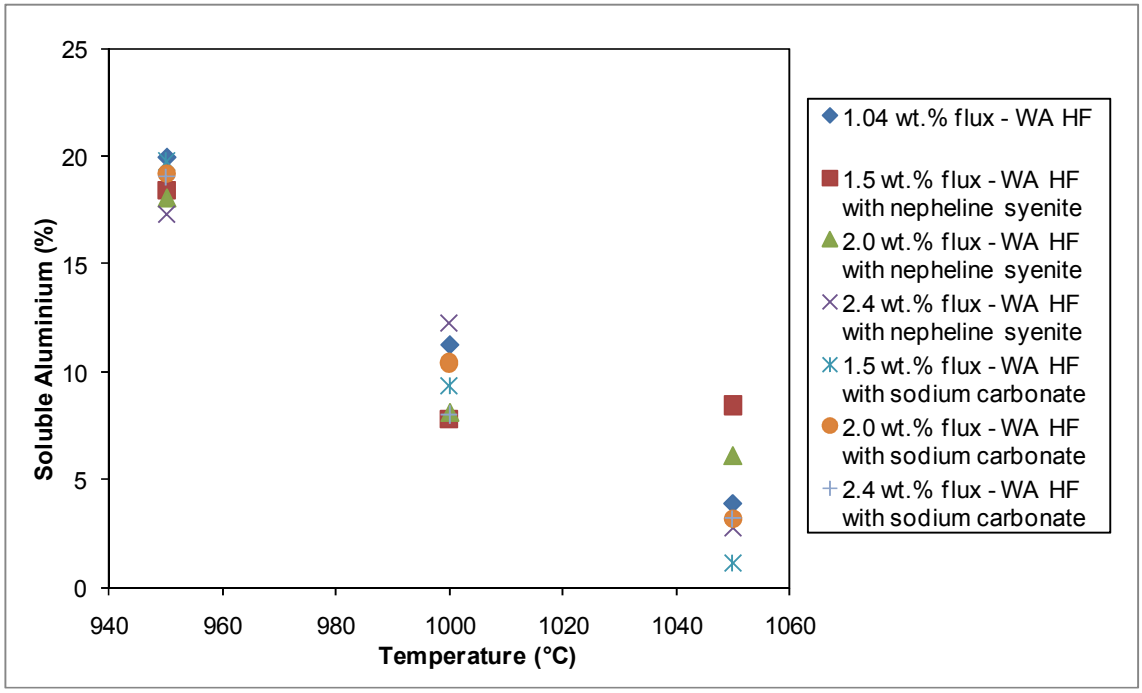

Figure 5-16: The soluble aluminium content of calcined product with regards to temperature

Table 5-16, which contains the XRF data for the different minerals involved in this study, specifies that there is some aluminium present in the nepheline syenite and this may be the reason values are so high. However, research by Ivanova (1961) carried out into the thermal degradation of nepheline syenite, found no thermal activity below 1200 °C [80]. By contrast, sodium carbonate has been found to be completely decomposed by 950 °C [81]. This suggests that the extra soluble aluminium present is not due to the chemical presence of nepheline syenite. Instead it may be due to more physical reason, such as a change in particle size due to

aggregation during the blending process or due to variations in heat transfer through the material.

5.6 Conclusions

It was already known when this work was implemented that kaolins with different mineralogy react differently when calcined at very high temperatures. The study of Brazil and Milled HF indicates that this difference is even more apparent at lower temperatures.

It appears that the presence of the organics does not have the dramatic effect suspected on the quality of the calcined product, however this could be further investigated in order to dismiss it completely. It seems more likely that a combination of different chemical factors is causing the decrease in colour.

The response of the Brazil blending work to temperature seems to indicate that the artificial blending of the different minerals in order to alter the proportion of kaolinite present in the kaolin was not successful in terms of changing the intrinsic chemistry of the blend. Instead, all blends continued to react in a similar manner to the main kaolin constituent, in this case, Brazil and that any effect on the product is one of dilution. This is also seen with the addition of nepheline syenite and sodium carbonate to Western Area HF, which does not alter the qualities of the calcined product and any gain achieved in the brightness of the product is insignificant as they are only fractions of a point.

However, with the magnet blending, where different kaolins in the form of magnet product and magnet rejects were blended together, the blending process was more successful. The similarity of the minerals used allowed the blending to take place at a more intimate level and this caused the blending process to have a greater effect on the calcination process.

This suggests that the intrinsic nature of minerals is highly important when determining how the chemistry affects the calcined product. Although artificially added minerals are used in other production areas of Imerys it is apparent that the addition of such minerals for the soft calcination of kaolin is not a workable solution to feed material issues.

6 Natural Chemistry

6.1 Introduction

As there was no discernible effect on the calcined product from the artificial blending of minerals into hydrous Brazilian kaolin, the focus of the work was changed, to examine the effect of natural chemistry variations. Samples were obtained from the Wheal Martyn production route in order to investigate the effect of subtle changes in chemistry which occur during beneficiation on both the hydrous kaolin and the product of calcinations at 500, 700, 950 and 1050 °C.

In order to perform accurate analysis on the product of the different calcination temperatures, it was decided to expand the data set and obtain samples from three further production routes; Blackpool, Lee Moor and Georgia, which originate from Cornwall, Devon and Georgia in the USA respectively. Due to significant differences in the response of the British (primary deposit) and American (secondary deposit) kaolins, the Georgia information was removed from the model data and work focussed on understanding relationships for the Devon and Cornwall kaolins.

The data set was then analysed to determine, first the influence of single factors on the quality of the calcined product at the four investigated temperatures and then the effect of multiple variables.

The effect of reductive bleaching was also examined by bleaching four Wheal Martyn beneficiation samples, the Dorr Oliver Product, the Centrifuge Product and the two magnet products at different levels of strong reducing agent. This work highlighted the detrimental effect of iron on the product, the importance of bleaching as well as other beneficiation stages on the calcined product. The results are discussed below.

6.2 The effect of beneficiation on the properties of hydrous kaolin

In order to compare subtle changes in the mineralogy of a kaolin and how that affects the properties of the calcined product, samples were obtained from several beneficiation stages along the Wheal Martyn production route. Wheal Martyn is a Cornish kaolin, mined from Wheal Martyn pit and contains several mineral impurities which include: mica, feldspar and quartz, but it consists of more kaolinite (94 wt.%) than the standard Herreschoff feed, Milled HF, which has a kaolinite content of around 89 wt.%. This can be seen in the quantitative XRD results shown in Table 6-2.

Table 6-1: XRD results for Milled HF Wheal Martyn (WM) Bleached sample

Mineral (wt. %)	WM Bleached	Milled HF
Kaolinite	94	89
Mica	5	3
Quartz	1	1
Feldspar	0	7
Tourmaline	0	0
Albite	0	0

Samples were obtained before and after the Dorr Oliver refiner and after the centrifuge, magnet and bleaching beneficiation stages. They were obtained in slurry form from production and were filtered and dried in the oven at 80 °C. Samples were then submitted for colour, particle size, XRD and XRF analysis, the results of which are shown in Table 6-2.

Table 6-2: XRD and XRF data for Wheal Martyn Production Samples

	Dorr Oliver Feed	Dorr Oliver Product	Centrifuge Product	Magnet Product 1	Magnet Product 2	Bleached Product
Colour (%)						
Brightness	77.4	78	80.2	82.2	84.7	86.4
Yellowness	7.6	8.3	8.8	8.5	7.1	5
Particle size (wt.%)						
< 2 µm	30.2	44.2	75.1	77.3	87.8	80.5
> 10 µm	25.9	9.4	1.3	1.5	1.3	1.2
XRD						
Kaolinite	74	82	91	92	94	94
Mica	21	12	6	5	4	5
Quartz	3	2	1	1	1	1
Feldspar	2	4	2	2	1	0
Tourmaline	0	0	0	0	0	0
Albite	0	0	0	0	0	0
XRF						
SiO_2	49.10	49.20	48.40	48.40	48.30	48.30
Al_2O_3	35.80	35.50	36.20	36.40	36.70	36.60
Fe_2O_3	0.91	0.90	0.82	0.65	0.58	0.57
TiO_2	0.04	0.03	0.03	0.02	0.02	0.02
CaO	0.06	0.08	0.08	0.07	0.06	0.06
MgO	0.21	0.25	0.26	0.23	0.18	0.22
K_2O	2.63	2.49	1.80	1.56	1.22	1.45
Na_2O	0.05	0.06	0.06	0.06	0.04	0.06
LOI	11.17	11.47	12.32	12.6	12.92	12.67

The information in Table 6-2 shows the importance of each beneficiation stage on the quality of the kaolin, with most stages showing an increase in brightness of around two points, although the yellowness remains fairly constant until the final bleaching stage. There is also a general decrease in particle size along the processing route, with an increase in particles less than 2 μm in size across the stages, except for a slight increase again after the bleaching stage. After the centrifuge stage, however, there is very little decrease in the proportion of particles over 10 μm in size with the content staying close to 1.5 wt.%. Between some of the beneficiation stages, there is some increase in contamination, this is particularly noticeable in the increase in potassium content between the second magnet product and the bleached product. This is partly due to contamination throughout the process from pipes and other equipment. The continuous nature of the processes also causes sampling difficulties, as obtaining samples that are directly related to each other is problematical.

The beneficiation stages which remove the largest amount of impurities are the Dorr Oliver and Centrifuge operations, with the non-kaolinite material decreasing by 8 wt.% and 9 wt.% over each of the two stages respectively. This is most likely due to the amount of large particles removed by each stage, as it has been proven that larger particles in unrefined kaolin contain the majority of impurities [2].

The impurities found in the larger particles can be identified in Table 6-2 as the quantity of material over 10 μm in size reduces from 25.9 wt.% down to 9.4 wt.% after the Dorr Oliver stage, and which is accompanied by a decrease in mica content

of 9 wt.%. The increase in feldspar content that occurs at the same time, is an example of the problem with obtaining plant samples, it is difficult to collect samples which are directly related to each other over each operation due to the inconsistencies found in the natural deposit and the continuous nature of the operations.

When examining the XRD results in Table 6-2, neither of the two magnet stages shows a large decrease in the quantity of mineral impurities in the kaolin but there is still a large increase in brightness for the two stages. This can be explained by examining the XRF results, which show a sizeable decrease in iron content from 0.82 wt.% for the centrifuge product, down to 0.65 wt.% after the first magnet stage and then to 0.58 wt.% after the second.

Much of the iron removed by the magnet operations is presumed to be located within the mica and feldspar portions of the kaolinite, as it is known that both contain a large amount of structural iron [34]. The removal of these mineral impurities also causes an accompanied decrease in the particle size, with an increase in 2 μm content to 87.8 wt.% for the product of the second magnet operation.

Bleaching reduces the amount of iron present on the surface of the kaolin by the reduction of solid ferric iron compounds, such as Fe^{3+} to ferrous, Fe^{2+}, which are soluble in an acid medium [82]. Not all iron in a kaolin found using XRF is bleachable, as it is contained within the crystal structure of the kaolin and so is not accessible by the bleaching chemicals. For this reason, there is only a very small

decrease in the amount of iron found in the kaolin over the bleaching stage, however, the significance of this small decrease can be seen in the brightness increase of 1.7 points and a yellowness decrease of 2.1 points, as shown in Table 6-2.

6.3 The effect of beneficiation on the properties of calcined kaolin

In order to investigate the effect of each beneficiation stage on the properties of the calcined product, samples obtained from production were calcined at 500, 700, 950 and 1050 °C using the batch method. From work carried out with Milled HF and Brazil, Section 5.2, it has been determined that these four temperatures are those at which the calcined product show significant changes in colour values and soluble aluminium content. The brightness data from these calcinations can be seen in

The significance of the iron content on the colour of a calcined kaolin has been stated by several researchers [33]. When iron is heated, it changes from the yellow ferrous form, Fe^{2+} to the ferric form, Fe^{3+} which is red in colour [36]. This has a detrimental effect on the brightness of the calcined kaolin due to the increase in the amount of light absorbed by the kaolin rather than reflected. Products with low iron content, such as the magnet and bleached products therefore have notably higher brightness values both before and after calcination, as detailed in Figure 6-1.

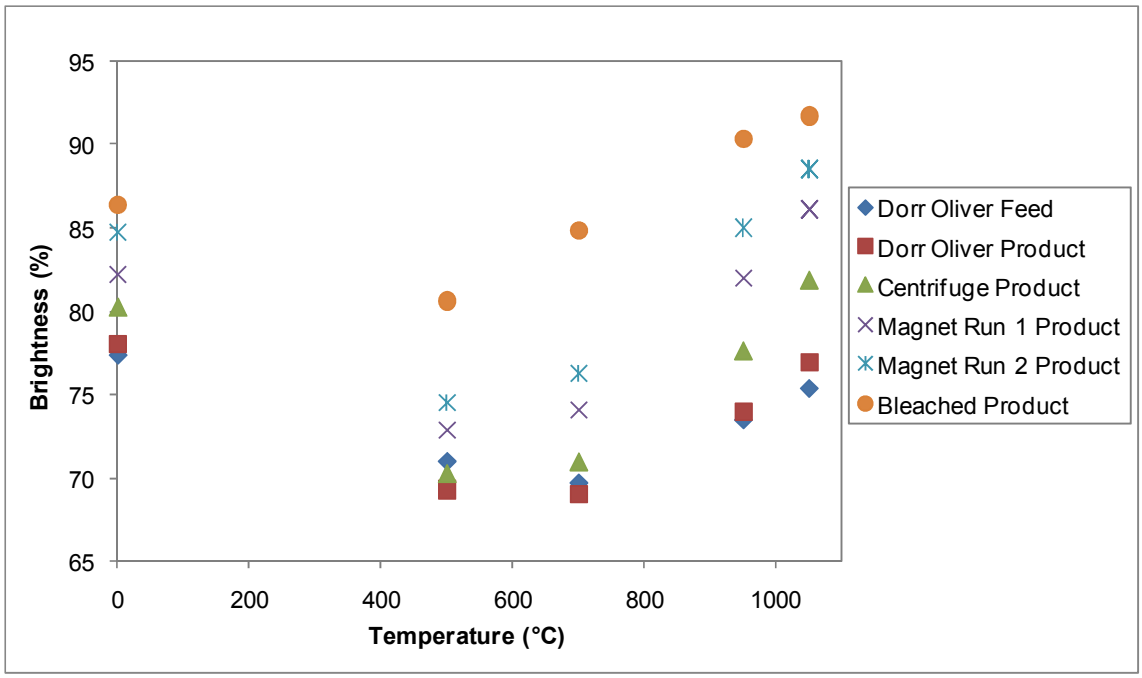

Figure 6-1: Brightness of Wheal Martyn Production Samples when calcined at 500, 700, 950 and 1050 °C compared with Milled HF when calcined at the same temperatures

As well as being linked to the iron content of the kaolin, the brightness of the calcined product is very closely linked to the total amount of impurities in the kaolin, as detailed in Table 6-2. At 950 and 1050 °C, the order of brightness is directly linked to the purity of the kaolin, with the purest kaolin, the bleached product, having the highest brightness value of 90.3 and 91.7 % and the most contaminated kaolin, Dorr Oliver Feed, having the lowest brightness values, of 73.5 and 75.4 wt.% at 950 and 1050 °C calcination, respectively.

At the two lower temperatures, 500 and 700 °C, the relationship is not so evident and is more complex, with both the Dorr Oliver Feed and Bleached Product samples exhibiting results which are not in processing order. The graph in **Error! Reference**

ource not found. shows a very dramatic decrease in the brightness for the bleached sample between the hydrous value and that for the 500 °C. With a drop of 11.9 brightness points, the decrease is larger than that for Milled HF which has been previously discussed and means the brightness for the bleached product is lower than that for the product of the second magnet run. This is probably due to the greater amount of mica present in the kaolin, and the accompanied increase in iron content.

The brightness for the calcined Dorr Oliver Feed is higher than both the Dorr Oliver Product and Centrifuge Product calcinations at 500 °C and higher than the calcined product of the Dorr Oliver Product at 700 °C, indicating that mineral impurities are not the only consideration when looking at the product properties of low temperature calcinations. As there is little difference between the XRF values for Dorr Oliver product and feed, but there is a significant decrease in mica content. It may be that coarse mica is not as rich in iron impurities as the fine and, hence, does not cause too much colour deterioration upon calcination. However, differences may also occur due to sampling inconsistencies.

The current products of the Herreschoff kiln are PoleStar 200P and PoleStar 200R, used in the Paint and Rubber industries, respectively. The brightness requirements for these two products are as follows [75, 76]:

- PoleStar 200P – 90.0 ± 1.5
- PoleStar 200R – 88.5 ± 2.0

Of the different samples calcined here, Wheal Martyn becomes suitable for use in the production of PoleStar 200R after the second magnet stage and only suitable for PoleStar 200P production, along with Milled HF, after bleaching. This highlights the importance of bleaching and the removal of as much iron as possible.

The amount of soluble aluminium found in the product is indicative of how far the calcination has progressed. According to the literature, the spinel reaction occurs at around 980 °C, during which the material reforms a crystalline structure after the amorphous metakaolin region, albeit different to that of a hydrous kaolin [8]. Once a spinel phase structure is obtained, aluminium can no longer be leached out with the nitric acid used in the soluble aluminium testing, causing values to decrease back to near zero.

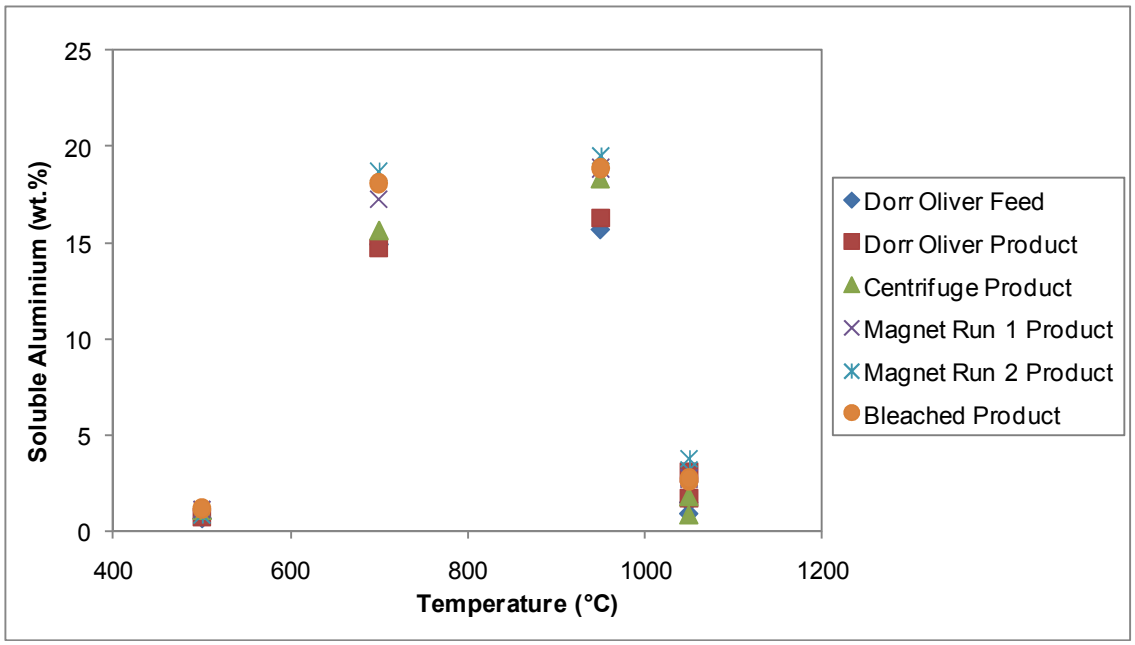

Figure 6-2: The soluble aluminium content of Wheal Martyn Production Samples when calcined at 500, 700, 950 and 1050 °C

Figure 6-2 shows that each of the kaolin samples examined exhibits the same trend for temperature and soluble aluminium content in the product. This indicates that, despite differences in chemistry and particle size, the same degree of calcination is occurring for the various kaolins, as with the blended samples detailed in Section 5.3.

The results for the calcinations carried out at 1050°C do show some variance, although all values are below 5 wt.%, which is the standard set for pharmaceutical grade material [83]. It appears that the purer kaolins show a higher level of soluble aluminium at 1050°C, with the bleached and both magnet product samples showing higher values than less refined samples, Dorr Oliver Feed and Dorr Oliver Product.

In order to identify the effect of both kaolinite content and particle size, additional samples from different production routes were obtained, including some from Georgia in the USA. The variation was obtained to create a better understanding of how the natural chemistry affects the calcined product and enable trends to be analysed and models developed.

6.4 Expanding the data set to other production routes

In order to develop an idea of which individual factors affect the properties of the calcined product, further plant samples were collected, with the intention of developing a general model for use with all kaolins. The three kaolins chosen were Lee Moor, which is mined in Devon and came from the same pit as Milled HF; Blackpool, which has a similar mineralogy to Wheal Martyn, as it is mined from Blackpool pit, a neighbouring deposit and Georgia, a very pure American kaolin from a secondary deposit, which is used as a calciner feed in the US. The samples obtained from each of the production routes are shown in Table 6-3.

Table 6-3: The samples that were obtained from each of the Georgia, Lee Moor and Blackpool production route

Blackpool	Lee Moor	Georgia
Centrifuge Feed	Centrifuge Feed	Magnet Feed
Centrifuge Product	Centrifuge Product	Magnet Product
Bleached Product	Magnet Product 1	Leached Product
	Magnet Product 2	Filter Cake
	Bleached Product	Calciner Feed

As with the Wheal Martyn samples, each of the kaolins were obtained as a suspension, which was filtered and dried before being calcined at 500, 700, 950 and 1050 °C. The information on the hydrous kaolins was then included with that of the Wheal Martyn samples and the data analysed in order to develop an understanding of the different factors which are important to the product.

The influence of several individual factors upon the particle size, brightness and soluble aluminium content of the calcined products was investigated. The factors included the particle size, brightness and yellowness of the hydrous kaolin alongside chemistry factors such as the kaolinite, mica, feldspar, potassium and iron content of the kaolin.

The influence of several factors on the brightness of the product for each of the four calcination temperatures was investigated using the data analysis feature in Microsoft Excel. The major influencing factors on the brightness of the product of the 1050 °C calcination, are shown in Table 6-4.

Table 6-4: The R^2 value for six different factors and the brightness of the 1050 °C calcination product for all four production routes and the three production routes, omitting Georgia

Factor	R^2 value for all production routes	R^2 value for production routes without Georgia
Hydrous Brightness	0.72	0.89
Hydrous Yellowness	0.43	0.54
Mineraliser content	0.3	0.51
Loss on Ignition	0.3	0.47
Potassium content	0.3	0.46
Iron content	0.28	0.44

As can be seen from the R^2 values in Table 6-4, when Georgia is included in the data set, the R^2 is detrimentally affected, decreasing in the case of all six of the major factors listed. This is due to the differences in chemistry between the American Georgia and British kaolins, with the purity of Georgia skewing the results. As the Georgia kaolin is from a secondary deposit, nature has already refined it and removed the impurities.

During the beneficiation of Georgia there is very little variation in the hydrous product when compared with the other production routes, due to very little impurities being present in the naturally beneficiated kaolin. Therefore, all of the production samples obtained from the Georgia production route are very similar, and consequently produce very similar calcined products. This can be seen in Figure 6-3, where all the Georgia samples are very closely grouped together with a hydrous brightness range of only 1.4 points, where hydrous samples from Lee Moor, Blackpool and Wheal Martyn production routes have brightness ranges of 9.8, 4.7 and 9 points respectively.

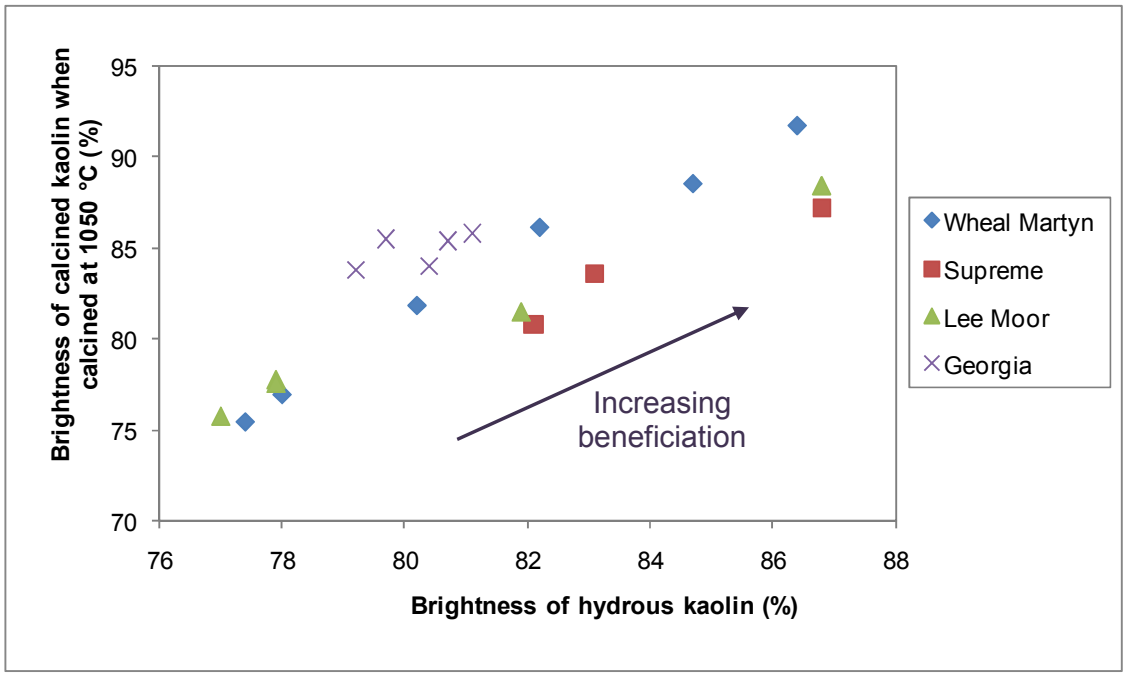

Figure 6-3: Brightness of the 1050 °C calcination for all four different production routes: Georgia, Lee Moor, Wheal Martyn and Blackpool

Due to the large differences in chemistry causing problems in the small data set, and the desire to build a model in order to predict the result of Herreschoff processing for various different kaolins, the Georgia data was removed from the development of the model. Consequently, the models produced would only be appropriate for use with British kaolins, which are all from primary deposits.

6.5 Single Factor Trend Analysis

6.5.1 Brightness

The brightness of the product from each calcination temperature, the particle size of the 1050 °C calcination product and the soluble aluminium content of the 950 and 1050 °C calcinations have all been compared with fifteen factors: aluminium, silica, potassium, iron, kaolinite, mica and feldspar content, which were obtained using XRF analysis, along with the LOI, the hydrous brightness and yellowness along with the less than 2 μm content, the d30, d50 and d70 of the hydrous feed.

The data set used for this analysis consisted of samples from the three British production routes; Wheal Martyn, Blackpool and Lee Moor. Analysis was carried out using the Data Analysis package in Microsoft Excel.

The colour of the calcined kaolin, at all four temperatures, is strongly related to the colour of the hydrous feed. The hydrous brightness is the most significant factor for the 950 and 1050°C calcinations, with R^2 values of 0.91 and 0.89 respectively. At the lower temperatures, 500 and 700 °C, the hydrous yellowness becomes more

important, with R^2 values of 0.78 and 0.91 respectively. The hydrous brightness, however, does continue to be a major influencing factor with an R^2 value of 0.75 for the 500 °C calcination and of 0.88 for the 700 °C calcination.

Other factors are less influential on the colour of the product. There is some influence of particle size, but the R^2 values are quite low, with R^2 values of around 0.37 for the 1050 °C calcination product, and lower for the other calcinations. This is most likely due to the overall effect of particle size on the brightness measurement. A sample with a fine particle size will experience a smaller amount of light scattering when the colour values are being tested when compared with a coarse sample [43]. This is why samples are generally milled before colour analysis. However, a large particle size distribution will still give a lower brightness values due to less scattering.

6.5.2 Soluble Aluminium

The amount of soluble aluminium found in each of the Devon and Cornish kaolins after calcination at 950 °C has a straight-line relationship to a large number of factors, both physical and chemical. The strongest relationships, as can be seen in Table 6-5 are with the particle size, the kaolinite content and the LOI value from the XRF data, all of which suggest links to the purity of the mineral.

The loss on ignition (LOI) value is obtained due to the OH groups within the material that form water at high temperature and evaporate off, reducing the weight of the material. The kaolinite portion of the kaolin is made of 13.9 wt.% of OH groups, while for mica this is reduced to 4.5 wt.%. Therefore, a mineral which contains more

kaolinite will have a higher LOI. It has been documented by previous research that larger particles contain more of the contamination, so upon removal the kaolin becomes finer and less contaminated, causing an increase in kaolinite content and, therefore, the purity of the material.

Table 6-5: The R^2 value for a number of different factors in relation to the amount of soluble aluminium found in the product of Devon and Cornish kaolins being calcined at 950 and 1050 °C

Factor	950 °C Soluble Aluminium Level R^2 value	1050 °C Soluble Aluminium Level R^2 value
Particle size of hydrous kaolin (wt.% <2 μm)	0.75	0.11
Kaolinite content of hydrous kaolin (wt.%)	0.74	0.097
LOI of hydrous kaolin from XRF data (wt.%)	0.74	0.022
Brightness of hydrous kaolin (%)	0.69	0.14
Potassium content of hydrous kaolin (wt.%)	0.65	0.0079
Mica content of hydrous kaolin (wt.%)	0.61	0.12
Iron content of hydrous kaolin (wt.%)	0.39	0.013
Silica content of hydrous kaolin (wt.%)	0.35	0.011
Aluminium content of hydrous kaolin (wt.%)	0.29	0.0092
Yellowness of hydrous kaolin (%)	0.21	0.088
Feldspar content of hydrous kaolin (wt.%)	0.17	0.0027

There is also a strong relationship to the amount of sample within the crucible and the soluble aluminium content after the 950 °C calcination. This can be seen in Figure 6-4, where the crucible that contains the most sample for calcination, has the lowest value for soluble aluminium. This sample can be identified as the Wheal Martyn Dorr Oliver Feed, which contains the largest amount of impurities, 26 wt.% as shown in Table 6-2. The presence of the impurities reduces the amount of aluminium that can be leached from the calcined product, as shown in Section 5.2.

Also, due to the higher density of both mica and feldspar when compared to kaolin, a higher amount of impurities in the kaolin will amplify the bulk density of the material and so increase the amount of material that is present in the crucible. Other samples which exhibited a higher weight prior to calcination were also more contaminated samples, with purer samples requiring less weight to fill the crucible.

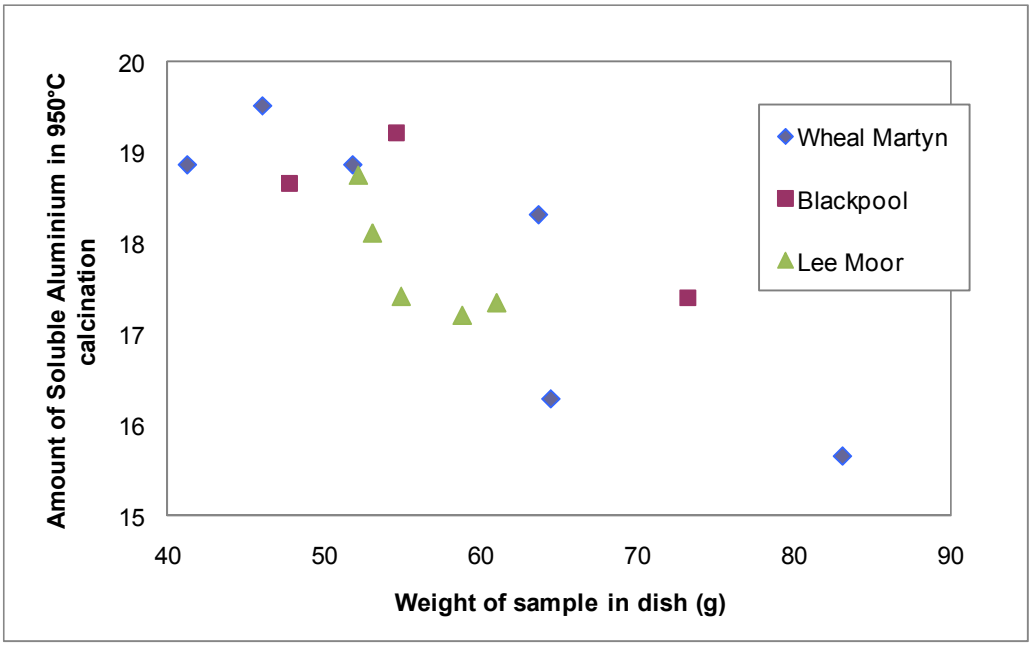

Figure 6-4: Soluble aluminium content of production samples when calcined at 950 °C and the weight of the hydrous sample used in the calcination

The amount of soluble aluminium found in the product of the 1050 °C calcinations seems to be unrelated to many of the investigated factors, as shown by the very low R^2 values in Table 6-5. The R^2 value of 0.0092 for the aluminium content of the hydrous kaolin suggests there is no relation at all to the soluble aluminium content available from the product of the 1050 °C calcination.

The effect of sample weight is not as evident as for the 950 °C calcination, shown in Figure 6-4, but there is some evidence of a general trend. This is particularly evident for the Wheal Martyn samples, as shown in Figure 6-5, where less soluble aluminium is released by samples that have a higher weight in the crucible, which is related to the bulk density of the material. The bulk density of the kaolin may affect the ability of the heat to penetrate the material. If the bulk density is too low and there is too much air present in the crucible, this may hinder the reaction as the air acts as an insulating layer, while for a kaolin that is well packed, the heat can easily pass from particle to particle.

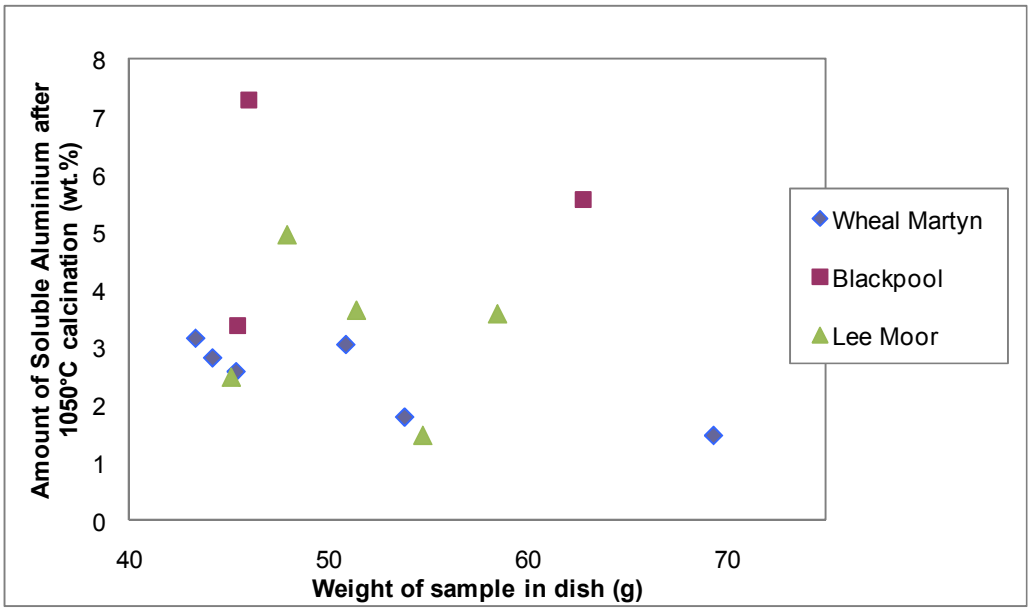

Figure 6-5: Soluble aluminium content of production samples when calcined at 1050 °C and the weight of the hydrous sample used in the calcination

It appears that the amount of soluble aluminium found in the soft calcined kaolin is not directly related to the chemistry of the product. Due to differences still evident between the different kaolins, it may be directly influenced by physical factors such

as the temperatures the kaolin was exposed to and for how long. Such variation may occur due to differences in heat penetration and kiln operation.

The effect of temperature and duration has already been shown in Section 4.4 and can also be seen in the work carried out by F. Onike, G.D. Martin and A. C. Dunham (1986) and Redfern (1987) who developed a Time-Temperature diagram for a pure kaolinite. This means that any kaolin, if calcined for long enough, will have a low soluble aluminium value [84, 85].

6.5.3 Particle size

The particle size of the product calcined at 1050 °C is largely dependent on the particle size of the hydrous feed, with an R^2 value of 0.76 for the amount of calcined product less than 2 μm in size compared with the amount of hydrous feed less than 2 μm in size, as shown in Figure 6-6. This relationship is increased to an R^2 value of 0.93 if the two highlighted Lee Moor samples are removed. These are the second magnet product and bleached samples, which contain slightly less kaolinite than the other samples and so are slightly coarser, skewing the results. There are two likely causes of the decrease; sample contamination from plant machinery and sampling inconsistencies.

The influence of the kaolinite content on the particle size of the calcined product can be seen in Figure 6-7, which has an R^2 value of 0.81. This is possibly because the 2 micron content is related to the kaolin content, where more refining results in less impurities in the kaolin with an accompanied decrease in particle size.

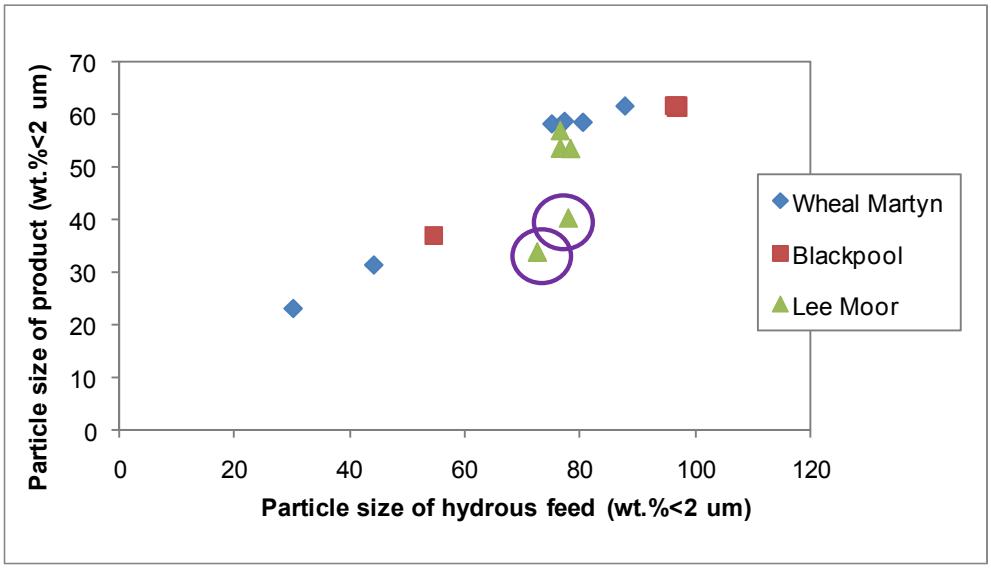

Figure 6-6: Particle size of the production samples after being calcined at 1050 °C compared with the particle size of the hydrous feed the ringed samples are Lee Moor, second magnet run product and bleached product which skew the trend

Alongside the kaolinite content, other factors such as the loss on ignition (LOI) and potassium content that are influenced by the purity of the kaolin, which have an R^2 value for the relationship upon the particle size of the product of 0.7 and 0.64 respectively.

It therefore appears that a kaolin which contains a lower value of potassium, which is generally found in the mica portion of the kaolin, contains a greater amount of kaolinite is also finer, and with a higher LOI. This suggests a great deal of interaction between factors, which should be considered when looking at the trends.

From the single factor analysis it appears that brightness of the product from the 1050 °C calcination is mainly influenced by feed brightness. The soluble aluminium from the same reaction is not linked to any of the kaolin properties and instead may be due to the heat transfer that occurs in the kiln. It has also been determined that both the maximum soluble aluminium and particle size values are mainly related to the purity of the kaolin, as factors such as particle size and kaolin content show dominance over other possible influences.

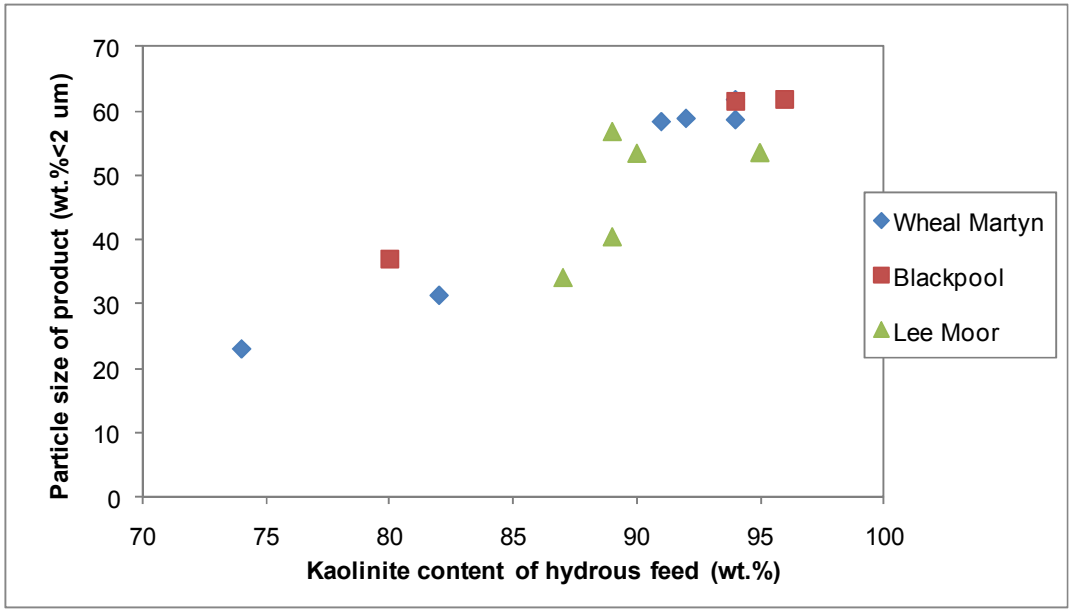

Figure 6-7: The particle size of the production samples after being calcined at 1050 °C compared with the kaolinite content of the hydrous feed

Due to the reasonably low R^2 values for many of the individual factors and the very few trends being proven, it appears that each of the calcined product properties are not reliant on any individual characteristics of the feed. The analysis was expanded by using multiple linear regression which allows more complex models to be

developed and with the prospect of creating a method for predicting the qualities of the calcined product form the feed properties.

6.6 Multiple Linear Regression

Multiple Linear Regression was carried out for the brightness of the product calcined at all four temperatures, 500, 700, 950 and 1050 °C, along with the soluble aluminium values for the 950 and 1050 °C calcinations and the particle size of the 1050 °C calcined product. The factors investigated were the same as for the single factor trend analysis, the aluminium, silica, potassium, iron, mineraliser, kaolinite, mica and feldspar content, the loss on ignition (LOI) obtained from XRF analysis, the hydrous brightness and yellowness along with the less than 2 μm content, the d30, d50 and d70 of the hydrous feed. The analysis was carried out using R version 2.8.1 (The R Foundation for Statistical Computing, USA).

The software allowed the analysis of the model and the plotting of Q-Q plots, which are used by statisticians to compare two distributions. In this work, the actual data was plotted against the model data. If the distributions being compared are similar then the points in the Q-Q plot will lie approximately on the line y=x. This is a useful tool to check the model as data points which skew the data, reducing the accuracy of the model can be detected, and if thought necessary, removed from the data set.

6.6.1 Brightness

It was found that the brightness of the product of the 500 °C calcination had the best fit model involving Aluminium, Kaolinite, Potassium, Feldspar and Iron content, along with the LOI and hydrous brightness. The relationship is shown in Equation 6-1 and the normal Q-Q plot shown in Figure 6-8, which has an R^2 value of 0.97.

$$Brightness\ after\ 500\ °C\ calcination$$
$$= 8.39\ Al - 0.16\ Ka - 43.37\ K + 4.30\ F + 12.48\ Fe - 37.47\ LOI$$
$$+ 2.30\ HB + 116.60$$

Equation 6-1: Determining the brightness of the product from the 500 °C calcination where Al = Aluminium content, Ka = Kaolinite content, K = Potassium content, F= Feldspar content, Fe = Iron content, LOI = Loss on Ignition and HB = Hydrous Brightness

Individual factors do not have a strong influence on the colour of the kaolin after the 500 °C with the hydrous brightness only showing an R^2 value of 0.78. However, the complicated nature of the formula shown in Equation 6-1 suggests that there is a complicated series of reactions happening at this point in the calcination reaction which is very hard to predict. This may include the location and phase of the iron particles and the ratios of minerals present, neither of which is known. There also may be several factors involved that have not been considered, such as the presence of organics, the surface area and shape factor of the particles.

The most accurate model to predict the colour of the 700 °C calcination is based on the Potassium, Feldspar and Iron content, and the Hydrous Yellowness, with a R^2 value of 0.99, is shown in Equation 6-2 and the normal Q-Q plot for the relationship is

shown in Figure 6-9. As with the colour of the 500 °C, the product colour for the 700 °C is difficult to predict, with several of the developed models having outlying points, reducing the accuracy of the model, point 1 can be seen as an outlier on Figure 6-9, and although other points are outliers for other models, they tend to be samples from early stages of the beneficiation route, suggesting that the impurities do have a strong effect on the product, despite factors such as mica and feldspar content being relatively insignificant single factors for brightness values.

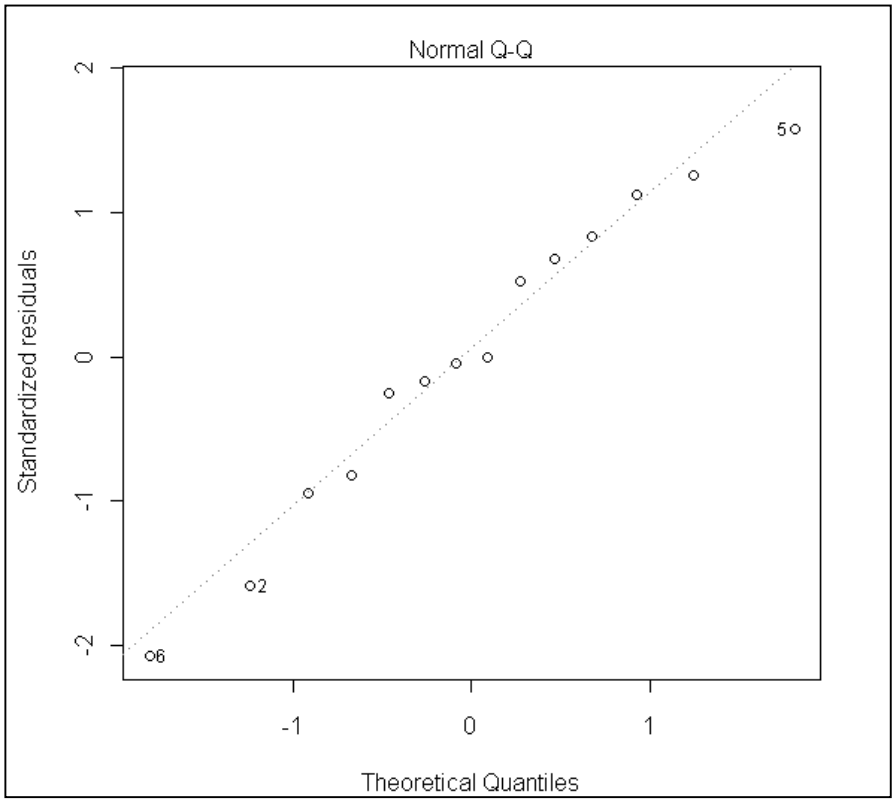

Figure 6-8: Q-Q plot for the brightness of production samples after calcination at 500 °C related to the Aluminium, Kaolinite, Potassium, Feldspar and Iron content along with LOI and Hydrous Brightness as detailed in Equation 6-1

$$Brightness\ after\ 700\ °C\ calcination$$

$$= 14.98\ K - 1.27\ F - 18.77\ Fe + 11.16\ LOI - 2.01\ HY - 58.89$$

Equation 6-2: Determining the brightness of the product of the 700 °C calcination, where K = Potassium content, F= Feldspar content, Fe = Iron content, LOI = Loss on Ignition and HY = Hydrous Yellowness

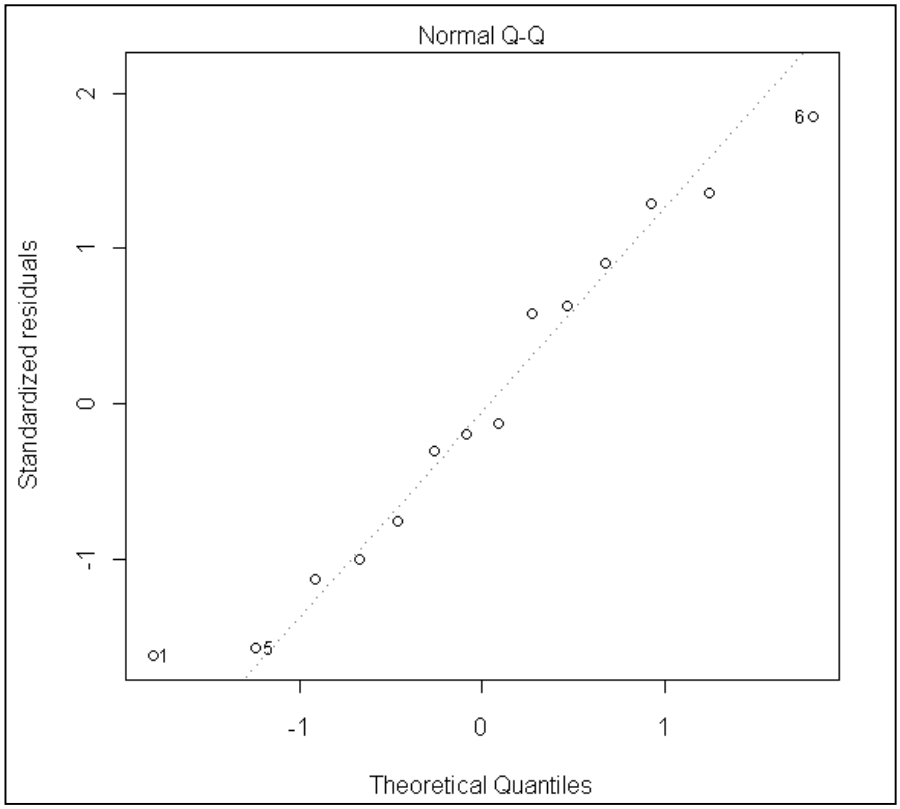

Figure 6-9: Q-Q plot for the brightness of production samples after calcination at 500 °C related to the Aluminium, Kaolinite, Potassium, Feldspar and Iron content along with LOI and Hydrous Brightness as described in Equation 6-2

Several of the factors in Equation 6-1 and Equation 6-2 are the same. Equation 6-1 also contains the kaolinite and aluminium content as part of the relationship for the brightness of the 500 °C calcination. However, the equation for the brightness of the calcined product at 700 °C contains the hydrous yellowness as a factor instead of the

hydrous brightness which is interesting as when compared as individual factors, for both calcinations, the hydrous yellowness was the most important factor. However, as the brightness and yellowness values for a kaolin are related, the relationship between hydrous and calcined colour is still evident.

There are several good models for the brightness of the 950 °C calcination and they are still primarily driven by the colour properties of the hydrous feed. The best fit model includes the aluminium, silica, iron and mica content as well as the hydrous yellowness; it has an R^2 value of 0.98 and is shown in Equation 6-3. The Q-Q plot for the model is shown in Figure 6-10, where it is noticeable that several of the data points lie directly on the line, which indicates where the model predicts the data should lie. There are also no very obvious outlying points.

$$Brightness\ after\ 950\ °C = 4.61\ Al + 2.97\ Si - 21.54\ Fe - 0.12\ M - 1.53\ HY - 203.49$$

Equation 6-3: Determining the brightness of the product from the 950 °C calcination where Al = Aluminium content, Si = Silica content, Fe = Iron content, M = Mica content and HY = Hydrous Yellowness

The different factors show greater significance for the 950 °C brightness compared with the previous models, all but two factors show a significance factor that is lower than 0.05, the point at which it is accepted by analysers that the factor is actually an important factor in the model [74]. The only factors that do not have such a low significance factor is the quantity of mica, which has a significance factor of 0.3 and the silica content which has a significance factor of 0.06. It should be noted that when the mica is removed from the model, the overall model suffers and the R^2 value

reduces to 0.97, which although only a small decrease, fewer of the points are directly on the line.

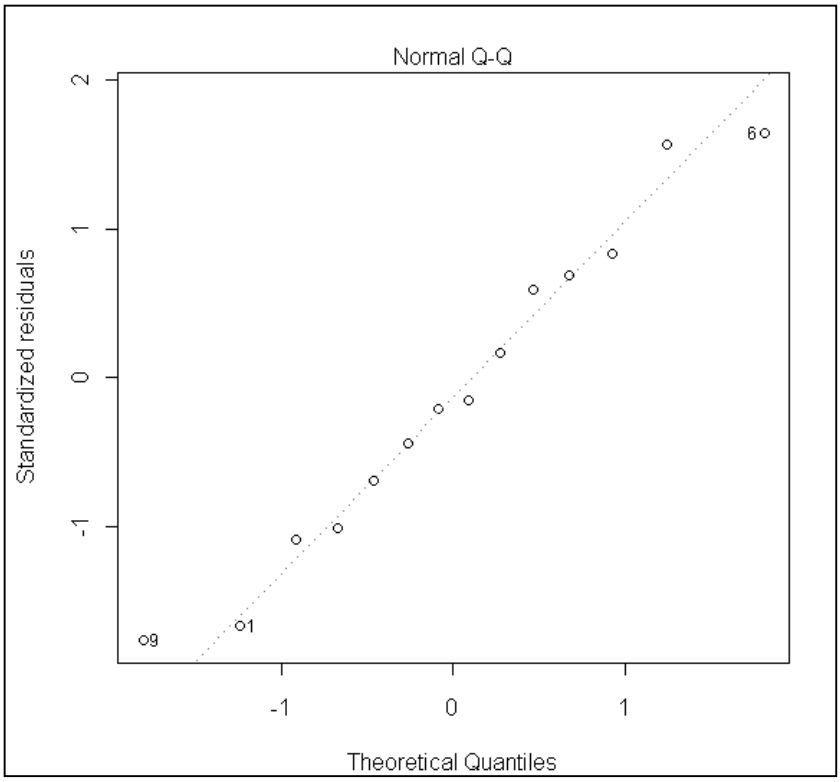

Figure 6-10: Q-Q plot for the brightness of production samples after calcination at 950 °C, related to the aluminium, silica, iron and mica content as well as the hydrous yellowness, as detailed in Equation 6-3

As was the case with the single influencing factors, the data for the product of the 1050 °C calcination it is not as easy to develop a model for as the 950 °C calcination. The best determined model has the following factors: kaolinite, mica, silica and aluminium content, along with the hydrous brightness, as described in Equation 6-4. The model has an R^2 value of 0.96 and the Q-Q plot is shown in Figure 6-11, which shows a reasonable fit and with no outlying data points.

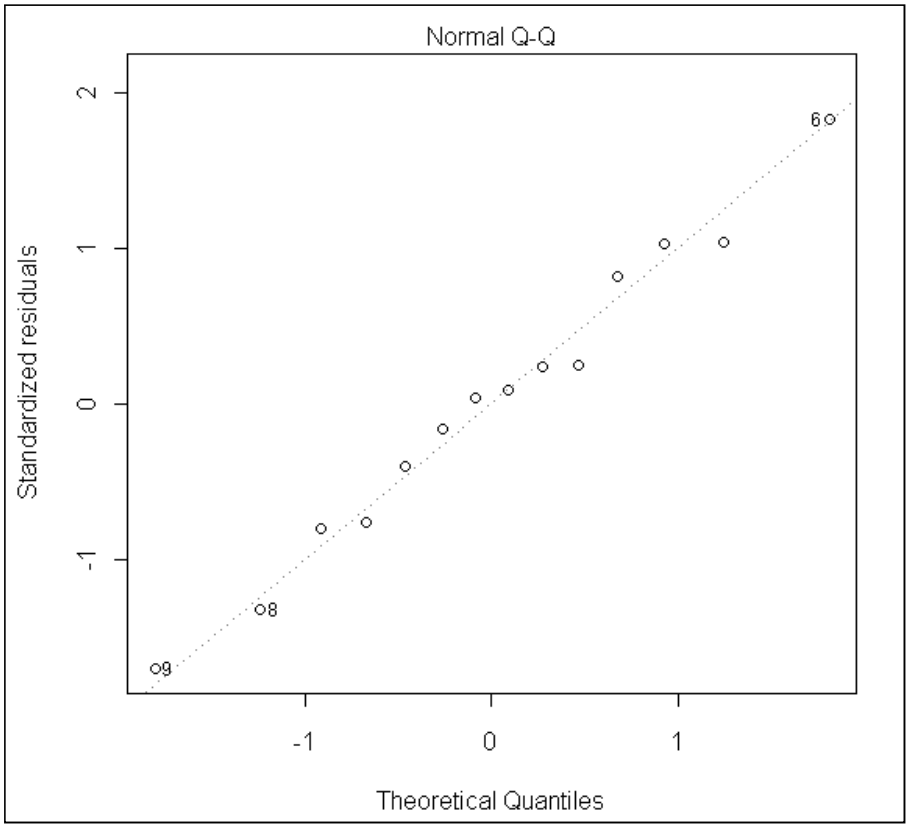

Figure 6-11: Q-Q plot for the brightness of production samples after calcination at 1050 °C, related to the aluminium, silica, kaolinite and mica content along with the hydrous brightness, as detailed in Equation 6-4

$$Brightness\ after\ 1050\ °C\ calcination$$
$$= 8.17\ Al + 4.73\ Si - 0.80\ Ka - 0.98\ M + 1.25\ HB - 465.5$$

Equation 6-4: Determining the brightness of the product from the 1050 °C calcination where Al = Aluminium content, Si = Silica content, Ka = kaolinite content, M = Mica content and HB = Hydrous Brightness

6.6.2 Soluble aluminium

Trying to predict the soluble aluminium content of the 950 °C calcination is very difficult because of the nature of the spinel reaction, which is very fast. The best-fit model for the amount of soluble aluminium obtained from the 950 °C was found to include five different factors; the potassium and mineraliser content (the amount of potassium, sodium, magnesium and calcium in the kaolin, all of which have been shown to promote fusion), the hydrous brightness and the d30 and d50 of the particle size distribution. The relationship, shown in Equation 6-5 has an R^2 value of 0.98, as exhibited in the Q-Q plot shown in Figure 6-12.

$$amount\ of\ soluble\ aluminium\ after\ 950\ °C\ calcination$$
$$= 4.92\ K + 0.09\ HB - 5.04\ Min + 1.76\ D30 - 1.49\ D50 + 13.90$$

Equation 6-5: Determining the soluble aluminium content of the product from the 950 °C calcination where K = Potassium content, Min = Mineraliser content, D30 = d30 of particle size distribution of hydrous feed, D50 = d50 of particle size distribution of hydrous feed and HB = Hydrous Brightness

Interestingly, the aluminium content is not included in the model and as part of the process of creating the multiple linear regression; it is removed from the list of factors quite early on in the process. Instead, the inclusion of the particle size factors suggests that it is the physical factors that are more important than the chemistry of the product. It has been theorised that smaller particles of kaolin release more soluble aluminium than the larger particles, due to the mechanisms of diffusion and surface area. This is reinforced by the d30 and d50 values, which represent the smaller size fraction of the particle size distribution, being present in the determined model rather than the d70 value, which is the larger size fraction [86].

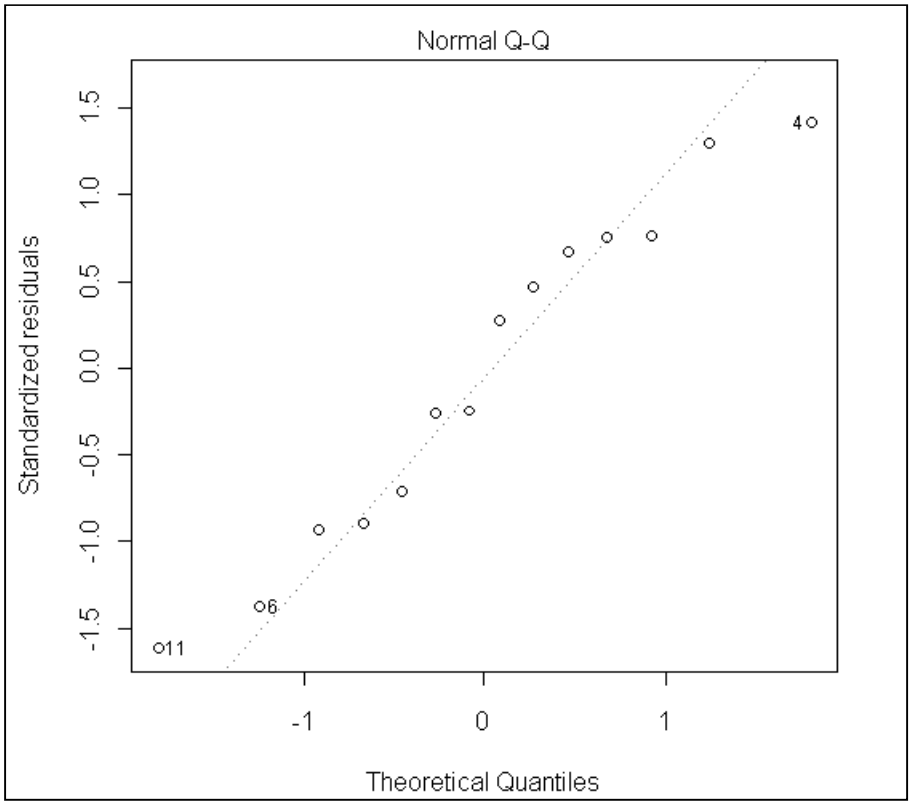

Figure 6-12: Q-Q plot for the soluble aluminium content of the 950 °C calcination related to the Potassium and Mineraliser content, the hydrous brightness and the D30 and D50 values of the particle size distribution as detailed in Equation 6-5

The S-shaped nature of many of the other Q-Q plots suggests that if a true relationship exists between the examined factors and the amount of soluble aluminium released after being calcined at 950 °C then it not a straight-line relationship.

It is very difficult to fit a trend to the amount of soluble aluminium retrieved after the 1050 °C calcination. The best model found contains nine different factors; the silica, feldspar, mineralisers, mica, kaolinite, iron and aluminium content along with the

hydrous brightness and the proportion of particles less than 2 μm in size. The equation is shown in Equation 6-6, which has an R^2 value of 0.95.

$$amount\ of\ soluble\ aluminium\ after\ 1050\ °C\ calcination$$
$$= 2.76\ Ka - 20.01\ Al - 3.65\ Si + 1.57\ F + 13.7\ Fe + 2.89M + 0.40\ HB$$
$$- 23.16\ Min - 0.34\ se + 664.26$$

Equation 6-6: Determining the soluble aluminium content of the product from the 1050 °C calcination where Ka = Kaolinite content, Al = Aluminium content, Si = Silica content, F= Feldspar content, Fe = Iron content, M = Mica content, Min = Mineraliser content, se = wt.% of particles less than 2 μm in size and HB = Hydrous Brightness

The high R^2 value is most likely due to the large amount of factors that are involved in the model as each of them compensate for issues with the others, as further factors are removed from the model, the R^2 value dramatically decreases and the issue of outlying values becomes more apparent. This can be seen in the model containing only two factors; the aluminium content and the hydrous brightness as shown in Figure 6-13 and as described in Equation 6-7, which has an R^2 value of 0.22.

$$amount\ of\ soluble\ aluminium\ after\ 1050\ °C\ caclination = 0.23\ HB - 0.54\ Al + 4.20$$

Equation 6-7: Determining the soluble aluminium content of the product of the 1050 °C, where HB = Hydrous Brightness and Al = Aluminium content

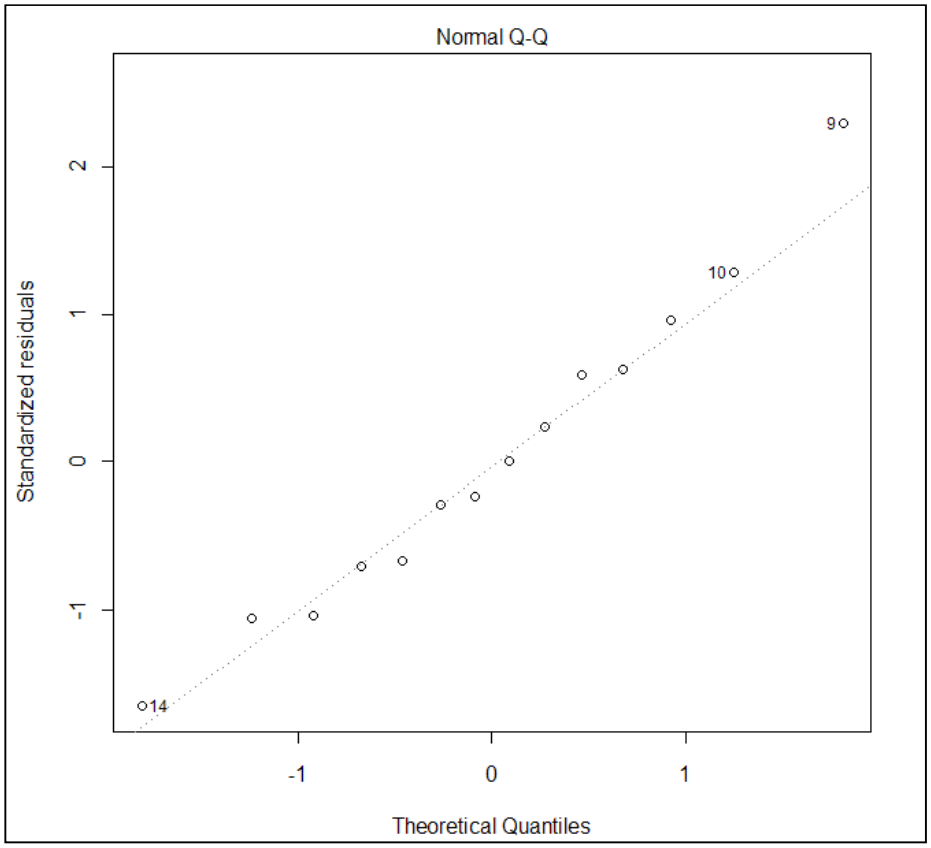

Figure 6-13: Q-Q plot for the soluble aluminium content of the 1050 °C calcination related to the hydrous brightness and the aluminium content as shown in Equation 6-7.

The outlying point in Figure 6-13, point 9 relates to a Blackpool sample which had an unexpectedly high soluble aluminium value, of 7.28 wt.% after the 1050 °C calcination. However, even when this point is removed, the R^2 value does not improve as the points are still spaced out, as shown in Figure 6-14, where point 10 from Figure 6-13 is now labelled point 9, as the removal of the sample altered the numbering of the samples.

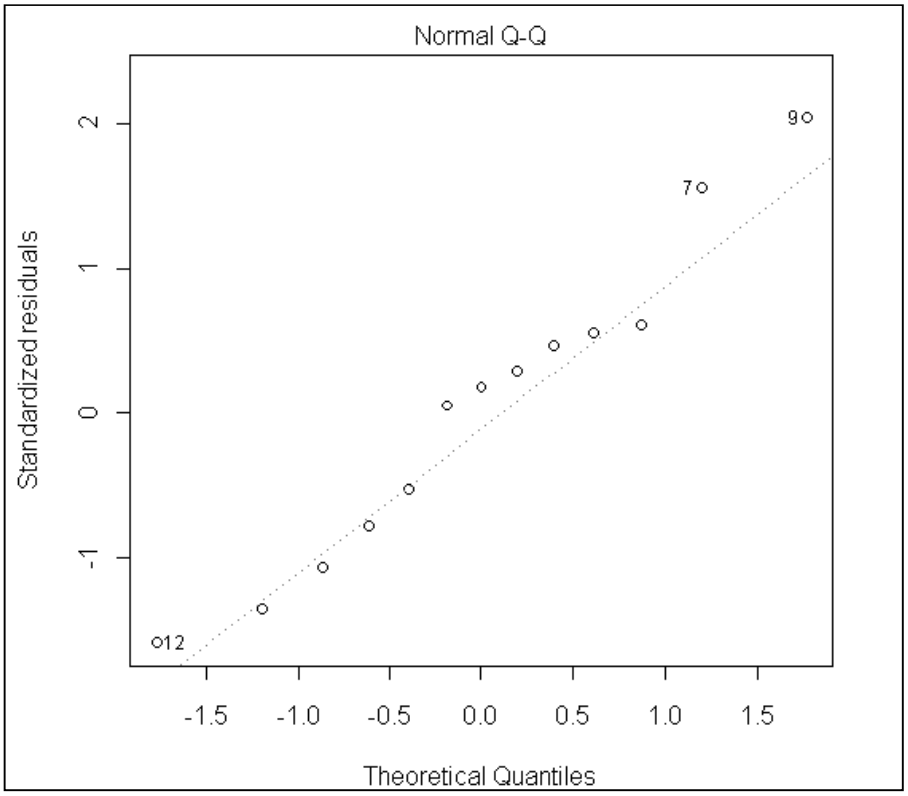

Figure 6-14: Q-Q plot for the soluble aluminium content of the 1050 °C calcination, with bleached Blackpool sample removed, related to the hydrous brightness and the aluminium content as shown in Equation 6-7

When trying to determine the standard properties of the reference material for a calcination, it was determined that there was a distinct range that the results fell into, as shown in Section 4.4.1. This suggests that if one feed, when calcined multiple times experienced a range in values, this means that most other samples will exhibit the same tendency. As most of the samples have a soluble aluminium value of less than 5 wt.%, this suggests that the amount of soluble aluminium released by a sample after the 1050 °C calcination is more related to physical rather than chemical factors.

6.6.3 Particle size

For all four particle size factors investigated, the d30, d50, d70 and the amount of sample less than 2 μm in size are most strongly linked to the single factors discussed in Section 6.5, Single Factor Trend Analysis, which are all particle size factors. This means that the calcined particle size is entirely reliant on the particle size of the hydrous feed and is linked through that to the chemistry of the kaolin.

6.6.4 Testing the models

Three samples were obtained from the magnet stage of the Littlejohns production route, the magnet feed, first magnet run product and second magnet run product. These samples were then reductively bleached under laboratory conditions. The samples were then batch calcined at 1050 °C for 30 minutes at high temperature.

The hydrous colour, particle size, XRF and XRD data are shown in Table 6-6. This information was used to determine the accuracy of the models detailed in Equation 6-4 and Equation 6-6 in predicting the brightness and soluble aluminium content respectively of the calcined product. The calcined properties and the values predicted by the two models that are displayed in Table 6-7 show that the model to predict the calcined brightness has an accuracy of more than 98 % for the three values, which means that the model is a good fit for British kaolins.

Table 6-6: Colour, Particles size, XRD and XRF data for hydrous Littlejohns Magnet Samples, obtained from production and reductively bleached under laboratory conditions

	Magnet Feed	Magnet Product 1	Magnet Product 2
Colour (%)			
Brightness	87.9	89.2	89.7
Yellowness	1	3.9	3.7
Particle size (wt.%)			
< 2 µm	78	80	80
> 10 µm	1.13	0.97	0.86
XRD (wt.%)			
Kaolinite	93	95	94
Mica	4	3	3
Quartz	1	1	1
Feldspar	2	1	2
Tourmaline	0	0	0
Albite	0	0	0
XRF (wt.%)			
SiO_2	47.66	47.72	47.63
Al_2O_3	36.69	36.79	36.92
Fe_2O_3	0.59	0.50	0.45
TiO_2	0.02	0.01	0.01
CaO	0.08	0.08	0.11
MgO	0.28	0.27	0.25
K_2O	1.18	1.02	0.90
Na_2O	0.08	0.09	0.09
LOI	13.41	13.52	13.64

The model to determine the soluble aluminium content of the product, however, is less accurate. For all three production samples, the predicted soluble aluminium results are higher than the actual results obtained. For the second magnet run product, the predicted level of soluble aluminium is almost eight times greater than the actual value obtained. This is not unexpected as the model only contains chemistry variables and no physical factors, such as bulk density, temperature of calcination and the amount of heat which enters the kaolin, which are considered to be dominant in determining how much soluble aluminium is present in the product of a 1050 °C batch calcination.

Table 6-7: The predicted and laboratory product brightness and soluble aluminium content results for the batch calcination at 1050 °C for 30 minutes (Herreschoff replicating conditions) of Littlejohns magnet feed, first magnet run product and second magnet run product the models used are shown in Equation 6-4 and Equation 6-6

	Predicted Results		Laboratory Results	
	Brightness (%)	**Soluble Aluminium (wt.%)**	**Brightness (%)**	**Soluble Aluminium (wt.%)**
Magnet Feed	91.2	5.92	89.6	1.05
Magnet Product 1	93.3	7.03	92.9	1.24
Magnet Product 2	93.2	5.79	93.9	0.74

6.6.5 Difficulties with the models

There is some relation between the proportion of the feed less than 2 μm in size, and the aluminium content and LOI. This is shown by the formula shown in Equation 6-8, which has a R^2 value of 0.97. This shows that the particle size of the hydrous kaolin is related to the purity of the kaolin, therefore the purity has an influence on the particle size of the calcined product. The other size values also show similar relationships.

$$proportion\ of\ hydrous\ sample\ less\ than\ 2\ \mu m\ in\ size = 38.29\ L - 10.82\ Al - 8.77$$

Equation 6-8: Determining the proportion of the hydrous sample less than 2 μm where L = LOI and Al = Aluminium content

This is also true for the four different brightness models, where the calcined colour is reliant on the colour of the hydrous feed. The hydrous brightness is related to the aluminium, silica, kaolinite, potassium, iron, mica and mineraliser content by the relationship shown in Equation 6-9, which has an R^2 value of 0.97.

$$hydrous\ brightness$$

$$= 2.41\ Ka - 19.44\ Al - 9.99\ Si + 42.70\ K - 14.06\ Fe + 2.4\ M$$

$$- 45.97\ Min + 1070.6$$

Equation 6-9: Determining the hydrous brightness where Ka = Kaolinite content, Al = Aluminium content, Si = Silica content, K = Potassium content, Fe = Iron content, M = Mica content and Min = Mineraliser content

The brightness of the product is also greatly affected by the bleaching process. The data set used for this analysis includes three samples that have been production bleached. It was, therefore, decided to investigate the effect of different levels of bleaching on the Wheal Martyn production samples.

6.7 The effect of bleaching on hydrous production samples

In order to investigate the effect of reductive bleaching, the four non-production bleached Wheal Martyn samples; Dorr Oliver Product, Centrifuge Product, Magnet Product 1 and Magnet Product 2 were all bleached at four different levels: 1.5, 3, 4.5 and 6 kg/t using sodium dithionite The results of the bleaching are shown in Figure 6-15.

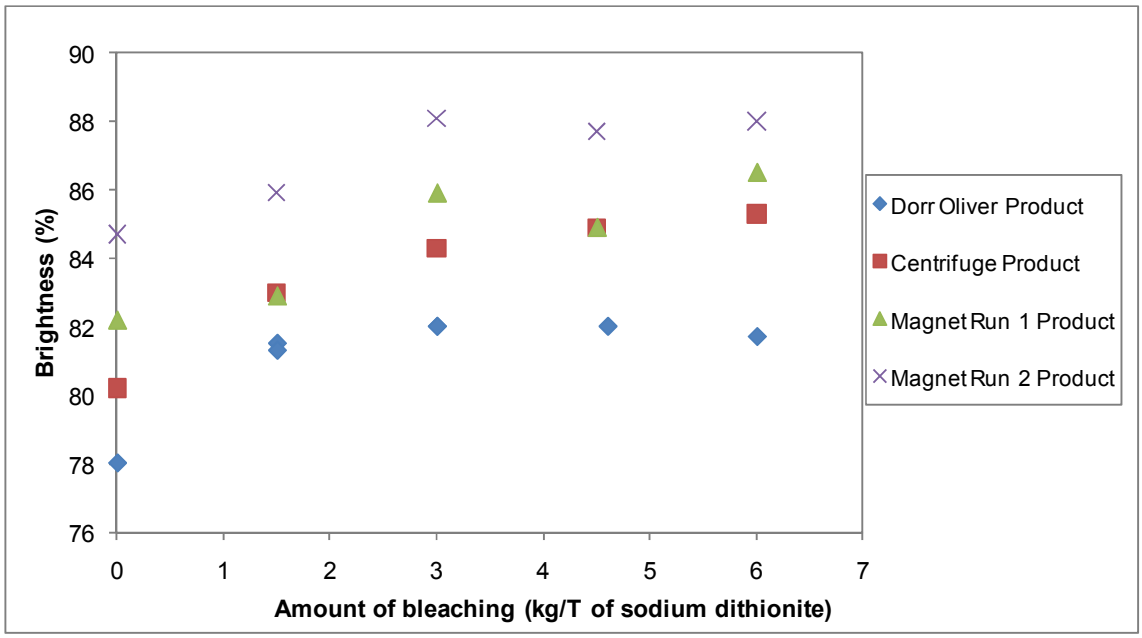

Figure 6-15: The brightness of Wheal Martyn production samples when bleached at four different rates; 1.5, 3, 4.5 and 6 kg t^{-1} using sodium dithionite

Figure 6-16 shows that the level of iron within the kaolin does not continue to decrease when in excess of 3 kg/t of sodium dithionite is used in the bleaching reaction. The limit in the reaction corresponds with the brightness data shown in Figure 6-15, where no further improvement in brightness is achieved as a result of the 4.5 and 6 kg/t bleaches. This is because there is a limited amount of surface iron for the sodium dithionite to react with. When 3 kg/t of sodium dithionite is exceeded, the remainder exists in the system as excess which is costly on a production scale. Therefore in production, kaolins are usually bleached at a maximum level of 3 kg/t, unless the kaolin is of superior quality and contains less iron contamination and consequently a lower level can be used.

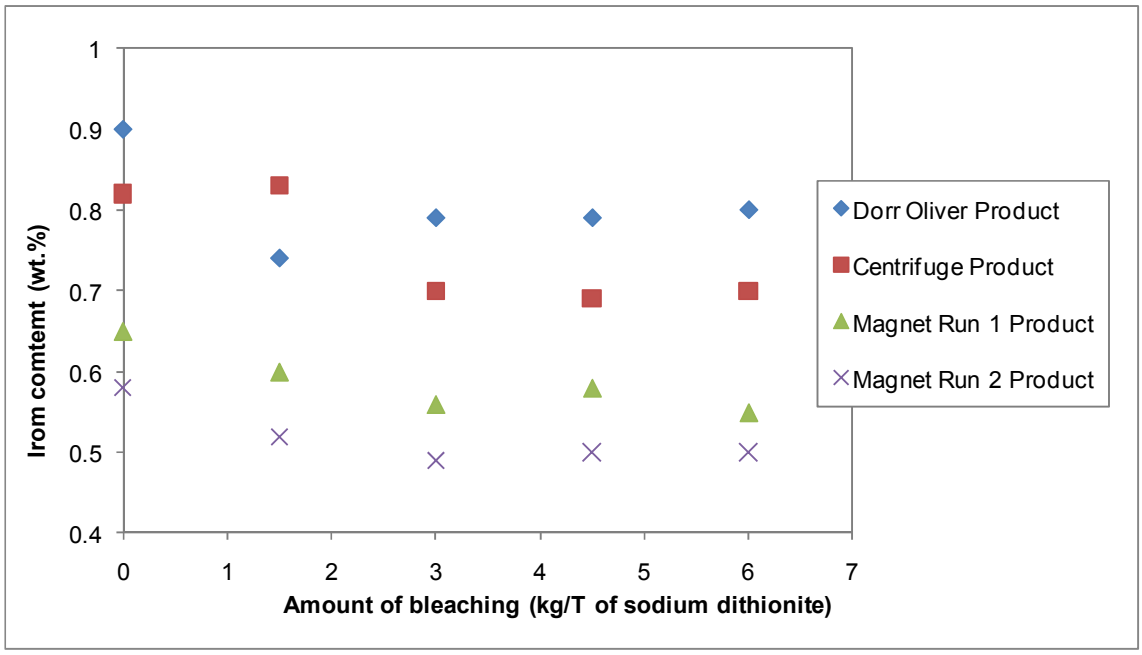

Figure 6-16: Effect of reductive bleaching with different quantities of sodium dithionite on the iron content of the kaolin

The link between the iron content and the brightness of the kaolin can be clearly seen in Figure 6-17, where a lower iron content is related to a brighter kaolin for all four different Wheal Martyn samples, a relationship which has an R^2 value of 0.85. This shows the importance of bleaching a kaolin on the brightness of the hydrous feed, which is in turn important for the calcined brightness, as shown in Section 6.6.

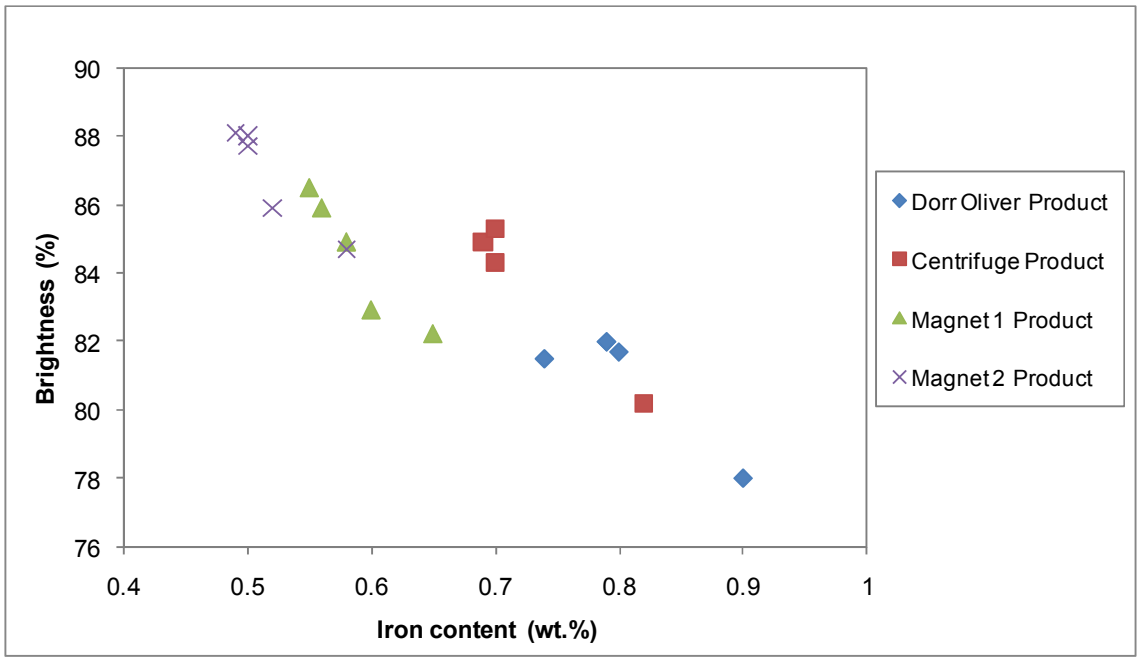

Figure 6-17: Effect of iron content on the brightness of the hydrous kaolin

6.8 The effect of bleaching on calcined samples

Four Wheal Martyn production samples were bleached using various levels of sodium dithionite; 1.5, 3, 4 and 6 kg t^{-1}. These samples were then calcined at 1050 °C for 30 minutes in order to determine the effect of bleaching on calcination. By bleaching the different samples to and beyond the production of 3 kg/t, the effect of each beneficiation stage could also be evaluated.

Figure 6-18 shows that, as with the hydrous kaolins, the brightness of the calcined samples peaks at 3 kg t^{-1}, after which there is no further advantage to the bleaching. The difference in calcined brightness achieved by the bleaching process to 3 kg/t, is around 4.5 points for the centrifuge and two magnet products and slightly lower for

the Dorr Oliver product, which has a brightness increase of 3 points. This may seem to contradict the fact that the Dorr Oliver product contains considerable more iron than the other three feeds, see Table 6-2. Due to the limited effect of bleaching, it is assumed that most of this iron is structural rather than surface and cannot, therefore, be reached by the sodium dithionite.

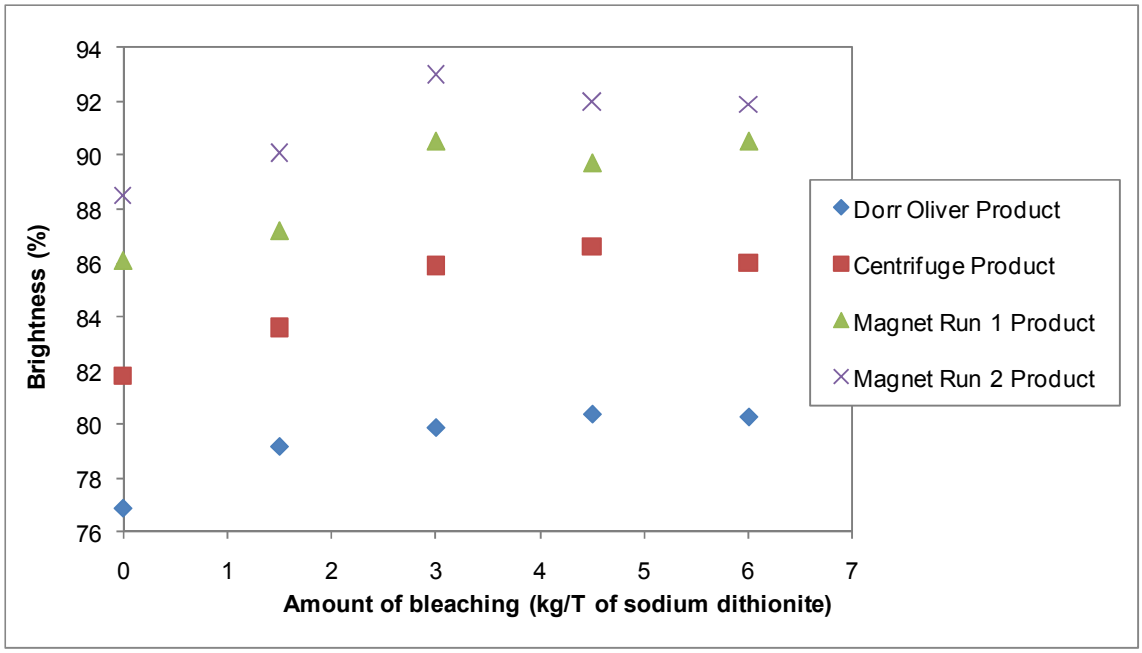

Figure 6-18: The effect of bleaching on the brightness of the Wheal Martyn production samples after calcining at 1050 °C for 30 minutes.

There is a distinct difference between each of the beneficiation stages and the quality of the calcined product, as with the unbleached samples shown in Figure 6-1. What is noticeable, from the production data shown in Figure 6-18, is that the Magnet 1 Product sample bleached at 3 kg t^{-1}, is upon calcination, suitable for use as the higher grade Herreschoff product, Polestar 200P, which has a brightness requirement of 90 ± 1.5 [75]. Although the magnet product 2 is suitable for use for

Polestar 200P when bleached at 1.5 kg t^{-1}, magnet product 1 is suitable for use as Polestar 200 R after the same level of bleaching [76].

The laboratory bleached second magnet run sample produces a brighter product upon calcination than the production bleached sample, as shown in Figure 6-1 as there is some iron reversion on drying for production samples. There is also the issue of contamination in production.

As operating the super-conducting magnet is much more expensive than bleaching, it is proposed that the second magnet operation be stopped in favour of bleaching. This has been proposed previously, although due to limitations with the bleaching process as it is currently carried out, in-line and with restricted mixing and control over the process as feed conditions vary it has not been carried out [33]. An improved bleaching process would reduce production costs significantly and would maximise the profit of not only the calcined product but also hydrous kaolins.

6.9 Conclusions

Each stage of the beneficiation process has an important influence on the quality of the hydrous kaolin. Both the Dorr Oliver and Centrifuge stages remove a significant proportion of larger particles, which are known to contain a significant proportion of contaminant materials [2]. The two magnet operations show an increase in brightness, which is due to the removal of iron-rich contaminants which have a detrimental effect on colour. The beneficiation process is completed by bleaching, which is important as it removes much of the surface iron.

The importance of bleaching as a beneficiation stage can be seen in that the Wheal Martyn kaolin that has only been put through a magnet once rather than the production standard twice meets the specifications of the highest quality Herreschoff product; Polestar 200P after it was bleached in the laboratory. This promotes the idea of reducing the amount of magnet processing which would create a large cost saving as the magnet operations are the most expensive part of the process. The current limitation in production scale bleaching prevents this from being implemented at the moment.

When determining models for a calcined product, if the feed properties are known, it was apparent that the Georgia kaolin was too chemically different from the British kaolins for inclusion in the data set as the Georgia results kept skewing the data. In order to develop a general model to determine the properties of the calcined product, more kaolins would have to be included in the data set so as to minimise this

difference. Kaolins from Brazil, China, France and other areas of the USA should all be included.

The colour of the calcined kaolin is dependent on the colour of the hydrous kaolin, along with other purity factors such as the Aluminium and Silica content, the amount of kaolinite and the Mica content. There is also some particle size influence, with finer kaolins having a better brightness value than coarse kaolins. This is a known phenomenon and is the reason for milling particles before colour analysis.

The amount of soluble aluminium retrieved from the sample after calcining at 950 °C, the point at which the amount of soluble aluminium has been found in other kaolins to be at its maximum value, is reliant on the potassium and mineraliser content, the brightness of the hydrous kaolin and the two smaller size fractions, the d30 and d 50 values. The inclusion of the two particle size values reinforces the belief that physical factors are very important in the calcination reaction.

It is very difficult to fit a trend to the amount of soluble aluminium retrieved after the 1050 °C calcination, with the best model containing nine different factors: silica, feldspar, mineraliser, mica, kaolin, iron and aluminium content along with the hydrous brightness and the amount of particles less than 2 μm in size. When trying to develop an idea of the standard properties of the proposed reference material, it was determined that there was a range that the soluble aluminium results fell into which guaranteed complete soft calcination had occurred. This suggests that if one sample, when calcined multiple times showed a range of possible results, other

samples will exhibit the same tendency. As most of the samples, with their very different chemistry, have a soluble aluminium content of less than 5 wt.% after the 1050 °C calcination, the theory that the amount of soluble aluminium is linked to physical features, such as the temperature of calcination, the bulk density and particle size of the powder and the amount of heat that penetrates into the material, rather than chemical factors seems likely. This will be examined further in Chapter 7. None of the four particle size characteristics of the 1050 °C product, the d30, d50 and the d70 of the size distribution, along with the proportion of particles less than 2 μm in size, show any reliance on factors other than the particle size of the hydrous feed. The particle size of the hydrous feed is in turn related to the purity of the kaolin, but the general trend is for the fine hydrous kaolins to produce finer calcined products.

7 The effect of heating/cooling rate on the calcined product

7.1 Introduction

Throughout this study, kaolin has been calcined in fused silica trays, using different heating and cooling regimes. These regimes influenced the soluble aluminium values of the product and it was deemed that further investigation was required into the temperature profile seen by the kaolin during calcination. Five K-type thermocouples were used to measure the temperature at five points throughout a tall, cylindrical alumina crucible.

The crucible used for the calcination was changed, in order to allow for the presence of the thermocouples, and to obtain a more varied temperature profile. However, a number of discrepancies with previous results were observed. After examining various factors that had changed, including the material of crucible construction, the height in the kiln and the effect of conduction from the walls, the temperature profile in the original tray crucibles was also investigated.

The temperatures in the tray crucibles were monitored by two thermocouples, one in the middle of the kaolin and one in the corner of the crucible. These results were, with the removal of the thermocouple support base, much more comparable with the original results. The results are discussed in full below.

7.2 Observed effects of different calcination methods

As part of the work trying to find laboratory conditions that replicate the effects of the Herreschoff, Milled HF has been calcined under several different conditions. Differences have been noted between the physical characteristics of the product from the two different calcination methods, most notably in the amount of soluble aluminium, as shown in Table 7-1.

Table 7-1: The brightness and soluble aluminium content of Mulled HF after calcining at 1050 °C for 30 minutes, using two different methods, batch and soak calcination.

	Soak Calcination	Batch calcination
Brightness (%)	89.0	90.3
Soluble Aluminium (wt.%)	10.75	0.44

This difference in values was investigated by carrying out a series of experiments which involved heating the kaolin using different cycles and then sectioning the kaolin into 6 parts, as in Figure 7-1, once it had been calcined. Each individual section was then separated into top and bottom samples when removing the calcined kaolin from the crucible and each individual sample was submitted for soluble aluminium testing.

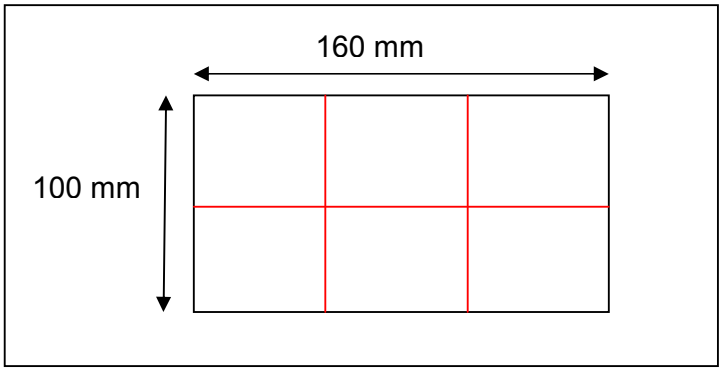

Figure 7-1: Division of calcined kaolin for soluble aluminium testing

Four different heating/cooling cycles were investigated using this technique:

- Inserting the sample into a cold kiln, heating up to 1050 °C at a rate of 10 °C per. minute, remaining at temperature for 30 minutes before cooling gradually back down to room temperature (Soak Method)
- Heating an empty kiln up to 1050 °C and placing a sample inside for 30 minutes before removing and cooling quickly outside the kiln (Batch Method).
- Inserting the sample into a cold kiln, heating up to 1050 °C at a rate of 10 °C per. minute, remaining at temperature for 30 minutes before removing and cooling quickly outside the kiln (Soak/Batch Method)
- Heating an empty kiln up to 1050 °C and placing a sample inside for 30 minutes at high temperature before switching off the kiln and allowing to cool gradually, removing when the kiln is room temperature. (Batch/Soak Method)

Previous research carried out by Imerys has shown that the cooling rate of kaolin after it has been in the kiln is highly significant when considering the colour of the product. If the kaolin is cooled either too quickly or too slowly, the iron form will revert and the colour will deteriorate, although the two investigations do disagree on the cooling rate to prevent this happening [87, 88].

Figure 7-2 shows the results of the soluble aluminium testing. All four experiments show that there is no sustained difference between samples taken from the side of the dish closer to the door and those taken from the back of the furnace, hence there is no effect of position in the furnace and the amount of soluble aluminium in the kaolin as results are uniform, front and back.

Soak Method

Top Layer			Back of Furnace	Bottom Layer		
3.89	5.45	2.05		9.17	12.64	9.41
3.49	4.7	2.4		10.91	14.6	8.69

Front of Furnace

Batch Method

Top Layer			Back of Furnace	Bottom Layer		
0.37	0.79	0.52		3.29	8.47	3.57
0.76	0.42	0.33		3.89	6.37	2.38

Front of Furnace

Soak/Batch Method

Top Layer			Back of Furnace	Bottom Layer		
4.05	6.36	2.16		9.3	12.47	10.76
4.49	7.19	4.24		9.96	15.59	9.52

Front of Furnace

Batch/Soak Method

Top Layer			Back of Furnace	Bottom Layer		
0.27	0.28	0.23		0.39	0.59	0.27
0.24	0.25	0.21		0.33	0.6	0.26

Front of Furnace

Figure 7-2: The amount of soluble aluminium found in sections of kaolin calcined under different conditions. Dishes were segregated into six sections and then samples were taken from the top and bottom of each section and submitted for testing.

There is a substantial difference between the amounts of soluble aluminium detected in samples that have been exposed to the different heating/cooling regimes. The Batch calcination method shows a large difference in the amount of soluble aluminium found in the top and bottom layers, which may explain the occasional large value for soluble aluminium that is obtained in testing.

The Soak calcination method shows a similar pattern to the Batch Method, with the top layer of kaolin being slightly more calcined than the bottom. This indicates that the kaolin is heated principally through radiation from the kiln itself, which is why the top of the kaolin is calcined before the bottom. However, the lower soluble aluminium values obtained in samples from the corner of the dish, on each layer and in all four experiments do indicate that conduction does take place. The Soak/Batch Method of calcination shows similar results to the Soak Method, which shows that it is the heating rate and not the cooling rate that is important in the amount of soluble aluminium present after calcination.

The method of calcination which produced the most evenly calcined product was the Batch/Soak Method. This is thought to be due to the extra time the kaolin remained at high temperature due to the long cooling cycle, allowing the entire dish of kaolin to be calcined. As the soluble aluminium levels were so low, a sample was submitted for XRD testing in order to check how far the calcination reaction had progressed. The results shown in Table 7-2 indicate that calcination has continued past the soft calcination stage and mullite has begun to form, hence the low soluble aluminium values.

Table 7-2: Table showing XRD results for Milled HF calcined using the Batch/Soak method of calcination

Mass%	Soak/Batch
Mullite	Detected
Quartz	1
Cristobalite	None Detected
Feldspar	2
Amorphous	Remainder

The four experiments highlight the relationship between the amount of soluble aluminium present in the samples and the amount of time spent at high temperature along the rate at which the kaolin is heated. Kaolin that is plunged into the furnace at high temperature, only spending 30 minutes being heated in the kiln has significantly lower soluble aluminium values than a kaolin that has been heated gradually to temperature before soaking for the same period of time. The initial difference in temperature of the kaolin and the kiln, therefore, seems to be a contributing factor to how successful the calcination is. This could be due to the intensity of the heat going into the kaolin.

This work can be expanded by investigating the actual penetration of heat through the kaolin with the aid of thermocouples placed strategically in a crucible. The kaolin sample can then once again be sectioned in order to determine the effect of specific heating/cooling rate on the product quality.

7.3 The use of thermocouples

In order to investigate how the heating rate affects the calcined product, a series of six thermocouples, five inside the dish and one outside, were arranged in a strategic manner in order to determine how quickly the kaolin heats up and cools down, as well as behaviour during the soak. The arrangement of the thermocouples in the tall crucible can be seen in Figure 3-1. The calcined material was then divided from top to bottom into 20 mm sections and submitted for separate analysis.

So that the spinel reaction could be properly investigated, it was deemed necessary to have a variance in soluble aluminium value throughout the crucible, so that in conjunction with the thermocouple data, the heating rates experienced by different sections of the crucible could be taken into consideration when looking at factors that affect the calcination reaction. Ideally, the top of the crucible will be fully calcined, with a very small soluble aluminium value and the bottom of the crucible will just be entering into the spinel reaction. The spinel reaction is considered to be a very fast reaction, as long as the necessary temperature has been reached [8]. Therefore, interrupting the reaction and obtaining the necessary variance in soluble aluminium throughout the crucible, was quite difficult to accomplish.

When FC Feed was calcined at 1050 °C for an hour, the brightness and soluble aluminium results, which are shown in Figure 7-3, indicated that the reaction had gone to completion, with all five sections producing very low values of soluble aluminium. The reaction time was, therefore, reduced to 30 minutes at temperature, which is the same conditions used for the Herreschoff replicating method as

described in Section 4.4, which used flat, tray crucibles. However, as shown in Figure 7-3, the experiment again progressed past the spinel phase to completion, with very low soluble aluminium obtained from the sample.

FC Feed 1050 °C soak calcination

	60 min	30 min	15 min
1	91.7 / 0.18	91.3 / 0.18	90.6 / 0.25
2	91.9 / 0.19	91.3 / 0.17	90.4 / 0.29
3	91.7 / 0.19	91.3 / 0.17	90.3 / 0.32
4	91.5 / 0.23	91.3 / 0.18	90.2 / 0.85
5	90.8 / 2.16	90.9 / 0.23	89.9 / 9.58

FC Feed 1000 °C soak calcination

	30 min	20 min	15 min
1	90.6 / 0.35	90.4 / 0.94	89.9 / 8.41
2	90.6 / 0.32	90.2 / 6.25	89.5 / 17.04
3	90.7 / 0.32	90.0 / 13.8	89.2 / 18.12
4	90.6 / 0.48	89.7 / 16.26	89.2 / 18.44
5	90.3 / 5.91	89.6 / 17.57	88.7 / 18.57

Figure 7-3: FC Feed calcined using the soak method at 1050 °C for 60, 30 and 15 minutes and at 1000 °C for 30, 20 and 15 minutes. Results shown are Brightness/soluble aluminium quantity (%/wt.%)

The kaolin was also found to have progressed past the spinel phase when the FC Feed was soak calcined at 1050 °C for 15 minutes, although the bottom sample did exhibit a slightly higher soluble aluminium result than the other sections, as shown in Figure 7-3. This, along with the slightly lower brightness results obtained when compared with the other experiments, suggests that the kaolin for this test has only just passed the spinel phase and that calcining for a slightly shorter time period would produce the range of values wanted. As the duration of this experiment was

only 15 minutes, the calcination temperature was lowered rather than adopting short soak durations.

By decreasing the temperature to 1000 °C, the thermocouple lifespan would be increased as a lot of breakage occurred at 1050 °C. Experiments were carried out with a 30 minute duration at temperature, for which the brightness and soluble aluminium results can be seen in Figure 7-3, where the soluble aluminium values are again low, apart from the bottom section, indicating that the reaction had gone to completion.

The duration at high temperature was halved and, on this occasion, the soluble aluminium results, shown in Figure 7-3, were deemed too high as the spinel reaction is only just beginning. The result obtained from the bottom of the 15 minute calcination crucible, seems to indicate that the sample is undergoing the end of the metakaolin reaction rather than the very start of the spinel reaction. This was considered to be the case due to two reasons:

- The high soluble aluminium level – the maximum found from an FC Feed when testing to use as a reference sample is about 20 wt.%, either the sample is building up to this value or it is coming away from it.
- The brightness value of 88.7, which is lower than that for the other samples. From previous testing, this brightness level was reached between 900 and 950 °C. This range also fits for the soluble aluminium level.

As shown in Figure 7-3, the results for the 20 minute calcination at 1000 °C are in between the results for the 30 and 15 minute calcination and show the required graduating soluble aluminium level throughout the dish. Therefore, this is the best method to replicate the variance in soluble aluminium results observed in the experiments detailed in Section 7.2 Observed effects of different calcination methods.

7.4 Investigating the different methods of calcination using tall circular crucibles and thermocouples

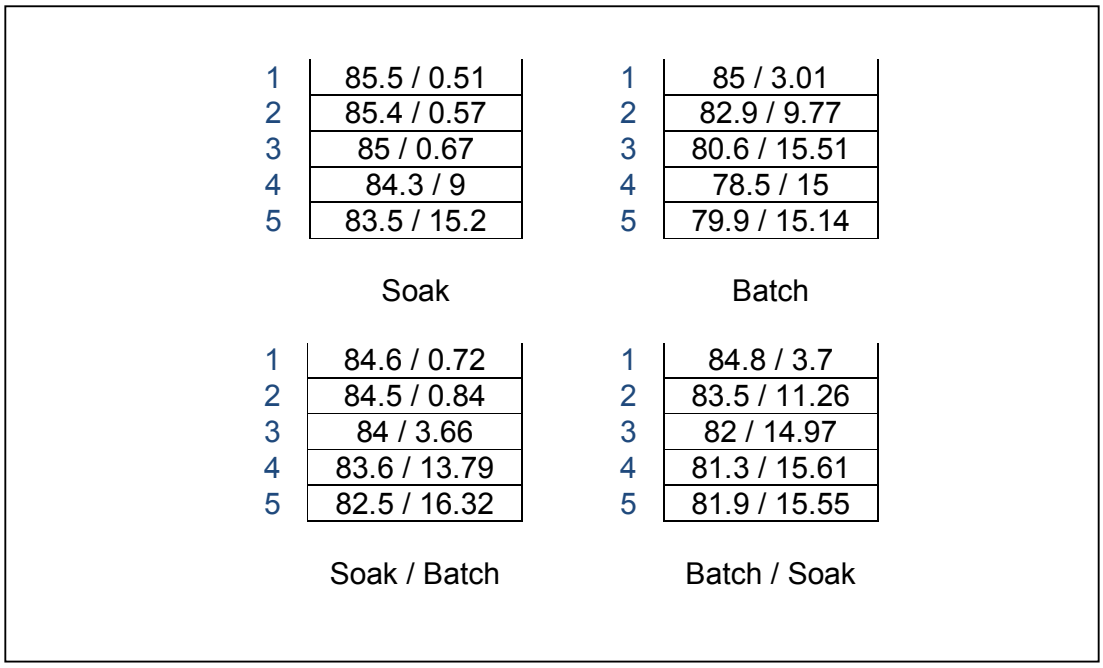

Figure 7-4: Milled Residue calcined at 1000 °C for 20 minutes using four different methods of calcination: soak, batch, soak/batch and batch/soak. Results are shown as Brightness / amount of soluble aluminium (% / wt.%)

Milled Residue was used for the different calcination method experiments, which were carried out at 1000 °C with a 20 minute duration at high temperature. The soluble aluminium and brightness results for the four calcinations; soak, batch, soak/batch and batch/soak, are shown in Figure 7-4.

The thermocouple data for the soak experiment are shown in Figure 7-5. It is apparent that the top three sections of kaolin all easily reach the furnace temperature of 1000 °C, which explains the low soluble aluminium values found for each section, as shown in Figure 7-4. The failure of the temperature in Section 4 of the crucible to rise above 880 °C, although it is around that level for a prolonged time, explains the medium value of 9 wt.% of the soluble aluminium found in that section.

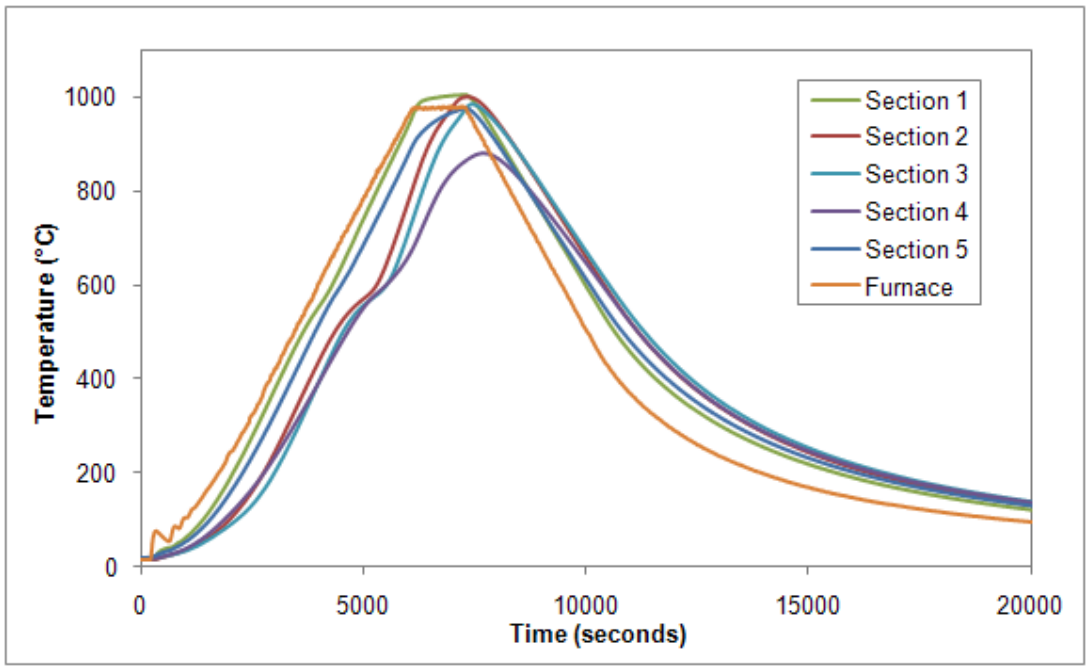

Figure 7-5: Residue Milled soak calcined at 1000 °C for 20 minutes thermocouple data

The soluble aluminium value obtained for the fifth section in the soak method experiment is much higher than expected. The thermocouple in the fifth section registers a maximum temperature of 976 °C while the section 4 thermocouple records a maximum temperature of 880 °C, yet section 4 yields a lower soluble aluminium result. The temperature monitored by the thermocouple may be related to the position in the crucible, which is near both the wall and the bottom and may, therefore, be an increased value over what is seen by the entire kaolin level. It should also be noted that the bottom of the dish is placed into the thermocouple support, which may be propagating the heat, causing the temperature of the walls to increase, which conducts into the kaolin.

An interesting feature of the data shown in Figure 7-5 is that the data for Sections 2, 3 and 4 all show some reduced heating rate between 550 and 650 °C, which is the temperature of metakaolin formation [6]. The phenomenon is less noticeable in the thermocouple data for Sections 1 and 5, although it is still present. This further suggests that the data for Section 5 is affected by the thermocouple location and that conduction from the wall and base of the crucible is distorting the heating experience of the kaolin.

The thermocouple data for the batch calcined Residue, displayed in Figure 7-6, shows a different heating mechanism than for the soak calcined sample in Figure 7-5, with less heat being seen by the middle section, Section 3 than the rest of the crucible. The initial heating rate for the thermocouple placed in the third section was initially at the same rate as the rest of the thermocouples, but it seemed to lag behind

after 4 minutes until 8 minutes into the experiment and the heating rate started to increase at the same rate as the other thermocouples. This is probably due to the heating elements no longer heating the kiln continuously once the kiln temperature has recovered from the heat escaping when the door was opened. Once the heating elements are only maintaining the temperature, there appears to be difficulty in getting heat into the crucible. The kaolin in the middle of the crucible is then heated again once the above and below sections start to conduct heat into the middle.

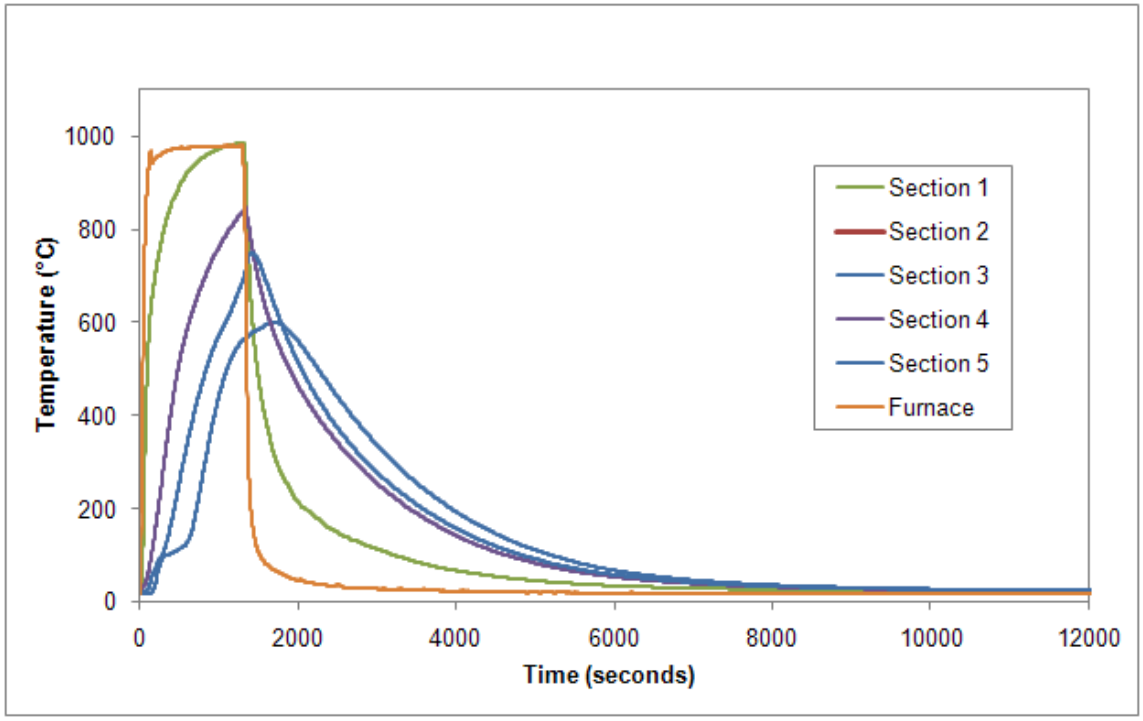

Figure 7-6: Residue Milled batch calcined at 1000 °C for 20 minutes thermocouple data

For the other four sections, the thermocouple data shows a very quick heating rate which begins to slow down after differing amounts of time. The heating rate drops in order from top to bottom, which suggests that heat is permeating through the kaolin over the twenty minute period.

The cooling rate of the different sections is also interesting, with the top section the quickest to cool, presumably because it is open to the air and therefore the heat is conducting away faster. Section 2 also cools quickly, albeit slightly slower than Section 1. Section 3 is the slowest to cool, retaining the heat for significantly longer than the top two layers, presumably because it is located in the middle of the crucible it is insulated by the surrounding kaolin and it is therefore harder for the heat to escape. Section 5 starts off the cooling cycle quite slowly, before speeding up suggesting that it expels the heat to the support structure once that has begun cooling.

The soak/batch calcination thermocouple data shown in Figure 7-7 shows amplified versions of the reduced heating rates due the endothermic metakaolin reaction in the various sections as seen in Figure 7-5, although for this calcination, the effect is also seen for Section 5.

Sections 1 and 2 both reach the same temperature as the furnace, 1000 °C, while the other three sections do not quite reach the maximum temperature. The soluble aluminium results shown in Figure 7-4, indicate that the top two samples are both fully calcined while the third sample, which has a soluble aluminium value of

3.66 wt.%, is just within the range for soft calcination. Sections 4 and 5 have not progressed as far in the calcination reaction, although they appear to be within the spinel reaction phase due to the higher brightness values.

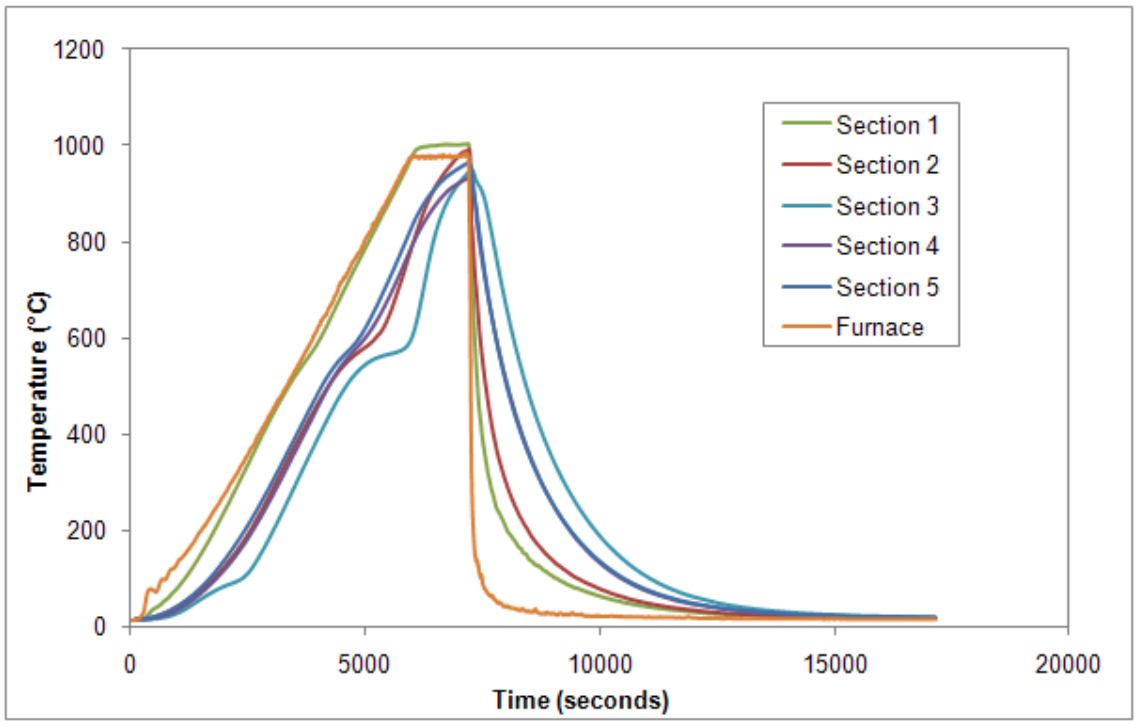

Figure 7-7: Residue Milled soak/batch calcined at 1000 °C for 20 minutes thermocouple data

In comparing with the soak calcination results, it therefore becomes apparent that the time spent at temperature is just as important as the temperature reached. The soak/batch system goes through the complete heating and cooling cycle in 236 minutes, which is just less than five hours. Other than section 1, which experiences the maximum temperature for the full 20 minute soak period, the other sections are only at their maximum temperature for less than a minute. In comparison, using the soak method, which lasts more than twice as long, at around 12.5 hours, the different

sections see the maximum temperature reached for around 17 minutes, including Section 3 which sees the lowest temperature. This increased exposure to temperature allows more of the calcination reaction to occur and for the soluble aluminium level to be lowered.

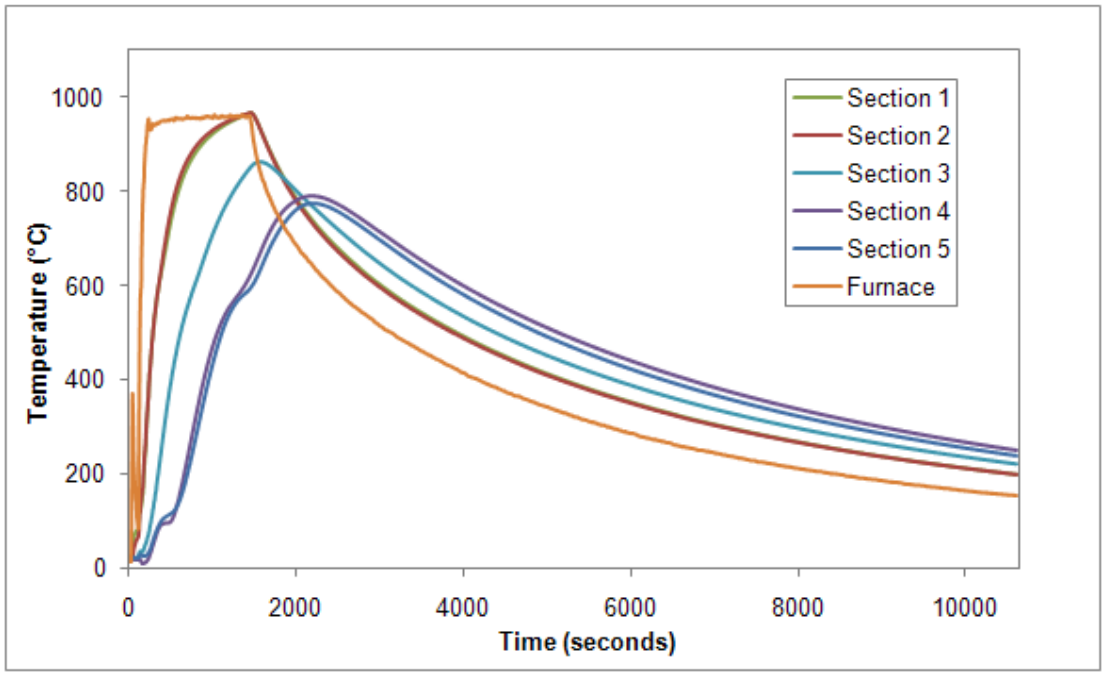

Figure 7-8: Residue Milled batch/soak calcined at 1000 °C for 20 minutes thermocouple data

The batch/soak thermocouple data shown in Figure 7-8 are reasonably comparable to the soak thermocouple data found in Figure 7-6 except for the heating of section 3, which appears to be better under batch/soak conditions. It is also noticeable that the second section, along with the first section, reaches kiln temperature during the reaction.

The soluble aluminium results shown in Figure 7-4 are reasonably similar for the batch/soak and batch experiments; however, the higher brightness levels obtained for the batch/soak experiment samples, suggest that these samples are undergoing the end of the spinel reaction, compared to the batch samples which are just starting the spinel reaction. This, as with the differences between soak/batch and soak, is thought to be due to increased exposure to temperature. The batch/soak experiment takes around 11 hours from start to finish while the batch calcination only takes just over 2 hours. This extra time means an increased exposure to heat, with Sections 4 and 5 remaining at the maximum obtained temperature for around 10 minutes. The other sections see slightly less time at temperature, however due to the long cooling time, the system stays above 600 °C for just under an hour.

The comparison of results from the batch and soak methods of calcination for the Milled Residue feed suggest that the tall, circular dish is not heating properly and the batch method is no longer more successful than the soak method. The opposite has been found with the small tray crucibles. The thermocouple data displayed in Figure 7-6 shows that only the very top of the crucible reaches the same temperature as the kiln, which is also reflected in the soluble aluminium data for the experiment, shown in Figure 7-4.

It was therefore theorised that the differences could be due to three factors:

- Change of crucible geometry – the new crucible is much taller, which affects the rate of radiation, due to heat variance in the kiln from top to bottom. There is also a greater amount of material to calcine.

- Changes in crucible material - The walls of the tall crucible are thinner and the material used in the manufacture of the dish is alumina instead of silica. Due to the difference in heat capacities, the alumina dish is easier to heat, causing wall convection to be more dominant than previously, with the flat crucibles.
- Heat gradient – the furnace was set at 1000 °C for this experiment and 1050 °C for the previous set. The decrease in temperature may be enough so that radiation is not as effective.

In order to determine which issue was dominant, each of the factors were investigated separately.

7.4.1 Height in the kiln

Experiments were carried out with FC Feed in order to determine if the height of the crucible affected the quality of the product. One tray crucible was raised in height, while the other was at normal height in the kiln. In order to raise the height of the tray crucible, it was rested on top of an upturned circular crucible. This meant it was slightly higher than the top level of the circular crucible on its own. Experiments were carried out at 1000 °C with 15 and 30 minutes at high temperature in order to compare with previous results.

As shown in Figure 7-9, the height of the crucible has a definite effect on the properties of the calcined product. The raised tray exhibits a product which is comparably calcined to the product of the top layer of the circular crucible for the 30 minute duration calcination, with both brightness and soluble aluminium level being very similar. However, for the 15 minute calcination, the slight gain in height means

that the raised tray product is significantly more calcined, with a reduction in soluble aluminium level and increase in brightness over the product obtained from the top layer of the circular crucible.

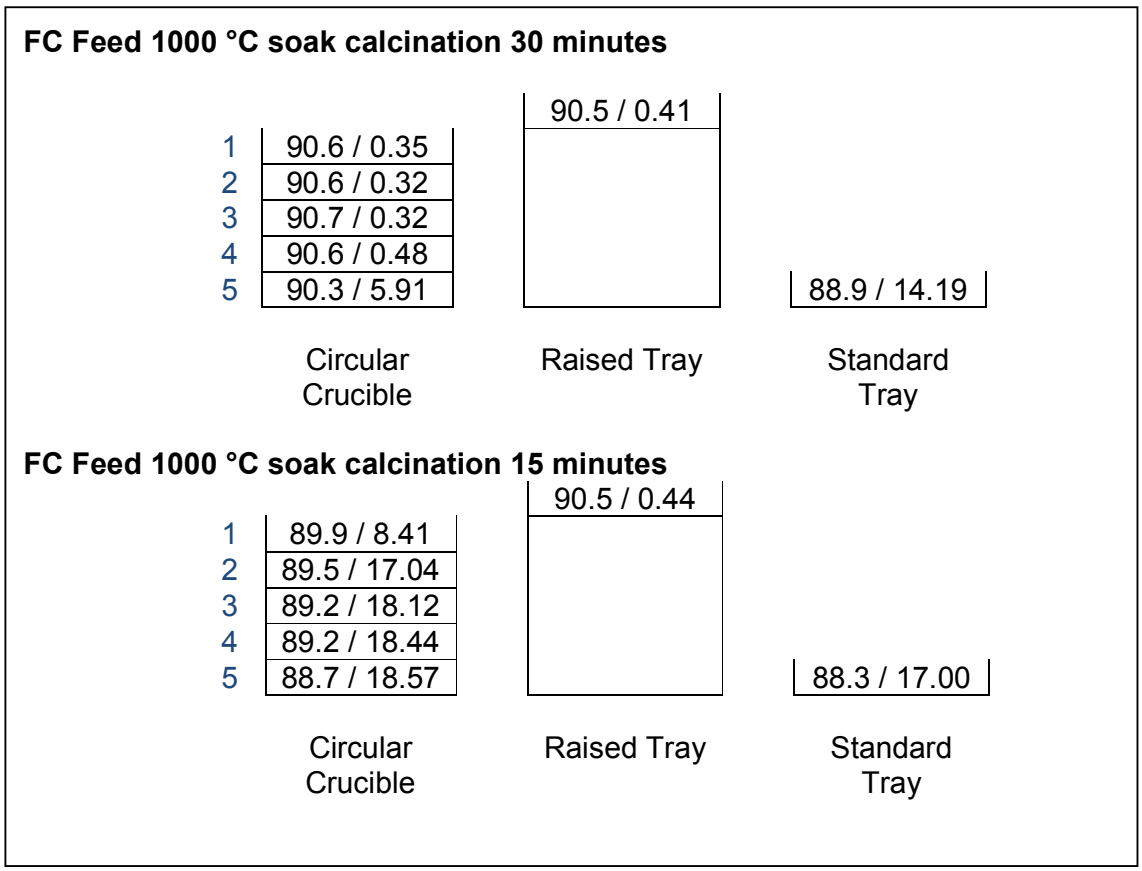

Figure 7-9: Brightness and soluble aluminium data for FC Feed calcined using the soak method at 1000 °C for 30 and 15 minutes in circular crucibles, raised trays and standard level trays. Results are displayed as Brightness/amount of soluble aluminium (% / wt.%)

For both experiments, the tray calcined at the standard height in the kiln has very high soluble aluminium levels and is only comparable to the results from the circular crucible for the 15 minute calcination, where the product shows similar signs of being toward the end of the metakaolin region rather than the start of the spinel region.

This can be seen in the comparison of soluble aluminium and brightness levels with those obtained previously in Section 5.2.

The continued low brightness value and high soluble aluminium content of the standard level tray crucible product for the 30 minute calcination, whilst the bottom level of the circular crucible increases in-line with the rest of the crucible, suggests that there is internal conduction, from top to bottom of the taller crucible and also that the construction material of the crucible is important.

7.4.2 Material of crucible construction

Experiments were carried out with FC Feed in order to determine if the material of the crucible was important in the characteristics of the product. A circular crucible was filled with kaolin to a level equal with the height of a tray crucible. This part-filled crucible was then calcined at 1050 °C for 15 minutes, alongside a tray crucible in order to compare with previous results, as shown in Figure 7-10.

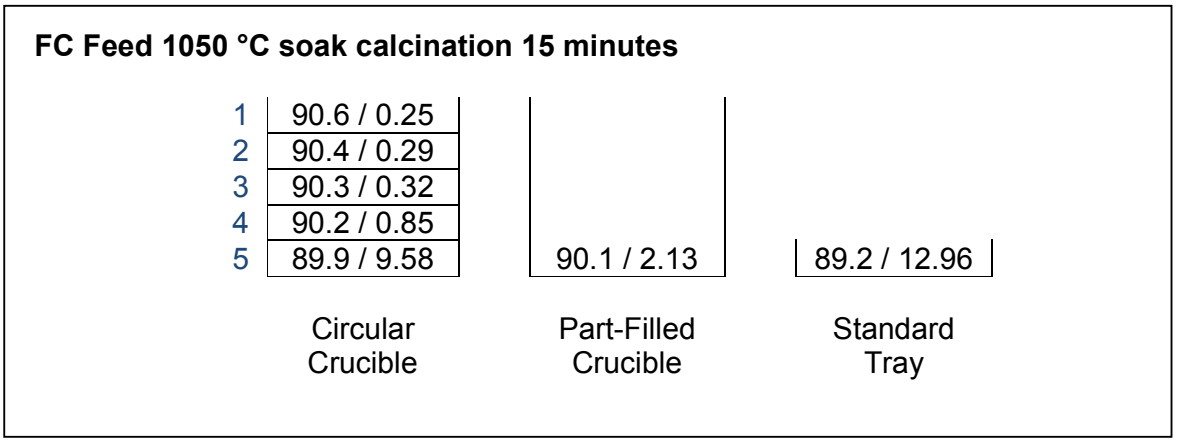

Figure 7-10: Brightness and soluble aluminium data for FC Feed calcined using the soak method at 1050 °C for 15 minutes in circular crucible, part-filled circular crucible and standard level tray. Results are displayed as Brightness/amount of soluble aluminium (% / wt.%)

The brightness and soluble aluminium results shown in Figure 7-10 indicate that the part-filled circular crucible produces a product that is more calcined than the bottom of the filled crucible. This suggests that the part-filled crucible conducts the heat better than the standard tray. This was expected due to the differences in conductivity between silica and alumina crucibles, although the differences in the calcination reaction were not expected to be so severe.

The presence of the material in the crucible, meanwhile, slows down the calcination reaction for the material in section 5, probably due to the amount of heat required for the contents of the other four sections to calcine before the bottom of the dish is reached, but may also be due to the insulating properties of kaolin powder, inhibiting the heat from reaching the material. There will also be less radiation in the system as the crucible is full of material. The heat permeation into the kaolin may, however, be improved with an increase in the heat gradient.

7.4.3 Heat gradient

In order to investigate whether the difference in kiln temperature was affecting the ability of the batch calcination method to produce a more evenly calcined product than the soak method, FC Feed was calcined at 1050 °C for 15 minutes in order to compare with the previously carried out soak experiment.

The soluble aluminium and brightness results for the two experiments are shown in Figure 7-11, indicating that the batch method calcination was again, not as successful as the soak calcination, with the soluble aluminium values all reasonably

high. The very low brightness values for the bottom three sections of the crucible suggest that the calcination reaction had only just started, as the brightness results obtained are lower than those obtained for FC Feed calcined at 350 °C for 30 minutes using the tray crucibles, see Section 4.4.1.

FC Feed calcination at 1050 °C for 15 minutes

	Soak
1	90.6 / 0.25
2	90.4 / 0.29
3	90.3 / 0.32
4	90.2 / 0.85
5	89.9 / 9.58

	Batch
1	88.5 / 8.85
2	82.7 / 11.28
3	80.4 / 10.84
4	79.3 / 11.54
5	77.9 / 14.80

Figure 7-11: Brightness and soluble aluminium data for FC Feed calcined using the soak and batch methods at 1050 °C for 15 minutes in a circular crucible. Results are displayed as brightness/amount of soluble aluminium (% / wt.%)

As the crucible was divided into the five sections, by the third layer it was noticed that the outside ring of kaolin was much whiter than the middle, which was greyer. This can be seen in the images in Figure 7-12. The increasing size of the ring of greyer uncalcined material, suggests that the calcined and uncalcined material exist in a domed pattern within the circular crucible, as shown in Figure 7-13.

This suggests that there is a much stronger conduction effect coming from the walls than was previously accounted for. This conduction through the walls may explain why the soluble aluminium values, shown in Figure 7-11, are not in ascending order from top to bottom, as depending on whether the sample came from the middle or

the edge of the crucible, there would be a very different result for both colour and reactivity.

(a) Third Layer (b) Fourth Layer (c) Bottom Layer

Figure 7-12: Photographs of sections through the crucible third layer (a), fourth layer (b) and the bottom layer (c). The ring of calcined kaolin around the outside of the crucible can be seen and is highlighted with a red dotted line in image (a).

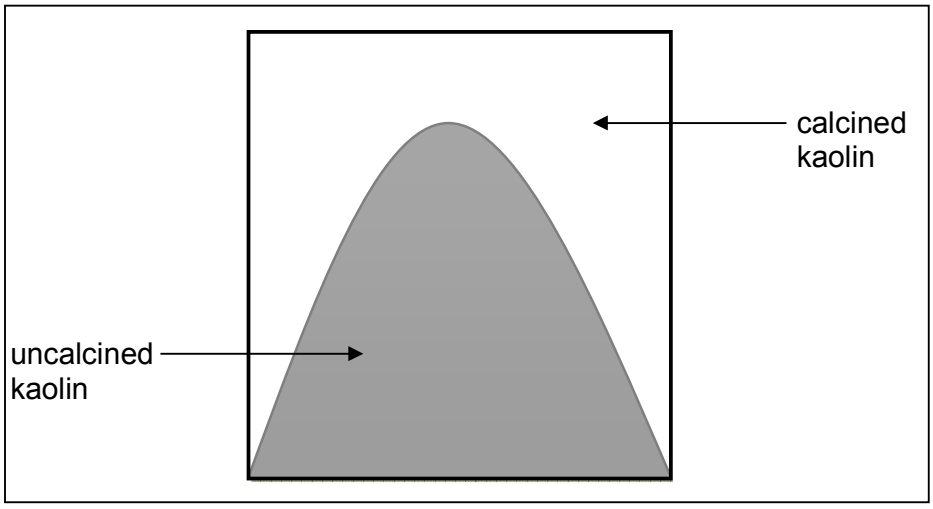

Figure 7-13: The appearance of calcined and uncalcined kaolin in a circular crucible calcined at 1050 C for 15 minutes using the batch method

Due to the influence of the wall conduction, the differences between the four different methods are not as apparent as anticipated. This is because the soak method, where the heat has a greater opportunity to permeate into the crucible, produces a much more calcined product than the batch method, where the heat is only just about reaching the bottom of the crucible after twenty minutes at temperature.

7.4.4 The effect of conduction from the walls of the crucible

In order to investigate the effect of the conduction coming off the wall, FC Feed was calcined in the tall, circular crucible with insulation in place around the crucible to try and minimise the effect of the conduction. FC Feed was calcined with this rig using both soak and batch methods of calcination at 1050 °C.

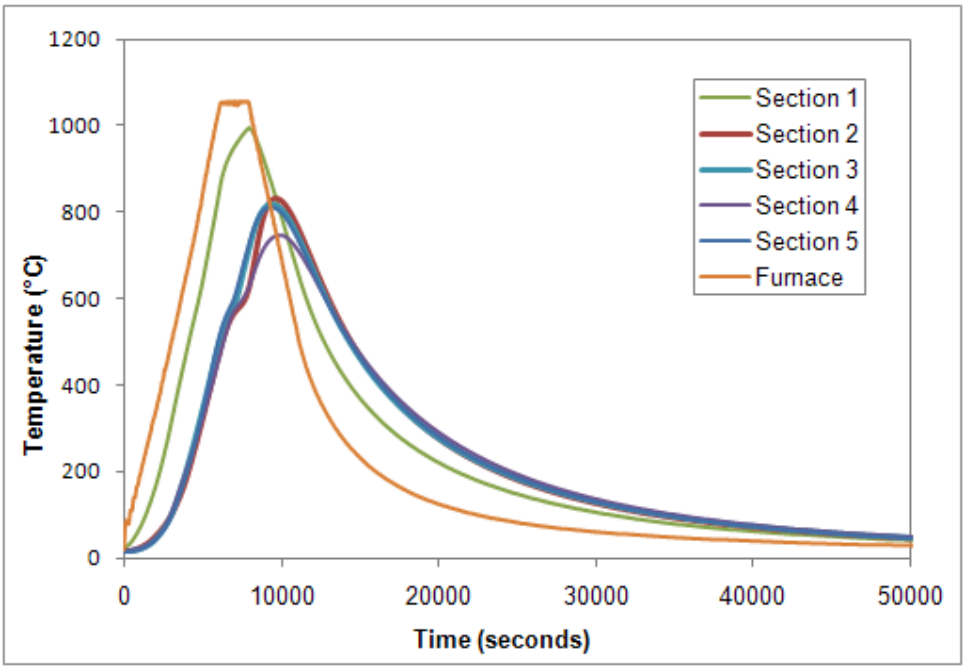

Figure 7-14: FC Feed soak calcined at 1050 °C for 30 minutes with insulation in place thermocouple data

The thermocouple data for the soak calcination with insulation in place, displayed in Figure 7-14, shows a decrease in temperature seen for sections 2 to 5 when compared with the soak experiment thermocouple data shown in Figure 7-5, despite the increase in furnace temperature, which means that the insulation is working. The soluble aluminium results for the soak experiment, shown in Figure 7-15, reinforce this, with the products being less calcined than the experiments without the insulation in place, the results for which are shown in Figure 7-3. The top of the crucible is the only section which appears to have been calcined, which proves that the conduction of through the sides of the crucible is important in the calcining of the material.

FC Feed calcination at 1050 °C for 30 minutes

	Soak		Batch
1	90.8 / 0.79	1	84.3 / 12.27
2	89.4 / 16.76	2	82.7 / 15.67
3	88.5 / 18.08	3	81.0 / 11.20
4	87.5 / 18.63	4	80.9 / 8.90
5	86.7 / 17.26	5	81.2 / 12.90

Figure 7-15: Brightness and soluble aluminium data for FC Feed calcined using the soak and batch methods at 1050 °C for 15 minutes in a circular crucible. Results are displayed as brightness/amount of soluble aluminium (% / wt.%)

The thermocouple data illustrated in Figure 7-16 indicate that the kaolin was exposed to significantly reduced temperatures during the batch calcination with insulation in place. Section 1 only reached a maximum temperature of 801 °C, which is a substantial decrease on both the maximum temperature measured in the kiln, 1059 °C and the maximum temperature registered in Section 1 of the soak experiment, 996 °C, as shown in Figure 7-14.

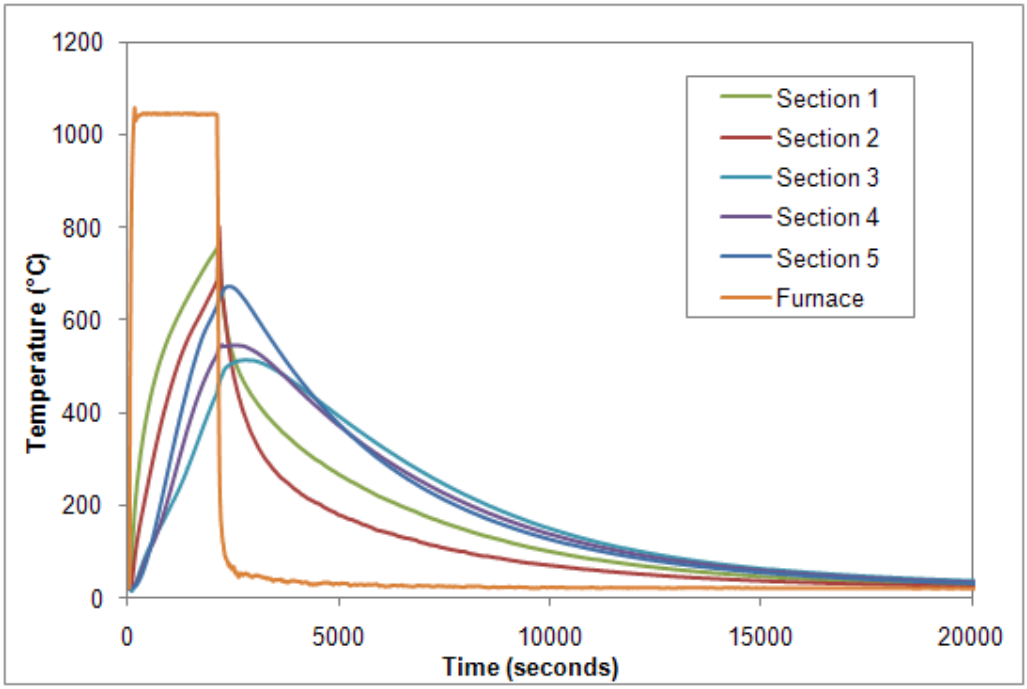

Figure 7-16: FC Feed batch calcined at 1050 °C for 30 minutes with insulation in place thermocouple data

The batch calcination results appear to indicate that the crucible is too large for the batch method to be successfully compared to the soak method under these conditions, with the soluble aluminium for the top section still very high, despite the increased level in the kiln, which has been proven to have an effect on the calcined product.

This means that the effect of heating rate and cooling rate on the calcined product could not be successfully investigated with the tall, circular crucible. Instead, the tray crucibles, as used for the initial experiments, are more suitable for further investigations.

7.5 Investigating the method of calcination with tray crucibles and thermocouples

The tray crucibles had a very shallow bed depth of only 20 mm, meaning that it was not possible to accurately measure different depths. Therefore, a rig was designed that would allow the temperature of the kaolin to be monitored in the middle of the crucible, and at one of the corners, as shown in Figure 7-17. A third thermocouple was used to measure the temperature at height of the furnace at the top of the crucible and a fourth the temperature at the height of the tall circular crucibles.

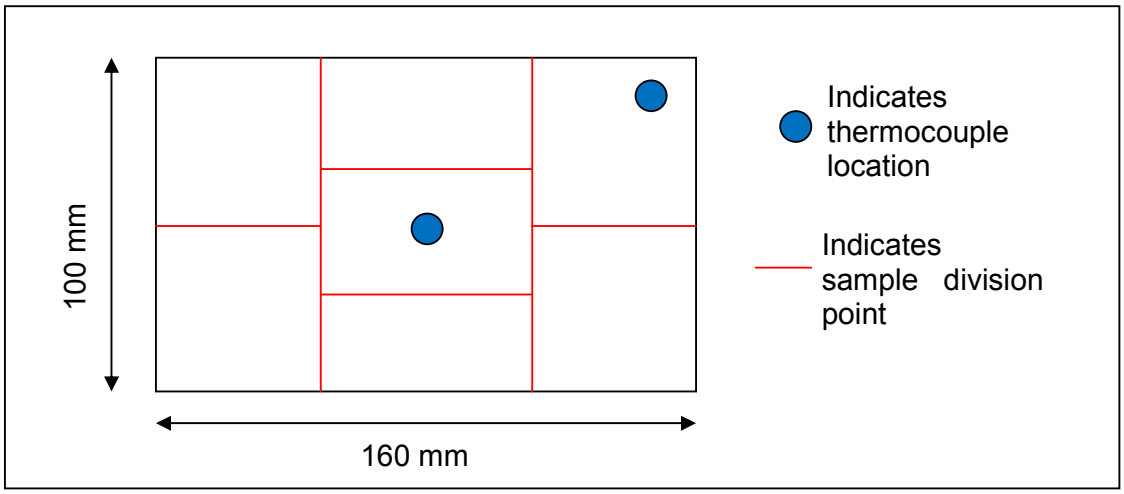

Figure 7-17: Location of the two crucible based thermocouples along with sample division markings

Figure 7-17 also indicates how the calcined sample was divided into sections, further division being performed for each section into top and bottom. It was divided into such an arrangement to allow the sample directly related to the thermocouple data to be collected, as well as to enable an understanding of the wall effects to be determined. A second crucible was also calcined simultaneously side by side, which was again separated into top and bottom sections, and which could be used for

colour and particle size analysis. The full thermocouple support design can be seen in Appendix A.

7.5.1 With support base in place

FC Feed was calcined at 1050 °C for 30 minutes at high temperature using both the soak and batch methods. The soluble aluminium results shown in Figure 7-18 indicate that the soak method has been the more successful calcination method, a similar result to the tall crucibles, shown in Figure 7-4. The brightness results for the second crucible also support this. The brightness values for the crucible calcined under soak conditions were 90.6 % for the top section and 90.4 % for the bottom, while for the batch calcined crucible the brightness values were 89.1 % for the top section and 88.7 % for the bottom.

The thermocouple data, shown in Figure 7-19, indicates that both the middle of the crucible and the corner of the crucible reach high temperature for a considerable amount of time, which explains the low values of soluble aluminium obtained from the dish samples. These values are much lower than those found in the experiment shown in Figure 7-2.

It is thought that the increase in height within the furnace for this experiment with thermocouples may be the cause of the difference, as the temperature profile through the kiln is not as even as stated by the manufacturers. There is a difference of 27 °C between the temperature recorded by the thermocouples at 100 and 20 mm from the support base when at high temperature. According to the chamber

uniformity data from Carbolite, there should be an overall temperature difference, from top to bottom of less than 5 °C when operated at either 900 or 1200 °C, see Appendix C.

Soak Calcination at 1050 °C

0.42	0.32	0.31
	0.35	
0.36	0.35	0.32

Top of crucible

0.49	0.40	0.40
	0.48	
0.52	0.58	0.43

Bottom of crucible

Batch Calcination at 1050 °C

1.74	1.57	0.56
	8.64	
6.47	10.74	2.32

Top of crucible

7.75	5.14	1.67
	14.89	
14.82	15.88	5.20

Bottom of crucible

Figure 7-18: Soluble aluminium results for FC Feed calcined at 1050 °C for 30 minutes in tray crucibles with full thermocouple rig, using the soak and batch calcination methods.

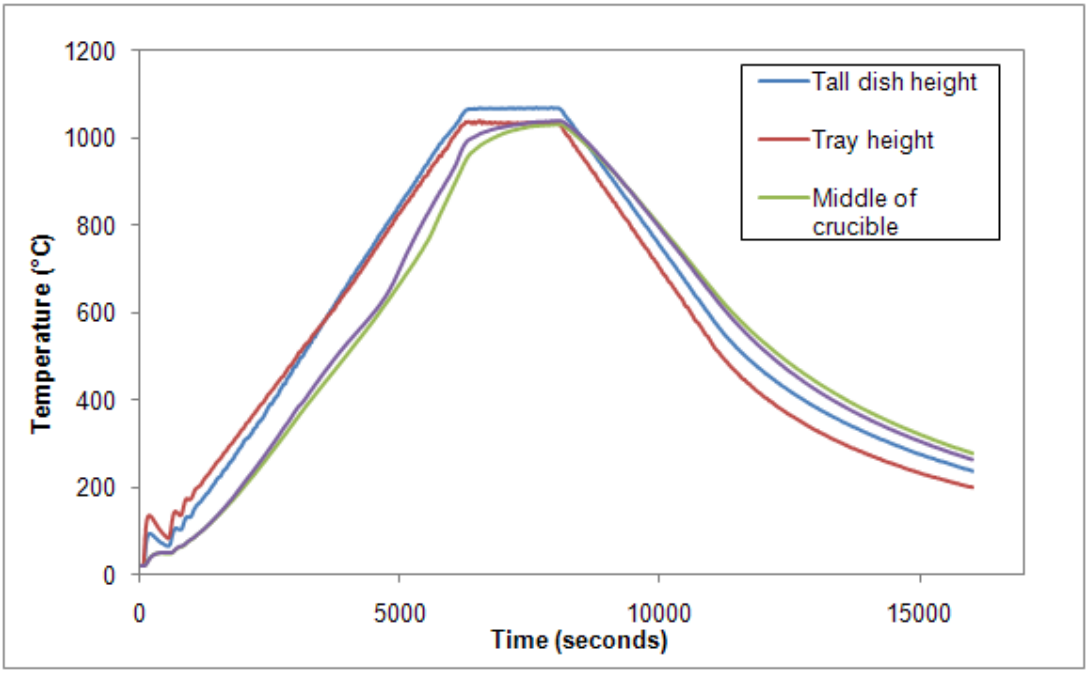

Figure 7-19: FC Feed soak calcined at 1050 °C for 30 minutes thermocouple data, tray crucibles

Under standard conditions, the furnace contains a base on top of which a tablet of fused silica sits, which is raised 20 mm from the base of the kiln. The thermocouple experiments were carried out using a rig made out of fibre board, which is 50 mm in height. Therefore, the experiments were repeated without the rig base in place, as the thermocouple stand was capable of supporting itself.

The thermocouple data shown in Figure 7-20 indicate that the middle of the crucible is not reading the same temperature as the corner, which just reaches 1050 °C at the end of the 30 minute heating period. When compared to the thermocouple data for the soak experiment, shown in Figure 7-19, the temperature of the dish is much lower for the batch experiment, and so the soluble aluminium levels achieved in the product, shown in Figure 7-18, are higher.

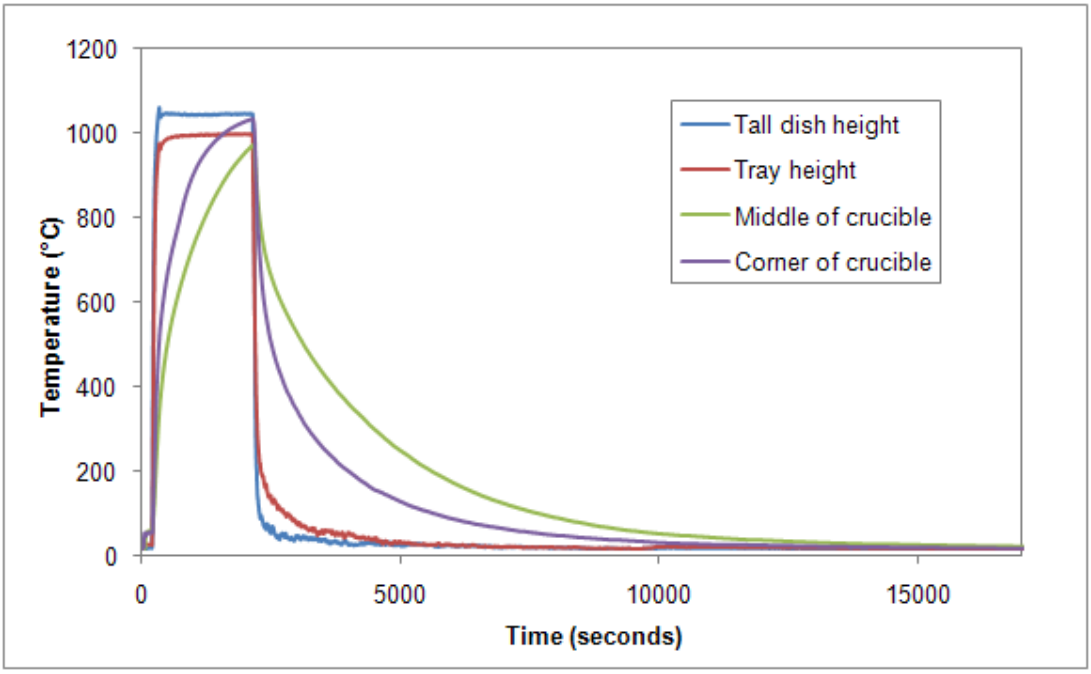

Figure 7-20: FC Feed batch calcined at 1050 °C for 30 minutes thermocouple data, tray crucibles, thermocouple support base in place

The soluble aluminium results for the batch calcination, shown in Figure 7-18, seem to show some variation across the dish, with one end showing higher levels than the other. This is thought to be due to the presence of the thermocouple stand, which may be acting as a heat sink. The soluble aluminium levels are much higher than those for the calcination shown in Figure 7-2 and it is possible that the change in feed has caused the differences, as all of the soluble aluminium results appear to be in the spinel phase of the reaction, if the experiment had continued for only couple of minutes longer, it is presumed that all of the levels would be low. Therefore, Milled HF was used for further experiments, as it was used in the original testing.

7.5.2 Without support base in place

Milled HF was calcined in two tray crucibles at 1050 °C for 30 minutes, using both soak and batch calcination methods. The temperature of the crucible that was divided into 14 sections was monitored using two thermocouples, one in the middle and one at the edge. The base for the thermocouple support was replaced with a slab of fused silica, which was the base used in the kiln under standard conditions, as with the calcinations shown in Figure 7-2.

Soak Calcination at 1050 °C

11.74	11.45	4.65
	12.33	
11.44	10.07	7.20

Top of crucible

16.45	13.65	10.72
	16.57	
16.95	16.22	12.49

Bottom of crucible

Batch Calcination at 1050 °C

0.49	0.57	0.86
	1.99	
0.44	0.74	0.78

Top of crucible

2.11	6.52	5.58
	12.87	
1.30	4.21	6.01

Bottom of crucible

Figure 7-21: Soluble aluminium results for Milled HF calcined at 1050 °C for 30 minutes in tray crucibles with only the thermocouple stand, resting on the fused silica base, using the soak and batch calcination methods.

The soluble aluminium results for the soak and batch method calcinations are shown in Figure 7-21. These are similar to the ones found in Figure 7-2, with the soluble aluminium content much higher for the soak calcined material than the batch calcined. As with the calcinations which included the thermocouple support base, there seems to be some evidence of shielding from the vertical section, with the sample that was next to the support having higher soluble aluminium values than the rest.

The thermocouple data displayed in Figure 7-22 show that the kaolin in the soak experiment did not reach the furnace set point, unlike the experiment shown in Figure 7-19, where the crucibles are slightly higher in the furnace. Both thermocouples measuring kaolin temperature reach similar temperature, as is the case in the other soak experiment, although they only reach the respective maximum point for a fraction of the amount of time compared to the previous. This lack of time at high temperature explains the higher soluble aluminium results, shown in Figure 7-21 compared with those in Figure 7-18.

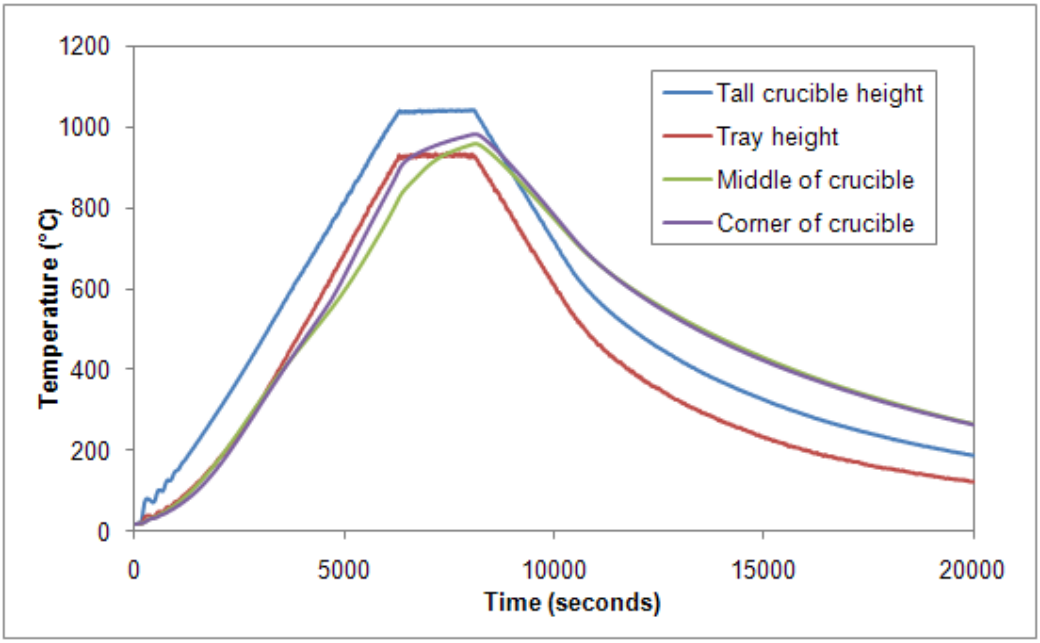

Figure 7-22: Milled HF soak calcined at 1050 °C for 30 minutes thermocouple data, tray crucibles, no base to thermocouple support

The thermocouple data for the batch calcination without a support base in place, shown in a Figure 7-23, displays a faster heating rate for the batch calcination with the support base, shown in Figure 7-20. The increased heating rate means that the kaolin has an extended duration at high temperature, which causes the decrease in soluble aluminium, shown in Figure 7-21 and compared with the data from Figure 7-18.

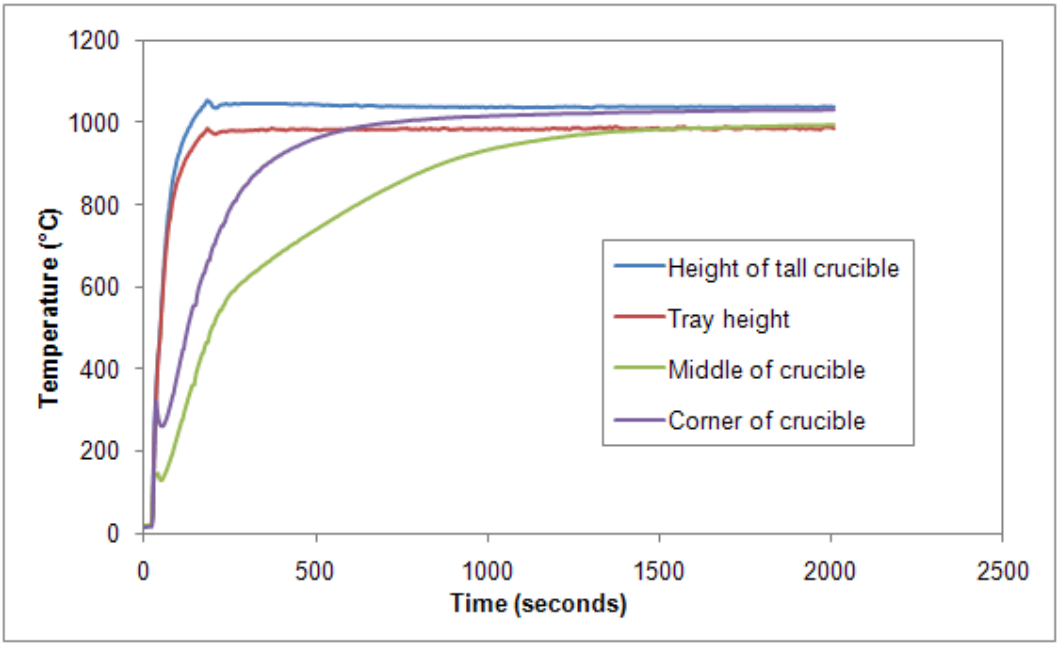

Figure 7-23: Milled HF batch calcined at 1050 °C for 30 minutes thermocouple data, tray crucibles, no base to thermocouple support

This increase in calcination, despite the accompanying drop in temperature seen by the crucible due to the drop in height in the furnace, may be due to the mechanism of heating. The most dominant form of heat transfer in the kiln, due to the lack of air flow to promote convection, is radiation, as shown in Appendix D.

Radiation is a very complex method of heat transfer. There is not only the temperature and the materials of the objects involved, but also the orientation of the object being heated to the heat source must be considered.

A surface generally emits radiation in all directions simultaneously. If the receiving surface is located some distance away from the radiation source, then not all the radiation leaving the source will impinge on the receiving surface. As the surface moves towards the source, increasingly more radiation will be received. Clearly, the source is not emitting more radiation as the object gets closer, but a larger proportion of the heat is landing on the object. This leads to the concept of the view factor, which takes the geometry of the system into account [89].

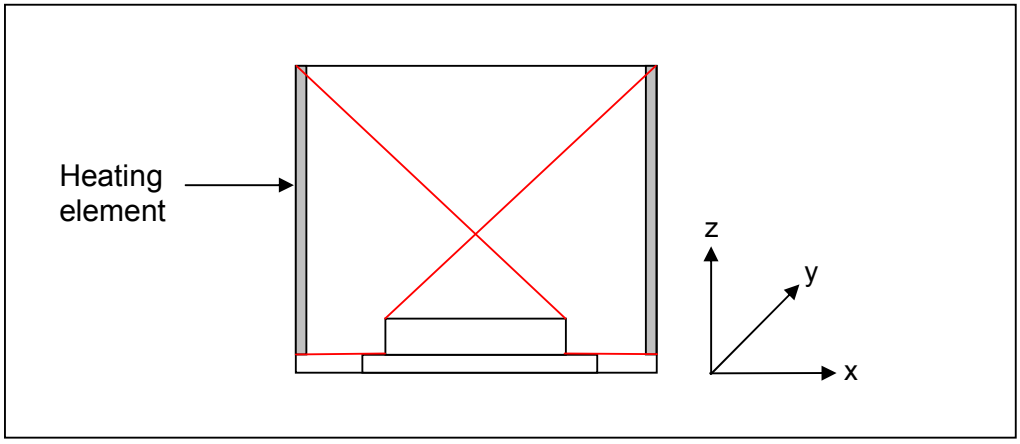

Figure 7-24: Diagram to show the path of radiation inside the furnace without the thermocouple support base present

Figure 7-24 shows the path of radiation inside the kiln. Due to the relatively square geometry of the furnace (H: 250 mm x W: 325 mm x L: 450 mm) when the dish is placed in the centre, all areas of the dish will receive the same amount of heat. Therefore, view factors are not relevant in this case.

However, when the crucible is raised in height, the presence of the thermocouple support in the kiln interferes with the path of the radiation, creating a complex situation, as shown in Figure 7-25, where the support base acts as a heat sink, drawing the heating energy away from the kaolin and thereby reducing the amount of calcination that can occur.

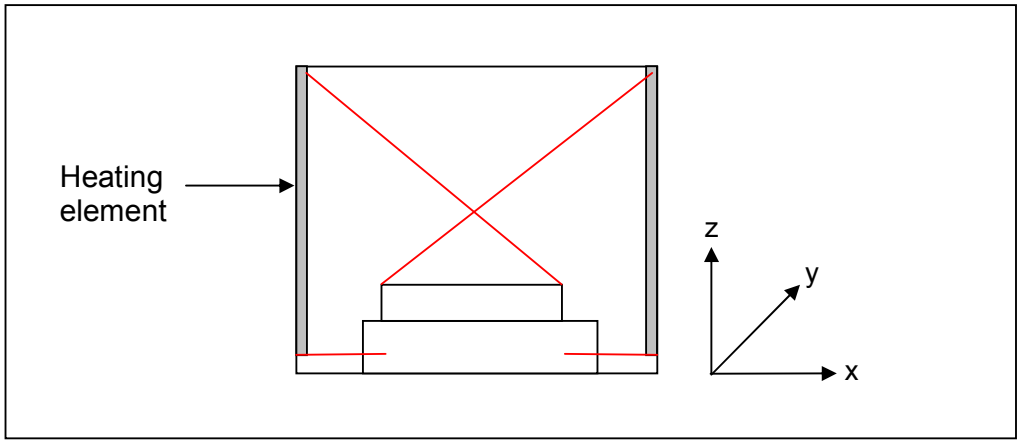

Figure 7-25: Diagram to show the path of radiation inside the furnace with the thermocouple support base present

It is, therefore, apparent that the amount of calcination that occurs within a sample is a delicate balance of temperature and duration at that temperature, otherwise incomplete calcination will occur.

7.6 Conclusions

Use of thermocouples within the crucible during calcination has determined that the maximum temperature reached and the time spent at that temperature during the reaction governs the amount of soluble aluminium remaining.

It has also been determined that the height of the sample in the kiln is very important, with samples placed higher in the kiln experiencing higher temperatures, which causes them to be more calcined than those lower down in the furnace.

This work has also proved that soluble aluminium content of the product is strongly linked to the temperature experienced by the kaolin during the calcination and is not related to the chemistry of the kaolin.

8 Particle size and morphology

8.1 Introduction

In order to investigate the effect of the particle size of the feed on the calcined product, a coarse kaolin was ground to produce a fine and a superfine kaolin. These three kaolins were then used to produce seven different feed forms: milled, spray dried, 3 mm prills, 6 mm prills, 9 mm prills, granules and lump. This allowed the intrinsic and bulk particle size to be investigated.

The different feed forms were calcined at four temperatures, using the batch method of calcination that had been established as representative of industrial conditions, to develop an understanding of how the aggregate size affected how the calcination reaction progressed. As a result of these experiments, the feed forms made out of the ultrafine kaolin were calcined in the thermocouple rig used to investigate the heat transfer through the product. This allowed the effect of bulk density and the nature of heating on the calcined product to be determined.

In addition to the feed form work, several kaolins that differed in particle size, shape and mineralogy were selected from Cornwall and France in order to determine the effect of particle morphology on the calcined product. Samples were analysed using a number of different techniques both prior to and after calcination in order to determine the cause of any differences in structure that may occur.

8.2 The effect of particle size on calcination

From the work carried out examining the effect of natural variances in chemistry as discussed in Chapter 7, it became apparent that the particle size of the kaolin had an effect on the soluble aluminium content of the calcined product, where smaller particles were yielding higher amounts of soluble aluminium, particularly as a result of the calcination carried out at 950 °C. There was also an effect on the brightness of the product, with finer kaolins exhibiting higher brightness values than coarser ones, although this is a known phenomenon and is not restricted to kaolin, it is related to the reduction in diffraction from the finer particles.

When investigating how particle size affects the calcination reaction, it was necessary to exclude the influence of chemistry. For this reason, Residue, a coarse, milled powder product that has a less than 2 μm content of approximately 40 wt.%, was chosen. This coarse kaolin was ground, using a stirred media mill in order to create two products with the same chemistry but differing particle size, a fine kaolin which has a 2 μm content of 70 wt.% and an ultra fine kaolin, that has a 2 μm content of 90 wt.%. The full particle size distributions for the three kaolins are shown in Table 8-1.

Each of these three kaolin products was then used as the starting material to create seven different feed forms: milled powder, spray dried powder, granules, 3 mm prills, 6 mm prills, 9 mm prills and lump product. This range of feeds allowed the effects of the intrinsic and physical particle size upon the calcined product to be investigated. After creating the different feed forms, the intrinsic particle size of the different kaolins

remains similar to that of the milled powder, as shown in Table 8-2. This was checked using the sedigraph technique detailed in Section 3.2.5.

Table 8-1: Particle size distributions for Milled Powder feed forms made from Residue obtained through sedigraph analysis

Particle size (wt.%)	Coarse	Fine	Ultrafine
10 µm	7.8	1.5	0.8
8 µm	13.8	2.4	1.2
5 µm	34	7.6	2.8
3 µm	45.9	83.0	92.7
2 µm	35.7	72.4	87.7
1 µm	24.3	53.1	75.8
0.75 µm	20.4	43.2	68.6
0.5 µm	15.2	28.7	53.4
0.25 µm	6.4	10.5	26.4

While the prill feed forms are uniform in particle size, and the spray dried material is between 200 and 400 µm in size, the other two forms, lump and granules do show variation and are detailed in Table 8-2. The differences between the lump feed size distributions for the three kaolins is minimal, with particular similarity in the coarse and fine kaolins, but the ultrafine feed shows a slightly finer particle size. The granular feeds are more similar in their particle size distribution.

Throughout the different calcinations, the three different prill feeds all showed a similar response to temperature in terms of product particle size, soluble aluminium content and brightness. Therefore, only the data for the 9 mm prills will be presented below to simplify the data set. In addition, while the data from all the different calcination experiments was being analysed, it was noted that the coarse and ultrafine feed forms exhibited the two extremes in product properties, with the fine

material in the middle. Therefore, only the ultrafine and coarse materials are discussed below.

Table 8-2: Particle size distributions for Lump and Granular feed forms made from Residue 40, 73 and 90 wt.% less than 2 microns obtained through sieve analysis

Particle size (wt.%)	40 wt.% < 2 µm		73 wt.% < 2 µm		90 wt.% < 2 µm	
	Lump	Granules	Lump	Granules	Lump	Granules
4 mm	25.9	0	27.1	0	17.1	0
2 mm	32.6	0	28.7	0	36.4	0
1 mm	19.8	53.6	17.4	53.4	21.2	55
850 µm	2.3	13.1	2.5	14.6	3.2	17
600 µm	5.1	23.9	4.8	24.2	5.0	19.6
425 µm	3.4	8.8	8.6	6.8	4.0	7.4
300 µm	3.8	0.2	3.9	0.7	3.6	0.7
180 µm	3.2	0.3	2.5	0.2	2.7	0.1
53 µm	3.9	0.1	4.4	0.1	6.9	0.2

8.2.1 Particle size

The fusion that occurs as a result of the 1050 °C calcination can be assumed to be due to an increase in the structure as a result of the spinel reaction, which follows on from the unstructured metakaolin phase. The amount of fusion that occurs appears to be consistent across all feed forms for those made out of the coarse material, as shown in Figure 8-1. The feed form that has the highest amount of fusion due to the calcination are the granules, which have an decrease of 18.2 wt.% in the less than 2 µm size fraction, which is accompanied by a drop in brightness as shown in Figure 8-8. The other feed forms all show slightly less fusion with a decrease in particle size ranging between 10 wt.% for 9 mm prills through to 15.4 wt.% for 3 mm prills.

As shown in Figure 8-1, the 9 mm prills show slightly less fusion than the other feed forms, with a less than 2 micron content of 28.4 %. The other feed forms all have a particle size of between 22 and 23 wt.% less than 2 microns as a result of the 1050 °C calcination.

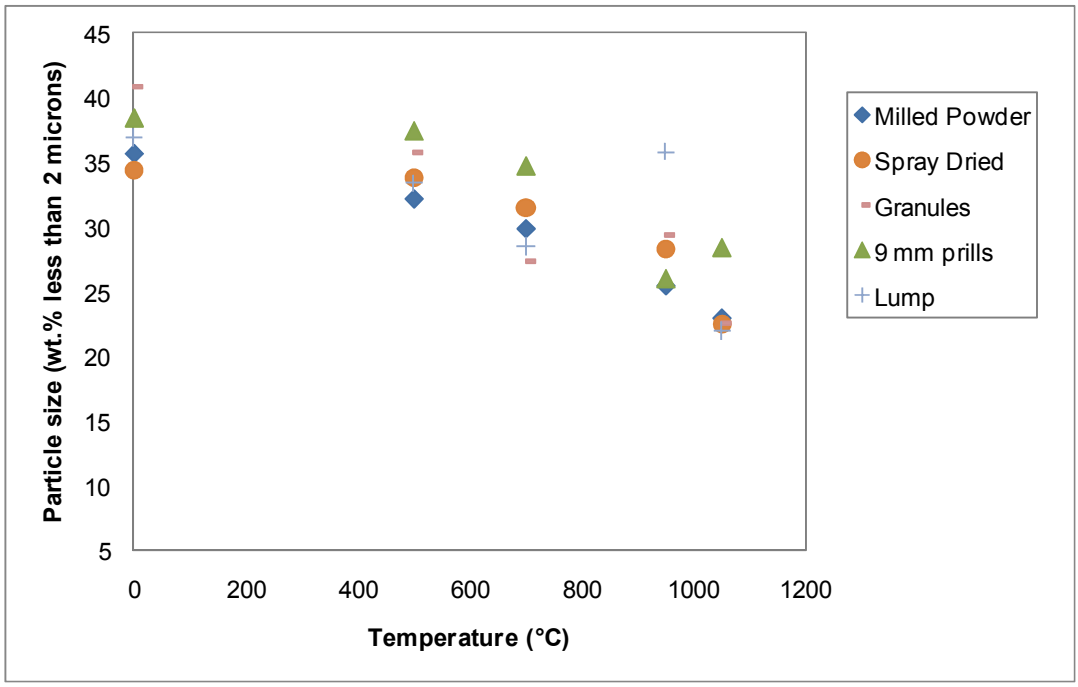

Figure 8-1: The effect of temperature on the particle size of the calcined product of different feed forms with an intrinsic particle size of 40 wt.% less than 2 microns.

The range of fusion that occurs for the different feed forms for the ultrafine material is a lot wider than for the coarse as a result of the calcination at 1050 °C. The amount of fusion occurring is also greater for the ultrafine materials, which is considered to be due to the increase in surface area making the kaolin more reactive [3, 4, 38]. This is in contrast with previous work [42]. The particle size of the ultrafine calcined products can be seen in Figure 8-2, with a range of between 62.4 and 9.3 wt.% less

than 2 μm for milled feed and spray dried feed, respectively, as a result of the 1050 °C calcination.

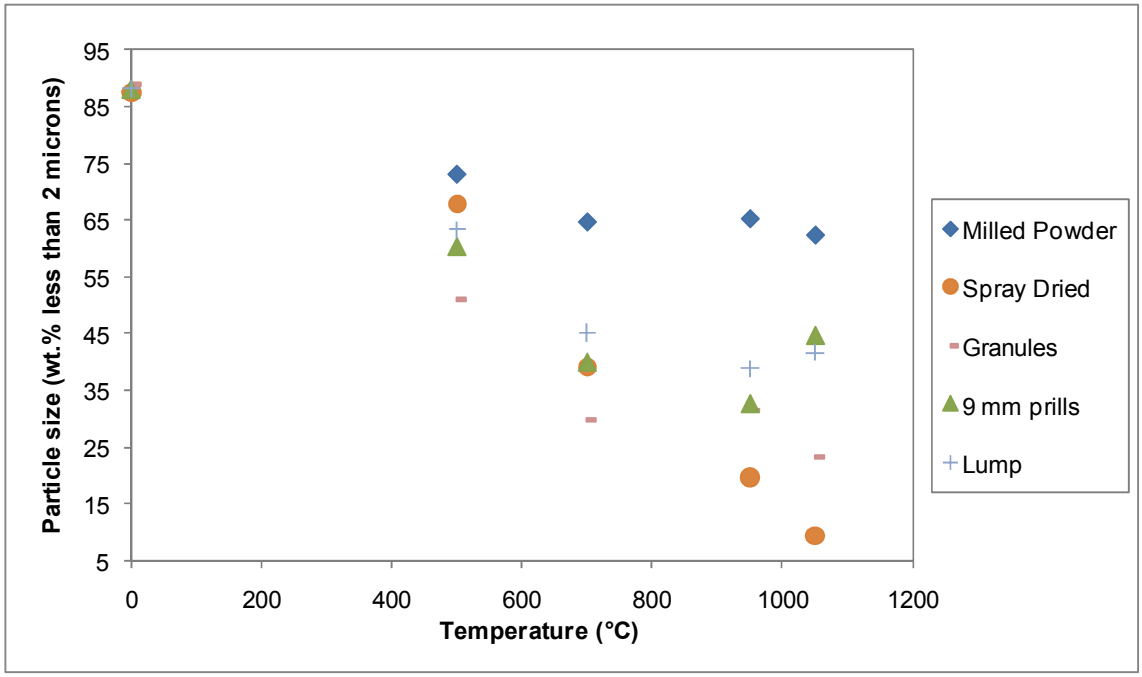

Figure 8-2: The effect of temperature on the particle size (wt.% less than 2 microns) of the calcined product of different feed forms created from the ultrafine material

For all four calcination temperatures, the feed form with the least amount of fusion is consistently the Milled Powder. The feed form with the most fusion occurring as a result of calcination varies until the 950 °C calcination, where the spray dried material begins to fuse considerably more than the other feed forms, and can be assumed to be as a result of the spinel reaction starting to take place. Above this temperature, the spray dried and granules feeds show more fusion than the other feeds.

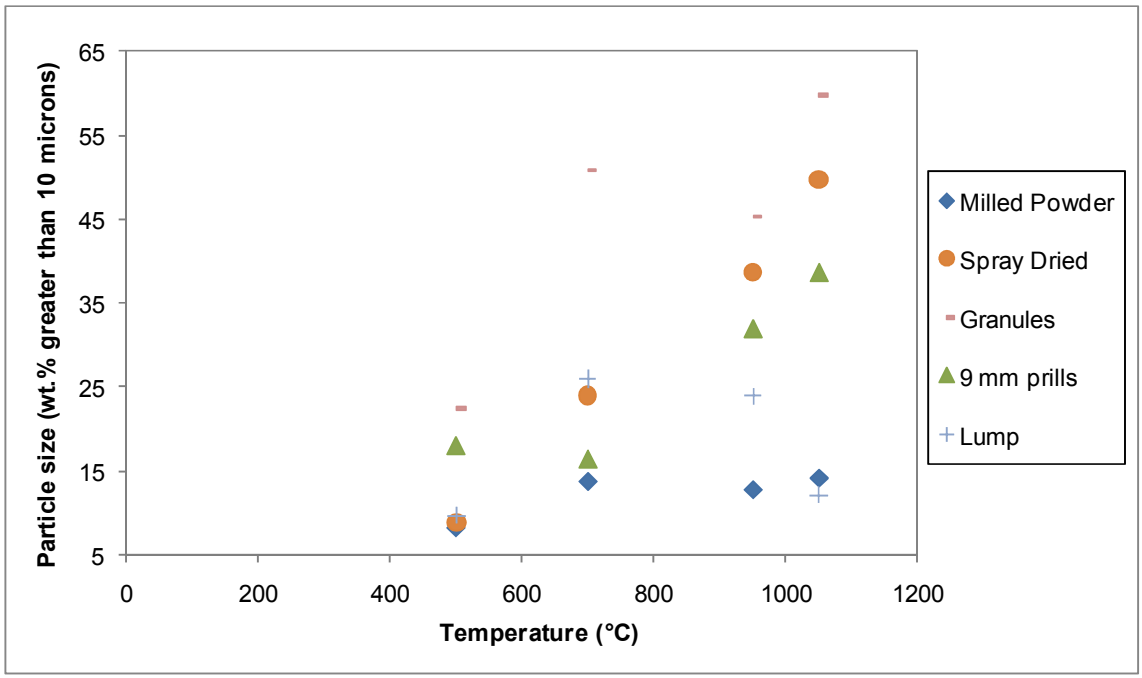

Figure 8-3: The effect of temperature on the particle size (wt.% greater than 10 µm) of the calcined product of different feed forms created from the ultrafine material

The extent of the fusion occurring for the different particles can be seen in the amount of product that is found to be larger than 10 µm, as displayed in Figure 8-3. After the 950 and 1050 °C calcinations for the 9 mm, spray dried and granules feeds, there is a high proportion of material found to be greater than 10 µm in the product, suggesting a great deal of fusion and that the spinel reaction is occurring at a lower temperature than for the other feed forms, hence the increased fusion. This suggests that these feeds are more difficult to mill than the others and means that they would not be suitable to use in production, even if they are proven to calcine more successfully.

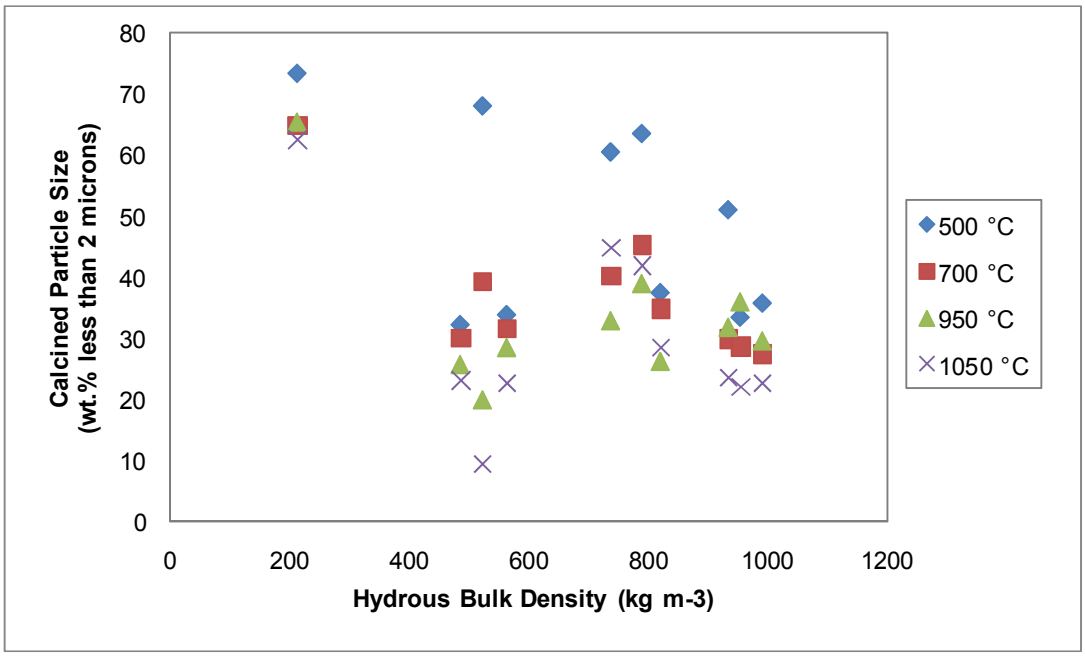

Figure 8-4: The relationship between calcined particle size and hydrous bulk density for coarse and ultrafine Residue feed forms calcined at 500, 700, 950 and 1050 °C

There is a trend evident in the relationship between bulk density and the size of the calcined product, as shown in Figure 8-4, but this is more evident in the lower calcination temperatures of 500 and 700 °C. For the higher calcination temperatures, 900 and 1050 °C, the trend of low bulk density hydrous feeds producing a finer particle sized calcination material is disturbed by the ultrafine spray dried feed, which although it had a lower bulk density than some of the other feeds, exhibited a large amount of fusion upon calcination, the product having a particle size of 9.3 wt.% less than 2 µm. This increase in particle size was also seen in the fine spray dried feed form. This suggests that the closer the particles are forced together in creating the feed form, the harder they are to break apart after calcination.

8.2.2 Soluble Aluminium

The soluble aluminium trend for the Residue feed forms follows the same trend as the other kaolins studied as part of this work, as discussed in Section 5.2. The results for the coarse Residue can be seen in Figure 8-5. Those for the ultrafine kaolin can be seen in Figure 8-6. The results are similar, with some minor variation in the maximum amount of soluble aluminium after the 950 °C calcination and the greater amount of soluble aluminium after the 1050 °C obtainable from the two finer feed forms, milled powder and spray dried material.

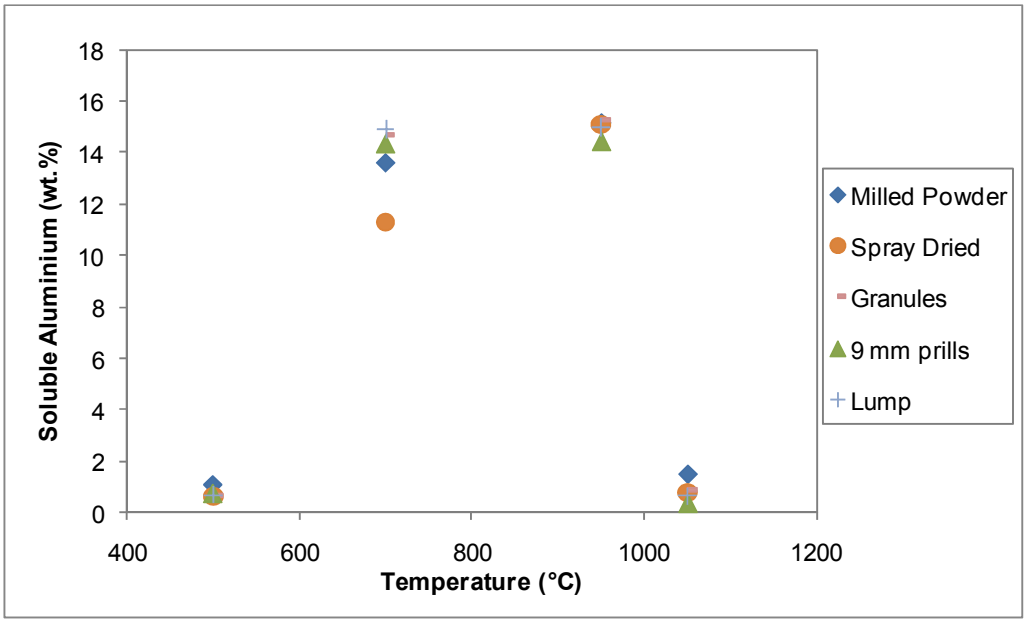

Figure 8-5: The relationship between the temperature and the amount of soluble aluminium obtainable from the calcined product for Residue feed forms made from the coarse material

The maximum soluble aluminium level seems to occur at a lower temperature for densified feeds, with a higher level of aluminium retrieved from the lump and granules for each particle size. These two feeds, along with the 9 mm prills also

have a lower soluble aluminium value after the 1050 °C calcination. This reinforces the theory discussed in Section 8.2.1 that these feed forms appear to be calcining better. This is in contrast with previous research which has stated that particles greater than 20 μm react much slower than fine particles, due to the reduction in surface area and difficulty in getting heat into the particle for the reaction to occur [40]. The absence of this effect may be due to the use of flat crucibles and what has been established as a delicate balance of radiation and conduction within the kiln (Section 7.5). The efficient heating method of the laboratory is unlikely to be what happens in production.

As with some of the other feeds experimented with, the amount of soluble aluminium present in the product of the 1050 °C calcination is higher than the other feed forms where there was more aluminium extractable as the result of the 950 °C calcination. This suggests that if more is released from the structure, it takes longer to be reabsorbed as the spinel reaction progresses.

The increase in reactivity is particularly evident in the milled and lump feed forms. The increased surface area present in both feed forms due to the presence of milled material means that they are more reactive than the coarser feeds [3, 4, 38].

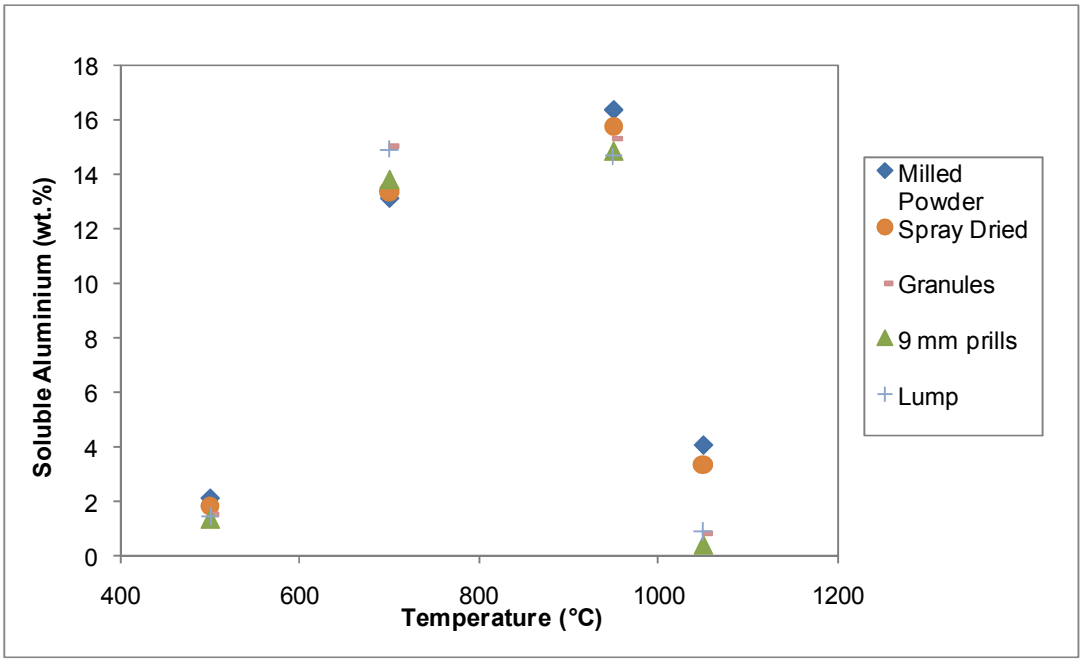

Figure 8-6: The relationship between the temperature and the amount of soluble aluminium obtainable from the calcined product for ultrafine Residue feed forms

As with the particle size of the calcined product, there appears to be a link between the bulk density of the feed and the amount of soluble aluminium in the calcined product. This can be seen in Figure 8-7, where the milled samples, which have low bulk density, have higher soluble aluminium values for the 500, 950 and 1050 °C calcinations than the higher density feeds. However, for the 700 °C calcination, the feeds with low bulk density have lower values of obtainable soluble aluminium. This suggests the nearness of particles has some influence on the metakaolin reaction, with particles that are spread further apart not calcining as well as those that are closer together. This may be due to the ability of heat to move through the crucible as any air gaps will be detrimental to the heating, as air is a good insulator.

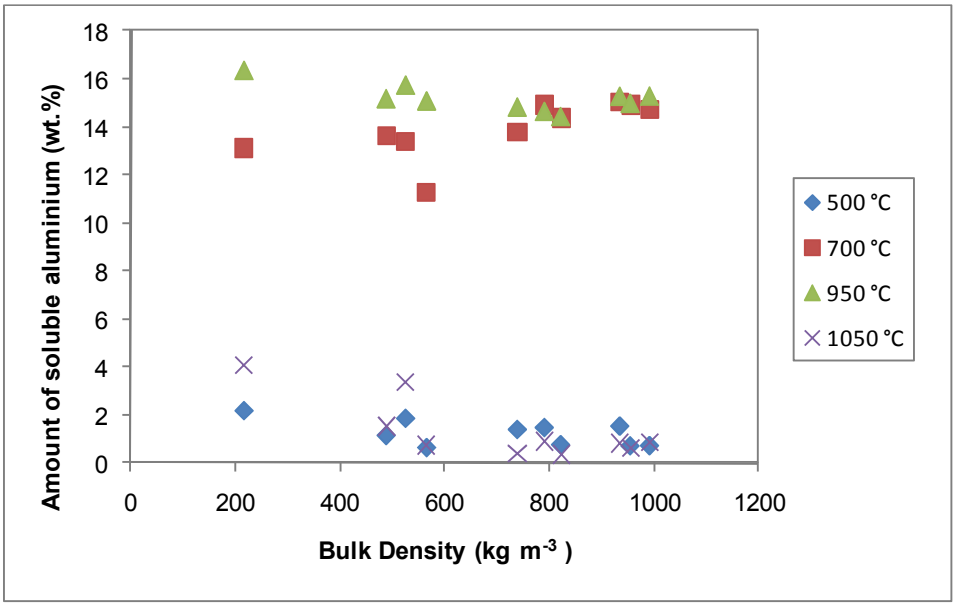

Figure 8-7: The relationship between the soluble aluminium content of the calcined product and the hydrous brightness for four different calcination temperatures

Kaolins that exhibit a lot of fusion upon calcination make a very abrasive product. This is one of the main concerns when calcining kaolin as if incorrectly fired, either at too high a temperature or for too long then mullite begins to form. Therefore, if in a feed form, such as granules, the particles are very close together, this enables conduction of heat throughout the agglomerate and so facilitates the reaction. The degree of heat retention within the crucible for the different feed forms can be identified using the thermocouple rig used in Section 7.3.

8.2.3 Brightness

Figure 8-5 shows that there is little variation in the brightness of the different feed forms created from the coarse kaolin when hydrous with all values within 1%. The spray dried material has the lowest brightness value, which is also true for the different calcination temperatures. This is not due to the particle size of the feed, as the other feed forms consistently produce a coarser product, as shown in Figure 8-1 and after calcination may be due to how the reaction has progressed in the feed. Prior to calcination, this may be down to natural variation in the feed used. The range in brightness values expands from the hydrous value for the calcined products, to 3.6, 2.2, 2.4 and 1.4 points for the 500, 700, 950 and 1050 °C calcinations respectively. This is still not a large variance and suggests that for each of the feed forms, the calcination reaction is progressing in a similar manner.

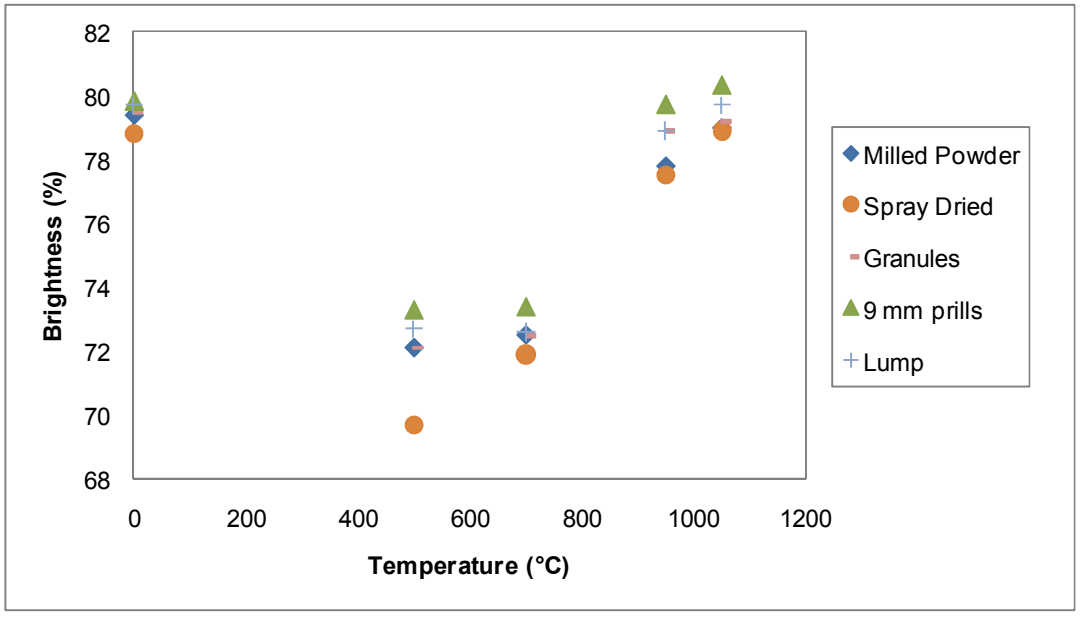

Figure 8-8: The effect of temperature on the brightness of the calcined product of different feed forms created from coarse Residue

The difference in brightness is more noticeable for the calcined product of the ultrafine material than for the coarse, as shown in Figure 8-9. The range in brightness values for the 1050 °C calcination is 9.4 points, between the milled powder and the granules. It is slightly less for the 500, 700 and 950 °C calcinations, with a variation of 5.7, 6 and 4.9 points, respectively.

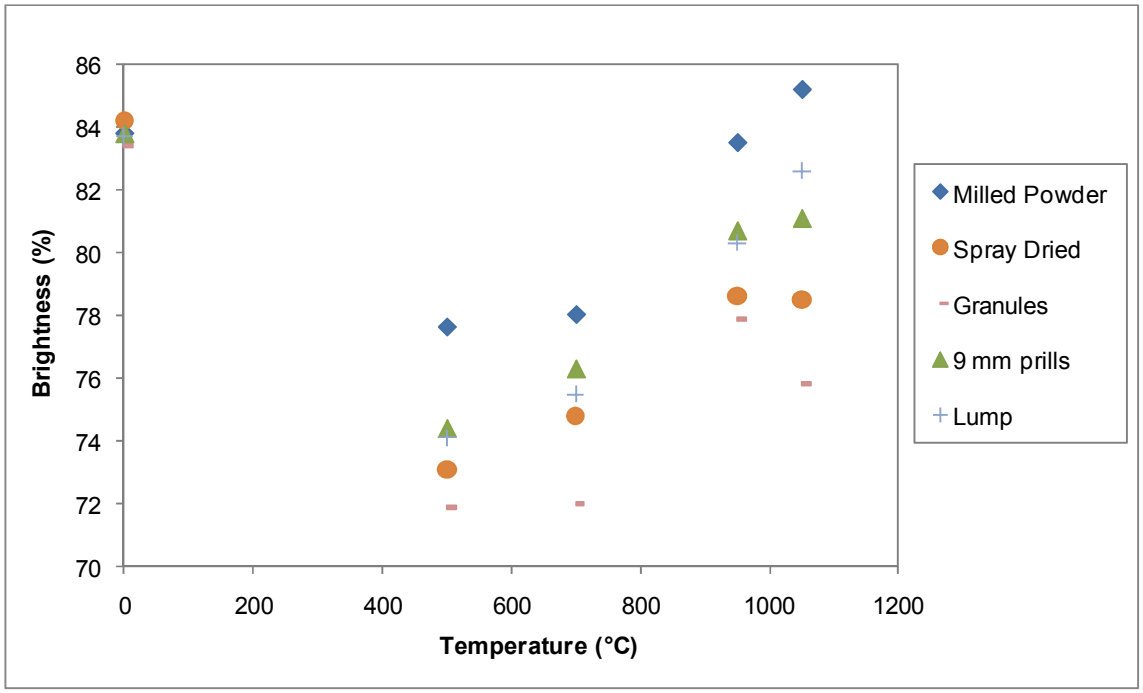

Figure 8-9: The effect of temperature on the brightness of the calcined product of different feed forms with an intrinsic particle size of 90 wt.% less than 2 micron

The product with the highest brightness for the ultrafine material is consistently the Milled Powder. This is likely to be attributable to the effect of the smaller particles causing reduced scatter from the sample being tested. The larger range of brightness values for the ultrafine material is attributable to the stronger bonds in the feed forms made out of the smaller particles, which causes greater agglomeration

during calcination and which are much harder to break up than the other particles. The larger particles then cause a deterioration in the colour of the kaolin [90]. The effect of particle size on the brightness of both the coarse and ultrafine feeds can be seen in Figure 8-10, where calcined product that has larger particles, and less material smaller than 2 μm, exhibits lower brightness.

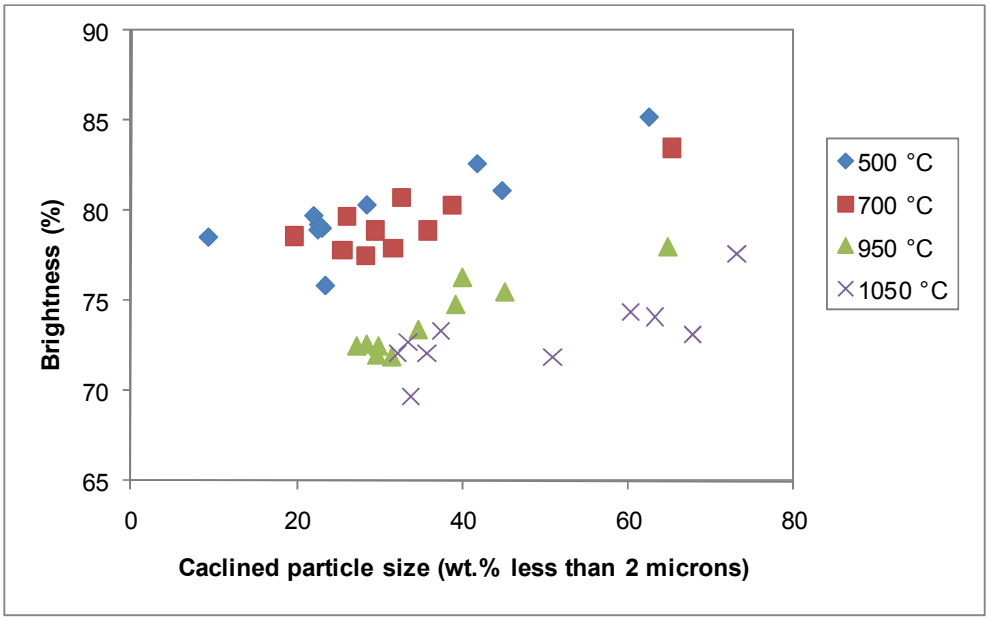

Figure 8-10: The effect of calcined particle size on the calcined brightness for coarse and ultrafine kaolins

This decrease in brightness is not attributable to the increase in bulk density, as other than the ultrafine milled powder, which has the lowest bulk density of the feed forms, there appears to be little variance for the other feeds, as shown in Figure 8-11. The fine milled material has similar bulk density and calcined brightness to the ultrafine material, suggesting that if there is an effect of bulk density on the brightness of the calcined product, it is eliminated once the bulk density increases beyond 400 kg m^{-3}.

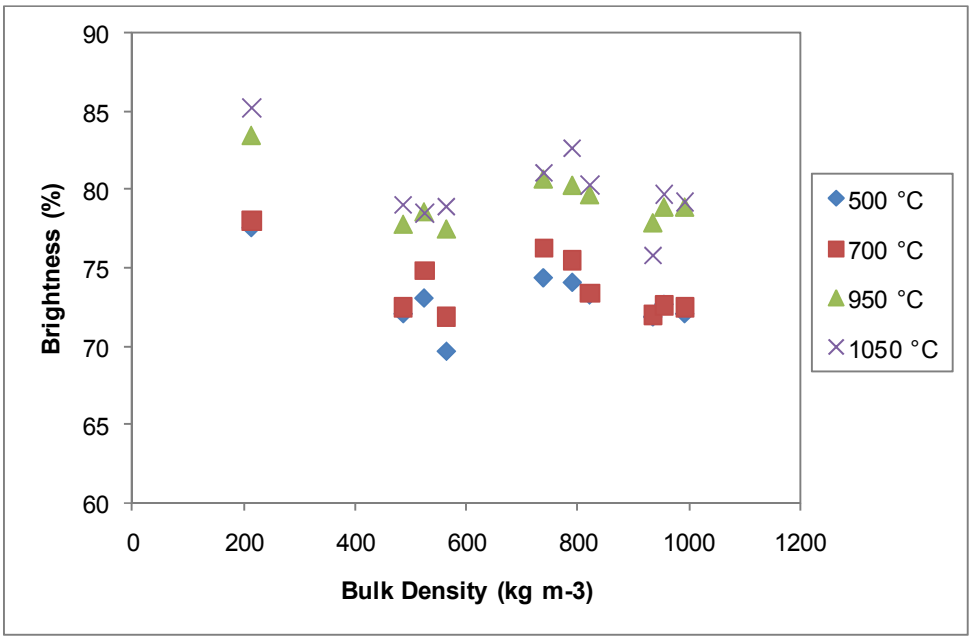

Figure 8-11: The relationship between calcined brightness and hydrous bulk density for ultrafine and coarse feed forms

As with previous kaolins, see section 6.6.1, there is a correlation between the hydrous brightness and the brightness of the calcined product, as shown in Figure 8-12. This is more evident for the 500, 700 and 950 °C calcinations which have R^2 values of 0.59, 0.61 and 0.78, respectively. The relationship between the hydrous brightness and the brightness of the product of the 1050 °C calcination is less apparent, with a R^2 value of only 0.08. This lack of trend may be due to the spread in results for the ultrafine material, as shown in Figure 8-9, which is due to the effect of the particle size distribution in the feed and the increased fusion that this causes [8, 39].

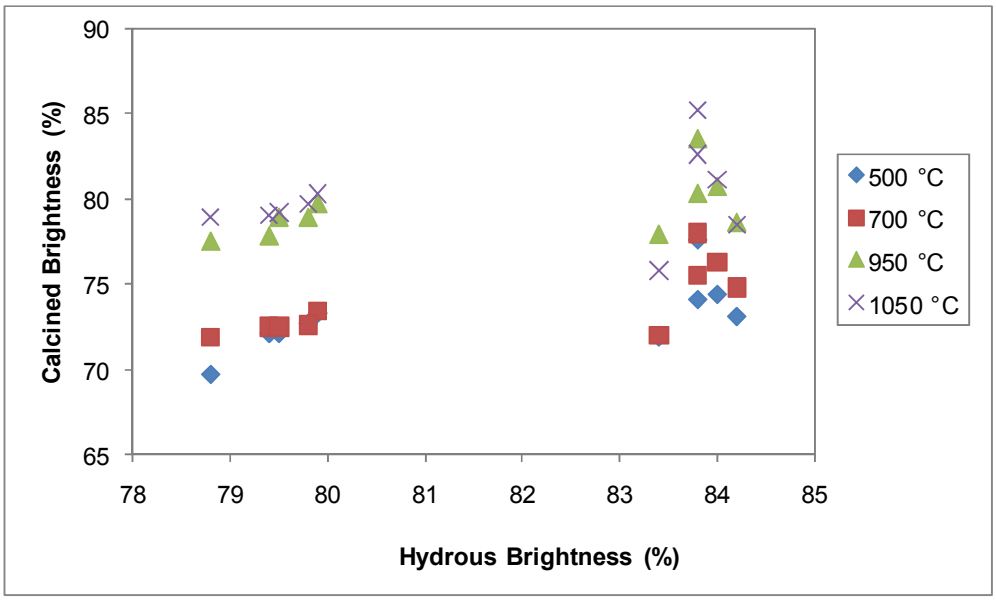

Figure 8-12: The relationship between hydrous brightness and calcined brightness size for all feed forms calcined at 500, 700, 950 and 1050 °C

8.3 Heat transfer through different feed forms

The feed form with the lowest bulk density, milled powder which was made from fine and ultrafine material, was found to have a lower soluble aluminium content after the 700 °C calcination and a higher soluble aluminium level after the 1050 °C. In order to investigate the differences, the thermocouple rig used to study the permeation of heat through the crucible in different densities of material. A sample of milled (lowest density), 9 mm prills (medium density) and granules (highest density) made from ultrafine Grade kaolin. The same method of calcination, soak was used for each experiment. The rig using the tall, circular crucible, is detailed in Appendix A.

Each of the feeds, made from the ultrafine material. was soak calcined using the thermocouple rig at 1000 °C with 20 minutes at high temperature. The soak method

of calcination was chosen for convenience and because it exerted less pressure on the rig, allowing it to be used for more experiments. The calcined material was split into five sections, labelled 1 to 5 from top to bottom. These sections corresponded with the location of the thermocouples, with a sixth thermocouple located outside of the crucible, monitoring the furnace temperature.

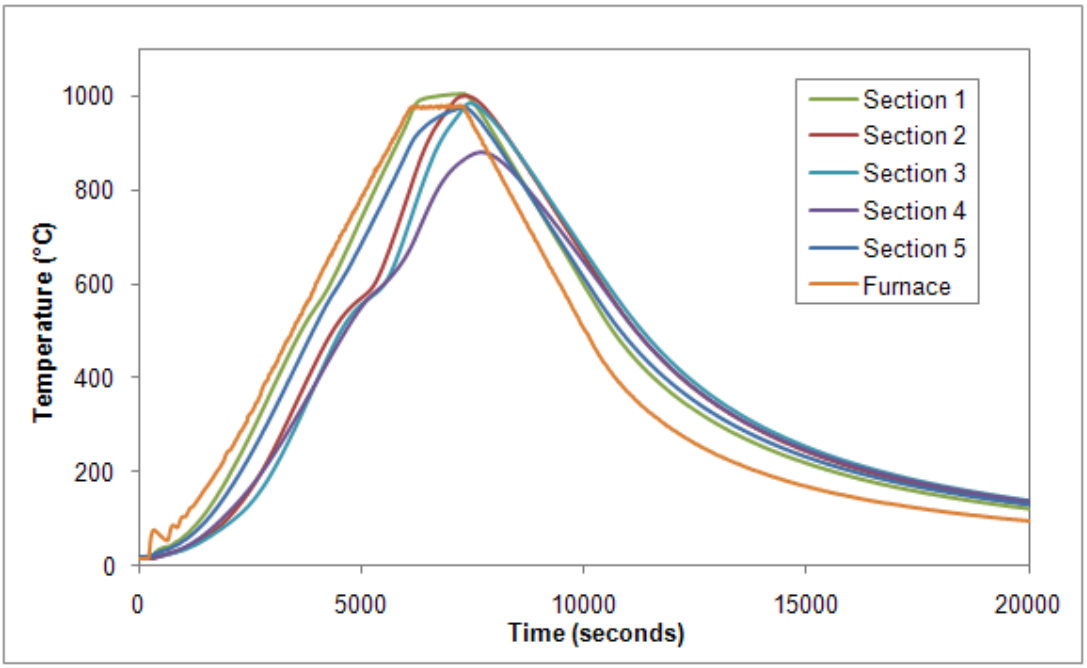

Figure 8-13: Thermocouple data for Residue Milled Powder with an intrinsic particle size of 90 wt.% less than 2 µm when soak calcined at 1000 °C with 20 minutes at high temperature

The temperature data for the Milled Powder feed is shown in Figure 8-13 and summarised in Table 8-3, where it can be seen that the furnace thermocouple does not register a temperature of 1000 °C and instead reaches a level of 964 °C before peaking at 981 °C, after which the furnace begins to cool. Potential reasons for this shortfall in temperature, include insulation from the thermocouple support, a variation

in temperature due to the height difference from the furnace thermocouple and a draught from thdene slightly open door caused by the presence of the thermocouples, going from the rig to the data plotter.

Table 8-3: Summary of thermocouple data for ultrafine Residue milled powder when soak calcined at 1000 °C with 20 minutes at high temperature

	Maximum temperature (°C)	Time to reach maximum temperature (seconds)	Onset of cooling (seconds)	Duration of soak (seconds)
Section 1	1007	7185	7332	1292
Section 2	1002	7313	7358	45
Section 3	985	7427	7489	62
Section 4	880	7662	7748	86
Section 5	976	7291	7337	46
Furnace	981	6978	7310	1358

From Figure 8-13 and Table 8-3 it can be seen that only the top two sections of the crucible reach the specified temperature of 1000 °C. As Section 3 reaches its highest temperature shortly after Sections 1 and 2, it is presumed that the heat to that section is coming from the top of the crucible. This is further evidenced by Section 4 reaching its maximum temperature of 880 °C shortly afterwards. As Section 5 reaches its maximum temperature soon after the first section, this suggests that the heat to that thermocouple has reached it from the side, through the crucible wall. This phenomenon has been shown to occur with this rig elsewhere, in Section 7.4.4.

The cooling for each section of the crucible starts around the same point, at approximately 7300 seconds, which is just over 121 minutes into the cycle. This is

21 minutes later than would be expected from the programming, a starting temperature of 18 °C, a heating rate of 10 °C min^{-1} and a soak time of 20 minutes gives the time for onset of cooling to be 100.2 minutes. As the delay is so short, it is likely that the heating rate of the furnace is a little slower than expected. As the crucible begins to cool soon after the furnace, there is little retention of heat within the crucible after the heating to the furnace stops.

The soluble aluminium and brightness data shown in Figure 8-14 for the milled powder reflect that insufficient heat reaches the fourth and fifth section in the crucible. However, the third section has a low soluble aluminium result. This may be due to errors in obtaining the sample, whether it is originating from a different area of the crucible or the edge of section 3, which has seen more heat than the middle, where the thermocouple was located. The error in sampling is also evident with the fifth section, which has a higher soluble aluminium level than the thermocouple data suggests, presumably because the sample came from the middle of the section rather than the edge, where the temperature was being measured.

	Milled Powder		9 mm prills		Granules
1	85.5 / 0.51	1	82.9 / 0.78	1	81.4 / 0.82
2	85.4 / 0.57	2	83.4 / 0.68	2	81.8 / 0.81
3	85.0 / 0.67	3	83.4 / 0.67	3	82.0 / 3.96
4	84.3 / 9.0	4	84.0 / 0.86	4	82.2 / 11.91
5	83.5 / 15.2	5	84.1 / 7.94	5	82.8 / 13.72

Figure 8-14: Brightness and soluble aluminium data for three ultrafine Residue feed forms; Milled Powder,9 mm prills and Granules, calcined at 1000 °C for 20 minutes in circular crucibles, with thermocouple support in place

The thermocouple data for the ultrafine 9 mm prills can be seen in Figure 8-15 and is summarised in Table 8-4. Only the top three sections reach the specified 1000 °C while the furnace only reaches 987 °C. As well as reaching a higher temperature than the milled product, the sections also remain at a higher temperature for longer, which results in a lower value of soluble aluminium for the fourth and fifth sections, as shown in Figure 8-14, when compared with the milled feed product. This may be due to the air gaps between the prills allowing the heat to penetrate deeper into the crucible. These air gaps will also allow the thermocouple to heat quicker, which may conduct into the surrounding material, affecting the result.

Table 8-4: Summary of thermocouple data for ultrafine Residue 9 mm prills when soak calcined at 1000 °C with 20 minutes at high temperature

	Maximum temperature (°C)	Time to reach maximum temperature (seconds)	Onset of cooling (seconds)	Duration of soak (seconds)
Section 1	1010	7131	7420	1034
Section 2	1003	6598	7444	1018
Section 3	1000	6695	7501	1301
Section 4	937	7498	7546	48
Section 5	972	7292	7530	722
Furnace	987	6769	7288	1178

The crucible sections begin cooling from top to bottom after 7400 seconds, two minutes after the furnace begins to cool. The temperature data for the 9 mm prill sections reaches below 80 °C, the temperature at which the kaolin is no longer greatly affected, between 30 minutes and 1 hour after the milled powder, again cooling from the top to bottom of the crucible. Overall, this shows a slight heat

retention over the milled powder and probably aids the reaction, producing the lower soluble aluminium results, as displayed in Figure 8-14.

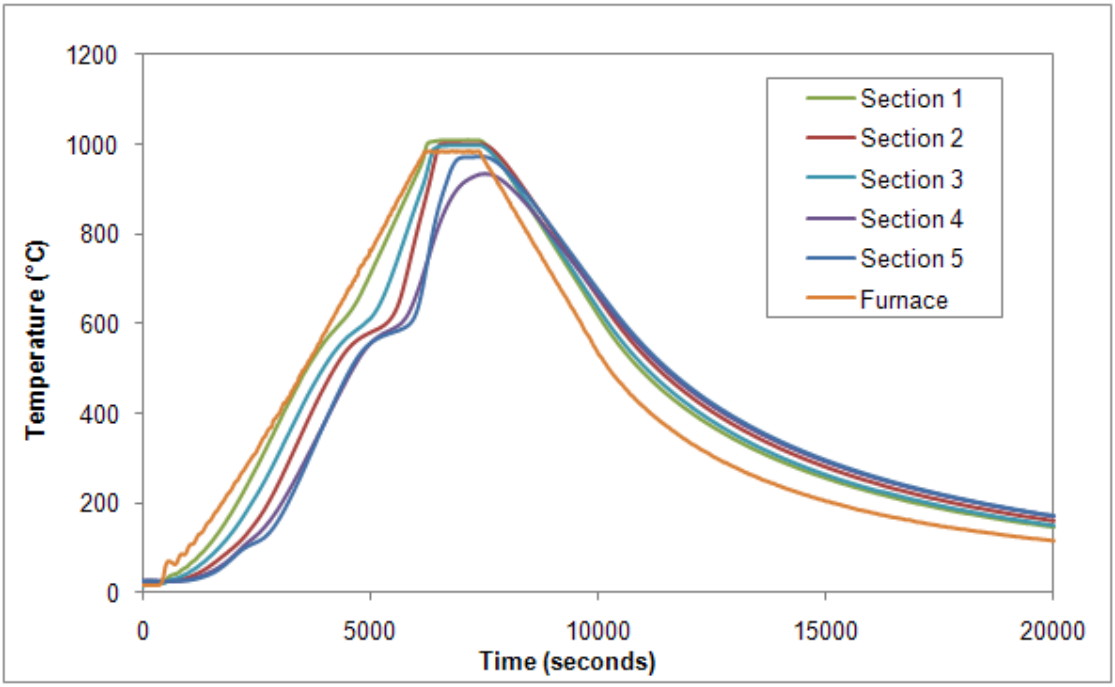

Figure 8-15: Thermocouple data for Residue 9 mm prills with a particle size of 90 wt.% less than 2 µm when soak calcined at 1000 °C with 20 minutes at high temperature

Figure 8-16 shows the thermocouple data for the Residue granules made from ultrafine feed, where it can be seen that none of the sections reach 1000 °C. The highest temperature, of 987 °C, is achieved by Section 1, with the other sections reaching progressively lower temperatures of 973, 948 and 866 °C for sections 2, 3 and 4 respectively. Section 5 reaches a slightly higher temperature, 941 °C, than section 4 which is attributable to wall effects.

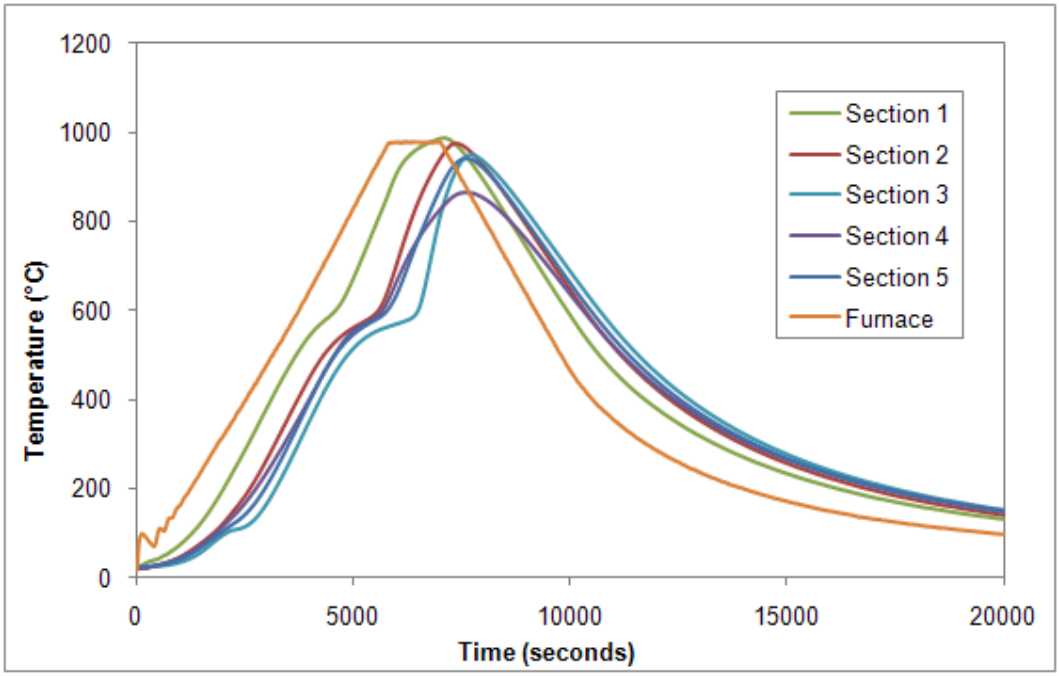

Figure 8-16: Thermocouple data for Residue granules with a particle size of 90 wt.% less than 2 µm when soak calcined at 1000 °C with 20 minutes at high temperature

The brightness and soluble aluminium results for the crucible filled with granules are displayed in Figure 8-14 and the thermocouple data is summarised in Table 8-5. Both the soluble aluminium and brightness results are lower for the granules than for the milled powder. The brightness values may be lower due to the effect of fusion on the particles making them difficult to break apart, as discussed previously in Section 8.2.3 [90]. The soluble aluminium results, however, reflect that the time spent at high temperature is as important as the high temperature reached.

Despite the furnace beginning to cool after 6866 seconds, the top section of the crucible does not reach the maximum temperature until 3 minutes later. It then takes a further 5 to 9 minutes for the other sections to reach their maximum temperature.

This suggests that the crucible is being heated from within as a result of the exothermic spinel reaction, allowing the rest of the crucible to heat up and continue the reaction. Due to the high bulk density of the kaolin and the lack of air within the system, this heat can be propagated and insulated within the dish, allowing for maximum use. Following on from the prolonged heating period, the crucible filled with granules appears to cool quickly and reaches 80 °C at around the same point as the other crucibles, around 466 minutes after the experiment started.

Table 8-5: Summary of thermocouple data for ultrafine Residue granules when soak calcined at 1000 °C with 20 minutes at high temperature

	Maximum temperature (°C)	Time to reach maximum temperature (seconds)	Onset of cooling (seconds)	Duration of soak (seconds)
Section 1	987	7065	7136	71
Section 2	973	7336	7426	90
Section 3	948	7691	7772	81
Section 4	866	7535	7696	161
Section 5	941	7556	7684	128
Furnace	979	6188	6866	1136

In order to calcine the kaolin, there needs to be a balance between the quantity of material and air in the crucible. Due to the high bulk density of the granules, the heat is unable to penetrate into the middle of the crucible, hindering the calcination reaction, however due to the amount of material the heat is propagated within the system, allowing the reaction to progress further than it otherwise would and produce lower soluble aluminium results than would otherwise be expected for the temperatures reached, as shown in Figure 8-14. The opposite is seen in the milled powder, the system reaches much higher temperatures, with a more uniform

distribution throughout the crucible but the heat is not retained, beginning to cool at the same time as the furnace. This leads to higher soluble aluminium results than for the 9 mm prills which propagate the temperature for longer, allowing the reaction to progress further.

8.4 The effect of particle morphology

Five kaolins; Double Ground, Beauvoir, Blackpool LR, Blackpool FR and SC Residues were selected due to natural variances in chemistry, particle size and particle shape. Except for Beauvoir, which is from France, the other kaolins are all Cornish in origin. Samples of each kaolin have been examined using Scanning Electron Microscopy (SEM) in their hydrous form and again when they have been calcined under Herreschoff replicating conditions, 1050 °C for 30 minutes using the batch method.

The brightness, particle size, XRF and XRD data for the five kaolins are detailed in Table 8-6, where it can be seen that the kaolins exhibit large differences in chemistry. All of the kaolins show high levels of potassium contamination, particularly Double Ground and Beauvoir which both contain high amounts of mineral impurities. Beauvoir shows a particularly high amount of mica and feldspar within the matrix, 13 and 4 wt.%, respectively, and this is reflected in the low brightness value for the kaolin. The low brightness value is also due to the coarse particle size and the unbleached nature of the kaolin, which can be identified due to the high brightness value, as displayed in Table 8-6.

Table 8-6: XRD, Brightness and Particle size, Surface Area and Oil Absorption results for hydrous Platy, Beauvoir, Blackpool LR, Blackpool FR and SC Residues

	Platy	Beauvoir	Blackpool LR	Blackpool FR	SC Residues
XRD (wt.%)					
Kaolinite	88	83	92	98	92
Mica	4	13	5	2	0
Quartz	2	4	1	<0.5	2
Feldspar	6	ND	2	ND	6
Tourmaline	ND	ND	ND	ND	0
Albite	ND	ND	ND	ND	0
Colour (%)					
Brightness	86.6	71.5	85.3	87.7	84.8
Yellowness	4	10.7	4.2	3.2	5.5
Particle size (wt.%)					
< 0.25 µm	18.4	8.9	22.4	31.6	39.3
< 2 µm	86.1	41	81.3	94.1	98.3
> 10 µm	0.7	18	0.4	0.3	1.3
Surface Area (g m^{-2})					
Area	13.4	6.5	12	16	18
Oil Absorption (g $100g^{-1}$)					
Absorption	57	40	42	46	47

The production route for Beauvoir is very simple and is shown in Figure 11-9 in Appendix B. The kaolin is extracted from the pit, screened at a particle size of 125 µm and passed through a hydrocyclone before being filtered and dried. The Blackpool LR production route is similar, with the pit wash being passed through a hydrocyclone, followed by a centrifuge before being bleached, filtered and dried. In order to produce Blackpool FR, the Blackpool LR product is passed through a centrifuge a second time before being bleached and dried. The routes to produce both kaolins are shown in Figure 11-10 in Appendix B.

In order to produce SC Residue, which is a by-product of the Paper group's operations, the pit wash is passed through a hydrocylcone and ground before being run through a centrifuge whereupon the fines are recovered, streamed through a magnet twice, before being bleached and dried. This production route is detailed in Figure 11-11 from Appendix B.

The production route, shown in Figure 11-12, Appendix A for the Double Ground kaolin is slightly more complicated, with the feed clay obtained from the 2nd stage Dorr Oliver residue. This sample is then ground until the particle size is 25 wt.% less than 2 μm, before being passed through a hydrocyclone and then close-circuit ground until the particle size is 90 wt.% less than 1 μm. The kaolin is then passed through a magnet twice before being bleached and dried.

Due to the different production routes, the kaolins differ much in appearance. The SEM images of the hydrous kaolins generated at a magnification of x20,000 are shown in Figure 8-17. The platy nature of both the Double Ground and Beauvoir kaolins can be seen in the images, with distinct flakes of the kaolin in Beauvoir visible and extended kaolin stacks appearing in the Double Ground image.

In contrast, the fragmented particles of SC Residues, Blackpool LR and Blackpool FR can be seen in the other three images. SC Residues show the most fragmentation, with the standard hexagonal shape of kaolin particles barely evident, while both Blackpool LR and FR have more reasonable particle shapes with the hexagonal shape more evident.

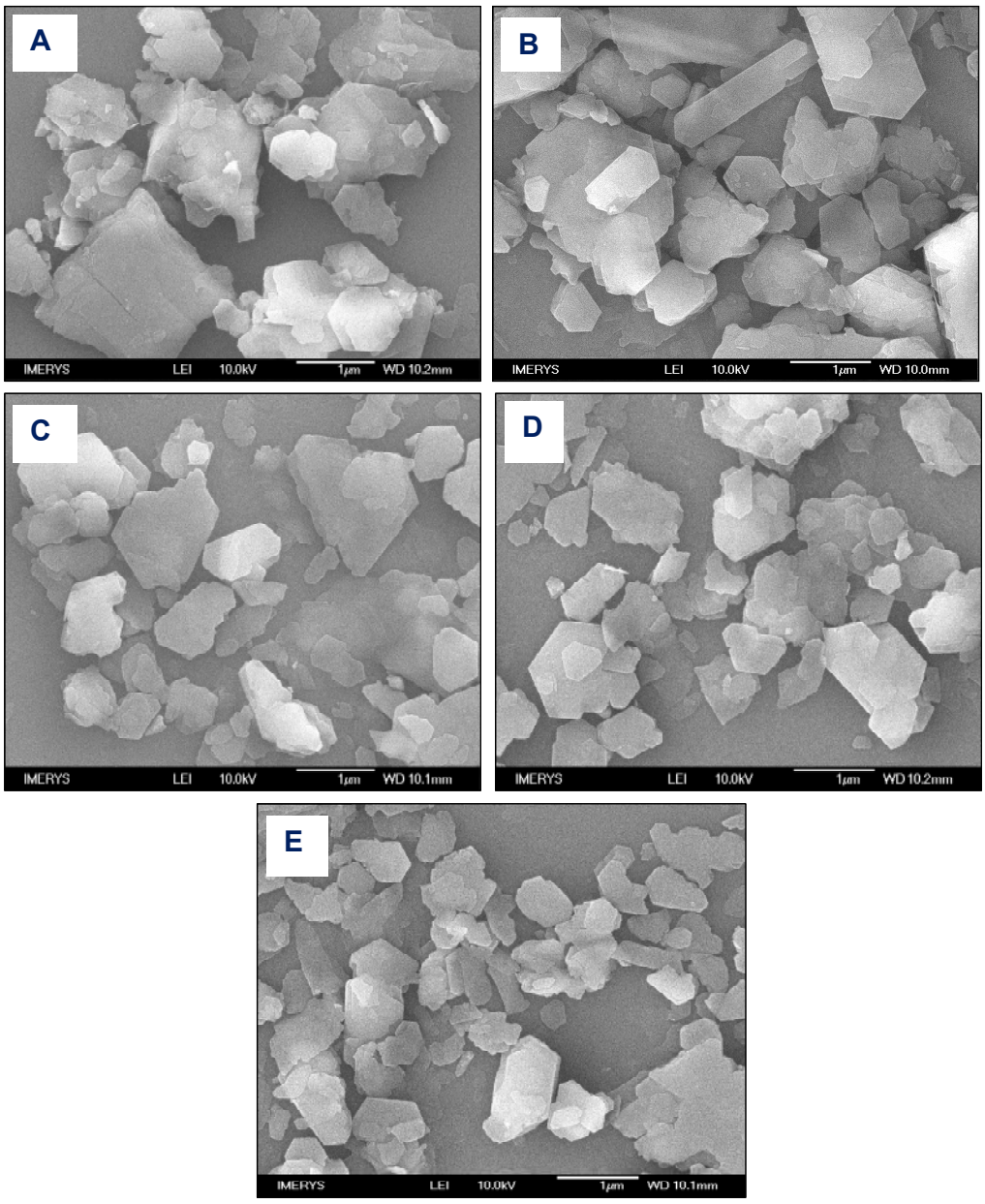

Figure 8-17: SEM images at a magnification value of x20,000 showing hydrous kaolins A) Platy, B) Beauvoir, C) Blackpool LR, D) Blackpool FR and E) SC Residues

The colour and particle size data for the calcined kaolins are shown in Table 8-7. Due to the large amount of impurities in the Beauvoir and the unbleached nature of the feed, the calcined product has a very poor colour with a brightness value of only 76.3 %. The other four kaolins all have very similar brightness values, although the SC Residues is slightly higher at 88.8%.

Table 8-7: Brightness and Particle size results for Double Ground, Beauvoir, Blackpool LR, Blackpool FR and SC Residues when calcined at 1050 °C for 30 minutes

	Double Ground	Beauvoir	Blackpool LR	Blackpool FR	SC Residues
Colour (%)					
Brightness	85.4	76.3	83.1	86.4	88.8
Yellowness	7.6	10.4	8.1	7	6.2
Particle size (wt.%)					
< 2 µm	24.1	20.8	36.6	32.4	44.5
> 10 µm	18.3	28.5	26.7	22	28.7
Surface Area (g m^{-2})					
Area	8.1	4.25	8.25	9.6	10.7
Oil Absorption (g $100g^{-1}$)					
Absorption	67	50	52	81	52

All of the kaolins show an increase in the amount of sample over 10 µm in size after calcination. The calcined SC Residues have a very broad particle size distribution, as although it has the largest smaller size fraction with 44.5 wt.% of the material less than 2 µm in size, it also has the largest oversize fraction with 28.7 wt.% of the material greater than 10 µm in size.

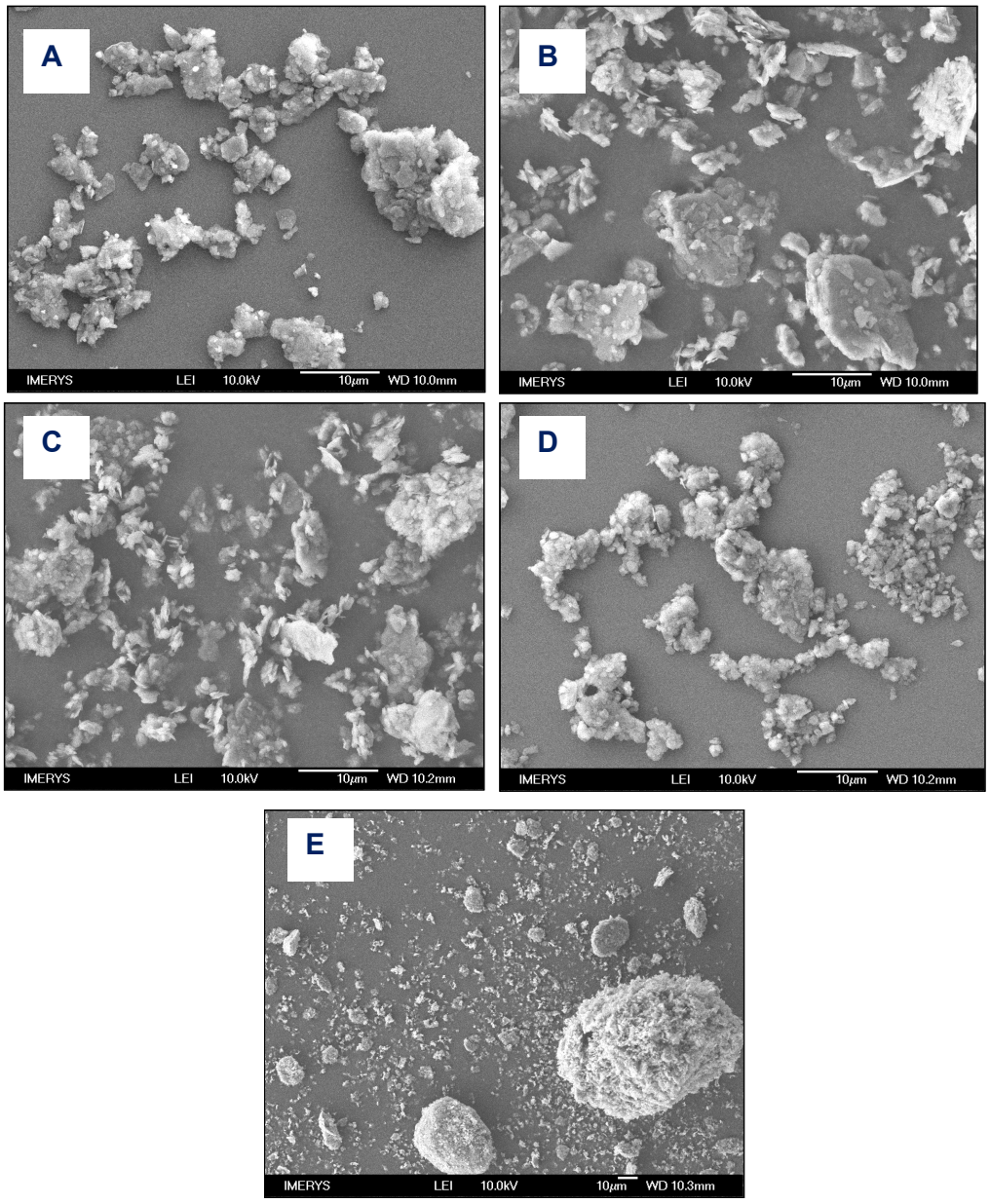

Figure 8-18: SEM images at a magnification value of x2000 showing kaolins calcined at 1050 °C for 30 minutes A) Platy, B) Beauvoir, C) Blackpool LR, D) Blackpool FR and E) SC Residues (shown at a magnification of x500)

From Table 8-7, Beauvoir has produced the coarsest calcined product, which is due to the amount of impurities in the hydrous form, the presence of mica and feldspar have been shown to have a fusing effect on the kaolin as calcination progresses, Section 5.3. Despite that the amount of material over 10 μm has only increased from 18 to 28.5 wt.%, the content of sample under 2 μm having significantly decreased.

SEM images for the calcined kaolins are shown in Figure 8-18 and indicate definite signs of aggregation, although the particles of several of the kaolins have distorted more than others. Platy in particular shows a loss of distinct flakes as the particles begin to take on a rounded appearance, which results in a messier agglomeration than the Beauvoir, for which the flakes are still partially evident.

The finer kaolins, predominantly SC Residues, show evidence of the small particles adhering to each other due to the high surface area that is available for the particles to touch each other and eventually fuse. This phenomenon is responsible for the large round particle seen in the SC Residues SEM image and is likely to be the cause of the large increase in the number of particles larger than 10 μm in size, as detailed in Table 8-7. The large agglomerate may be montmorillonite particles, which are found in some samples of SC Residues, adhering together, a phenomenon witnessed in work with plastics [91].

For Blackpool LR, there is still some hexagonal morphology apparent, despite the slight rounding of the particle and the aggregation. Blackpool FR, however, is more like SC Residues and is more agglomerated. Upon calcination, for all kaolins, the

2 µm content and surface area both decrease upon calcination. This is due to the fusion of particles as the calcination reaction progresses. The change in 2 µm content is related to the less than 0.25 µm content of the hydrous feed, as shown in Figure 8-19, where the high fines content in the two finer feeds, Blackpool FR and SC Residues leads to a larger amount of fusion than the coarser Beauvoir. This is considered to be due to the tendency of fine particles to act as an aid to adhesion, sticking to larger particles and causing them to stick together [39].

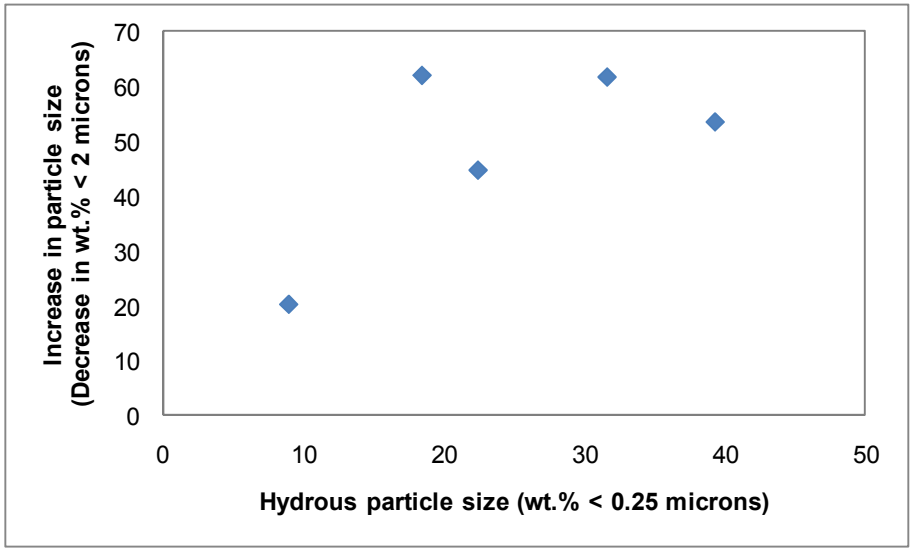

Figure 8-19: The relationship between the quantity of fines in the hydrous feed (wt.% < 0.25 µm) and the change in particle size (wt.% less than 2 µm) as a the result of calcination at 1050 °C for 30 minutes, batch method

All of the kaolins show a decrease in surface area upon calcination. This can be linked to the decrease in particle size, as fine kaolins, such as Blackpool FR and SC Residues, show a greater decrease in surface area, as displayed in Figure 8-20, when compared with the coarser Beauvoir. The decrease in surface area is also strongly linked to the quantity of fines within the hydrous kaolin, hence the coarser Beauvoir sees less of a decrease than the other kaolins. During the spinel reaction,

the fine particles adhere both to each other and the larger particles, thereby decreasing the available surface for the nitrogen to adhere to in testing.

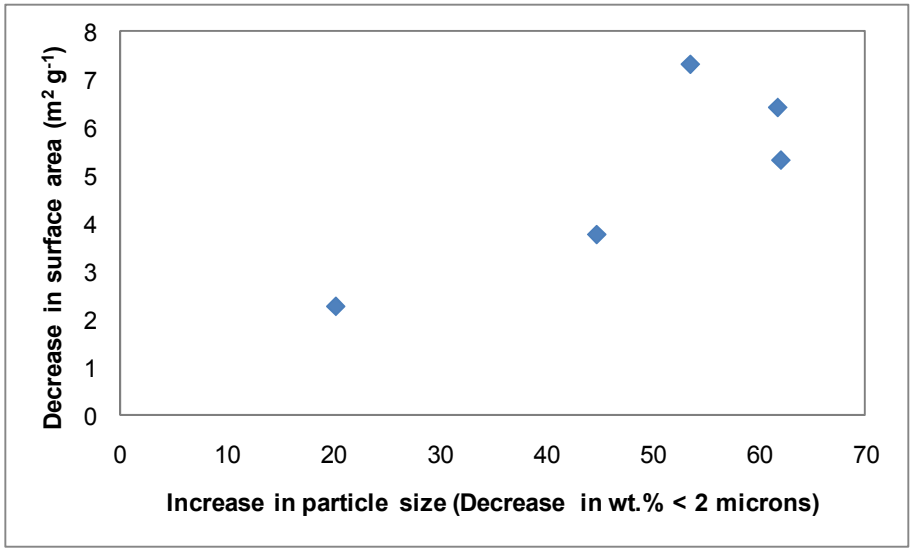

Figure 8-20: The relationship between the change in particle size (wt.% less than 2 microns) and the change in surface area as the result of calcination at 1050 °C for 30 minutes, batch method

While the surface area and particle size of the kaolins decreases upon calcination, the oil absorption for the calcined product is higher than that for the hydrous feeds, as shown in Figure 8-21. The change in oil absorption is most noticeable in the Blackpool FR kaolin, which changes from a value of 46 g per 100 g, which is of similar value to the other hydrous feeds, to 81 g per 100 g upon calcination. The increase in oil absorption may be due to the creation of a pore structure upon the fusion of particles. It is not known how the particles fuse together, but there are two main theories, the “house of cards” theory and the “face to face” theory, as detailed in Figure 8-22. A third theory is a combination of the two.

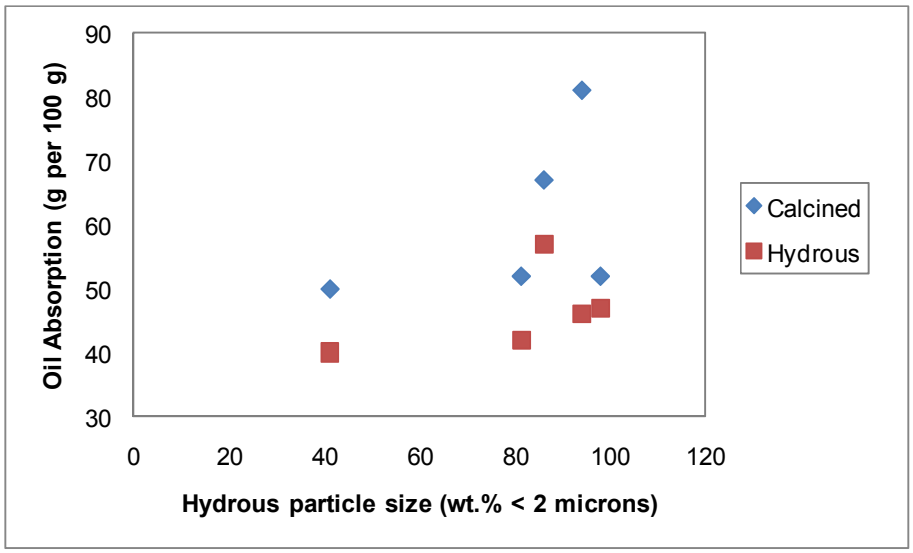

Figure 8-21: The oil absorption values for hydrous feeds and products after 1050 °C calcination for 30 minutes, batch method

Some “face to face” fusion can be seen in the SEM images in Figure 8-18 for all of the kaolins, but the balling which occurs in some of the kaolins, particularly ND1690.01, suggests that there is also some “house of cards” fusion occurring.

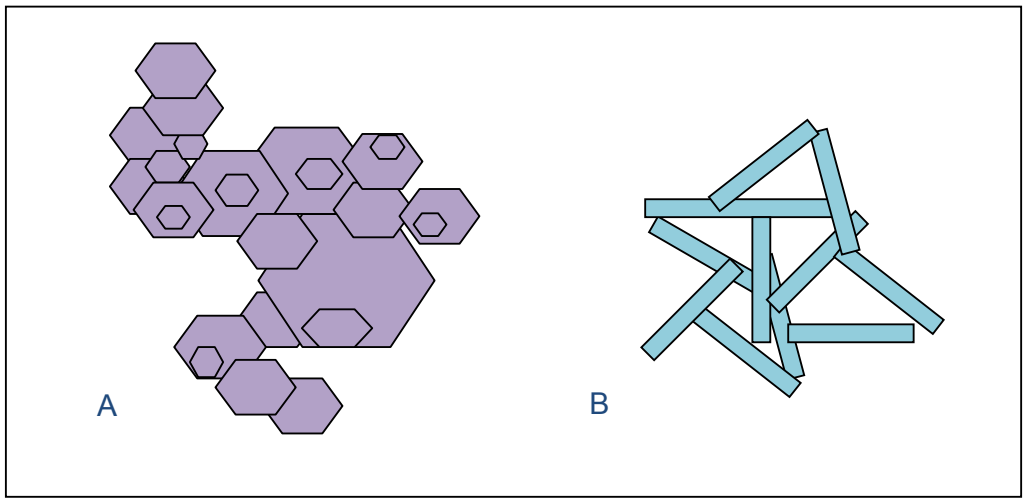

Figure 8-22: Theories of particle fusion, A) Face to face and B) House of cards

The calcination process can destroy the internal pore structure within individual particles, but allows inter-particle structures to be formed. This leads to a change in the surface area and oil absorption measurements after the calcination process. While the nitrogen used in the surface area measurements is able to adsorb onto the surface of the particles, which decreases as a result of the fusion that accompanies calcination, while the oil moves into the structure of the kaolin and is trapped into pockets, giving an indication of the porosity of the material. The lack of pockets within the hydrous structure may also be a factor in the values of oil absorption being so similar for the hydrous kaolins.

For all kaolins there is an increase in porosity due to calcination, indicating that a complex structure is created upon calcination. The highest oil absorption values per given surface area are for Platy and Blackpool FR, both of which show evidence of house of cards fusion in the SEM images displayed in Figure 8-18, with the other kaolins that show more “face to face” fusion and produce products that are similar in porosity. The SC Residues, which exhibits a large amount of fusion in the SEM image has an oil absorption value of 52 g $100g^{-1}$ which is the same as the calcined Blackpool LR. The reason for this may be that the large agglomerates are sporadic in the calcined SC Residues material, or that the oil is unable to penetrate into the structure. This highlights the importance of using several techniques to analyse the product to gain a full understanding of what is happening.

There is some correlation between the surface area of the calcined product, as shown in Figure 8-23, with the oil absorption, where for increased surface area there is also increased oil absorption, except for the very platy Double Ground kaolin and the fragmented FC Residues. This suggests that, upon fusion, the platy clay obstructs the pore network created upon calcination, which prevents the oil from being able to be absorbed by the material. In contrast, the fine FC Residues does not appear to create a pore network and the surface area value is caused by the fineness of the particles. Where there is a balance of fine and large particles, as in Blackpool FR, however, the network and small pockets can be formed, thereby increasing the oil absorption.

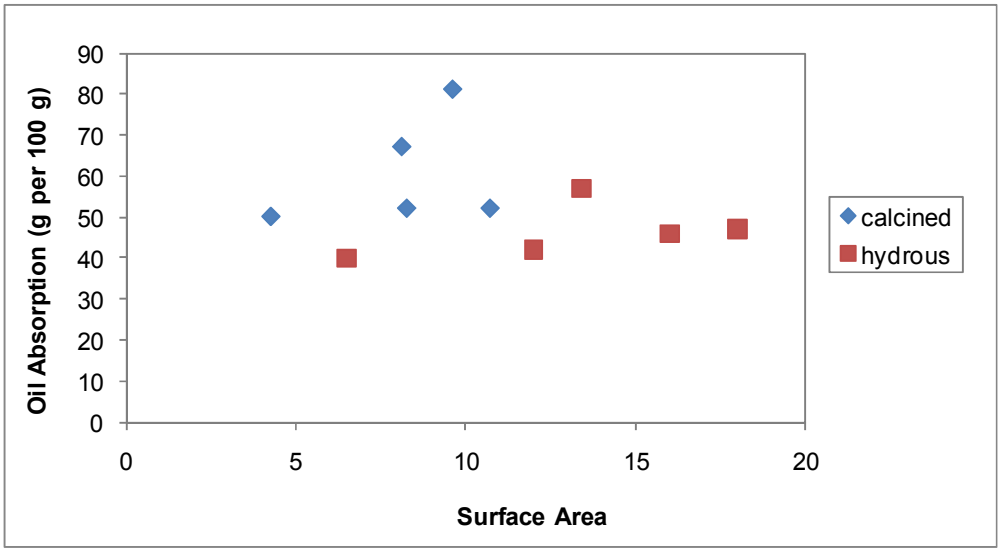

Figure 8-23: The oil absorption and surface area values for hydrous feeds and calcined products after 1050 °C calcination for 30 minutes, batch method

8.5 Conclusions

It is apparent from this work that as well as feed chemistry, the size and shape of the feed is very important in the calcination reaction. The physical nature of the feed should, therefore, be determined and taken into consideration as well as impurities that are present in the kaolin.

As some of the feed forms produce highly fused material upon calcination and these aggregates are unable to be broken up upon milling, they have a detrimental effect on the brightness of the product which skews the results. This is because larger particles affect the reflection of the light that is used in the test method [90]. This could be overcome by using the colour in oil method of analysis.

There appear to be no significant differences in the heat transfer through each of the three Residue materials, as all feeds batch calcined in flat rectangular crucibles show similar soluble aluminium results. There is more fusion in the ultrafine kaolin than the coarse, particularly if the feed form is compacted during the manufacturing process, such as with the granules. This is a potential issue in milling.

There is some suggestion that the bulk density of the kaolin affects the product properties, with low bulk density products struggling to reach the temperature required for the spinel reaction, hence yielding higher soluble aluminium results after calcining at 1050 °C. This is thought to be related to air gaps in the feed hindering the conduction of heat between particles. High bulk density products, however, appear to calcine well with a limited bed depth, although they produce an inconsistent product in very deep beds. This is thought to be due to the amount of

material that has to be heated to temperature through conduction and the limited amount of heat that is able to penetrate during the heating cycle.

From the investigations with the different feed forms, it appears that the granules retain heat within the crucible much longer than the milled powder, although the high bulk density of the material means that the heat cannot penetrate into the middle of the crucible, creating an inconsistent calcined product which is very difficult to mill. The milled powder is considered the best feed for use in production as it is much easier to mill, preventing the appearance of agglomerates which could be detrimental to machinery in the product. However, it is not the best feed form for heat transfer within the bed of material as it is unable to retain heat once the furnace begins to cool, due to the low bulk density of the material.

All of the five kaolins with differing morphology exhibited an increase in oil absorption and decrease in surface area upon calcination. The increase in oil absorption was more noticeable with the platy kaolins than the blocky kaolins, as they created a more complicated and porous structure as the particles aggregated.

9 Conclusions and Further Work

9.1 Conclusions

Under standard operating conditions, with a throughput of 5.3 tonnes h^{-1} of 0 wt.% moisture feed, the mean residence time inside the Herreschoff has been determined to be a mean of 42 minutes with the use of talc as a tracer. Talc was discovered to represent the flow properties of kaolin more accurately than titiania, which is understood to move at a different rate and by a different mechanism through the kiln to kaolin. This is probably due to discrepancies in the powder flow behaviour, as reflected in the properties determined with the Powder Flow Rheometer, and also the significant difference in specific gravity between the hydrous/calcined kaolin and the titania.

In order to develop a suitable method of replicating Herreschoff conditions on a laboratory scale, samples were obtained from production of Kiln Feed, Kiln Outlet and Milled Kiln Product. By calcining the Kiln Feed under different conditions, varying the temperature, duration and method of calcination, it was determined that the most representative method of replicating commercial firing was to calcine samples for 30 minutes at 1050 °C in rectangular silica trays.

Due to the unpredictable nature of the calcination reaction, it was considered appropriate to use a reference sample in each experiment. The Kiln Feed, obtained from production, was used and was calcined numerous times, before submitting samples for brightness, particle size and soluble aluminium content analysis. The

results were then analysed in order to determine an acceptable range for the reference sample values to fall into. When the store of Milled HF was used up, the same testing procedure was performed with FC Feed, also originating from Devon, which exhibited slightly different product properties upon calcination due to deposit location and variations in beneficiation.

It was already known when this work was implemented that kaolins with different mineralogy react differently when calcined at very high temperatures. The study of Brazil and Milled HF indicates that this difference is even more apparent at lower temperatures.

It appears that the presence of organics does not have the dramatic effect suspected by previous Imerys researchers on the quality of the calcined product; however, this could be further investigated in order to dismiss it completely. It seems more likely that a combination of chemical factors, such as mineralogical differences, is causing the dramatic decrease in colour.

The response of the Brazil blending work to temperature seems to indicate that the artificial blending of the different minerals in order to alter the proportion of kaolinite present in the kaolin was not successful in terms of changing the intrinsic chemistry of the blend. Instead, all blends continued to react in a similar manner to the main kaolin constituent, in this case, Brazil and that any effect on the product is one of dilution. This is also seen with the addition of nepheline syenite and sodium

carbonate to Western Area HF, which does not alter the qualities of the calcined product.

With the magnet blending, where different kaolins in the form of magnet product and magnet rejects were blended together, the blending process was more successful. The similarity of the minerals used, allowed the blending to take place at a more intimate level and this caused the blending process to have a greater effect on the calcination process. This suggests that the intrinsic nature of minerals is highly important when determining how the chemistry affects the calcined product. Although artificially added minerals are used in other production areas of Imerys, it is apparent that the addition of such minerals for the soft calcination of kaolin is not a workable solution to feed material issues.

Each stage of the beneficiation process has an important influence on the quality of the hydrous kaolin. Both the Dorr Oliver and Centrifuge stages remove a significant proportion of larger particles, which are known to contain a significant proportion of contaminant materials [2]. The two magnet operations show an increase in brightness, due to the removal of iron-rich contaminants which have a detrimental effect on colour. The beneficiation process is completed by bleaching, which is important as it removes much of the surface iron.

The importance of bleaching as a beneficiation stage can be seen in that the Wheal Martyn kaolin that has only been put through a magnet once rather than the production standard twice meets the specifications of the highest quality Herreschoff

product, Polestar 200P, after it was bleached in the laboratory. This promotes the idea of reducing the amount of magnet processing which would create a large cost saving as magnet operations are the most expensive part of the process. The current limitation in production scale bleaching prevents this from being implemented at the moment.

When evaluating kaolin deposits for their suitability as alternative Herreschoff feeds, there are two product properties that are of most interest, namely brightness and soluble aluminium content. If it were possible to predict these without carrying out full-scale trials, it would save a great deal of time and money, in removing the need to produce large batches of kaolin for the trial and also any disposal issues of an unsuitable product. Therefore, several samples were taken from different production routes in Cornwall, Devon and Georgia and calcined at different temperatures. The influence of several individual factors upon the soluble aluminium, particle size and brightness results of these products were then investigated using single and multiple factor linear analysis. The factors included the particle size, brightness and yellowness of the hydrous kaolin alongside chemical and mineralogical factors such as the potassium, iron, mineraliser, kaolinite, mica and feldspar content of the kaolin.

When determining models for a calcined product where the feed properties are known, it was apparent that the Georgia kaolin was too chemically different from the British kaolins for inclusion in the data set, as the Georgia results kept skewing the data. In order to develop a general model to determine the properties of the calcined product, more kaolins would have to be included in the data set so as to minimise

this difference. Kaolins from Brazil, China, France and other areas of the USA should all be included.

From this work it has been shown that the colour of the calcined kaolin is dependent on the colour of the hydrous kaolin, along with other purity factors such as the aluminium and silica content, the amount of kaolinite and the mica content. There is also some particle size influence, with finer kaolins having a better brightness value than coarse kaolins. This is a known phenomenon and is the reason for milling samples before colour analysis [43].

As a result of the dehydroxylation reaction which occurs between 450 and 700 °C, the material is very reactive. This reactivity is identifiable by the amount of aluminium which can be leached out of the material using nitric acid. Once the spinel phase is reached at around 980 °C, the reactivity of the material, and so the amount of soluble aluminium obtainable from the sample, begins to decrease.

Different samples of kaolin have been calcined at a variety of temperatures and the maximum soluble aluminium is usually removed from a sample calcined at 950 °C. The amount of soluble aluminium retrieved from the sample after calcining at this temperature is reliant on the potassium and mineraliser content, the brightness of the hydrous kaolin and the two smaller size fractions, the d30 and d 50 values. The inclusion of the two particle size values reinforces the belief that physical factors are very important in the calcination reaction.

In order to reach production demands, a soft calcined product ideally contains less than 5 wt.% soluble aluminium. It has been found to be very difficult to fit a model to the amount of soluble aluminium retrieved from the sample after the 1050 °C calcination, the temperature which replicates Herreschoff production conditions, with the best model containing nine different factors: silica, feldspar, mineraliser, mica, kaolin, iron and aluminium content along with the hydrous brightness and the amount of particles less than 2 μm in size.

When trying to develop an idea of the standard properties of the proposed reference material, it was determined that there was a range that the soluble aluminium results fell into which guaranteed complete soft calcination had occurred. This suggests that if one sample, when calcined multiple times showed a range of possible results, other samples will exhibit the same tendency, making the prediction of the soft calcined materials soluble aluminium content from chemical factors alone impossible. This has been shown by the use of thermocouples within the crucible during calcination, where instead of chemical factors, the maximum temperature reached and the time spent at that temperature during the reaction govern the amount of soluble aluminium reached in the final product.

None of the four particle size characteristics of the 1050 °C product, the d30, d50 and the d70 of the size distribution, along with the proportion of particles less than 2 μm in size, show any reliance on factors other than the particle size of the hydrous feed. The particle size of the hydrous feed is in turn related to the purity of the kaolin but the general trend is for the fine hydrous kaolins to produce finer calcined products.

It is apparent from this work that as well as feed chemistry, the size and shape of the feed is very important to the calcination reaction. The physical nature of the feed should, therefore, be determined and taken into consideration as well as impurities that are present in the kaolin.

Some of the feed forms used as part of this work produce highly fused material upon calcination. As the aggregates are unable to be broken up using a laboratory mill, they have a detrimental effect on the brightness of the product, due to their affecting the reflection of the light that is used in the test method. This could be overcome by using the colour in oil method of analysis.

There is some suggestion that the bulk density of the kaolin affects the product properties, with low bulk density products not reaching the temperature required for the spinel reaction, hence yielding higher soluble aluminium results after calcining at 1050 °C. This is thought to be due to air gaps in the feed hindering the conduction of heat between particles. High bulk density products, however, appear to calcine well with a limited bed depth, although an inconsistent product was created in very deep beds. This is thought to be due to the amount of material that has to be heated to temperature through conduction and the limited amount of heat that is able to penetrate during the heating cycle.

9.2 Further Work

There is a variety of work that could be carried out in order to expand the study. If a range of samples were to be obtained from different deposits around the world, then the different models could be expanded so that they are applicable for all kaolins and not just those originating in Cornwall. This would be an extensive exercise but would aid the understanding of what particularly governs the reaction. Each of the samples should also be examined to determine the form of iron present in the kaolin, whether Fe^{2+} or Fe^{3+}. This may help improve the bleaching process and increase productivity for both hydrous and calcined kaolin.

The thermocouple experiments could be expanded by investigating different regimes of heating and cooling and with different kaolins to try and determine the effect of heating on the product. Additionally, by varying the feed forms present in each experiment, creating a greater variation in bulk density, the influence of packing and feed size could be better investigated. This could be further expanded by introducing an air flow into the system, allowing the influence of conduction, radiation and convection to be properly determined and the relevance of each mechanism calculated, allowing better design of future and current kiln operations.

The amount of fine particles, wt.% of material less than 0.25 μm, has a large influence on the amount of fusion that occurs during the reaction, with large quantities increasing the amount of fusion that takes place, as it is believed that the small particles adhere not only to each other, but also to the larger particles, thereby increasing the total amount of fusion taking place. By altering the size fractions

present in the feed kaolin, this phenomenon could be properly studied and understood. This would be useful in determining how a kaolin would react in the kiln.

In order to determine how the different feed forms react to temperature, it would be beneficial to perform some trial work either using the Herreschoff kiln in Devon, or perhaps more practically using a pilot scale facility. It would be interesting to carry out such trials with materials that have a varying bulk density. This would allow some understanding of how the kaolin moves through the kiln influences the product as well as more standard variables such as feed chemistry and particle size.

10 Appendix A

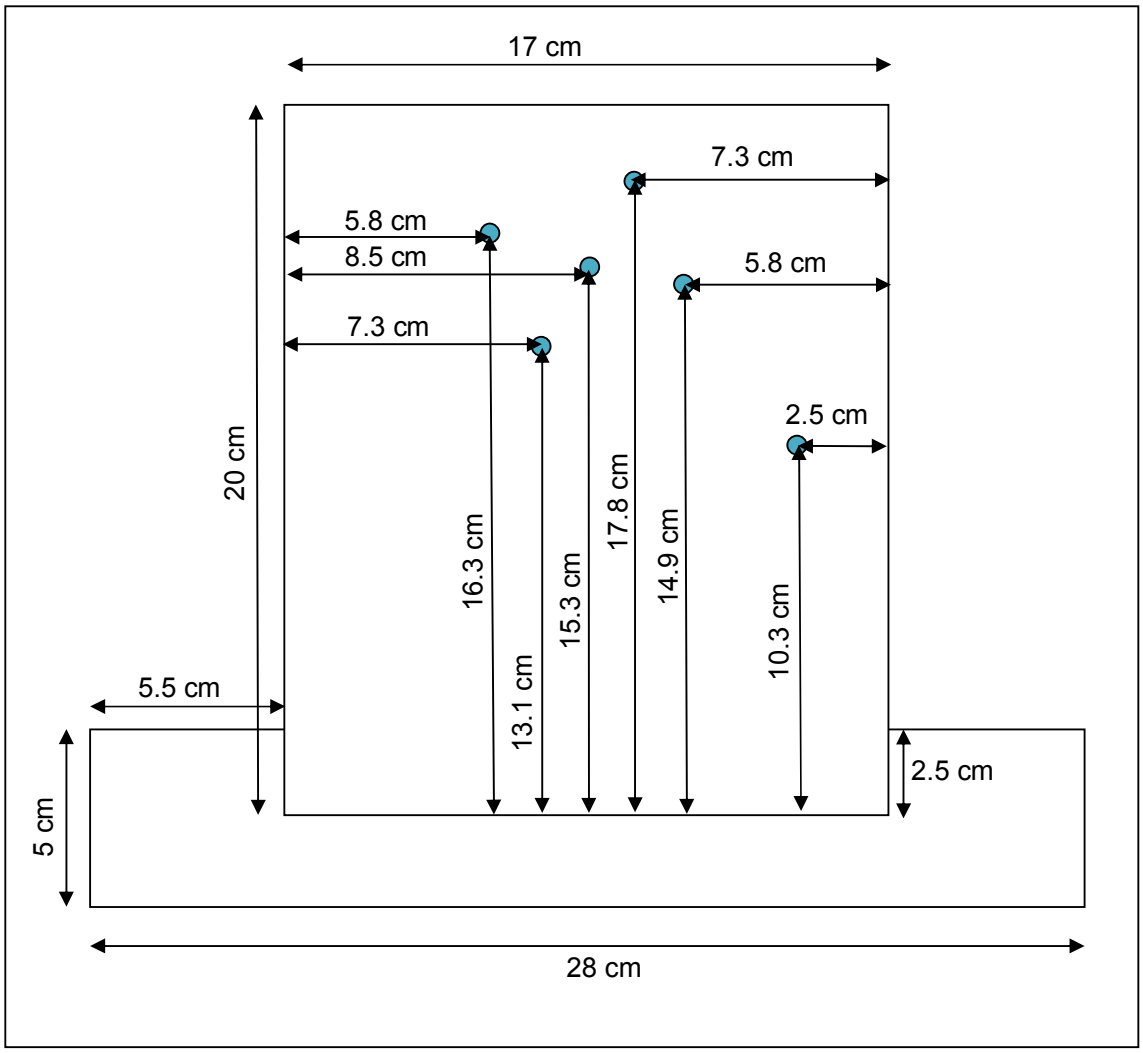

Figure 10-1: Front View of thermocouple support for use with tall circular crucible. Blue circles are 5 mm in diameter and are drilled completely through the support.

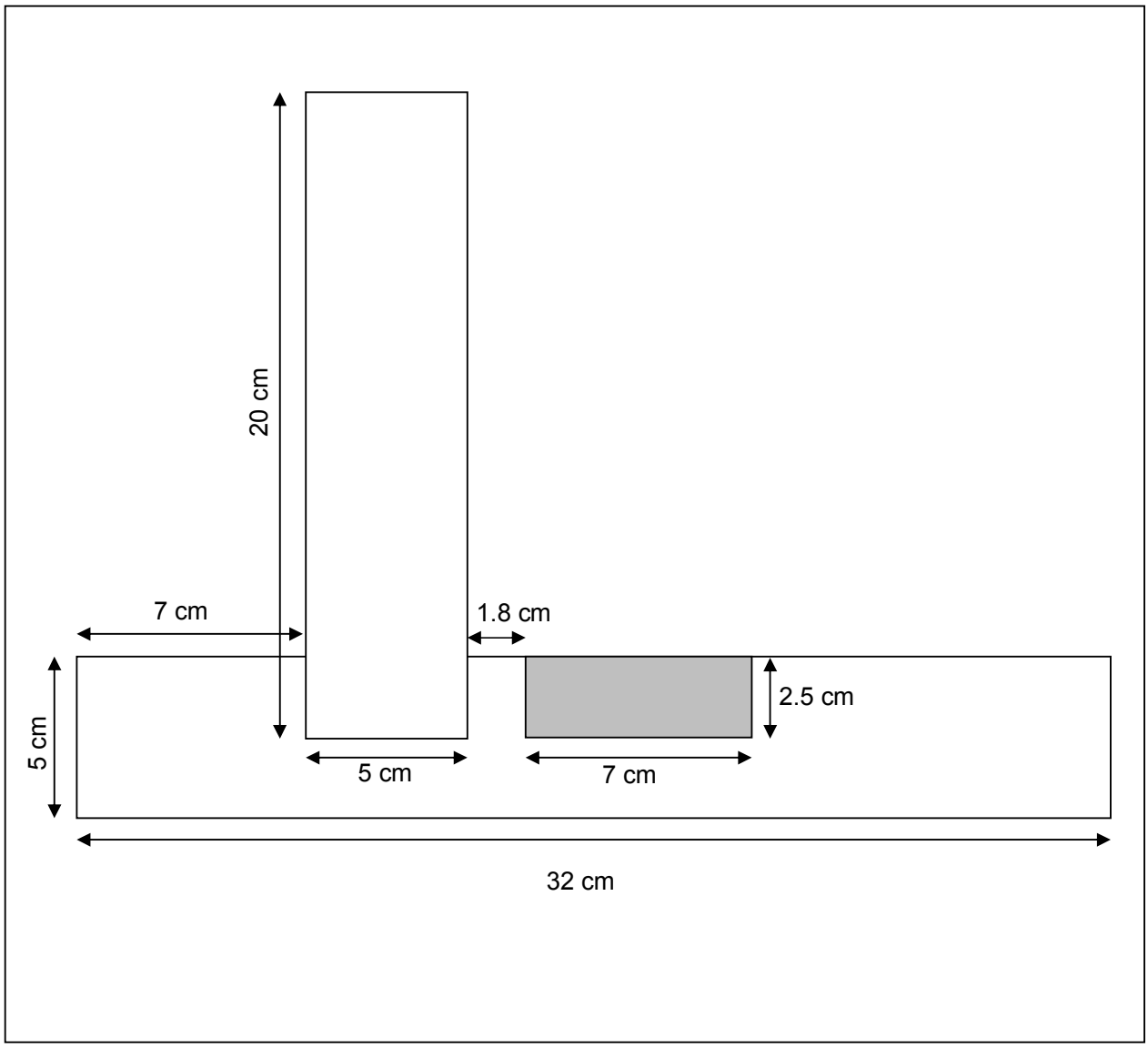

Figure 10-2: Side View of thermocouple support for use with tall circular crucible. Shaded areas should be cut to 2.5 cm deep.

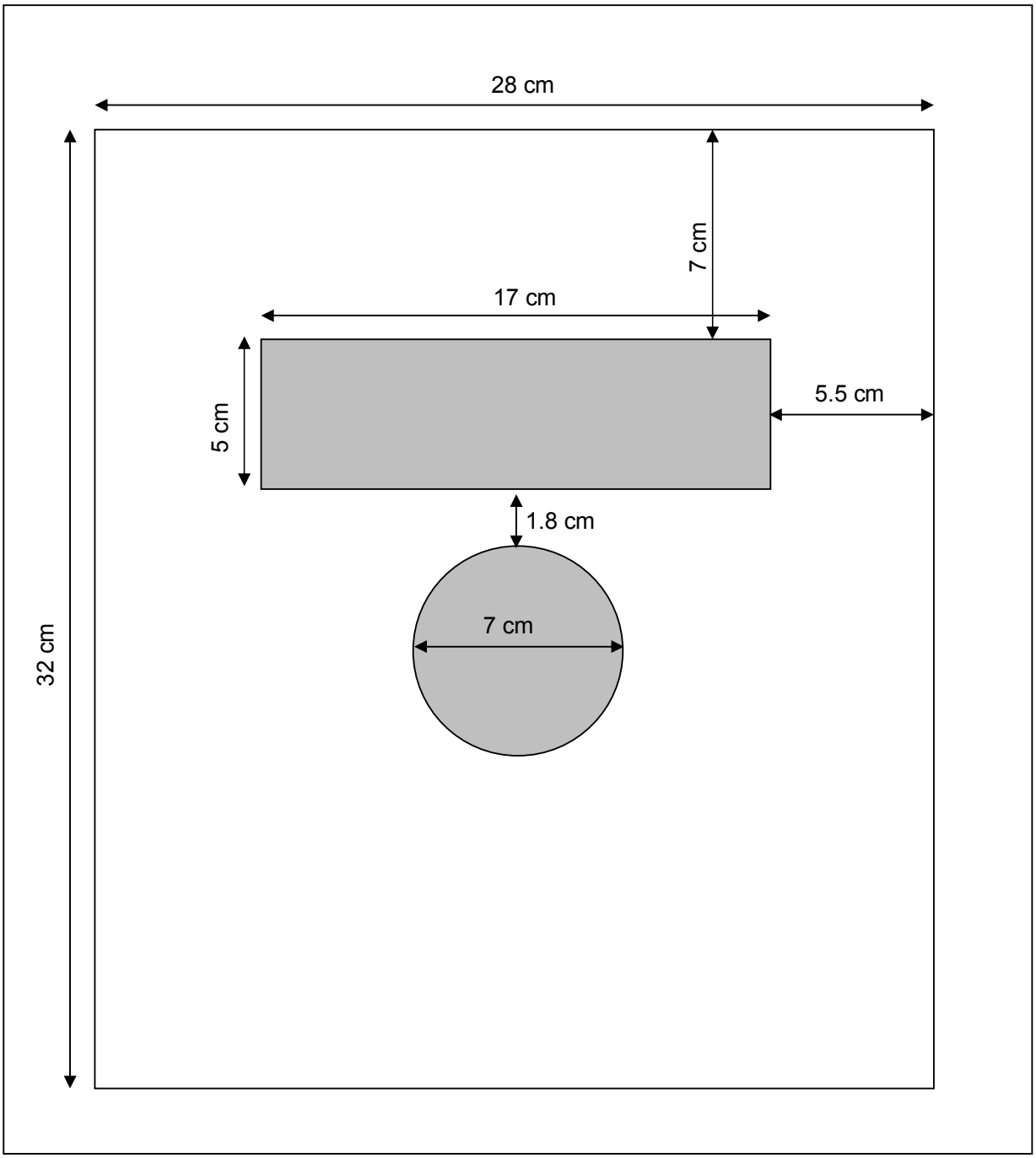

Figure 10-3: Top View of thermocouple support for use with tall circular crucible. Shaded areas should be cut to 2.5 cm deep.

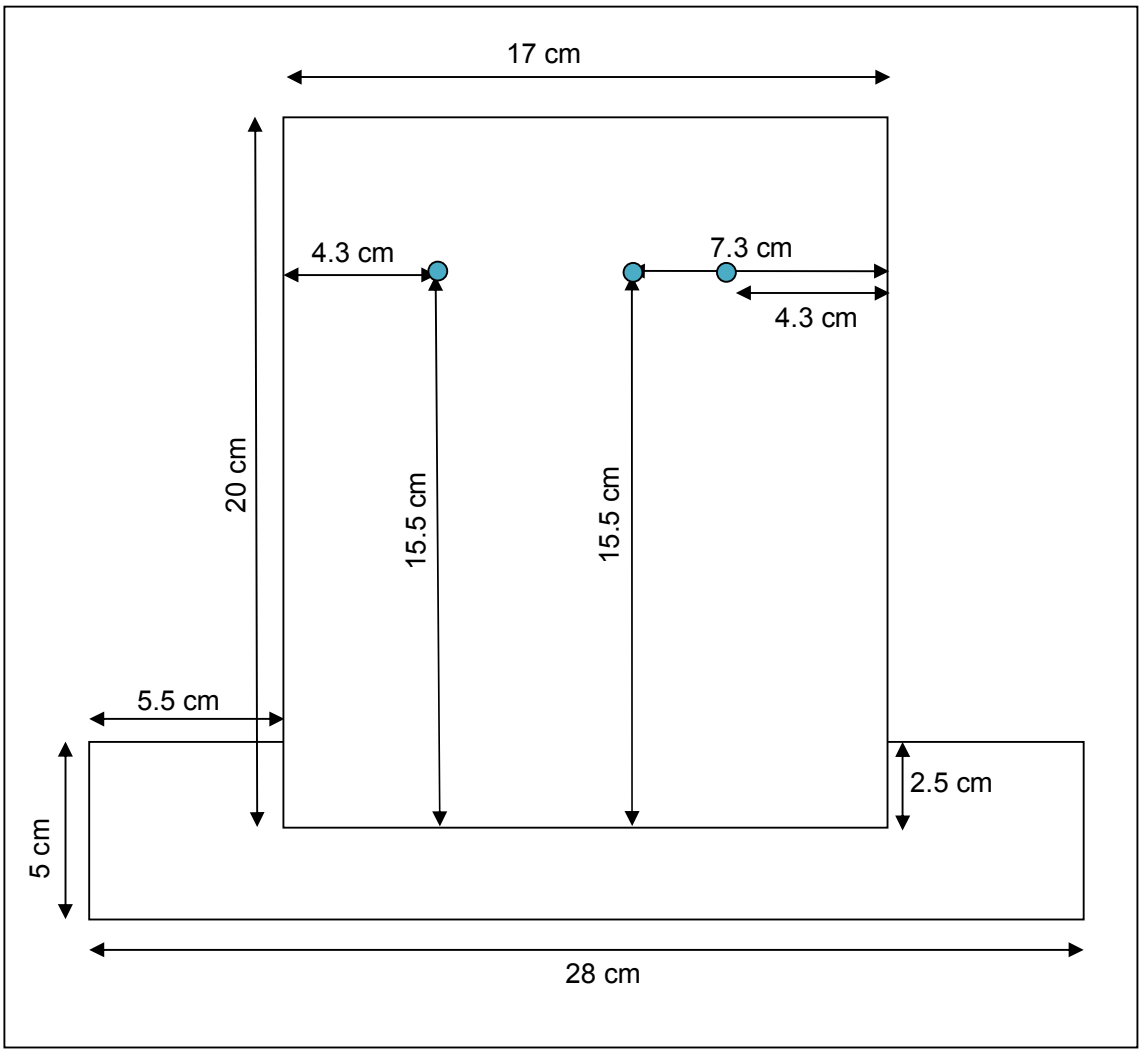

Figure 10-4: Front View of thermocouple support for use with flat rectangular crucibles. Blue circles are 5 mm in diameter and are drilled completely through the support.

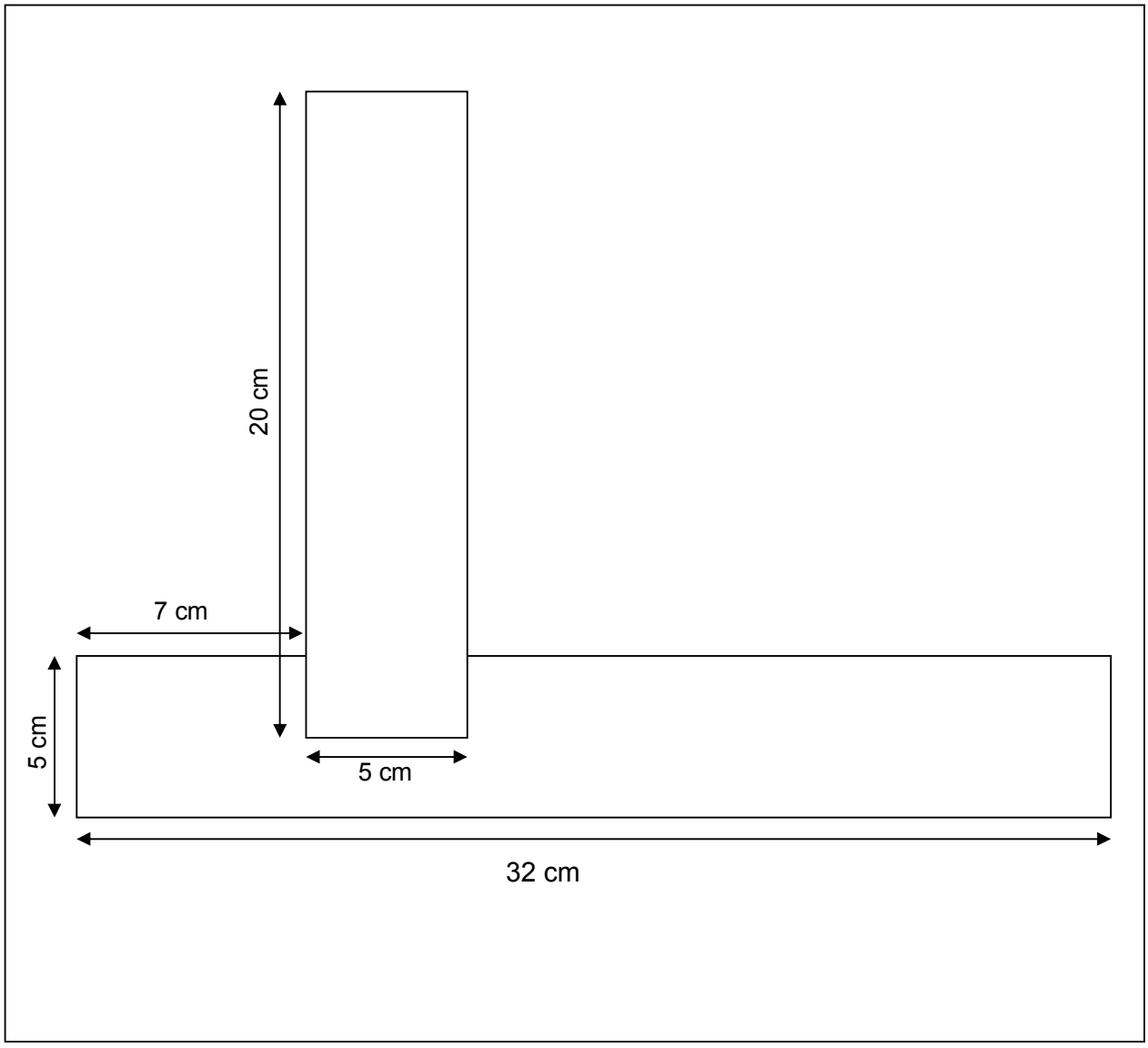

Figure 10-5: Side View of thermocouple support for use with flat rectangular crucibles

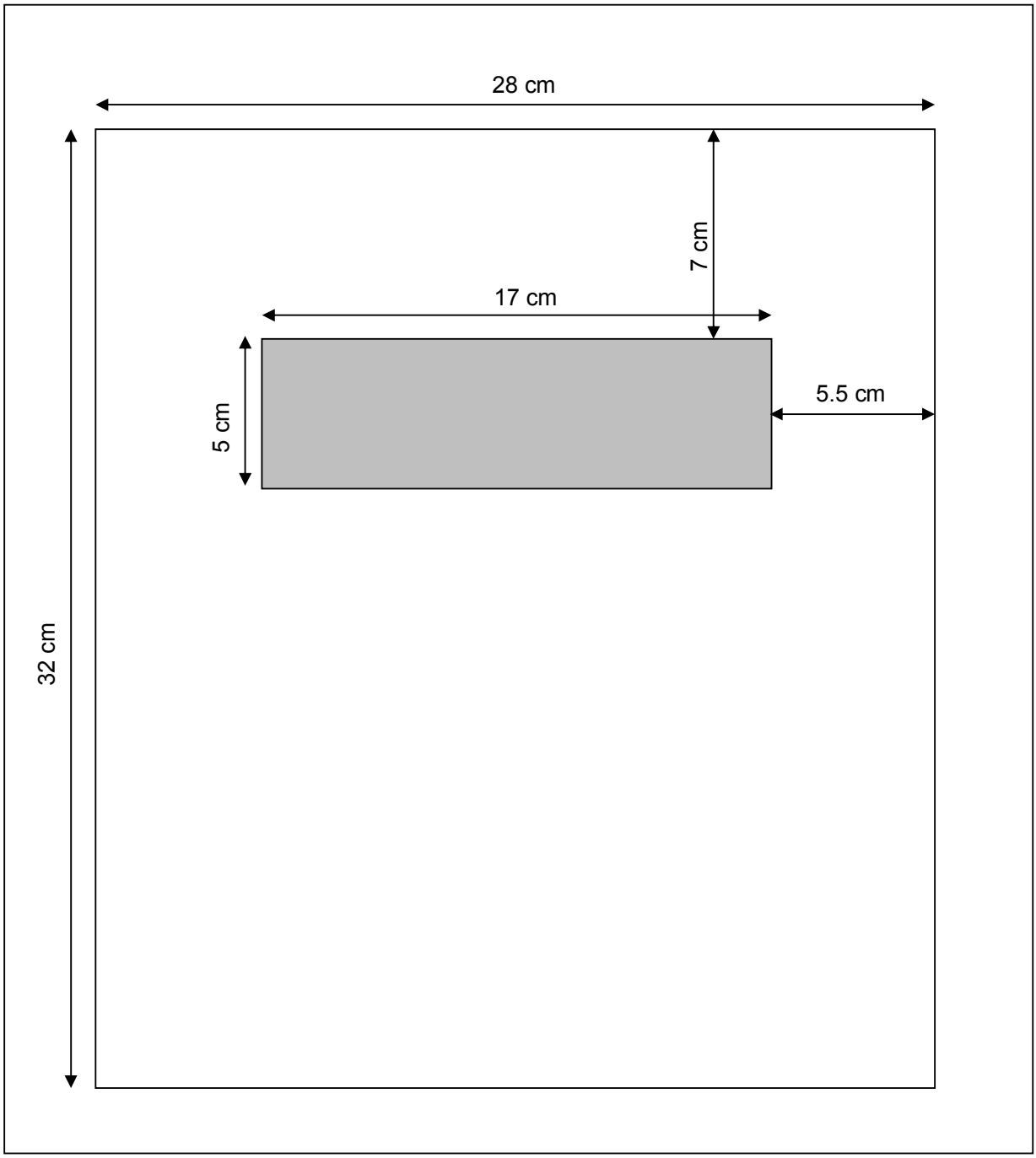

Figure 10-6: Top View of thermocouple support for use with flat rectangular crucibles. Shaded areas should be cut to 2.5 cm deep.

11 Appendix B

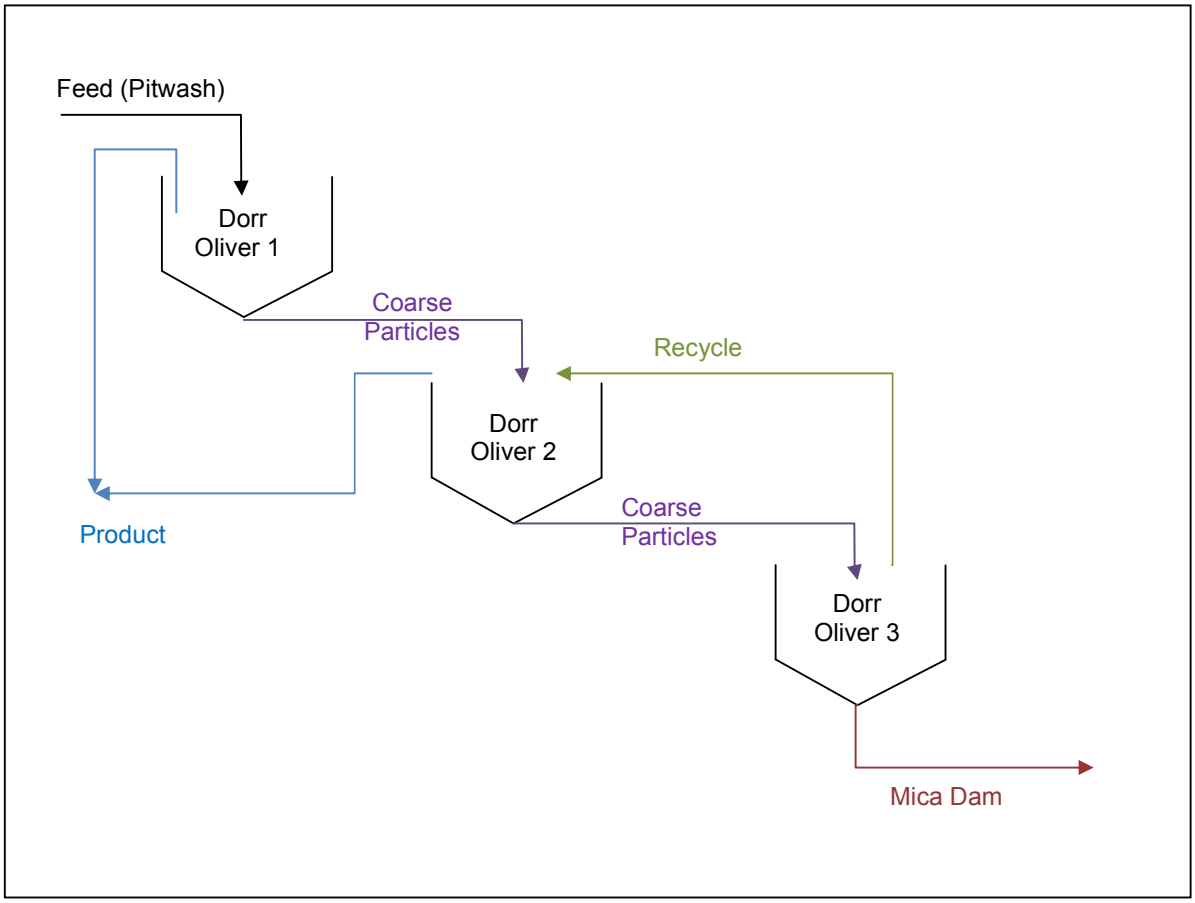

Figure 11-1: Dorr Oliver Operation in Production

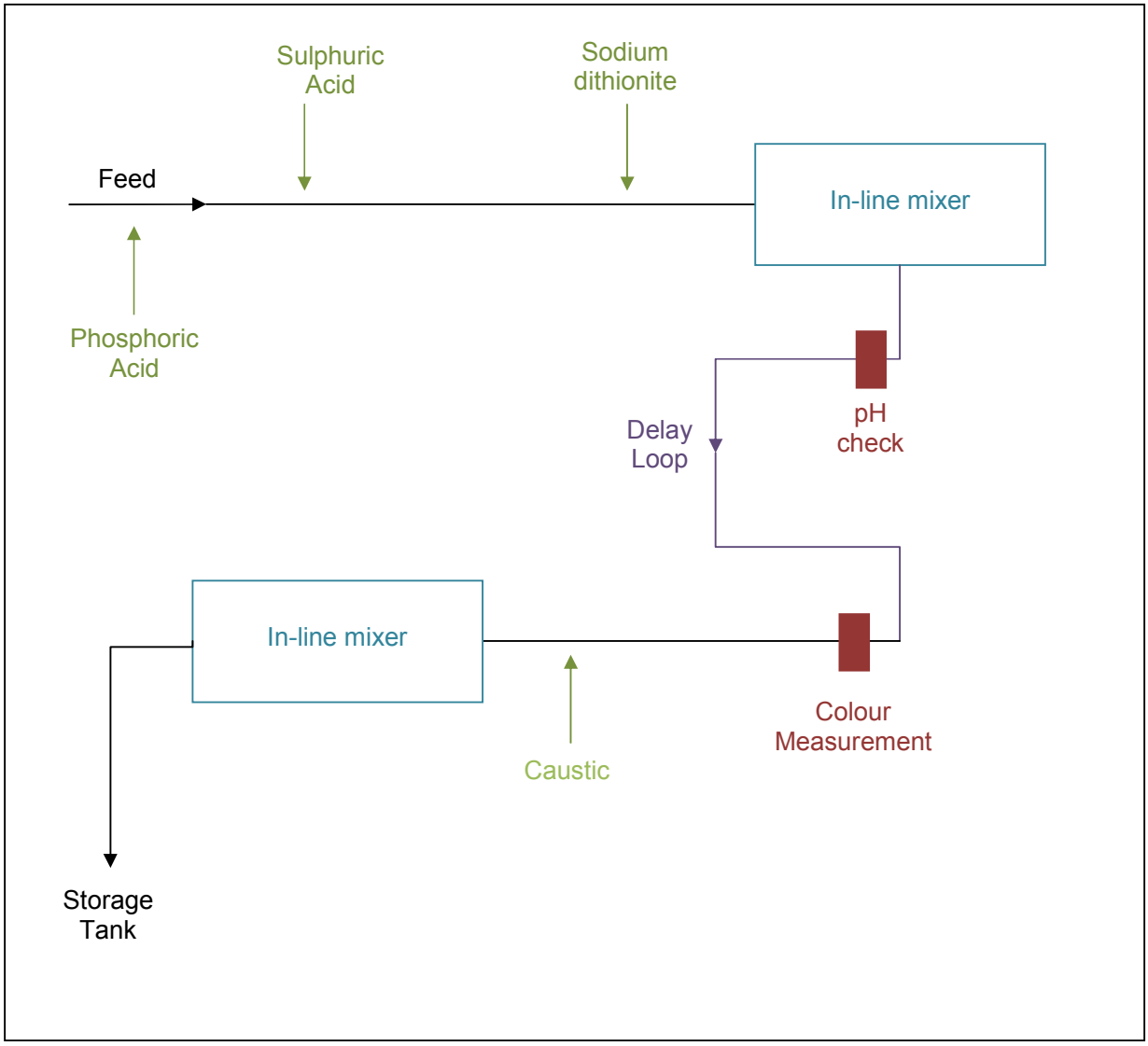

Figure 11-2: Bleaching Operation in Production

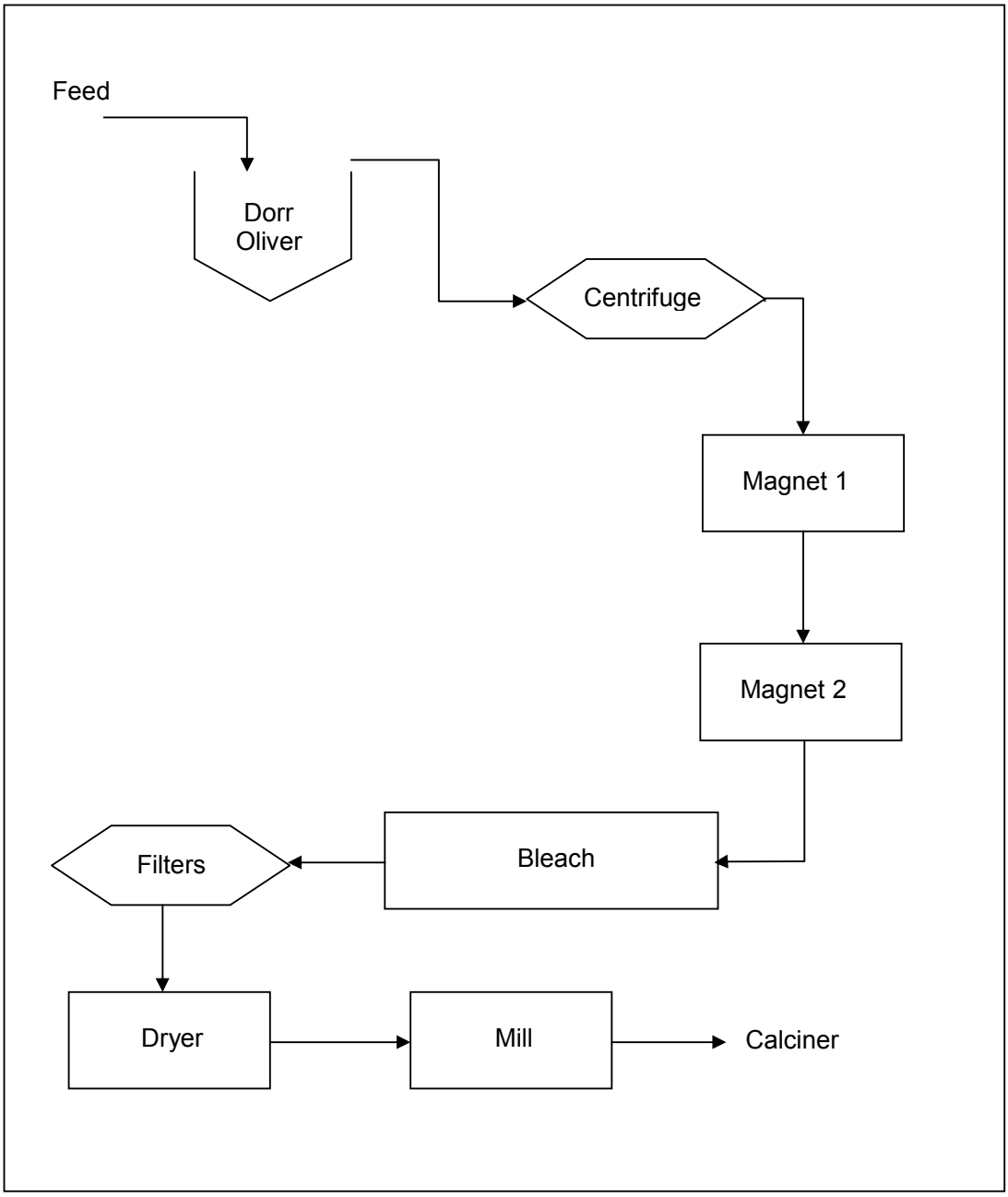

Figure 11-3: Milled HF Production Route

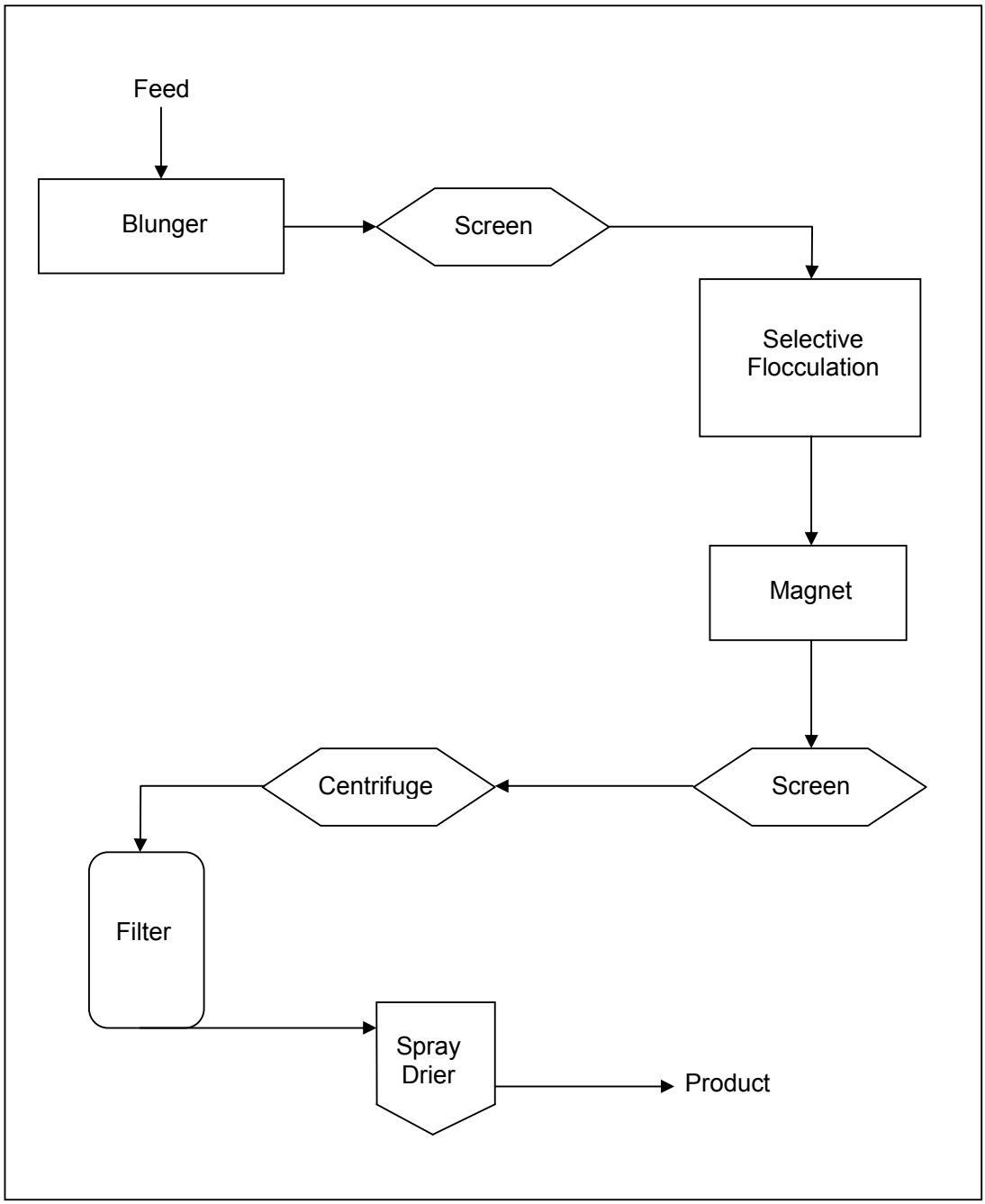

Figure 11-4: Brazil Production Route

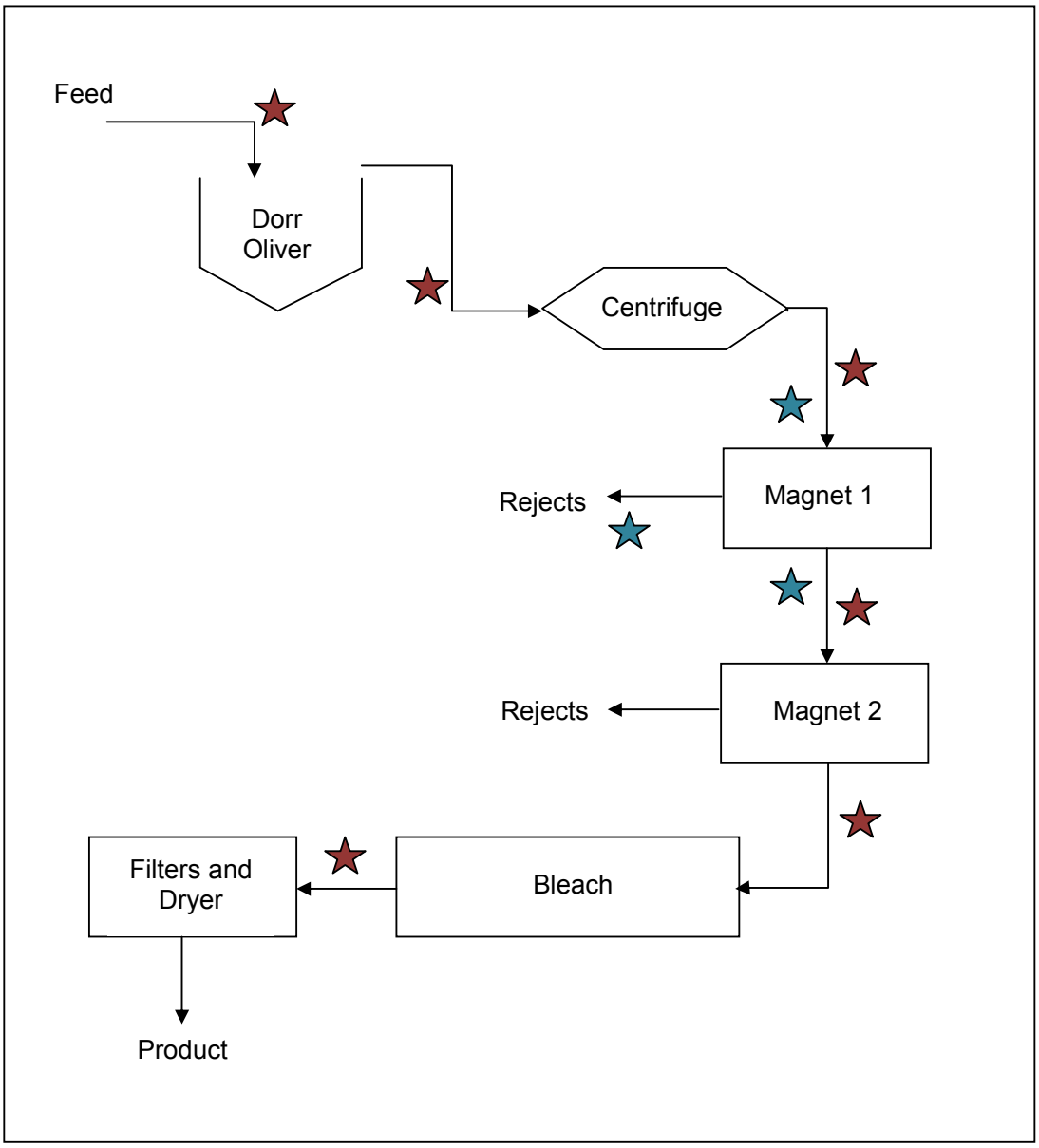

Figure 11-5: Wheal Martyn Production Route. Samples were taken at points marked with a blue star for Chapter 4: Artificial Chemistry and at points marked with a red star for Chapter 5: Natural Chemistry

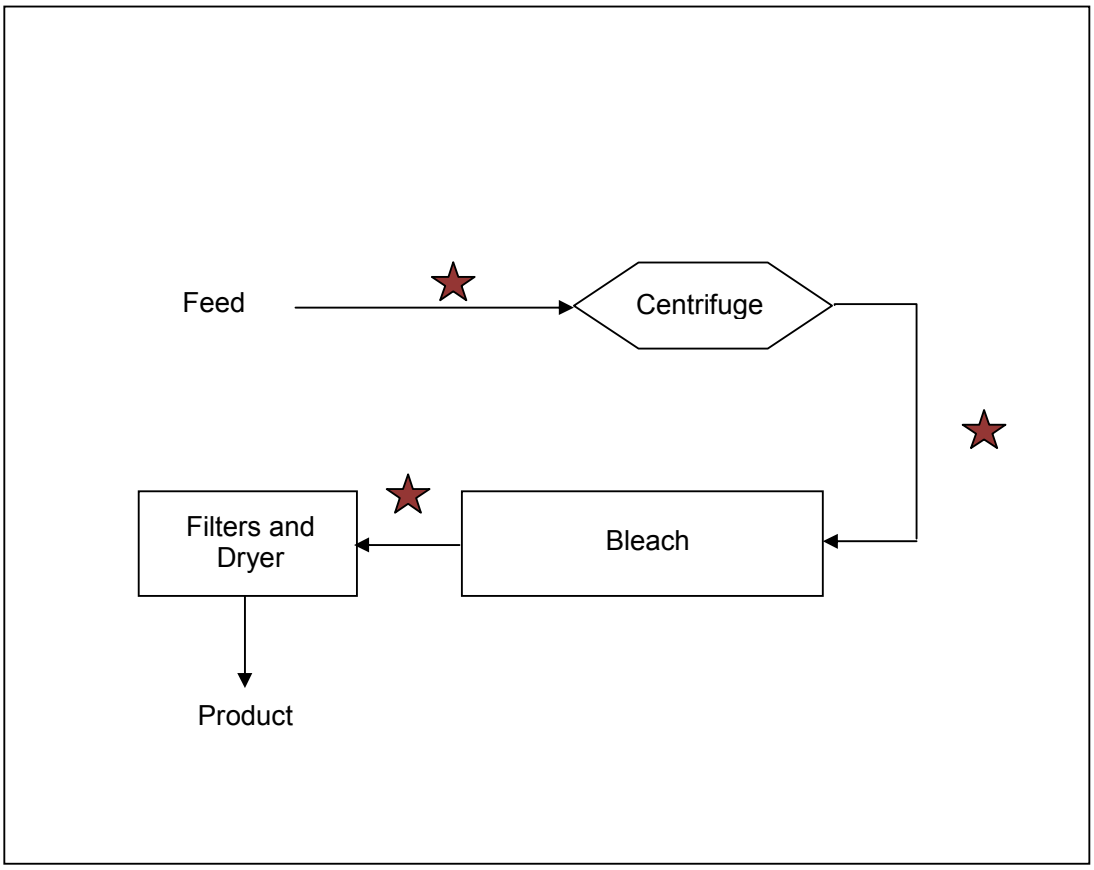

Figure 11-6: Blackpool Production Route. Samples were taken at points marked with a red star for Chapter 5: Natural Chemistry

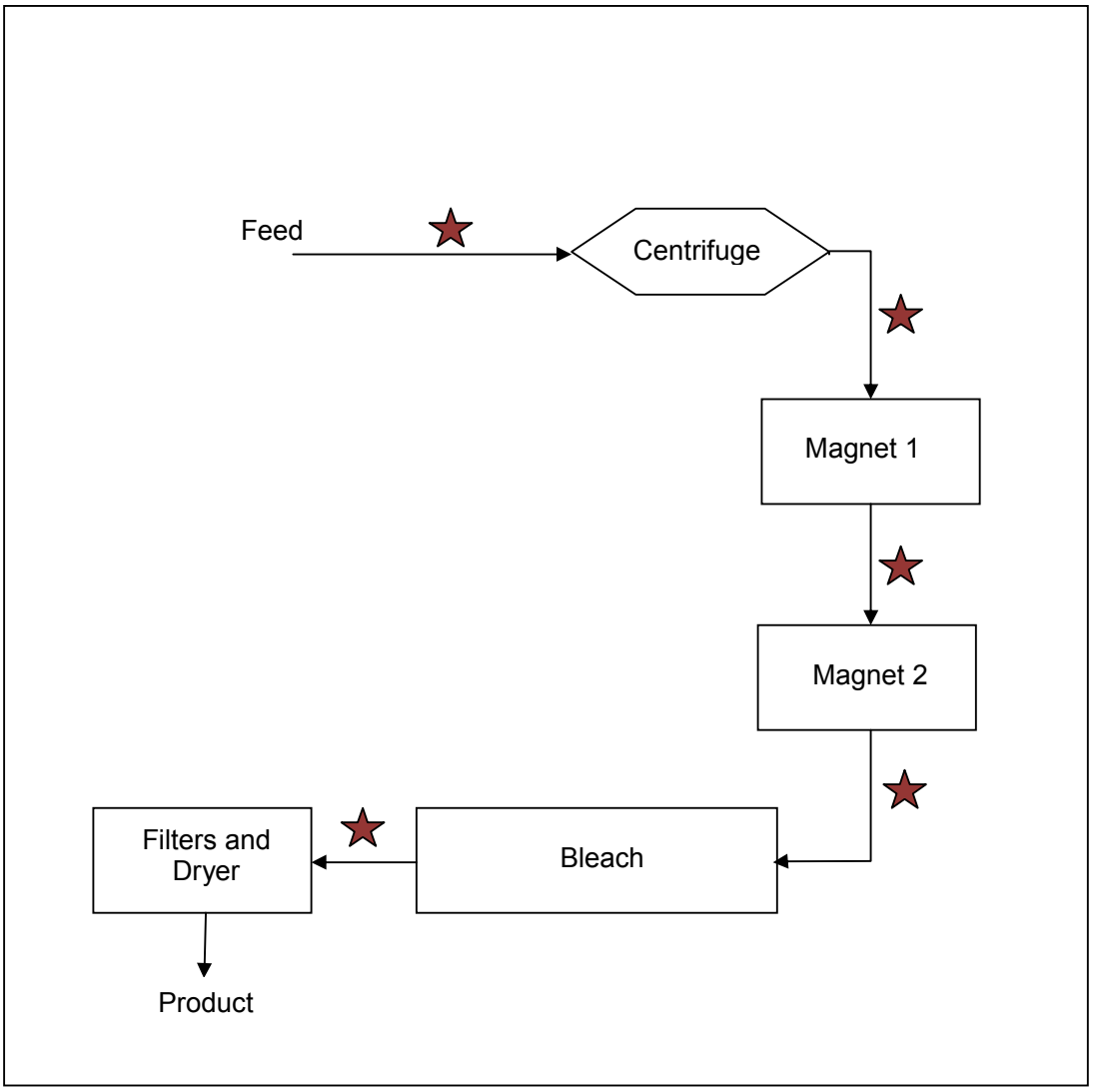

Figure 11-7: Lee Moor Production Route. Samples were taken at points marked with a red star for Chapter 5: Natural Chemistry

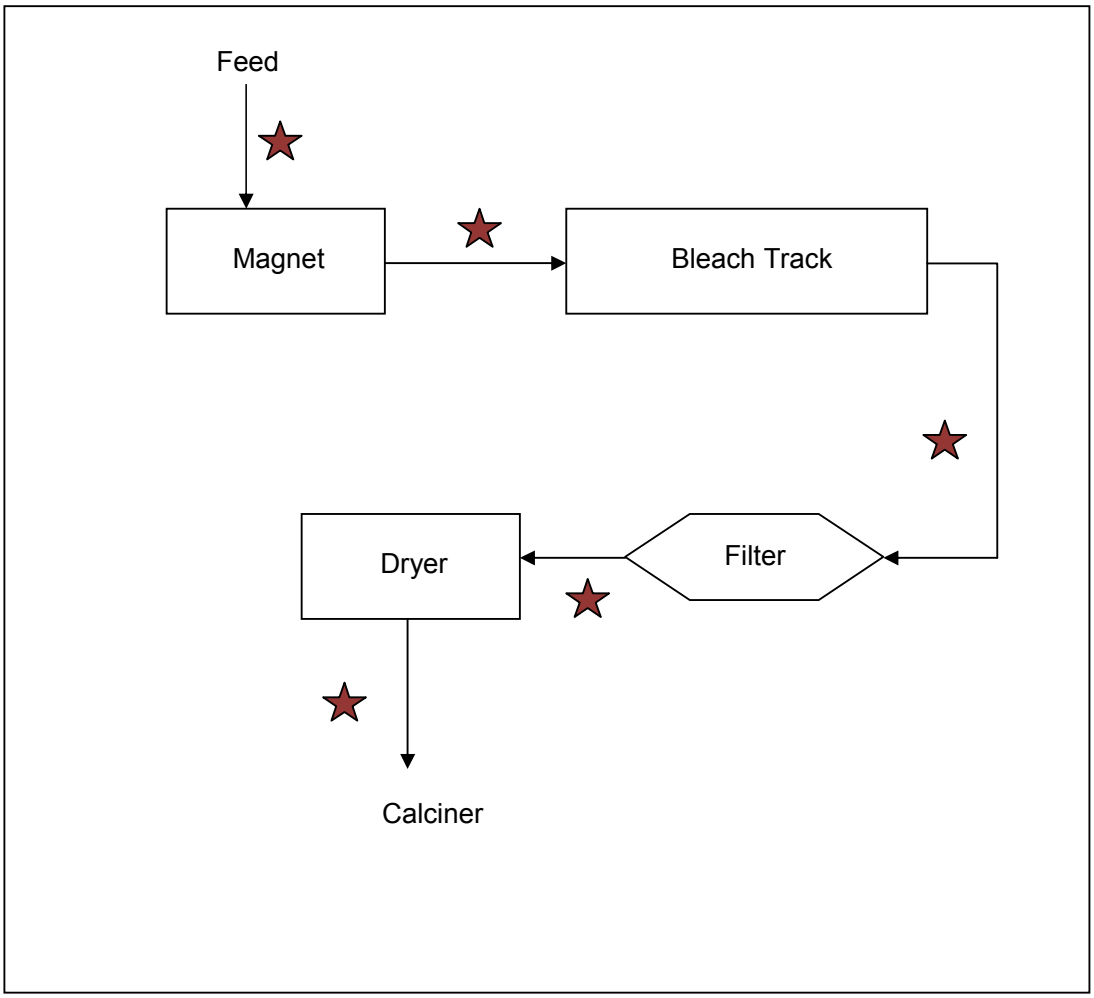

Figure 11-8: Georgia Production Route. Samples were taken at points marked with a red star for Chapter 5: Natural Chemistry

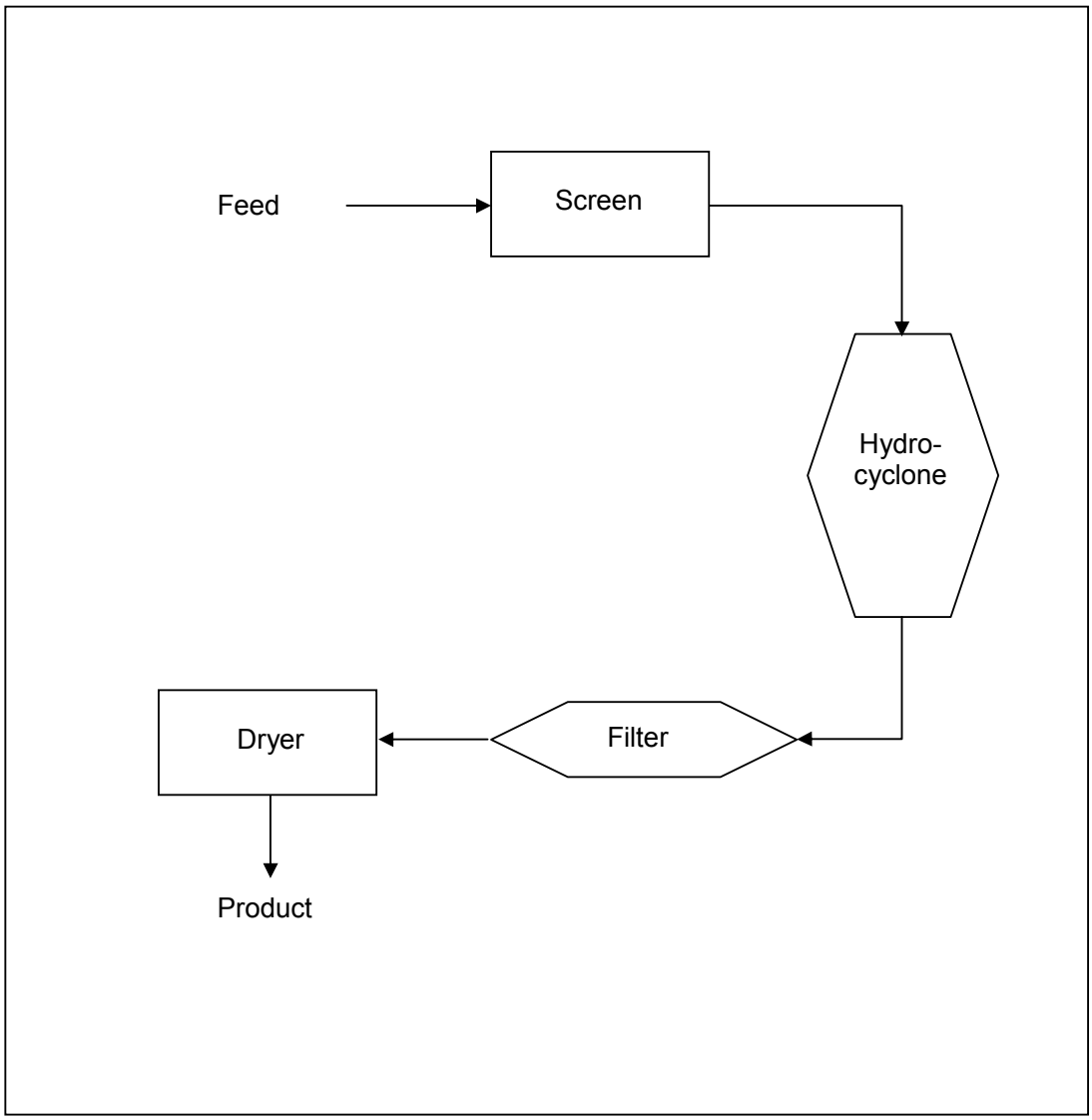

Figure 11-9: Beauvoir Production Route

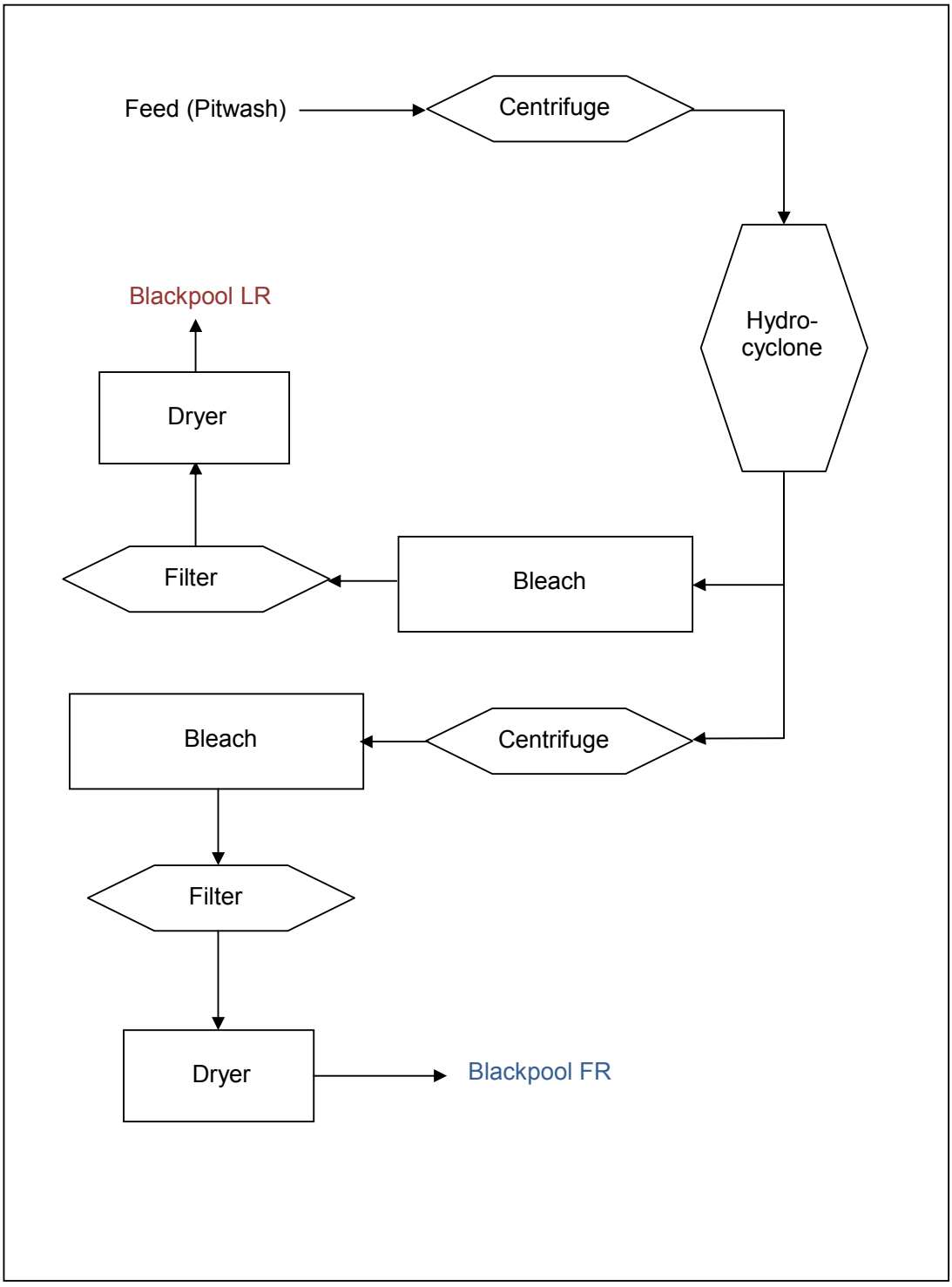

Figure 11-10: Blackpool LR and Blackpool FR Production Routes

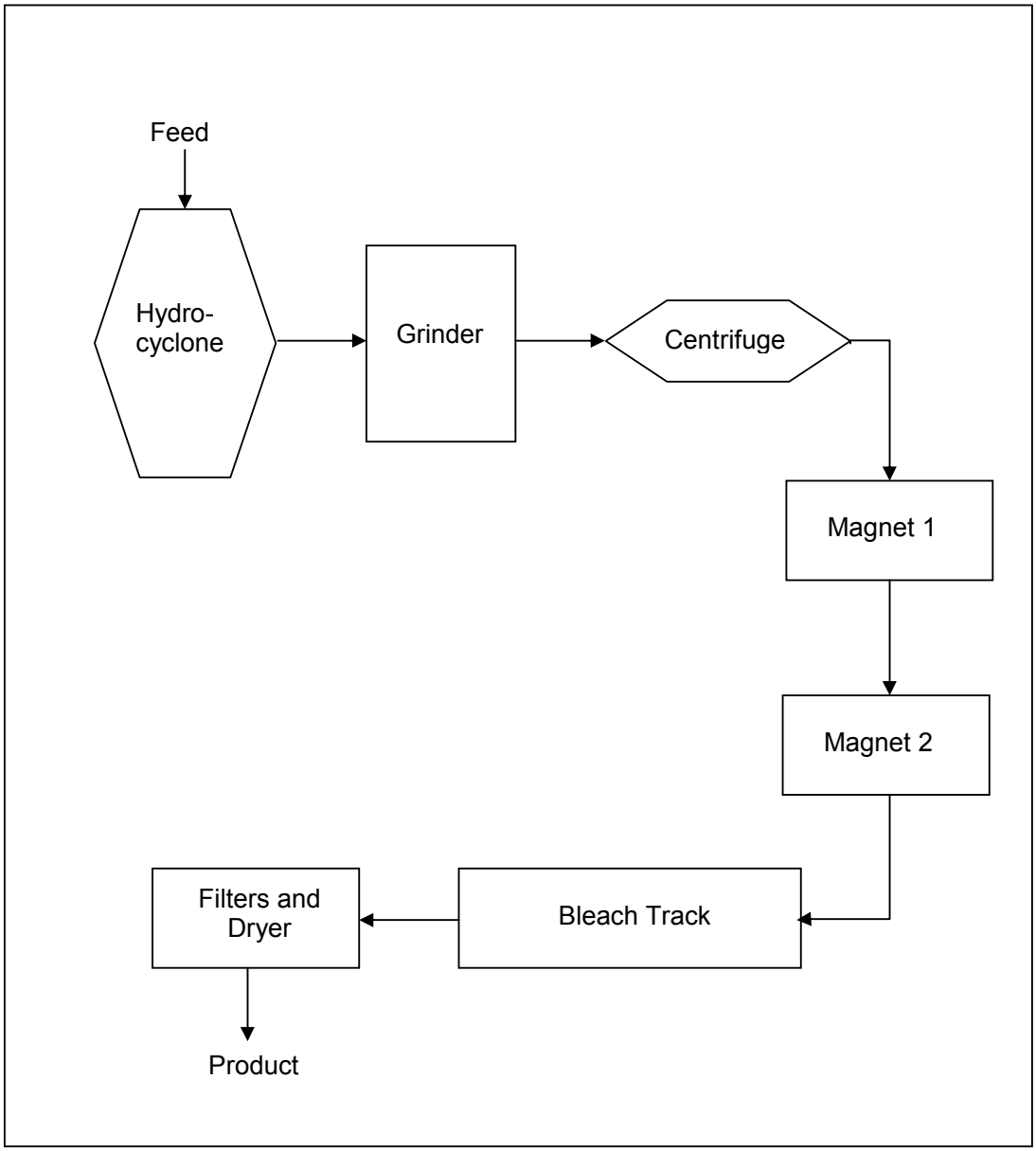

Figure 11-11: Scalping Residues Production Route

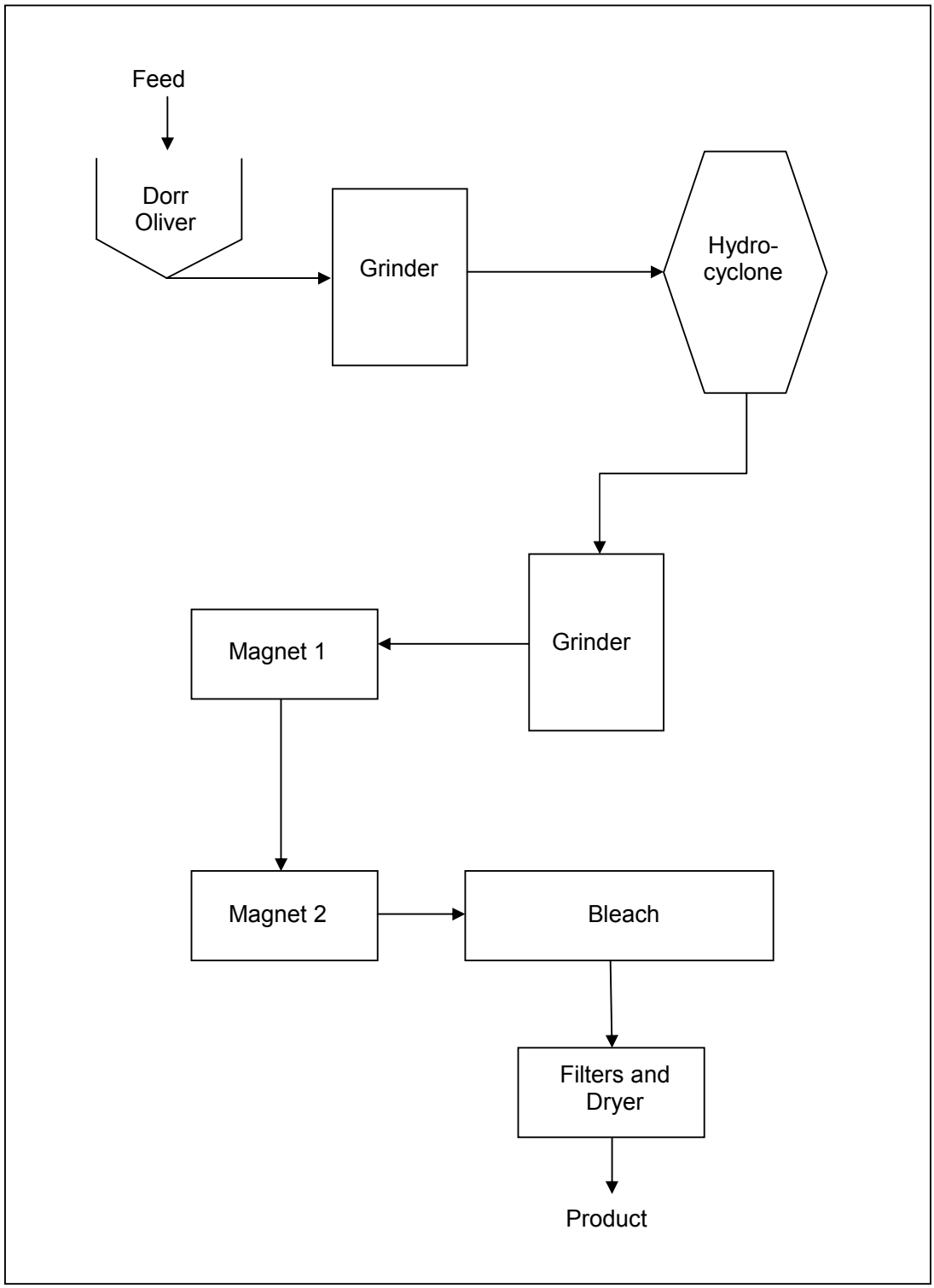

Figure 11-12: Double Ground Clay Production Route

12 Appendix C

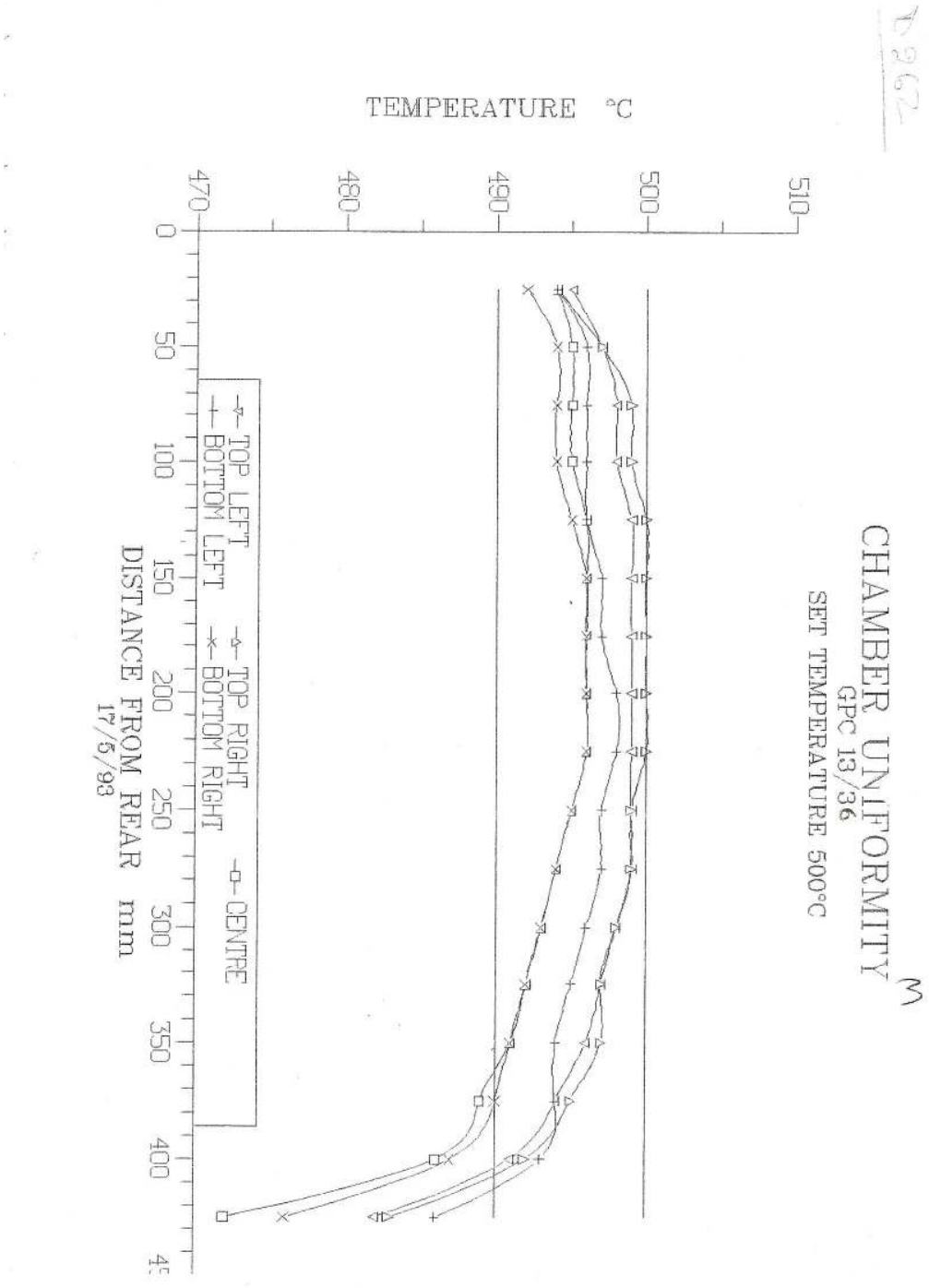

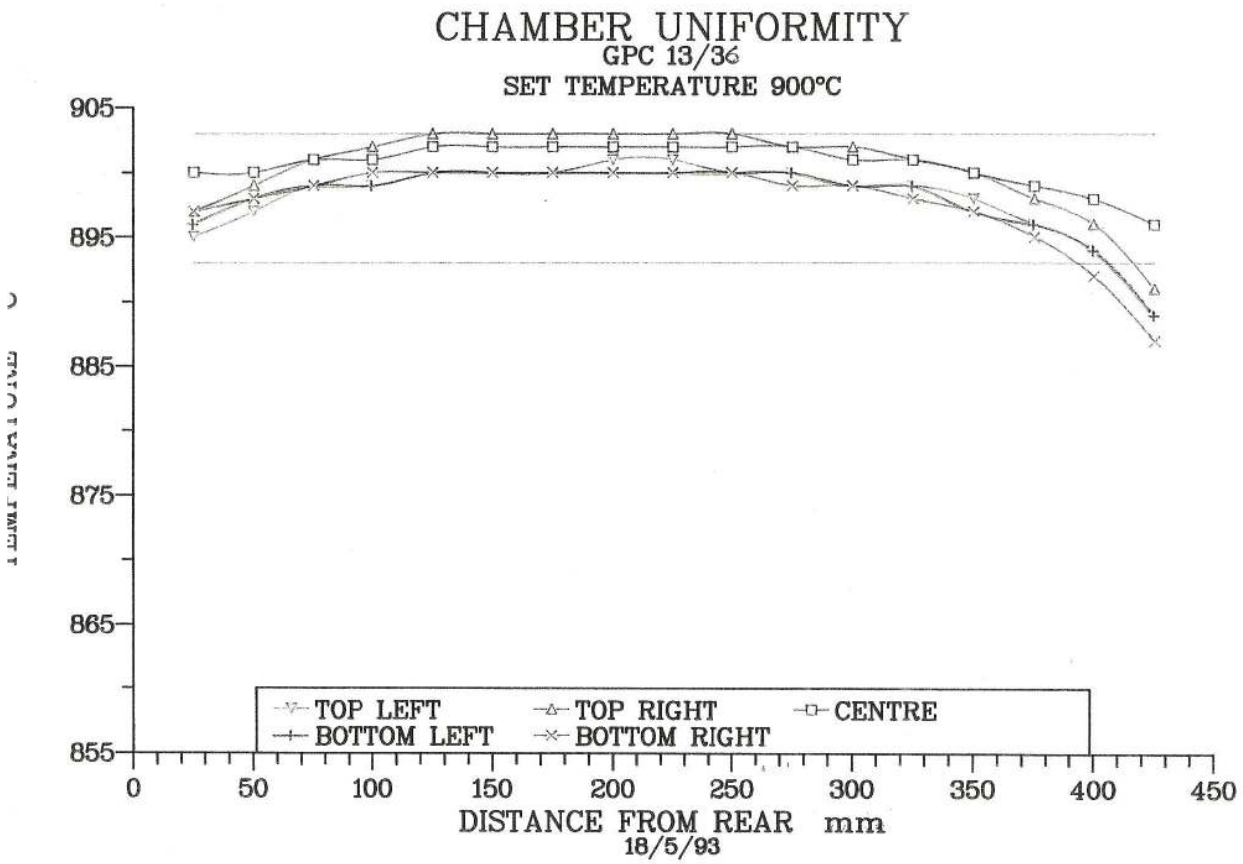
CHAMBER UNIFORMITY
GPC 13/36
SET TEMPERATURE 900°C
905
895
885
875
865
855
TOP LEFT
TOP RIGHT
CENTRE
BOTTOM LEFT
BOTTOM RIGHT
0
50
100
150
200
250
300
350
400
450
DISTANCE FROM REAR mm
18/5/93

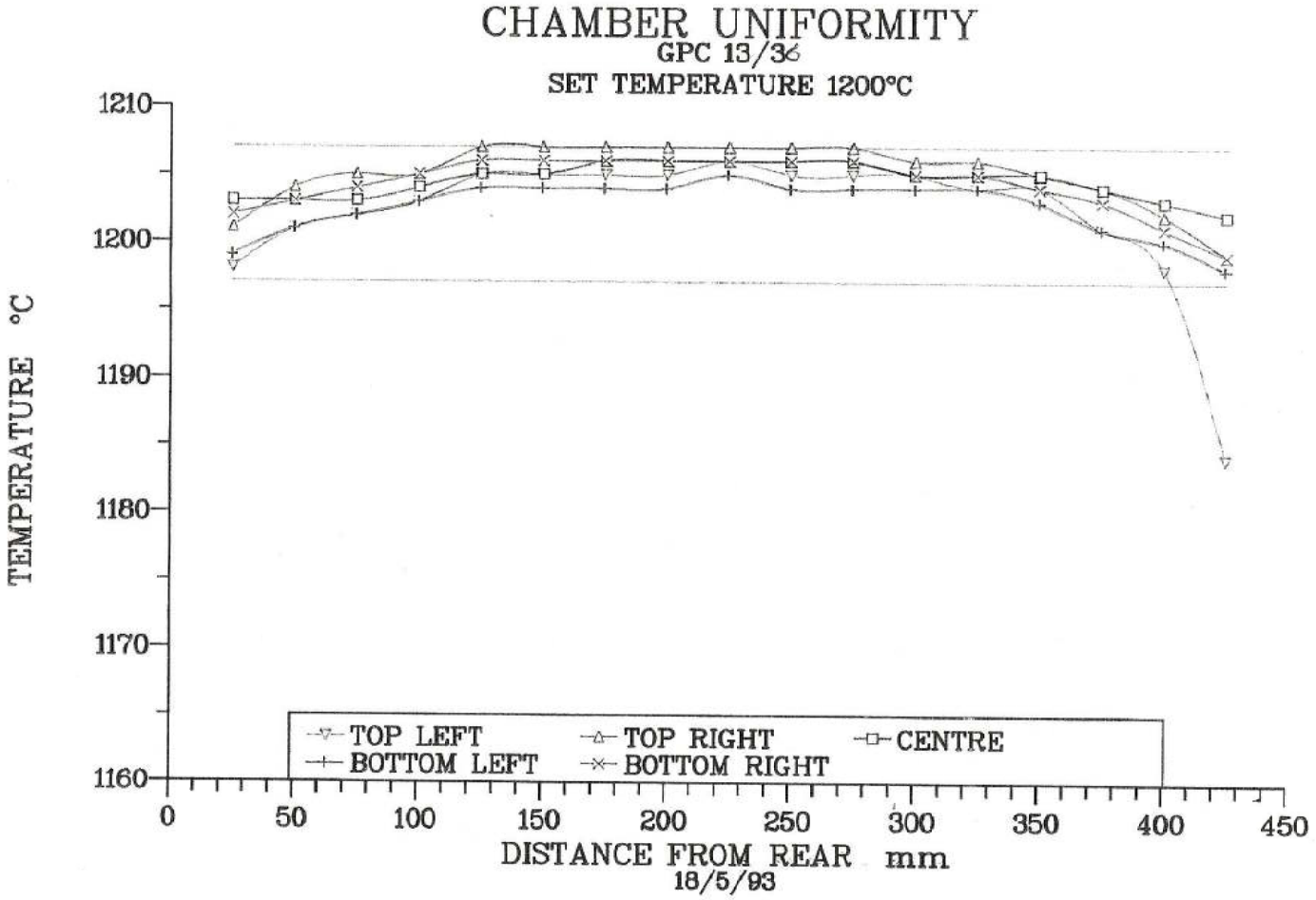
CHAMBER UNIFORMITY
GPC 13/36
SET TEMPERATURE 1200°C
TEMPERATURE °C
1210
1200
1190
1180
1170
1160
TOP LEFT
TOP RIGHT
CENTRE
BOTTOM LEFT
BOTTOM RIGHT
0
50
100
150
200
250
300
350
400
450
DISTANCE FROM REAR mm
18/5/93

13 Appendix D

13.1 Determining the dominant mechanism of heat transfer in the kiln

The conditions being considered are illustrated in Figure 13-1. There is one fixed temperature, T_f, and one variable, T_d. A model needs to be developed for the change of T_d with time, so that the time taken for the dish to reach temperature equilibrium with the furnace can be determined. The dish is being modelled as a slab of fused silica, due to problems caused by the sides of the dish relating to geometry and corner effects, they have been removed from the problem.

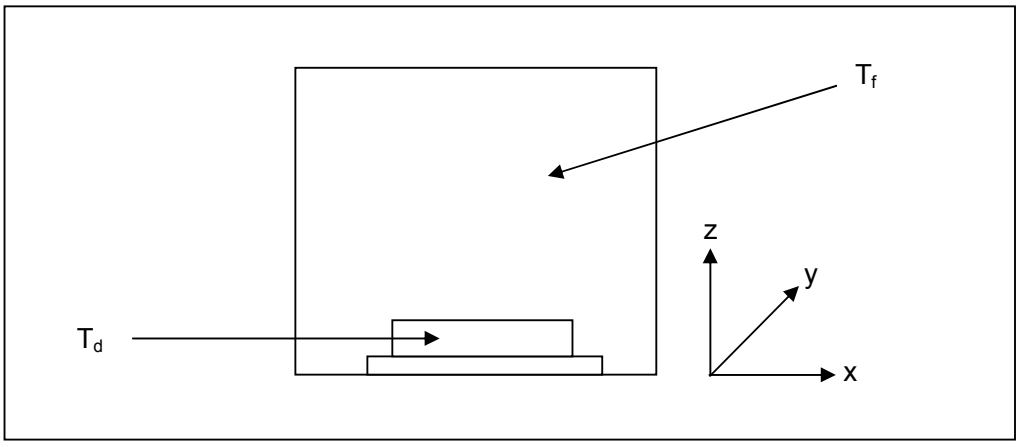

Figure 13-1: Illustration of the problem

The heat transfer from the surrounding air inside the furnace to the dish is governed by the relationship shown in Equation 13-1.

$$m \ C_p \ \frac{dT_d}{dt} = h \, A \left(T_f - T_d\right)$$

Equation 13-1: Determining the heat transfer from air in the furnace to the crucible where m = mass in the dish (kg), Cp = specific heat capacity of the dish (kJ kg-1 K-1), T_d = temperature of the dish (K), h = heat transfer coefficient (W m-2 K-1), A = surface area of the dish (m2), T_f = temperature of the furnace (K), t = time (s) [92]

13.1.1 An analytical model

In order to develop a simple analytical model the following assumptions have been made:

- There is a uniform temperature distribution throughout the furnace; therefore T_f is only a function of time and not space and it can be considered fixed
- The temperature of the kiln is unaffected by the introduction of the dish
- There is a uniform temperature distribution throughout the dish; therefore, T_d is only a function of time and not space
- The specific heat capacity of the dish is not a function of temperature
- The heat transfer coefficient is not a function of temperature
- Radiative heat transfer is not important, the main mechanism of heat transfer is natural convection
- There is no conduction occurring in the system

The heat transfer relationship from Equation 13-1 can be rearranged as in Equation 13-2.

$$\frac{dT_d}{T_f - T_d} = \frac{hA}{mC_p} t$$

Equation 13-2: Rate of heating, rearranged from Equation 13-1, where m = mass in the dish (kg), Cp = specific heat capacity of the dish (kJ kg-1 K-1), T_d = temperature of the dish (K), h = heat transfer coefficient (W m^{-2} K-1), A = surface area of the dish (m^2), T_f = temperature of the furnace (K), t = time (s)

When this is integrated it becomes what is shown in Equation 13-3.

$$\left[\ln \frac{1}{T_f - T_d}\right]_{T_{do}}^{T_{de}} = \left[\frac{h\,A}{m\,C_p}\,t\right]_0^t$$

Equation 13-3: Integration of Equation 13-2, where m = mass in the dish (kg), Cp = specific heat capacity of the dish (kJ kg-1 K-1), T_d = temperature of the dish (K), h = heat transfer coefficient (W m-2 K-1), A = surface area of the dish (m^2), T_f = temperature of the furnace (K), t = time (s)

It is known that:

T_f = 1050 °C = 1323 K

T_d = 1039.5 °C = 1312.5 K

A = 0.0123 m^2

m = 0.3253 kg

C_p = 703 J kg^{-1} K^{-1}

$$h = \frac{\text{thermal conductivity of air}}{\text{thickness of dish}} = \frac{0.059}{0.0035} = 16.9 \text{ W m}^{-2} \text{ K}^{-1}$$

The heat transfer coefficient is a function of the thermal conductivity, the thickness of the dish and the Nusselt number. It can be roughly determined by the thermal conductivity divided by the thickness of the dish, disregarding the Nusselt number

[92]. The heat transfer coefficient for an air based system should be between 2 and 25 $Wm^{-2}K^{-1}$ which this value is [93]. Therefore, for the basic, analytical model it will be used.

The increase of T_d with time is exponential; for the dish to reach the same temperature as the furnace will take an infinitely long time and therefore the value of T_d to be used in the calculation will be 99% of T_f which is 1039.5 °C.

When these values are used the time taken for the dish to reach 1039.5 °C is 84 minutes. This is a longer time than expected and considered mainly due to the small heat transfer coefficient. Hopefully, by increasing the complexity of the model, by introducing the fact that the heat transfer coefficient is dependent on temperature, the accuracy of the model can be increased.

13.1.2 Numerical model

A numerical model can be developed for the system, if the heat transfer coefficient is allowed to become a function of temperature. This is determined using a correlation which was developed between the Nusselt, Prandtl and Grashof numbers in a natural convection system. This relationship is shown in Equation 13-4.

$$\sqrt{Nu} = \sqrt{Nu_0}\left[\frac{\left(\frac{Gr\ Pr}{300}\right)}{\left(1 + \left(\frac{0.5}{Pr}\right)^{9/16}\right)^{16/9}}\right]^{1/2}$$

Equation 13-4: Correlation of Nusselt, Prandtl and Grashof numbers in a natural convection system. This correlation is valid for 10-4 ≤ Gr Pr ≥ 4x1014 and 0.0022 ≤ Pr ≥ 7640, where Nu = Nusselt number, Pr = Prandtl number and Gr = Grashof number [94]

The following assumptions are applicable in this situation:

- There is a uniform temperature distribution throughout the furnace, therefore T_f is only a function of time and not space and it can be considered fixed
- The temperature of the kiln is unaffected by the introduction of the dish
- There is a uniform temperature distribution throughout the dish, therefore T_d is only a function of time and not space
- The specific heat capacity of the dish is not a function of temperature
- Radiative heat transfer is not important, the main mechanism of heat transfer is natural convection
- There is no conduction occurring in the system

The density of air can be calculated from a simple relationship with temperature and pressure, shown in Equation 13-5.

$$\rho = \frac{P}{R\,T} RMM_{air} = 0.267\ kg\ m^{-3}$$

Equation 13-5: Determining the density of air, where ρ = fluid density (kg m-3), P = standard air pressure, R = specific gas constant (kJ kmol-1 K-1), T = Temperature (K), RMM = Relative Molecular Mass [92]

The viscosity of the air is more difficult to calculate but it can be done using Sutherland's formula, shown in Equation 13-6.

$$\mu = \mu_0 \frac{0.555\,T_{fs} + S}{0.555\,T_0 + S} \left(\frac{T_{fs}}{T_0}\right)^{3/2} = 0.0241\ cP = 2.41\ x\ 10^5\ Pa\ s$$

Equation 13-6: Determining the viscosity of air, where μ0 = reference viscosity (cP), T = Temperature (K), S = Sutherland's constant = 120, T_{fs} = temperature of furnace (° R), T_{d0} = initial temperature of the dish (K) [92]

Due to the complexity of the problem, it was encoded in Matlab and solved. The Matlab code for the m-file named ftemp1 is displayed below:

```
function dT=ftemp1(t,T)

%calc temp of fused silica dish in a muffle furnace
mu=2.41e-5; %(Pa s) calculated using Sutherland's formula from
www.limoeng.com/Flow/GasViscosity.htm
rho=0.267; %(kg/m^3) calculated using (P/(R*Tm))*RMMair
Pr=0.68;      %Prandtl      number      for      air      from
www.engineeringtoolbox.com/air-properties.html
Tinf=1050+273; %(K) temperature of kiln, set value
L=0.0035; %(m) thickness of dish, measured value
g=9.81; %(m/s^2)acceleration of gravity
Nu0=0.67;       %initial       Nusselt       number       from
www.cheresources.com/convection.shtml
Ah=0.0123; %(m^2) surface area of dish, measured value
md=0.3253; %(kg) weight of dish, measured value
Cpd=703; %(J/kg.K) from www.sciner.com/Opticsland/FS.htm
Cpa=1068;     %(J/kg.K)from     www.engineeringtoolbox.com/air-
properties.html
```

```
k=(Cpa*mu)/Pr; %(W/m.K) thermal conductivity of air at Tinf

%the following calculations are from www.cheresources.com/convection.shtml and are used in order to calculate the heat transfer coefficient in terms of Temperature
beta=1/((Tinf+T)/2);
Gr=L^3*g*rho^2*beta*abs(T-Tinf)/mu^2;
x1=Gr*Pr/300;
x2=(1+(0.5/Pr)^(9/16))^(16/9);
x3=(x1/x2)^(1/6);
sNu=sqrt(Nu0)+x3;
Nu=sNu^2;
htc=k*Nu/L;%(W/m^2.K)heat transfer coefficient


%the following is an ordinary differential equation for temperature and time developed from the standard heat transfer equation
dT=htc*Ah*(Tinf-T)/(md*Cpd);
```

The program in the function m-file, named ftemp1prog then consists of the following:

```
Ti=20+273
[t,T]=ode23('ftemp1',[140*60],[Ti]);
plot (t,T)
title('heat transfer into a fused silica dish')
xlabel('time (s)')
ylabel('Temperature (K)')
```

When the program is run, the graph shown in Figure 13-2 is produced. This shows that the time taken for the dish to heat up to 1050 °C is 140 minutes. The time taken for the dish to reach 99% of the required temperature is 86.4 minutes, a slightly increased duration compared to that found with the analytical model. This graph does show a time taken for equilibrium of temperature, something which cannot be determined with the analytical model, this stage is shown to take 135.4 minutes.

It is known from practical experiments performed that the dish glows red-hot after 30 minutes at temperature. Therefore, the model is not as accurate or realistic as it

could be. By incorporating some aspect of the radiation that is occurring in the furnace into the model the accuracy can be increased.

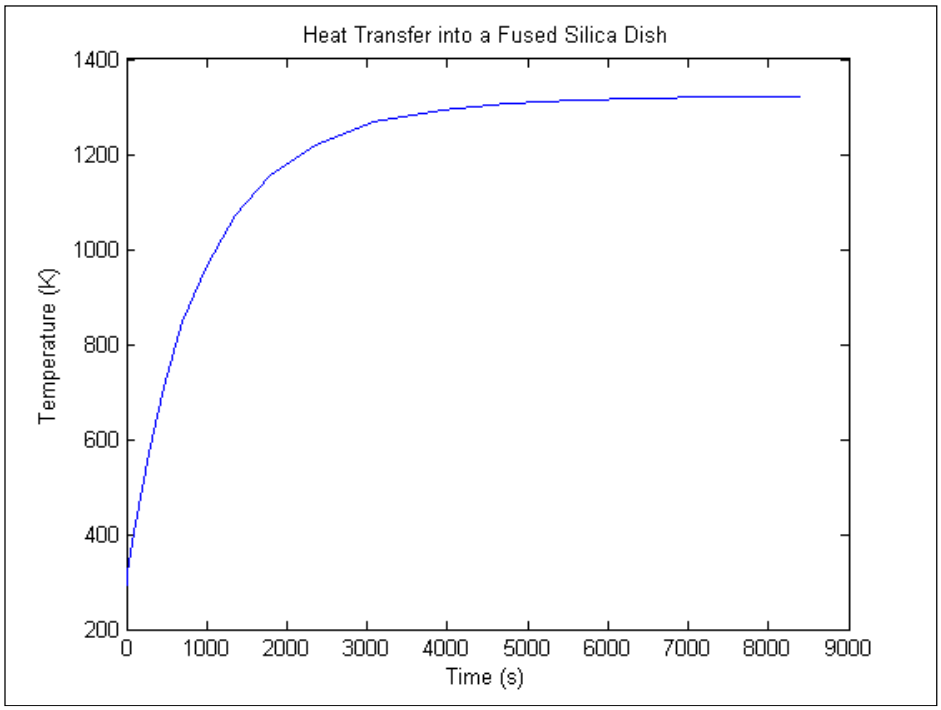

Figure 13-2: Graph to show heat transfer into a fused silica dish

As radiation is incorporated into the model, the following assumptions are applicable:

- There is a uniform temperature distribution throughout the furnace, therefore T_f is only a function of time and not space and it can be considered fixed
- The temperature of the kiln is unaffected by the introduction of the dish
- There is a uniform temperature distribution throughout the dish, therefore T_d is only a function of time and not space
- The specific heat capacity of the dish is not a function of temperature
- There is no conduction occurring in the system

Radiation can be introduced into this situation by calculating the heat transfer coefficient due to radiation and combining it with the heat transfer coefficient due to free convection, which has already been calculated. This combined heat transfer coefficient can then be used in Equation 13-1.

The radiative heat transfer coefficient can be calculated using Equation 13-7.

$$h_f = e\,\sigma\left(T_f^3 + T_d T_f^2 + T_d^2\,T_f + T_d^3\right)$$

Equation 13-7: Determining the radiative heat transfer coefficient, where e = emissivity of grey body, σ = Stefan-Boltzman constant, T_d = temperature of the dish (K), T_f = temperature of the furnace (K) [89]

In this case, the APM (a nickel, chromium, and aluminium alloy) wire heating elements at the sides of the furnace are the grey body that radiates heat. This material has an emissivity value of 0.7 [95]. The emissivity value is the radiation per unit area emitted from a 'real' or grey surface relative to that emitted by a black body at the same temperature, and it is used in order to simplify equations [89].

Therefore, by incorporating this modification, the whole model can be made more accurate. The lines added to the ftemp2 m-file are shown below.

```
em=(0.83+0.96)/2;  %emissivity of silicon carbide heating
elements,                                          from
www.omega.com/literature/transactions/volume1/emissivityb.html
sigma=5.67e-8; %Stefan-Boltzman constant

htcf=k*Nu/L;%(W/m^2.K)heat transfer coefficient due to free
convection
```

```
%the following calculations are from C&R 1 Page 444 and relate
to
%developing a radiative component of the heat transfer
coefficient
x4=(Tinf^3)+(T*Tinf^2)+(Tinf*T^2)+(T^3)
htcr=em*sigma*x4; %(W/m^2.K) heat transfer coefficient due to
radiation

htc=htcf+htcr; %(W/m^2.K) total heat transfer coefficient
```

The rest of the code remains as before, except for the time component in the ftemp2prog function m-file, which is reduced from 140 to 10 minutes.

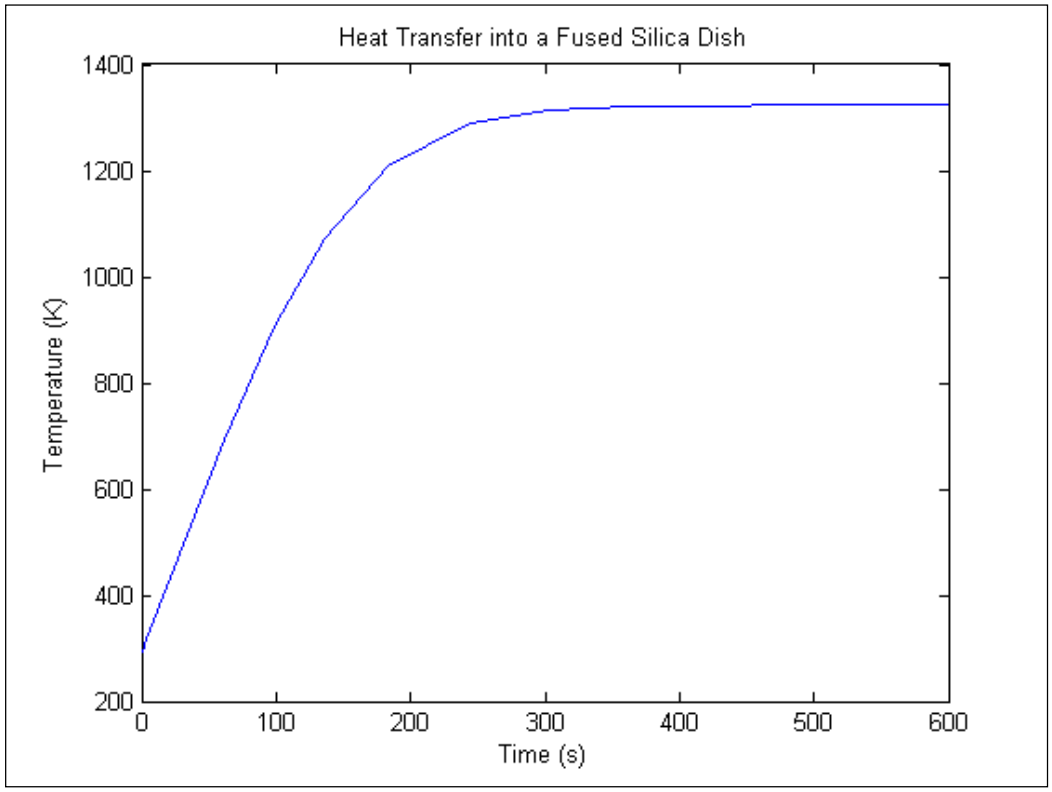

Figure 13-3: Graph to show the heat transfer into a fused silica dish when radiation is considered

When the program is run, the graph shown in Figure 13-3 is produced, showing that it only takes 6.9 minutes to reach equilibrium temperature with the furnace, and only

5.3 minutes to reach 1039.5 °C (99% of high temperature) when radiation is included in the model.

The difference between the two models that have been developed as part of this piece of work is illustrated in Figure 13-4. The dramatic reduction in time taken for the dish to reach its final temperature once that radiation is included in the model shows that radiation is the considerably more dominant form of heat transfer occurring in the system compared to convection.

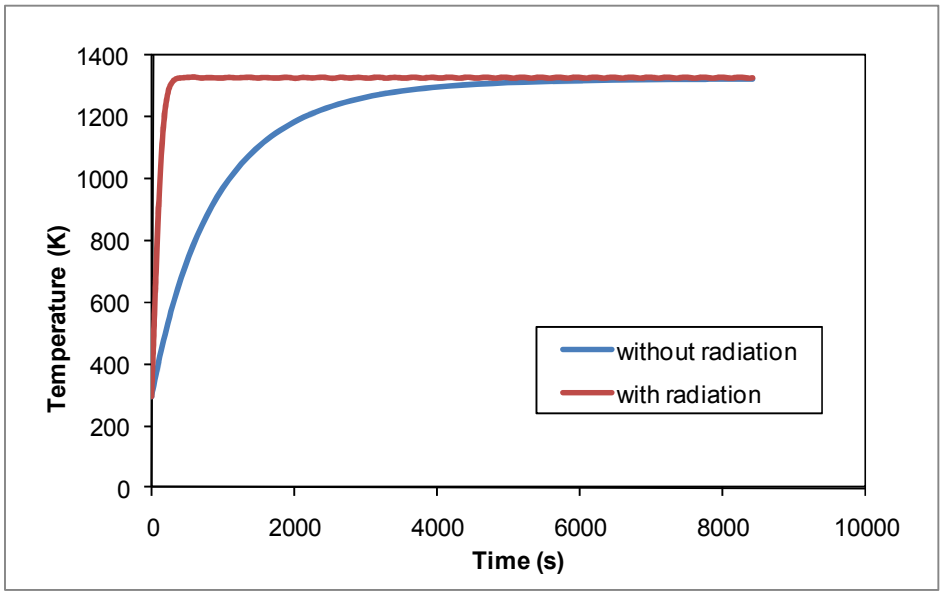

Figure 13-4: The impact of radiation on the time taken for the fused silica dish to reach high temperature

14 References

1. (2009) 2008 Annual Report Imerys Minerals Ltd.
2. Chandrasehar S, Ramaswamy S (2002) Influence of mineral impurities on the properties of kaolin and it's thermally treated products. Applied Clay Science 21: 133-142
3. Grim RE (1968) Clay Mineralogy, 2 edn Mc-Graw-Hill Book Company, New York, USA
4. Noble FR (1980) A study of sintering and other phenomena related to calcination in the Lee Moor No.3 Herreschoff Imerys Minerals Ltd.
5. Taylor R (2000) Microwave assisted firing of kaolinite Imerys Minerals Ltd.
6. Drzal LT, Rynd JP, Fort T (1983) Effects of calcination on the surface properties of kaolinite. Journal of Colloid and Interface Science 93: 126 - 139
7. Gamiz E, Melgosa M, Sanchez-Maranon M, Martin-Garci JM, Delgado R Relationships between chemico-mineralogical composition and color properties in selected natural and calcined Spanish kaolins. Applied Clay Science 28: 269-282
8. Schneider H, Oka K, Pak JA (1994) Mullite and Mullite Ceramics John Wiley and Sons, Chichester, England, pp. 105 - 145.
9. Taylor DA, Preston JS, Dingle KB, Gate LF, Hogg CS (1995) Flash calcined kaolin in paint: A brief summary of current understanding Imerys Minerals Ltd.
10. Enos R (2003) Calcining Strategy Fact Pack, Version 1 Imerys Minerals Ltd.
11. Wellman B, Hampton K (1999) Living Networked On and Offline. Contemporary Sociology 28: 648 to 654
12. Manning DAC (1995) Introduction to Industrial Minerals Chapman and Hall, London, pp. 35 -71.
13. Kawano M, Tomita K (1995) Formation of mica during experimental alteration of K-feldspar. Chemistry and Clay Minerals 43: 397 - 405
14. Bristow CM (1993) The genesis of the china clays of south-west england - A Multistage Story. In: Murray H, Bunday W, Harvey C (eds) Kaolin Genesis and Utilization The Clay Minerals Society, Boulder, Colorado, pp. 171 - 204.
15. Murray HH, Keller WD (1993) Kaolins, Kaolins, and Kaolins. In: Murray H, Bunday W, Harvey C (eds) Kaolin Genesis and Utilization The Clay Minerals Society, Boulder, Colorado, pp. 1 - 24.
16. Whitten DGA, Brooks JRV (1987) The Penguin Dictionary of Geology Penguin Books, Middlesex
17. Taylor R (2005) Kaolin pit operations presentation Imerys Minerals Ltd.
18. Jepson WB (1988) Structural Iron in kaolinites and in associated ancillary minerals. In: Stucki JW, Goodman BA, Schwertmann U (eds) Iron in Soils and Clay Minerals D. Reidel Publishing Company, Boston, pp. 467 - 536.
19. Lefond SJ (1983) Industrial Minerals and Rocks Society of Mining Engineers, New York
20. Weaver C, Pollard L (1973) KaoliniteChemistry of Clay Minerals Elsevier Scientific Publishing Company, Amsterdam, pp. 131 - 144.

21. Deer WA, Howie RA (1975) Rock Forming Minerals Longman Group Ltd., Lonodn
22. Bristow CM, Exley CS (1985) Kaolin Deposits of the United Kingdom Imerys Minerals Ltd.
23. Barth TFW (1969) Feldspars Wiley Interscience, New York
24. Dunham AC, McKnight AS, Warren I (1992) The determination and application of time-temperature-transformation diagrams for brick, tile and pipe clays Department of Geology, University of Leicester.
25. Silica: Summary of Data Reported and EvaluationIARC Monographs On The Evaluation of Carcinogenic Risks to Humans IARC, pp. 41.
26. Chakraborty AK (2003) New data on thermal effects of kaolinite in the high temperature region. Jounal of Analysis and Calormetry 71: 799 - 808
27. Chakraborty AK, Das S, Gupta S (2003) Evidence for two stage mullite formation during thermal decomposition of kaolinite. British Ceramic Transactions 102: 153 - 157
28. Haines PJ (2002) Principles of Thermal Analysis and Calorimetry The Royal Society of Chemistry, Cambridge, UK
29. Lemaitre J, Delmon B (1977) Study of the sintering mechanism of kaolinite at 900 and 1050 °C; influence of mineraliser. Journal of Material Science 12: 2056-2064
30. Hogg CS, Stewart RGS (1997) The effects of temperature, soak time and alkali content on the products of china clay calcination Imerys Minerals Ltd.
31. Grofcsik J (1961) Mullite, its structure, formation and significance Publishing house of the Hungarian academy of sciences, Budapest
32. Noble FR, Stewart RGS, Golley CRL (1971) The transformations of heated kaolinite Imerys Minerals Ltd.
33. Thrale DS, Smith DN, Williams AA (1990) The colour of calcined clays Imerys Minerals Ltd.
34. Adams JM, Williams AA, Thrale DS (1989) The Colour of Calcined Clays I: Preliminary Work with Lee Moor Clays Imerys Minerals Ltd.
35. Grose DF (2004) The enhancement of flash calcined clay by secondary calcination - MSc Dissertation University of Exeter.
36. Thrale DS, Adams JM (1991) Methods for improving the colour of calcined clays Imerys Minerals Ltd.
37. Dover EL, Skuse DR, Williams AA (1990) A Laboratory Study of the Effects of variation in Lee Moor works water composition on the beneficiation of kaolinite, Imerys Minerals Ltd.
38. Sugden A (2003) An introduction to whiteware fluxes Imerys Minerals Ltd.
39. Bouchetou ML, Ildefonse JP, Poirier J, Danielou P (2005) Mullite grown from fired andalusite grains: the role of impurities and of the high temperature liquid phase on the kinetcs of mullitization and the consequences on thermal shocks resistance. Ceramics International 31: 999 - 1005
40. Arens PL (1951) A study of the differential thermal analysis of clays and clay minerals Excelsiors Foto-offset, Wageningen, Netherlands
41. Grim RE (1962) Applied Clay Mineralogy McGraw - Hill Book Company, New York, USA
42. Stewart D (2008) Calcined Kaolin in Decorative Matt Emulsions Presentation Imerys Minerals.

43. Hunt RWG (1987) Measuring Colour John Wiley and Sons, New York
44. (1999) ISO 2470:1999 Paper, board and pulps - Measurement of diffuse blue reflectance factor (ISO brightness) International Organization of Standardization, pp. 9.
45. Bennett G (2002) Brightness Test Procedure Imerys Minerals Ltd.
46. (2006) Datacolor Elrepho 450X Product Information Sheet Datacolor.
47. Weast RC (1968) Handbook of Chemistry and Physics, 49th Edition edn The Chemical Rubber Company, Ohio, US
48. Beard G (2006) Soluble Aluminium Test Method Imerys Minerals Ltd.
49. Boumans PWJM (1987) Inductively Coupled Plasma Emission Spectroscopy. In: Winefordner JD (ed) Chemical Analysis: A Series of Monographs on Analytical Chemistry and its Applications John Wiley and Sons, New York.
50. Beard G (2009) The Determination of Total Nitrogen content in Alumino Silicates and associated Minerals test method Imerys Minerals Ltd.
51. Beard G (2009) Carbon and Sulphur content of clay (general) using infra-red absorption detection in the SC-444DR test method Imerys Minerals Ltd.
52. Wills BA (2007) Mineral Processing Technology, 7 edn Elsevier, Oxford, UK
53. Bennett G (2001) Particle size (sedigraph) test procedure Imerys Minerals Ltd.
54. (2006) Innovative solutions in materials characterisation, process solutions, technology focus: laser diffraction technology Malvern Instruments Ltd.
55. Bennett G (1991) Particle Size (Dry sieving) test procedure Imerys Minerals Ltd.
56. Jenkins R (1974) An Introduction to X-Ray Spectrometry Heyden, London
57. Beard G (2007) Chemical Analysis by XRF, using Pressed Pellet sample preparation Imerys Minerals Ltd.
58. Anderson JC, Leaver KD, Leever P, Rawlings RD (2003) Materals Science for Engineers, 5 edn Nelson Thornes, Cheltenham, UK
59. Brindley GW, Brown G (1980) Crystal structure of clay minerals and their X-Ray indentificaton Mineralogical Society, London
60. Goldstein J, Newbury DE (2003) Scanning Electron Microscopy & X-Ray Microanalysis, 3 edn Springer Publishing Company, New York, USA
61. Shaw DJ (1991) Introduction to Colloid and Surface Chemistry Butterworth-Heinemann
62. Brenton D (2005) Surface Area testing method Imerys Minerals Ltd.
63. Powlesland B (2003) Evaluation of the FT3 Powder Rheometer Imerys Minerals Ltd.
64. Bennett G (2009) Oil Absorption Test Procedure Imerys Minerals Ltd.
65. Decanter Centrifuges Product Information Ashbrook Simon-Hartley.
66. Rabey T (2004) Goverseth Refinery Information Pack Imerys Minerals Ltd.
67. Fooks JA (2001) Why Use Cryogens in the China Clay Industry?CRYO - users meeting Imerys Minerals Ltd.
68. Fooks JA (2004) Reductive Bleaching of Clays, Laboratory Method Imerys Minerals Ltd.
69. Hawken WA (1998) A Practical Review of the Methods of Colour Enhancement of Kaolin Clays Imerys Minerals Ltd.
70. Dunn M (2008) Polwhite E Continuous Grinding Report Imerys Minerals Ltd.
71. Freund RJ, Wilson WJ, Sa P (2006) Regression Analysis Study Guide Elsevier Science

72. Montgomery DC, Runger GC (2006) Applied Statistics and Probablity for Engineers Wiley
73. Acton FS (1984) Analysis of Straight-Line Data Dover Publications
74. Braun WJ, Murdoch DJ (2008) A First Course in Statistical Programming with R, 3 edn Cambridge University Press, Cambridge, UK
75. (March 2008) PoleStar 200P Specification Sheet, Third Edition edn Imerys Minerals Ltd.
76. (March 2008) PoleStar 200R Specification Sheet, Fourth Edition edn Imerys Minerals Ltd.
77. Cabrera MI (1996) Absorption and Scattering Coefficients of Titanium Dioxide Particulate Suspensions in Water. The Journal of Physical Chemistry 100: 8
78. Kenkel J (2002) Analytical Chemistry for Technicians, 3 edn CRC Press, Florence, Kentucky, USA
79. McConaghy K (2001) Flux Process Description. In: Wang Q (ed) World Minerals.
80. Mackenzie RC (1970) Differential Thermal Analysis Academic Press, London
81. Todor DN (1976) Thermal Analysis of Minerals Abacus Press, Tunbridge Wells, Kent
82. Rowse JB (1979) Bleaching Review Imerys Minerals Ltd.
83. Taylor R (2005) Soluble Aluminium in the Herreschoffs Imerys Minerals Ltd.
84. F. Onike, G.D. Martin, Dunham AC (1986) Time-Temperature-Transformation Curves for Kaolinite. Materials Science Form 7: 73-82
85. Redfern SAT (1987) The kinetics of dehydroxylation of kaolinite. Clay Minerals 22: 447 - 456
86. Goodman R (2004) Soluble aluminium and sandgrinding of calcined clays Imerys Minerals Ltd.
87. Fooks JA (1994) Low Yellowness Calcined Clay for the Paint Industry` Imerys Minerals Ltd.
88. Grose DF (2005) Reductive Calcination - Prevention of Colour Reversion Imerys Minerals Ltd.
89. Jones HRN (2000) Radiation Heat Transfer Oxford University Press, Oxford
90. Billmeyer FW, Satzman M (1966) Principles of colour technology Interscience Publishers
91. Agra-Gutierrez C (2003) RR0610/02 Imerys Minerals Ltd.
92. Coulson JM, Richardson JF (2000) Coulson and Richardson's Chemical Engineering, Volume 1: Heat Flow and Mass Transfer, Sixth Edition edn Butterworth Heinemann, Oxford
93. Incropera FP, DeWitt DP, Bergman TL, Lavine AS (2006) Fundamentals of Heat and Mass Transfer, Sixth edn John Wiley and Sons, New Jersey
94. Winterton RHS (2000) Heat Transfer Oxford University Press, Oxford
95. (2006) 1200 °C and 1300 °C Medium laboratory furnaces Carbolite.